A STUDY OF THE APPLICATION OF ULTRASONIC STANDING WAVES TO THE SEGREGATION OF FINE BIOLOGICAL PARTICLES FROM LIQUIDS.

Gareth Bowen Davies

Thesis submitted for the degree of Doctor of Philosophy
in Biochemical Engineering,
December 1992.

Department of Chemical and Biochemical Engineering,
SERC Advanced Centre for Biochemical Engineering,
University College London,
University of London.

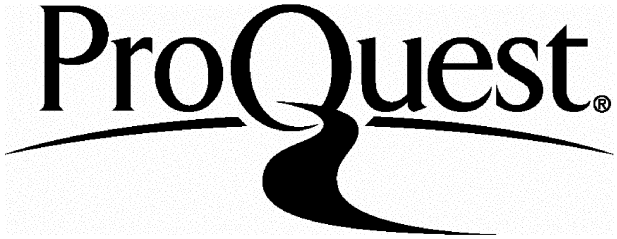

Summary

This thesis describes research to evaluate the application of megahertz (1 to 10 MHz) ultrasonic standing waves to the segregation and separation of fine biological particles, in the size range of 0.1 to 10 μm, from liquids. Research has focused on the development of an alternative separation technique through the ability to selectively manipulate delicate, highly hydrated particles typical of many biological process streams where the sedimentation characteristics of the particles preclude traditional centrifugation–based separation methods and the requisite for non–invasive in line processing rules out filtration.

A survey of both acoustic and ultrasonic research concentrating on the application of ultrasonic energy to processes involving biological particles has been carried out. An in–depth analysis of the theories of ultrasonics in relation to the stated aims of the work is presented in which the mechanisms controlling the migration of fine particles under the influence of a megahertz frequency standing wave field are discussed.

Results of investigations to determine the feasibility of concentrating micron–sized particles in a standing wave field are presented. These confirm that the small–scale separation of biological particles is achievable. The subsequent design of an experimental separation device and detailed experiments to elucidate the parameters of importance in determining the segregation of biological particles from liquids using this apparatus are described. Ultrasonic power input and fluid velocity were found to be the most critical process parameters and operational constraints as functions of particle size and ultrasonic frequency were identified.

The design and development of a novel laser scanning technique for the monitoring of the migration of particles in an ultrasonic standing wave field is presented. Data obtained using this equipment has been used when discussing the design of large–scale continuous solid–liquid separation devices.

Details of an ultrasonic system for the non–invasive, *in–situ* sample preparation of material for dynamic laser light scattering analysis of particle size distributions in the monitoring and control of bioprocesses are presented together with data from experimental trials. Results showed this to be a promising method for rapid

and controlled sample preparation and well suited to handling process streams containing heterogeneous particle sizes.

The thesis concludes by giving consideration to the necessary future work and to the application ot the techniques described in the thesis to relevant biological separation problems.

To Anne and Owen.

Contents

List of Figures

List of Tables

Nomenclature.		Units
a	particle radius	m
c	sound velocity	$m.s^{-1}$
f	frequency	Hz (s^{-1})
g	acceleration due to gravity	$m.s^{-2}$
h	a function of ... (See **Equation 2.2**)	–
k_B	Boltzmann's constant	$J.K^{-1}$
l	length	m
r	radial distance from axis	m
t	time	s
u	velocity	$m.s^{-1}$
x	displacement	m
z	axial distance	m
A	amplitude of vibration	m
D	distance between two particles	m
E	energy density	$J.m^{-3}$, Pa
$\bar{E}$	time averaged energy density	$J.m^{-3}$, Pa
J	density correction factor	–
F	density and compressibility factor	–
I	sound intensity	$W.m^{-2}$
P	pressure	Pa
P_a	acoustic pressure	Pa
R	radius of cylinder	m
T	period	s
U	streaming velocity	ms^{-1}
V	voltage	V
V_p	peak voltage	V
α	striation condition	–
κ	wave number	m^{-1}
λ	wavelength	m
μ	viscosity	Pa.s

		Units
ρ	density	$kg.m^{-3}$
σ	c_1/c_0	–
ν	ρ_1/ρ_0	–

Subscripts

T	travelling or progressive wave
S	standing wave
0	medium
1	particle

Superscripts

-	time averaged
i	incident wave
r	reflected wave

CHAPTER 1 INTRODUCTION

1.1 Introduction

The focus of this work is to examine the selective application of ultrasonic standing waves to provide an alternative and non-invasive process capable of achieving rapid separation and concentration of fine biological particles without the addition of contaminating reagents.

Many of the physical effects of ultrasound have been known and exploited for some time. In the area of biotechnology, however, its use has been limited to small scale cell disruption and to sensors. This thesis examines a novel use of ultrasonic standing waves for the selective manipulation of biological particles of diameters ranging from submicron sizes to tens of micrometers. Key applications in the field of biochemical engineering are identified together with details of novel techniques developed to measure scale-up parameters.

In many industrial biological processes it is necessary to separate extremely small and fragile particles from suspension. Traditionally this is achieved using high-speed centrifugation or filtration [Hoare and Dunnill (1989)]. Such techniques suffer from problems associated from the shear sensitivity and compressibility of typical biological particles such as whole cells and protein flocs [Devereux (1984)].

Centrifugation exploits the difference in density between solid and liquid phases to effect a separation. Living cells are highly hydrated and therefore have a very similar density to the complex dilute solution of nutrients required to support their growth from which they must be separated efficiently. Consequently lengthy processing times are often needed causing expensive loss of labile products. Another characteristic of industrial scale high-speed centrifugation is that the extremely high rates of acceleration experienced by particles (typically 2,000 - 20,000 g) on entering the working volume of the centrifuge can develop damaging shear forces which destroy some delicate particles [Dunnill (1983)].

Filtration suffers from limitations imposed by particle compressibility leading to a reduction in the voidage of the particle cake, concentration polarisation effects [Dunnill (1983)] and permanent fouling of membranes. Biological particles, and whole cells in particular, exhibit significant compressibilities that can cause blinding of filters

and membranes alike when the bed voidage reduces as the particles are compressed. This problem is frequently overcome by the addition of a filter aid such as diatomaceous earth or perlite which does however incur cost and contamination of the filter cake.

Megahertz frequency ultrasonic standing waves cause migration of fine particles suspended in the sound field to the nodal planes of the sound field which are spaced at half-wavelength distances. The mechanisms behind this phenomena have been the subject of research since their initial observation by Kundt (1874). The driving force for migration is the radiation pressure exerted on the particle by the sound waves. This phenomenon forms the basis of the novel separation technique examined in this thesis.

Ultrasound is usually defined as being sound of frequency too high for the human ear to detect. The normal upper frequency limit of hearing is taken as being somewhere in the region of 16–25 kHz [Mason (1990)].

In this study ultrasound of frequencies in the range of 1–10 MHz will be studied during experimental work. However research in the field of sound wave and particle interactions has been carried out at sound wave frequencies ranging from 1 Hz to over 20 MHz and for this reason the following literature survey will investigate research performed at acoustic or sonic and ultrasonic frequencies which are outside the experimental range of this work.

1.2 Literature Survey

Ultrasound is only distinct from audible sound because of the upper frequency threshold of the human ear and indeed the physical properties and effects of audible sound can be similar to those of ultrasound. For this reason much of the research published on high frequency ultrasonic phenomenon has been guided by research into low frequency ultrasound and audible sound. The following literature survey therefore includes a consideration of acoustic operations as well as ultrasonic operations.

1.2.1 Physical Effects of Ultrasound

A number of physical effects are attributed to the irradiation of a material with ultrasound. These are discussed in detail in the following sections together with a review of the applications of ultrasound investigated by other researchers. (Theoretical and mathematical aspects of the physical effects of ultrasound are described in detail in **Chapter 2.**)

1.2.1.1 Acoustic Aerosol Agglomeration

The experiments of Kundt and Lehmann (1874) of Berlin were the first illustration of the ultrasonic agglomeration of fine particles. Essentially the method used involved producing ultrasonic (30 kHz) standing waves in a closed glass tube, where the nodes of the waves were shown by the gathering of a light dust of fine particles, such as lycopodium spores.

Further work on the agglomeration of suspended particles was carried out by various authors in the 1930's and excited widespread interest in the practical applications of acoustic and low frequency ultrasonic waves.

St.Clair (1949) brought together the work of King (1934) and Smoluchowski (1918), among others, to formulate a theory on the agglomeration of smoke, fog or dust particles by sonic waves. He concluded that the behaviour of suspended particles being subjected to sonic vibrations in the enveloping gas may be considered as being influenced by a combination of the following effects:

- Covibrations of particles in a vibrating gas
- Attractive and repulsive hydrodynamic forces between neighbouring particles
- Radiation pressure.

It was noted that the forces causing particle agglomeration were associated only with the vibration of the gas and hence were acoustic forces.

> "The forces acting to cause sonic agglomeration are complex; it seems fairly certain that the major effects are the result of acoustic forces, and are not purely kinetic effects."
>
> [St.Clair, (1949)]

St.Clair's experiments showed that aerosols made from ammonium chloride, zinc oxide and carbon, and water and oil fogs could be flocculated in seconds under moderate acoustic energy densities of 50 – 100 ergs.cm^{-3} (5 – 10 J.m^{-3}).

Mednikov (1965) presented a theory of acoustic coagulation and precipitation of aerosols in which he combined particle and hydrodynamic interactions. Particulate agglomeration mechanisms can be classified into several categories, the most important being orthokinetic interaction. This is a process where the smaller (mobile) particles collide with the larger (relatively stationary) particles. This agglomeration process is sensitive to changes of frequency and to the initial size distribution of the particles such that there is an optimum frequency range for a specified particle size distribution as described in **Equation 1.1**.

$$f_{opt} = \frac{9\,\eta}{4\,\pi\,\nu_p\,r_2^2}\,r_{2rr} \qquad \textbf{Eq. 1.1}$$

where r_2 is the radius of the smaller particle, r_{2rr} is the reduced radius of the smaller particle and equals r_2/r_1, η is the viscosity of the gas and ν_p is the relative velocity of the particle to the gas.

Hydrodynamic interactions occur due to the distortion of the flow field around the particles and can be grouped under the following terms, parakinetic interaction, attractional interaction between particles, and pulsational interactions between particles. Parakinetic interaction occurs due to unilateral or bilateral distortion in the fields of flow of the gas around particles of different diameters.

The attractional interactions between particles include Bernoulli forces, Bjerknes forces, Oseen forces, and Stokes forces are discussed in more detail in **Chapter 2**. By these mechanisms the coagulation rate increases only monatonically with frequency.

According to Shaw & Tu (1979) acoustic agglomeration by hydrodynamic collision is important for particles with radii larger than 0.5 μm in the audible frequency range (less than 10 kHz). It was experimentally determined that the acoustic

agglomeration of these large particles is relatively insensitive to frequency change being more dependent on particle diameter. In contrast orthokinetic interaction is sensitive to changes in frequency as the optimum frequency for coagulation increases as the diameter of the particles decreases. This finding agrees with the change in optimum frequency suggested by Mednikov in **Equation 1.1.**

In the 1950's acoustic agglomerators were being sold commercially, with applications to remove mists and dust from process gas streams. However, industrial interest soon declined due to the high running costs of such units. With the upsurge in emphasis on energy and environmental conservation in the early 1970's a renewal of interest in acoustic agglomeration was evidenced. New applications, such as removal of dust from power station emissions, suppression of molten sodium aerosols in nuclear power plants and the collection of toxic dusts, were developed and as a result the research field became very active.

Rajendran (1979) investigated experimentally the saving in energy consumption when standing wave conditions were set up in an agglomerator chamber as compared to the use of travelling waves. It was found that effective acoustic precipitation could be achieved at a sound intensity one order of magnitude lower than that required for travelling wave agglomerators.

Higher frequency ultrasound has not found a role in aerosol agglomeration due to the increase in attenuation of ultrasound with increasing frequency. The intensity of an ultrasonic wave at a specified distance from the source decreases exponentially with increasing sound frequency, indeed ultrasound of frequency above 500 kHz does not propagate further than a few centimeters through air. For this reason higher frequency ultrasound has only found an application in the aggregation of particles in liquid media where the coefficients of absorption are significantly reduced.

1.2.1.2 Acoustically and Ultrasonically Enhanced Sedimentation

Burger and Sollner (1936) studied the action of ultrasonic waves in colloidal and semi-colloidal suspensions. When examining the neutralisation of dilatancy they observed increased sedimentation rates and a reduction of the final settled volume.

Thielsch (1946) examined the effect of acoustic vibrations on the settling rates of ground rock particles in water. At 60 Hz increased sedimentation rates and dewatering were observed; these effects were attributed to coagulation in the suspension and closer packing of particles in the settled phase.

Megahertz and lower frequency ultrasound were used by Thompson and Vilbrandt (1954) to affect the settling of solids in phosphate ore tailing. The phosphate tailing consisted of a mixture of clay, quartz and phosphate mineral with a size range of 0.1 – 10 μm. Suspensions of 5 weight % were used during most experiments. Mild sonication of intensities below approximately 3 $kW.m^{-2}$ increased the rate of sedimentation by at least five times but did not affect the concentration of solids in the sediment due to the very strongly thixotropic nature of the suspension. Ultrasonic intensities above 3 $kW.m^{-2}$ caused cavitation in the suspension and actually hindered the settling of the slurry by increasing the effective number of charged particles in suspension. The presence of charged particles in turn increased and strengthened the thixotropic gel structure. The authors did not attribute the increased settling rates to any specific mechanism of particle interaction.

Obiakor (1965) and Matskevich & Skalozubiv (1969) sonicated kaolin and carbonate slurries, respectively and noted an increase in sedimentation rate of between 150 and 200%. Small particles were observed to grow into large particles (coagulation) and a reduction in the filtration resistance of the slurry of 14% was observed. An increase of 600–700% in the rate of sedimentation of industrial pigment slurries of concentrations of 0.02 and 0.06 $kg.m^{-3}$ when sonicated at 540 and 765 kHz was reported by Anada (1974).

Little research into the effects of ultrasound on the settling of biological suspensions was published until the late 1970's. Kowalska *et al* (1979) and Bien *et al* (1979) discussed the use of ultrasound to supplement the addition of flocculating agents to sludges from sewage treatment plants. Ultrasound of frequency 20 kHz used alone produced beneficial effects, but used in conjunction with the addition of polyelectrolyte flocculating agents ultrasound was found to be most useful in increasing the rate of sedimentation and the strength and density of the flocs, reducing the final volume of the solid phase to 20% of the volume of normally treated sludge.

The authors suggest that their results indicated an economically important method of improving the treatment of municipal sewage.

King and Forster (1990) subjected samples of activated sludge from domestic sewage to ultrasound of 20 kHz frequency and power outputs of between 0 and 60 W transmitted via a probe for various periods of time. Their conclusions were that high ultrasonic intensity levels caused an increase in settling rate but at the expense of supernatant clarity. Sonication of the sludge in the range of 7.5 – 75 W.min (authors derived units from the electrical power supplied to the sound source, multiplied by the duration of sonication) caused shear disruption of the sludge flocs and a significant reduction in ease of filtration of the sludge due to a reduction of the mean particle size in both the sludge and the supernatant. A review of the research field [King and Forster, (1990)] highlighted the need for further detailed studies of the application of ultrasonic energy to activated sludge,in order to explain the seemingly contradictory findings [Bien (1979) and King and Forster (1990)].

Bell and Dunnill (1984) studied the effect of acoustic frequencies (20 – 200 Hz) on the rate of sedimentation and dewatering of soya protein precipitates. Increased coagulation, sedimentation rate and dewatering were observed and an overall improvement in an undefined separation efficiency of 20 – 30% was achieved. Treatment was most effective when the particles were undergoing orthokinetic growth. This finding gave support to the concept of the sound waves enhancing the mechanisms of aggregation by covibration.

Bien (1988) discussed the use of low frequency ultrasound (20kHz) in the preparation of mineral and organic sludges to improve the levels of dewatering achieved by filtration. Sonication was found to reduce final hydration by around 10%. As a result of the joint action of ultrasound and polyelectrolytes it was possible to reduce the dose of the polyelectrolyte added by 50%. The levels of dehydration achieved were in some cases even better than those obtained when using only electrolytes at their full dose.

In conclusion despite the diverse research that has been conducted there is little evidence to suggest that large–scale sonically–enhanced processes are widespread in industry. There may be various reasons for this including the high capital cost of installing industrial scale acoustic and ultrasonic equipment, the relative paucity of

process scale data, and the lack of concensus as to the mechanisms and effects of sonication.

1.2.1.3 Ultrasonic Particle Manipulation

Ultrasonic particle manipulation in the context of this thesis covers the application of ultrasonic standing waves to specifically manipulate particles in suspension for the purpose of solid liquid separation or applications involving the aggregation of particles.

Sollner and Bondy (1936) studied the emulsifying and coagulating effects of ultrasound on toluene–water, mercury–water emulsions and suspensions of various sizes of quartz particles. They produced stationary waves in narrow tubes containing the suspensions.

> "These stationary waves in the liquid are obviously the cause of the accumulation of droplets, a phenomenon identical with Kundt's dust figures. In such a zone coagulation takes place, in part owing to the much higher concentration, in part owing to a kind of ortho-kinetic coagulation: drops of different size moving with different velocity, then colliding and coalescing."
>
> [Sollner and Bondy, (1936)].

The authors also noted that the rate of accumulation was very strongly dependant on particle size and on the wavelength of the ultrasound. The accumulation of particles at half wavelength distances proceeded rapidly with particles of diameter above 1 μm but was not observed with particles of truly colloidal size.

In the following decades extensive work on ultrasonic emulsification and enhanced sedimentation was performed but little interest was shown in using the ultrasonic forces alone to manipulate particles in suspension. Fresh interest was aroused in the early 1970's when investigations into possible harmful effects of ultrasound on unborn foetuses by Dyson (1971) reported that the flow of red blood cells *in vivo* was stopped by the application of ultrasound at therapeutic intensities (under 10 $kW.m^{-2}$). The cells were seen to aggregate into sharp edged clumps spaced at half wavelength intervals. The aggregates rapidly collapsed as irradiation ceased, supporting the theory that the radiation pressure was the sole cause of the effect. Baker (1972) repeated the

experiments *in vitro* and reported threshold intensities for the onset of aggregation of red blood cells in standing waves of 0.3 $kW.m^{-2}$ in whole blood and for red blood cells in blood diluted 1:10 with plasma, threshold intensities of 0.03 $kW.m^{-2}$. No aggregation was observed under travelling ultrasonic wave conditions even up to intensities of 50 $kW.m^{-2}$, again indicating that the radiation pressure exerted on a particle suspended in a standing wave field was the primary cause of particle aggregation.

Similar experiments were repeated by Gould and Coakley (1973) who examined the phenomenon under conditions more amenable to the quantitative analysis of the forces involved. Using red blood cells and polystyrene spheres they compared experimental results with theoretical relationship for the minimum anti-nodal sound pressure required for striation formation over a hundred-fold concentration range. The forces considered in the analysis were those arising from gravitation, buoyancy, acoustic microstreaming and acoustic radiation pressure. Reasonable agreement was obtained between the predicted and observed thresholds for particle accumulation at the antinodes of the standing wave field and for the rate of particle migration of the polystyrene microspheres.

Higashitani (1981) formulated a generalised theory of time-averaged motion of particles in a plane stationary sound field in which the effect of particle diffusion is taken into account. The particle distributions at the rather early stage and after a sufficient period of irradiation were also derived analytically from theory. Results from subsequent experiments using polystyrene latex dispersions with particle diameters of 0.78, 1.24 and 1.62 μm were well predicted by the theory. The condition for formation of the Kundt's tube striations was characterised and it was predicted that the accumulation of colloidal particles of diameter less than 0.1 μm would be "rather difficult" due to the large diffusional forces exerted on the particles.

Peterson (1987) described a technique utilising two opposing ultrasonic transducers operating at slightly different frequencies to produce pseudo-standing waves that move through the test chamber at the beat frequency of the two transducers. This technique was used to separate red blood cells from whole blood. Separation of a feed stream of 40 % v/v red blood cells in plasma resulted in a suspension of 80 % v/v cells and a plasma stream of 1.5 % v/v red blood cells at a

feed flowrate of 3.33×10^{-8} $m^3.s^{-1}$. It was suggested that red blood cells, platelets and the various white blood cells may be separated with this technique due to their different acoustic properties.

Schram (1985 and 1986) in two European Patent Applications described inventions for the fractionation of a suspension of particles of different diameters into separate fractions containing different particle size distributions with varying ratios of large and small particle diameters. The process involved the use of standing waves of 2.02 MHz frequency and transducer signals of 50 volts to separate a mixture of yeast and bacteria cells which were of different diameter into fractions where the ratio of number concentration of one particle to the other was 80:1 at its highest value at flow velocities of 6.67×10^{-3} $m.s^{-1}$.

Patat *et al* (1991) investigated the application of ultrasonic waves as an alternative to centrifugal separation in agglutination serological tests. The permanent binding of antibodies on the blood cells and the test antigens in suspension cause the blood cells to form clumps that are not easily disrupted. The standard procedure is to centrifuge the microplates to bring the blood cells into contact so that agglutination can occur and then to agitate the plate to detect the non-agglutinated negative results by visual observation, a process that can take up to 30 minutes. Ultrasonic waves at 20 $kW.m^{-2}$ were transmitted through the bottom of a standard polystyrene microplate containing the sample and standing waves were created as the sound wave reflected off the sample-air interface. The ultrasonic standing waves caused the blood cells to migrate to the nodes of the sound field in a matter of seconds allowing agglutination to occur. A second application of ultrasound at 40 $kW.m^{-2}$ caused acoustic streaming of sufficient intensity to disperse the weak aggregates formed in negative results and to allow the results to be read by a human operator. [It is interesting to note that no measures were taken to avoid the formation of potentially hazardous aerosols from the air-sample interface.]

The upper limits of sound pressure amplitude applicable to the aggregation of fine particles in a megahertz frequency standing wave field were investigated by Gould *et al* (1992). The upper sound pressure limits were taken as the sound pressures required to cause the disruption of the concentrated bands of particles through the onset of cavitation or acoustic streaming. For the concentration of 9 μm polystyrene

latex particles in air-saturated water at 1.02 MHz an upper peak sound pressure limit of 1.9 x 10^6 Pa even though cavitation was detected at 1.1 x 10^6 Pa. At 3.14 MHz cavitation was detected at peak sound pressures of 2.150 x 10^6 Pa however vigorous acoustic streaming in a portion of the test vessel disrupted the banding pattern at sound pressure levels of 1.1 x 10^6 Pa.

In conclusion, there appears to be little work published on investigations into the development of a practical separation technique for the segregation of biological particles or the feasibility of larger scale standing wave separation devices.

1.2.1.4 Cavitation

This section describes the phenomenon of ultrasonic cavitation which is of importance to the experimental work of this thesis since cavitation is an undesirable effect that must be avoided if efficient particle segregation in a standing wave field is to be performed. The theoretical background and mechanisms of cavitation are discussed and followed by a literature survey of the physical, chemical and biological effects of cavitation. Careful consideration of the direct physical effects of ultrasound upon a suspension of biological particles must be applied prior to the design of experimental apparatus.

Cavitation may be said to occur whenever a new surface or cavity is created within a liquid, a cavity being defined as any bounded volume, whether empty or containing gas or vapour, with at least part of the boundary being liquid. This broad definition includes such phenomena as boiling and effervescence, which involve only expansion of the gas phase [Neppiras, (1984)]. The term 'acoustic cavitation' is therefore usually restricted to cases involving both expansion and contraction of cavities or bubble nuclei. In the literature the term cavitation is often loosely applied to the effects, as well as the formation and motion of cavities in liquids (For the chemical and biological effects of cavitation see **Section 1.2.2.1**).

Cavitation voids originate in an ultrasonic wave field at nuclei that are ever-present in a liquid in the form of solid, vapour or gas micro-inhomogenities. When the rarefaction (reduced pressure) portion of an ultrasonic wave is powerful enough

to overcome the intermolecular forces binding the fluid very small cavities or microbubbles will be formed that collapse during the compression portion of the ultrasonic wave to release large amounts of energy. As during cavitation the continuity of the medium is destroyed this phenomenon must also be regarded as a nonlinear effect. In the course of several cycles of the ultrasonic field each cavity that develops from a nucleus becomes, due to rectified and convective diffusion, infused with a finite quantity of the gas dissolved in the liquid. Over the subsequent few periods these cavities implode creating localised 'hot spots' of tremendous temperature and pressure (6000 K and 1000 bar [Mason, (1990)]) at the point of implosion (see **Figure 1.1**).

An important question arises as to how the liquid ruptures in an ultrasonic wave at acoustic pressures far below the theoretically predicted rupture strength of the ideal liquid (the sound pressure amplitude at which a perfectly pure liquid is unable to sustain the cyclical compression and rarefaction imposed by the ultrasonic wave and discontinuities form in the liquid during the rarefaction phase creating cavities of vapour). For a cavity of radius **R** to form in an ideal liquid a tensile stress S_T equal to the Laplace Pressure generated by the surface tension, σ_s, of the liquid must be applied. S_T is described in **Equation 1.2**.

$$S_T \approx \frac{2\sigma_s}{R} \qquad \textbf{Eq. 1.2}$$

To cause cavitation in an ideal liquid the molecules must be forced apart to a distance, **R**, approximately equal to twice the intermolecular distance. In water this distance is approximately 0.2 nm. Substituting **R** into **Equation 1.2** we obtain a value of S_T of 10,000 atmospheres (approximately 3.5×10^8 kW.m^{-2}).

However all real liquids, and especially water, contain solid and gaseous impurities which act as cavitation nuclei. As the hydrostatic pressure in the rarefaction wave drops gas diffuses out of solution forming bubbles containing the dissolved gas and liquid vapour. This process occurs at sound intensities greater than 10–30 kW.m^{-2} which is orders of magnitude less than the sound intensity required to produce cavitation in an ideal liquid.

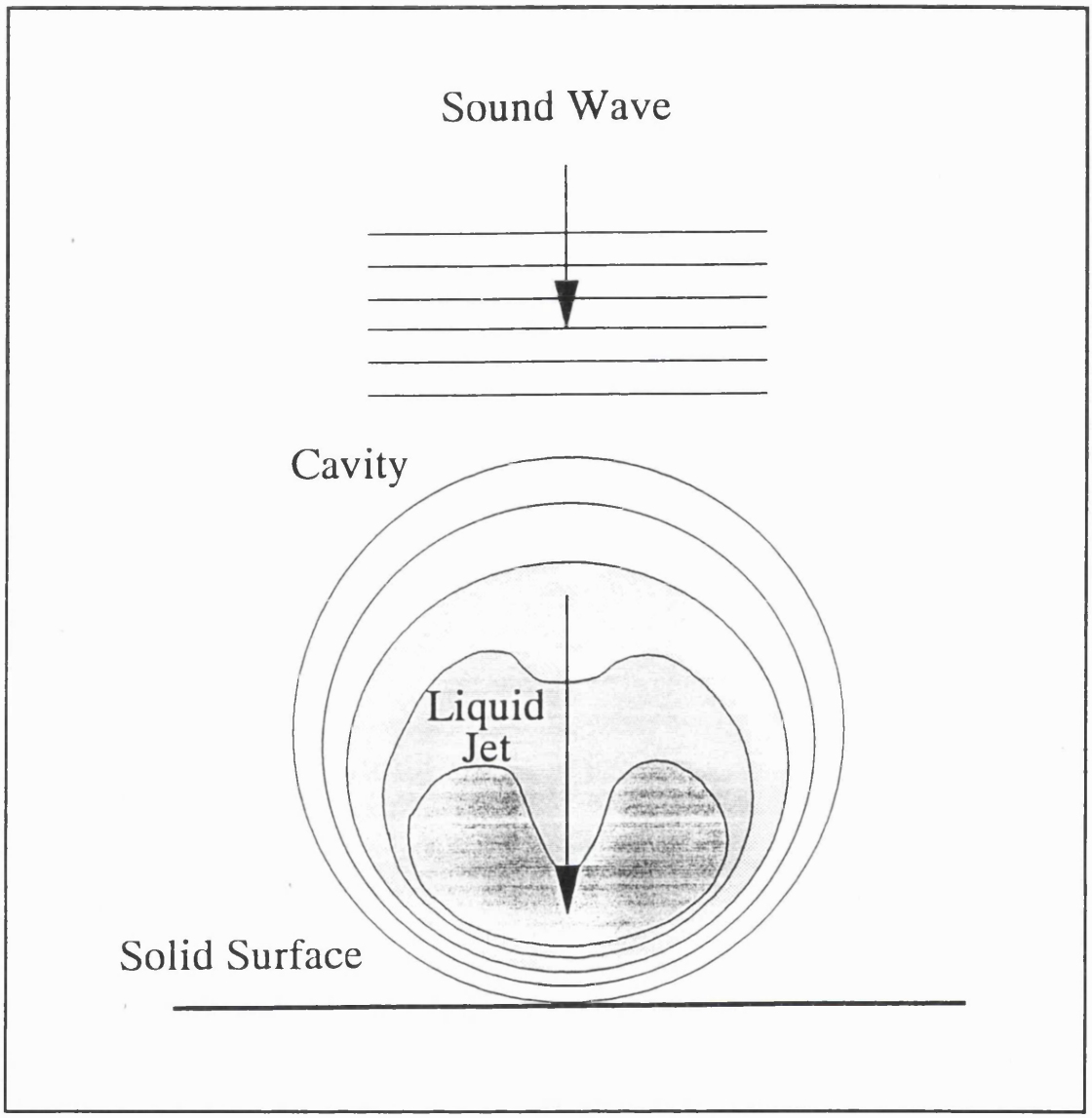

Figure 1.1 *Collapse of a Cavity at a Surface in an Ultrasonic Field.*

Two types of cavitation in liquids have been identified stable cavitation and transient cavitation categorised by the lifetime of the cavitation microbubble formed which is dependent on the original size of the gas bubbles inherently present in the liquid.

- **Transient Cavitation**

Ultrasonic intensities in excess of 100 $kW.m^{-2}$ are required to produce transient cavitation [Mason (1990)]. Transient cavitation bubbles are voids or vapour filled bubbles that exist for only a few cycles of the sound wave and expand to more than

twice their original size before collapsing violently during a compression wave. The collapse of the cavities is very violent because although the bubbles contain the gas dissolved in the liquid there is insufficient time to allow significant diffusion of the gas or vapour into the bubble and therefore the cavity is essentially a void.

Noltingk and Neppiras (1950) derived equations to estimate the maximum temperature and pressure developed on the implosion of a transient cavity.

$$T_{MAX} = T_0\left(\frac{P_m[\gamma - 1]}{P}\right) \qquad \textbf{Eq. 1.3}$$

$$P_{MAX} = P\left(\frac{P_m[\gamma - 1]}{P}\right) \qquad \textbf{Eq. 1.4}$$

where T_0 is the ambient temperature, γ is the ratio of specific heats of the gas, **P** is the pressure in the bubble at its maximum size and is usually assumed to be equal to the vapour pressure of the liquid. Calculations using these equations for the collapse of a cavity containing nitrogen (γ = 1.33) in water at 293 K and atmospheric pressure give values for the maximum temperature and pressure at the point of implosion of $T_{MAX} \approx$ 4,273 K and $P_{MAX} \approx$ 970 bar respectively. It is these "hot spots" that are thought to be the main mechanism for the increased yields of certain chemical reactions and sonochemical effects (See **Section 1.2.2.1**).

- **Stable Cavitation**

Stable cavitation can be described as the linear pulsation of gas–filled bodies in low–amplitude sound fields. Stable cavitation bubbles have a much greater lifetime than transient microbubbles and may exist for as many as a thousand cycles of the sound wave. They are believed to contain mainly gas and little vapour and are produced at relatively low intensities (10–30 $kW.m^{-2}$). Stable cavities oscillate in the sound field giving rise to a microstreaming field around the bubble which can lead to increased yield and reaction rates of mass transfer limited chemical and biochemical reactions and also cause mechanical damage due to the hydrodynamic shear stress generated by the enormous velocity gradients in the microstreaming field.

Both forms of cavitation, transient and stable, cause disruptive mechanical effects at the locality of the cavity and also in the bulk of the liquid through acoustic streaming caused by the chaotic motion of the microbubbles produced. In the scope of this thesis cavitation of any nature is undesirable and experiments and equipment will be designed carefully to avoid cavitation if possible.

The following section examines the process factors which determine the onset of cavitation and which will be carefully controlled in this study.

1.2.1.5 Factors Affecting Cavitation

The multi-phase, aqueous process streams normally encountered in bioprocess operations dictate that the prevention of cavitation will be an important factor in the design of ultrasonic equipment for the segregation of biological particles. Certain important measures in the avoidance of cavitation, such as the reduction of the dissolved gas concentration of the liquid, are not practical in the majority of bioprocesses and these issues are discussed in the following sections.

- **Properties of the Solvent**

Water is the universal solvent for biochemical processes and therefore there is little scope for preventing cavitation by changing to a solvent of lower vapour pressure and higher intermolecular forces to increase the ultrasonic intensity required for the onset of cavitation. However many biochemical reactions and fermentations produce solvents as products (i.e. ethanol, methanol) and this factor must be considered before attempting ultrasonic separation in such a system as the presence of volatile solvents may reduce the ultrasonic intensity required to induce cavitation.

- **Temperature**

Connolly and Fox (1954) examined the thresholds of ultrasonic cavitation in water in relation to a number of external factors including the temperature of the liquid. The dependence of the cavitation sound pressure threshold on temperature was found to non-linear and increased by a factor of 2.5 as the temperature decreased from 303 K to 273 K. Therefore operating ultrasonic standing wave particle

segregation systems at the low temperatures normally required in the downstream separation processing of sensitive biological materials has the effect of decreasing the risk of cavitation.

- **Ultrasonic Frequency**

The sound pressure threshold for the onset of cavitation increases with increasing ultrasonic frequency. At very high frequencies the microbubbles have insufficient time for growth during the rarefaction phase of the wave before being influenced by the compression phase of the wave. This frequency relationship is further complicated by the dependency of the threshold on the size of the microbubbles already present in the liquid since there is an optimum bubble size that corresponds to a resonant frequency. As the frequency increases the optimum bubble radius for cavitation decreases (Lewin & Bjorno, [1981]). Ultrasonic cavitation is unlikely to occur at frequencies greater than 3 MHz even at very high sound intensities.

- **Dissolved Gas Content**

The presence of dissolved gas in a sonicated liquid greatly increases the risk of cavitation. Galloway (1954) found that the sound pressure required to initiate cavitation in de-aerated water at 20–40 kHz was in the order of $2x10^7$ Pa and fell to $1x10^5$ Pa at 100% saturation. Degassing liquids before sonication would significantly decrease the risks of cavitation.

- **Overpressure**

The cavitation threshold depends on the rarefaction phase of the sound wave generating negative pressures that overcome the ambient pressure on the system. Therefore increasing the external pressure has the effect of increasing the cavitation threshold for the system.

- **Ultrasonic Intensity**

Increasing the intensity of the ultrasonic wave increases the risk of the onset of cavitation. Through consideration of the factors listed above it is possible to avoid cavitation at intensities below 10–30 $kW.m^{-2}$, the application of higher ultrasonic intensities must be coupled with an increase in the frequency of the sound wave applied to avoid the onset of cavitation.

1.2.2 Chemical and Biological Effects of Ultrasound

The enhancement of many chemical reactions can be directly attributed to the cavitation events produced in high intensity ultrasonic fields (See **Section 1.2.2.1**), however the rate of chemical and biochemical reactions alike have been increased by the application of ultrasonic energy well below the appropriate threshold intensities for cavitation and suggests a further mechanism for the enhancement of reactions (See **Section 1.2.2.2**). Therefore this topic is divided into the following two sections which discuss the mechanisms of increased rate of chemical and biological reactions: 1.2.2.1 The Sonochemistry of Cavitation and 1.2.2.2 Enhanced Biocatalysis.

1.2.2.1 The Sonochemistry of Cavitation

The term 'sonochemistry' was introduced in 1953 by Weissler to describe the chemical and biological effects produced by ultrasonic waves. **Section 1.2.1.4** describes the physical effects of cavitation and factors that influence the onset and extent of cavitation and mathematically describes the mechanisms of all forms of cavitation.

It is universally accepted that the immense temperatures and pressures developed in "hot spots" of imploding microbubbles are the main cause of sonochemical effects, and that the extreme conditions provide a unique catalytic environment. In water the effect of cavitation is to decompose the H_2O molecule forming extremely reactive protons (H^+) and hydroxyl radicals (OH^-). These radicals can recombine, as the local "hot spot" is instantly cooled, to form hydrogen peroxide

(H_2O_2) and molecular hydrogen (H_2). Evidently when other chemicals are added to the water, cavitation can support a wide range of reactions.

Organic liquids also yield interesting reactions. For example, crude oil can be "cracked" into smaller compounds at room temperature (the normal process requires temperatures in excess of 723 K [Suslick (1989)]). Ultrasonic cavitation can also produce chemicals that cannot be synthesised by simple heating or chemistry. For example the action of heat and ultra-violet light on iron pentacarbonyl $Fe(CO)_5$ yield pure iron and $Fe_2(CO)_9$ respectively whereas ultrasonic cavitation yields the unusual product $Fe_3(CO)_{12}$ as a product.

Langevin (1917) was probably the first to produce ultrasound at intensities sufficient to induce cavitation. It was noted that millions of minute bubbles were produced in the path of the ultrasound, killing small fish that swam through, and giving the impression that the bones of ones hands were being heated (later proved to actually be the case).

The biological effects of cavitation were examined by Wood and Loomis (1927) who noted the following phenomena:

- Rupturing of red blood cells.
- Death of unicellular organisms.
- Harmful to lethal effects on small fish, frogs and mice.
- The internal heating of liquids and solids.
- The formation of emulsions and fogs.
- Preliminary observations on chemical reactions and crystallization.

In the late 1920's and early 1930's substantial research was carried out on the biological effects of cavitation and ultrasound in general; the majority of which was guided towards lethal or harmful effects. Although it was noted that ultrasound and cavitation in particular could increase the rate of chemical reactions, interest diminished and little work was carried out in the area in the following forty years.

Interest was rekindled in the early 1970's by the medical use of ultrasonic imaging equipment and the fear of possible hazardous side-effects. Abdulla *et al* (1972) studied the effect of ultrasound on the chromosomes of lymphocyte cultures.

The intensities used were equivalent to those used in medical equipment (0.5 – 35 $kW.m^{-2}$). No damage was detected in the chromosomes and there was no mention of other forms of damage even after eight hours sonication at 35 $kW.m^{-2}$. However under these conditions no cavitation of any nature was reported to have been present in the test cultures.

The sonochemical yield of cavitation centres was examined by Coakley and Sanders (1973). By using solutions of potassium iodide, carbon tetrachloride and starch in water, cavitation events were made visible by the appearance of a blue spot or streak caused by the release of iodine. This method also allowed the total yield to be easily measured by taking optical density measurements. It was found that the yield varied with sound intensity, the number of cavities produced, the type of cavity and the life span of the cavities. Similar experiments performed on the same chemical reaction by Cum *et al* (1992) show that there is an optimum ultrasonic frequency that is capable of driving the chemical reaction to its maximum yield. The optimum frequency for the oxidation of iodine ions to iodine was found to be 60 kHz. The authors suggested that at the optimum frequency rectified diffusion shifted the size distribution of the micro bubbles present in the liquid towards a different range where transient cavitation could occur and hence increase the yield of the reaction.

A review of the recent research into the biological effects of cavitation was conducted by Nyborg (1973) who found that information on the effects of cavitation in tissue was scarce compared with that of the effects on suspensions of cells and molecules. With the dramatic increase in the use of ultrasound in medical imaging this situation has changed somewhat in the intervening years. Nyborg (1973) also researched the effects of single resonating bubbles in suspensions of red blood cells, noting the release of haemoglobin during irradiation. He also determined a direct relationship between release and the amplitude of vibration of the bubbles.

The use of ultrasound in physiotherapy and wound healing led Webster *et al* (1980) to study the role of cavitation in the stimulation of collagen synthesis in human fibroblasts. It was found that synthesis was enhanced only when cavitation was present. Graham (1980) and his colleagues studied cavitational bioeffects at 1.5 MHz. Observations were made on the retardation of plant root growth: which was found not to be a direct result of cavitation but probably due to the resonance of air pockets in

the roots themselves (a process later described by Nyborg). They also researched cell death and DNA degradation in bacteria, finding that bacterial cells were killed before cavitation was sufficiently intense to rupture the cell membranes. It was discovered that the DNA strands were detached from the cell membranes thus deactivating the cells. Further sonication however, caused the DNA strands to break.

Polymerisation is initiated by ultrasonic cavitation. Dupont *et al* (1983) initiated the polymerisation of pure methyl methylacrylate and pure styrene under certain conditions, 20 – 75 watts (undefined power) but an unspecified frequency. It had previously been believed that both small amounts of the polymer and contaminating agents were required for polymerisation to occur. These results effectively disproved this. Substantial research continues in this area particularly in the area of control of molecular size and hence polymer characteristics.

1.2.2.2 Enhanced Biocatalysis through Microstreaming

Ultrasound has long been known to increase the rate of certain chemical reactions. It is widely accepted that such increases are caused by the processes of cavitation and the extreme conditions of temperature and pressure in the 'hot spots' caused when the cavities collapse inwards (See **Figure 1.1,** [Suslick, (1990)]). In the case of biological systems cavitation is largely associated with cell disruption and protein denaturation for which purpose ultrasound has wide spread use.

High intensity sound waves in liquids and gases are also accompanied by stationary (time independent) flows known as acoustic streaming (also 'acoustic wind' or 'quartz wind'). These flows occur either in a free non–uniform sound field or, particularly, near solid or gaseous obstacles immersed in a sound field. These flows are always of a rotational character. There are three types of streaming known to date:

- Streaming in a viscous boundary layer near obstacles in a sound field (sometimes known as micro streaming). Under the influence of a sound wave the stationary flows in a boundary layer have a rotational vortex character. The scale of the boundary vortices is, as a rule, determined by the thickness of the acoustic boundary layer, and their dimensions are much smaller than the ultrasonic wavelength. See **Figure 1.2** and **Figure 1.5**.

- Streaming outside the boundary layer. The vortex scale in this case is considerably larger than the scale of the boundary layer vortices. One form of this type of streaming has been investigated by Rayleigh (1948), namely the two dimensional flow between two plates (or in a cylindrical tube) under the action of a stationary wave; the vortices in this case have a scale equal to the acoustic wavelength. See **Figure 1.3**.

- Streaming in a free non-uniform sound field in which the inhomogeneity scale of the sound field is much larger than the ultrasonic wavelength. Eckart (1948) was the first to solve the problem of the flow generated in a confined volume by a well collimated sound field ie. where the transducer dimensions are greater than the ultrasonic wavelength. The vortex scale of this streaming is determined by the volume of fluid and greatly exceeds the ultrasonic wavelength. See **Figure 1.4**.

Microstreaming, which perturbs the boundary layer, does much to explain a number of observed effects involving the acceleration of transport processes under the influence of sound waves.

Chetverikova *et al* (1985) and Schmidt *et al* (1987) examined the effects of ultrasound on solutions of purified enzymes and enzymes immobilized on inert carrier particles. Chetverikova *et al* (1985) found that ultrasonic intensities far too low to produce cavitation could increase the activity of certain enzymes but only when they were immobilized on inert particles. Schmidt found that the maximum activity increase achieved in experiments on immobilized enzymes was more than 200%. This increase in activity could be attributed to a reduction in the thickness of the static boundary layer surrounding the inert particle thus facilitating a more rapid diffusion of substrate and product to and from the enzyme molecule. However a number of issues were raised by the results:

- The ultrasonic effect was dependent upon the molecular weight of the substrate. The larger the molecule the more pronounced the effect. This may be due to the dominance of diffusion effects at large molecular weights.
- The effect increased with increasing inert particle diameter.

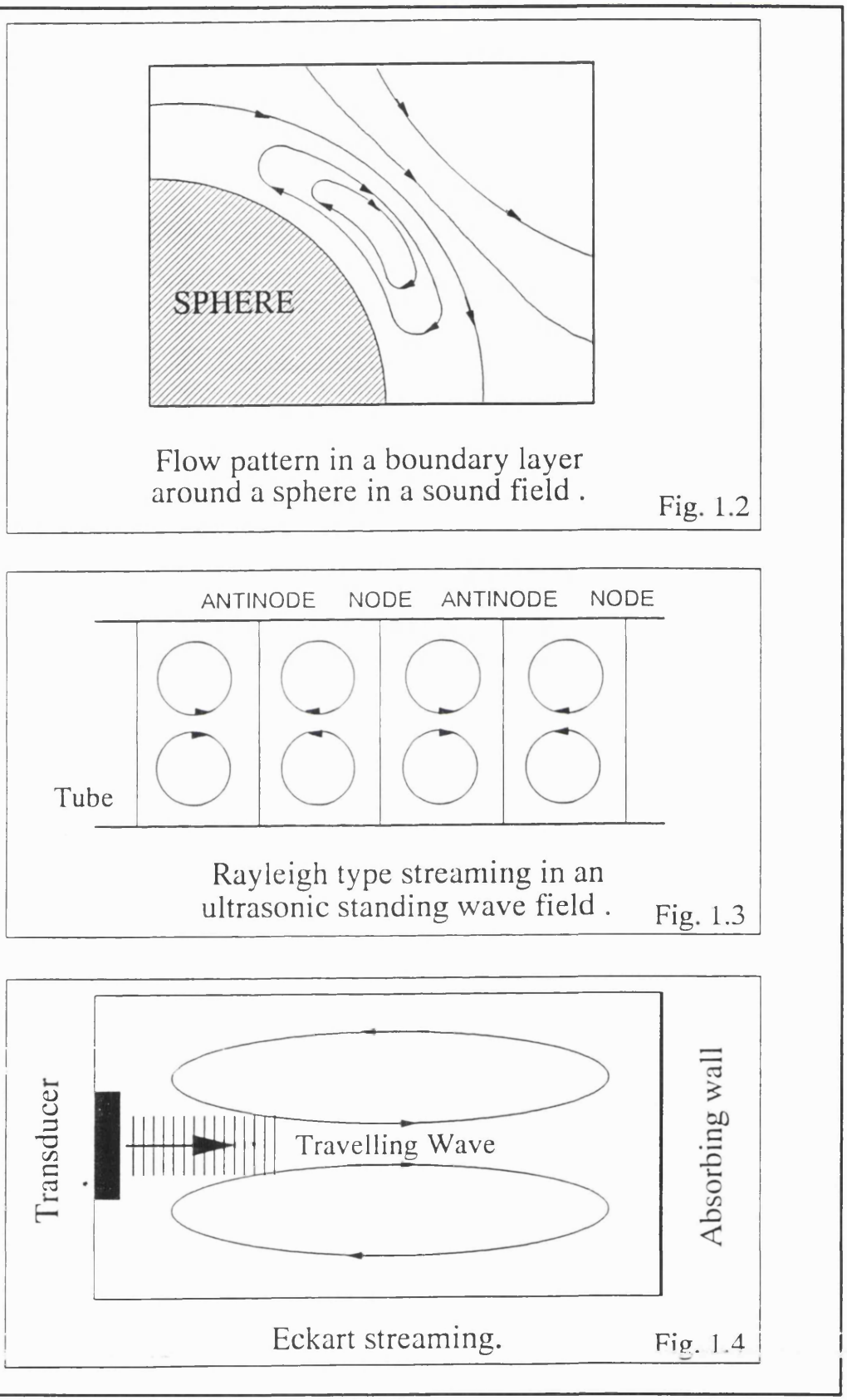

Figures 1.2 to 1.4 *Forms of Acoustic Streaming Found in Ultrasonic Wave Fields.*

- The effect increased with decreasing substrate concentration.
- The effect decreased with increasing fluid flow rate.
- In the ultrasonic field, a decrease of the apparent rate constant values and the apparent activation energies was observed.
- The effect increased with the square of the sound frequency and decreases with the viscosity of the medium.

A comparison of the effect of ultrasound on a cell catalysed reaction (the oxidation of cholesterol by *Rhodococcus erythropolis*) and the same enzyme catalysed reaction was conducted by Bar (1988). The microbial slurry was irradiated for five seconds every ten minutes at approximately 21 $kW.m^{-2}$. This intensity and duration of irradiation caused no cell disruption or loss of viability. The rate of conversion of cholesterol was greatly increased by sonication, whereas the ultrasound had no effect on the enzymatic conversion of cholesterol. The effect of sonication decreased with increasing cholesterol concentration.

Increases in the rate of cholesterol conversion were attributed to a reduction in the thickness of the boundary layer around the cell (or an enhancement of mass transfer across the boundary layer due to vortex motion), and also, to an enhancement of mass transfer across the cytoplasmic membrane and cell wall of the bacteria. This phenomena has often been termed 'phonophoresis', a process whereby ultrasound facilitates the penetration of chemicals through membranes [Sanghvi and Banakar (1991)]. Microstreaming of the cytoplasm was also determined to be a possible contributing factor.

1.3 Applications of Ultrasound to Bioprocesses.

1.3.1 Introduction

The application of ultrasound to bioprocesses for the purposes of increasing reaction rates and rates of conversion may be favourable for a number of reasons:

- Ultrasonic radiation is easy to control; it is readily adaptable to computer control allowing accurate timing and power dosage.

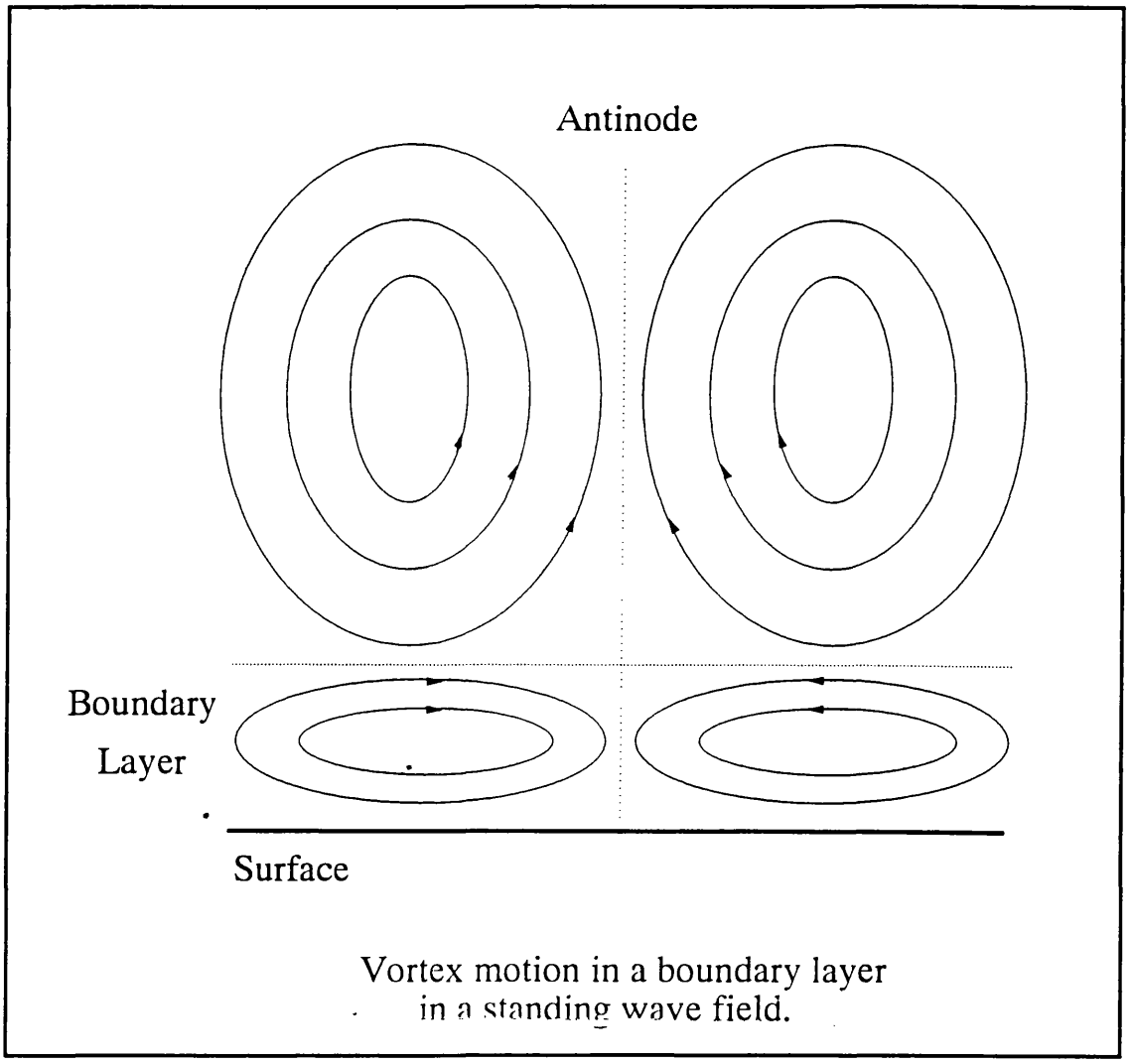

Figure 1.5 *Vortex Motion of Acoustic Streaming in the Boundary Layer Within a Standing Wave Field.*

- Systems can be designed that are non-invasive and robust; transducers can be separated from the medium and will withstand steam sterilization.

- Ultrasound lends itself to batch and continuous systems with modular units overcoming some of the problems of scale up.

- A single transducer geometry may be capable of performing more than one role.

The application of ultrasound to bioprocesses will now be considered under the following headings which are related to specific ultrasonic phenomena: 1.3.2 Particle Separation In Ultrasonic Standing Waves, 1.3.3 On-Line Analysis, 1.3.4 Flocculation and Precipitation and 1.3.5 Enhancement of Biocatalysis.

1.3.2 Particle Separation In Ultrasonic Standing Waves

It has already been shown that ultrasonic standing waves can be used to fractionate whole blood into red cells and plasma in a continuous system on a small scale [Peterson (1987)]. A suspension of equal concentrations of two different microorganisms has been separated into two suspensions where the number ratio of one organism to the other is 1:80 [Schram (1985)].

Ultrasonic separation techniques are very dependent on particle properties such as diameter, density, shape (or internal structure) and the velocity of sound through the particle (which is related to the hardness of the particle material). These properties of megahertz frequency ultrasonic standing wave fields theoretically enable particles that would be very difficult to separate in a centrifuge, ie those with the same diameter and density, to be effectively separated if they possess differing internal structures and different shapes. For example, whole blood could be separated into two red blood cell fractions (young and mature erythrocytes), plasma, platelets and each type of white blood cell due to their different sizes and structures without subjecting the cells to the high acceleration environment of a centrifuge.

With the development of high power, high frequency ultrasonic (100's of MHz) sources research into the separation of proteins and other macromolecules, at present too small to be manipulated with this method, will be possible. The technique although being limited to an analytical scale due to the high rate of absorption of ultrasound of this frequency would compete with electrophoresis and similar techniques.

1.3.3 On-Line Analysis

The on-line analysis of process fluids such as fermenter broth and protein fractions is essential where effective control systems are to be employed. Accurate measurements made by reliable systems with short response times are required to provide data for the controllers. In this study the use of ultrasonic techniques to remove particles from a liquid stream or concentrate particles ready for analysis will be investigated.

1.3.3.1 Polishing

Two quite different approaches to the production of a clarified liquid sample are possible:

- A batch system for producing a small volume (5 – 10 mL) of polished liquid. This would involve the use of travelling pseudo-standing waves to aggregate and remove particles over a certain limiting size (dependent on the sound frequency, intensity and the rate of travel of standing waves) from suspension, or separate stable emulsions into component liquid phases for example.

- An in-line continuous system for producing a small stream ($\simeq 2\times10^{-8}$ $m^3.s^{-1}$) of clarified liquid suitable for flow injection analysis for example. This would be achieved by passing a laminar flow of suspension through a tubular ultrasonic transducer a few centimetres in length. The axial element of the

flowing liquid would rapidly become particle free and could be collected as shown in **Figure 1.6**.

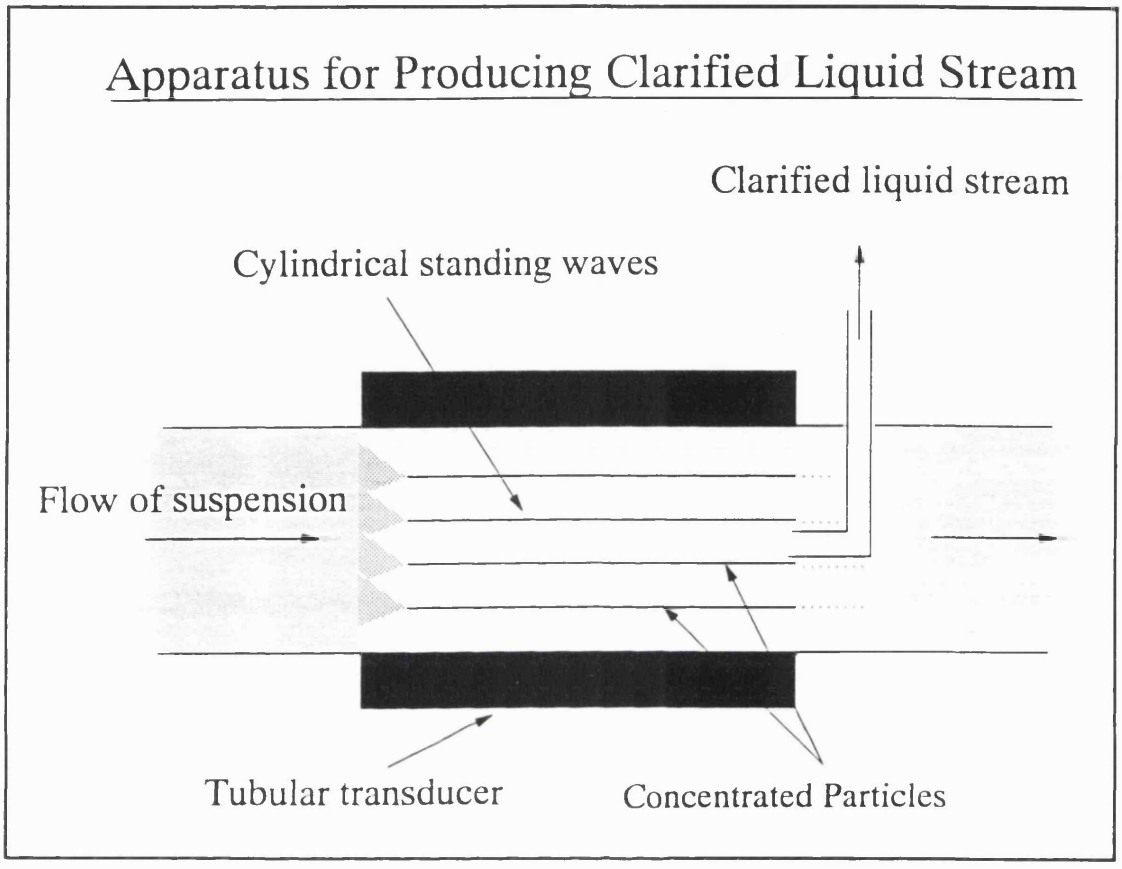

Figure 1.5 *Transducer Apparatus to Produce a Continuous Sample of Clarified Liquid.*

1.3.3.2 Particle Concentration

Ultrasonic separation techniques may be capable of rapidly concentrating a specific fraction of the particles from a known volume of suspension without the problems of fouling and contamination, thus providing a sample for particle size analysis, biomass concentration measurements etc.

1.3.4 Flocculation and Precipitation

The use of ultrasonic standing waves may significantly increase the rate of flocculation of a suspension by causing flocculating particles to come closer together as they accumulate at the nodal planes of the sound field [Kilburn (1989)]. The ultrasonic vibrations will significantly increase the collision frequency of the extremely small primary particles, through the action of covibration of fluid and particle, hence increasing the rate of aggregation of these primary particles to form flocs.

Radiation pressure causes orthokinetic interactions as large particles achieve larger velocities than small particles as they move towards the nodes. Along with this axial process there are attractive forces (Bernoulli's and Bjerknes forces [See **Section 2.3.3**]) in the plane of the nodes and antinodes that cause particles to come into very close proximity with one another when they have come to rest at the nodes of the sound field therefore enhancing any particulate process that is concentration dependent or that relies on particles coming into direct physical contact with one another [Tilley, Coakley, Gould and Payne (1987) and Vienken *et al* (1985)].

1.3.5 Enhancement of Biocatalysis

Most biological particulate systems are subject to mass transfer limitations across liquid boundary layers surrounding the particles. Often mass transfer across these layers becomes the rate limiting step in fermentations and immobilized enzyme systems. Ultrasound causes the liquid in close proximity to an obstacle such as a suspended cell to flow in a vortex motion (**Figure 1.2**). This phenomenon is known as acoustic streaming.

Ultrasonic waves cause acoustic streaming in the static boundary layer around particles and also a reduction in the thickness of the layer due to an increase in the relative fluid velocity. Obviously reducing the thickness of the boundary layer and promoting turbulence within the layer will increase the rate of diffusion of solutes across the layer. Ultrasound can also increase the rate of mass transfer across cell walls, cell membranes and reticulum membranes within the cell. Increased ion,

molecule and macromolecule uptake rate has been reported by several workers [Chapman and Al-Hashimi (1979) and Bar (1988)].

Therefore ultrasonic waves may be used to enhance fermentations and enzyme reactions that are mass transfer limited.

1.4 Aims of Research

This work aims to examine and assess the selective application of megahertz frequency ultrasonic standing waves, in the range of 1 – 10 MHz, as an alternative, non-invasive for achieving the segregation and separation of fine biological particles from liquids without the addition of contaminating reagents.

More specifically the aims of this research are:

- to determine the parameters of importance in determining the segregation of biological particles from liquids using megahertz frequency ultrasonic standing wave fields.

- to experimentally determine the magnitudes and relative importance of these parameters in the application of standing wave fields to the segregation of biological particles – for example the ultrasonic power levels required to effect separation;

- to investigate the application of ultrasonic standing waves in key areas of bioprocessing such as large scale separation and analytical uses;

- in the light of data obtained from experimental results, to provide design criteria for larger-scale continuous solid-liquid separation devices exploiting ultrasonic standing waves.

CHAPTER 2 THEORETICAL CONSIDERATIONS

2.1 Introduction

This chapter covers theoretical aspects of areas of ultrasonics and biochemical engineering that are pertinent to the scope of this thesis. The objective of the chapter is therefore to outline and describe the mechanisms involved in the application of megahertz frequency ultrasonic standing waves to the separation of fine biological particles.

2.2 Theory of Sound Waves.

Harmonic sound waves are used in this research project to effect particle segregation and therefore the following sections briefly define the physical phenomena of sound and develop key expressions for predicting the properties of sound waves.

2.2.1 Introduction

Sound is defined as a mechanical disturbance from equilibrium in an elastic medium (that is, after being disturbed the material will return to its original equilibrium state after the disturbing influence has been removed). Most solids, liquids and gases display such elastic behaviour and can therefore act as sources, transmitters and receivers of sound. Transmission takes place through an elastic medium by means of wave motion where a wave is defined the motion of a disturbance through a medium and is distinct from the motion of the medium as a whole (such a phenomenon is known as vibration).

Most sound waves are transmitted compressional disturbances, that is, disturbances in which the pressure or density at any point in the medium is caused to vary from its equilibrium value (See **Figure 2.1**). The velocity at which a disturbance propagates through a medium is dependent on the type of wave in question and with the nature and temperature of the medium. The most important type of sound waves are harmonic waves.

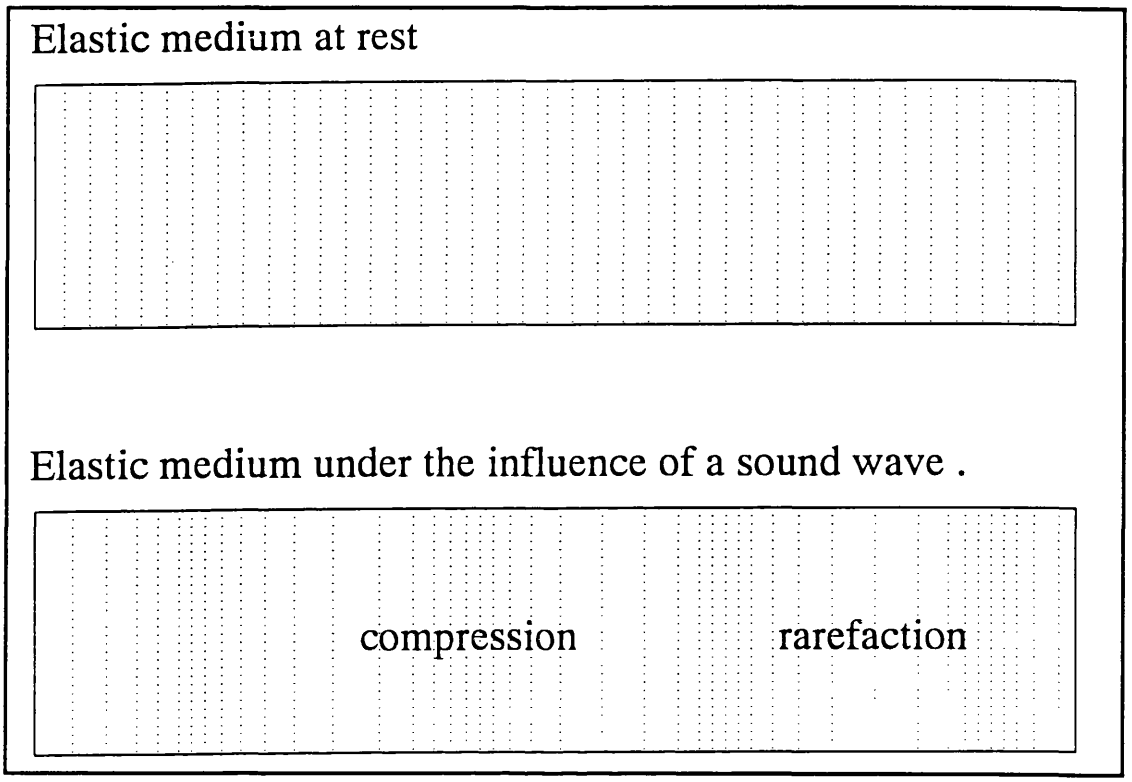

Figure 2.1 *An Elastic Medium Under the Influence of A Sound Wave.*

In a harmonic wave the propagated disturbance at any point in the direction of the wave varies sinusoidally with time and with a definite frequency or number of complete cycles per unit time. The disturbance at any instant repeats itself in magnitude and phase at intervals, along the direction of propagation. This interval is called the wavelength, λ, of the disturbance and is equal to the sound velocity divided by the frequency of the disturbance.

$$\lambda = \frac{c_0}{f} \qquad \textbf{Eq. 2.1}$$

For sound propagated in one direction **z** with velocity **c**, the excess pressure $\mathbf{P_a}$ in the medium due to the wave motion can be represented by an expression of the form described in **Equation 2.2**:

$$P_a = h(z - ct) \qquad \textbf{Eq. 2.2}$$

Clearly $\mathbf{P_a}$ is a function of the variable **(z–ct)** and hence dependent upon both space and time. The disturbance $\mathbf{P_a}$ at the point $\mathbf{z_1}$ at time $\mathbf{t_1}$ moves to the point $\mathbf{z_2}$ at time $\mathbf{t_2}$ as shown by **Equation 2.3**.

$$h(z_1 - ct_1) = h(z_2 - ct_2) \qquad \textbf{Eq. 2.3}$$

This relationship is only valid when the following equality holds, where a change in position **z** equals the product of the velocity of sound and a change in time **t**.

$$(z_2 - z_1) = c(t_2 - t_1) \qquad \textbf{Eq. 2.4}$$

From **Equations 2.3** and **2.4** it is possible to deduce that the wave moves a distance $(\mathbf{z_2 - z_1})$ in time $(\mathbf{t_2 - t_1})$ with velocity **c**. In order to consider the generalized case in which wave motion can occur in all three spatial dimensions it is necessary to write the equations above in a partial derivative form:

$$\frac{\partial^2 P}{\partial t^2} = \frac{c^2 \partial^2 P_a}{\partial z^2} \qquad \textbf{Eq. 2.5}$$

This is the 'wave equation' and the description of sound propagation through media is essentially the study of the solutions of **Equation 2.5** when generalised to three spacial dimensions.

2.2.2 Harmonic Waves

Under the influence of a harmonic wave any point in time the displacement of an individual element of fluid from its equilibrium position is given by **Equation 2.6**.

$$x = x_{max} \cos(2\pi ft) \qquad \textbf{Eq. 2.6}$$

Differentiation of **Equation 2.6** gives an expression for the elemental velocity

$$u = \frac{dx}{dt} = v_{max} \cos(2\pi ft) \qquad \textbf{Eq. 2.7}$$

where $v_{max} = 2\pi f x_{max}$ is the maximum velocity of the element.

Besides the variation in the position of the fluid element when the sound wave travels through the fluid, there is a variation in pressure. The excess pressure P_a is given by:

$$P_a = P_{max} \cos(2\pi ft) \qquad \textbf{Eq. 2.8}$$

Equations 2.6 and **2.7** are represented in diagram **Figure 2.2**.

The amplitude of the pressure wave is defined as the maximum value of the excess pressure P_{max}.

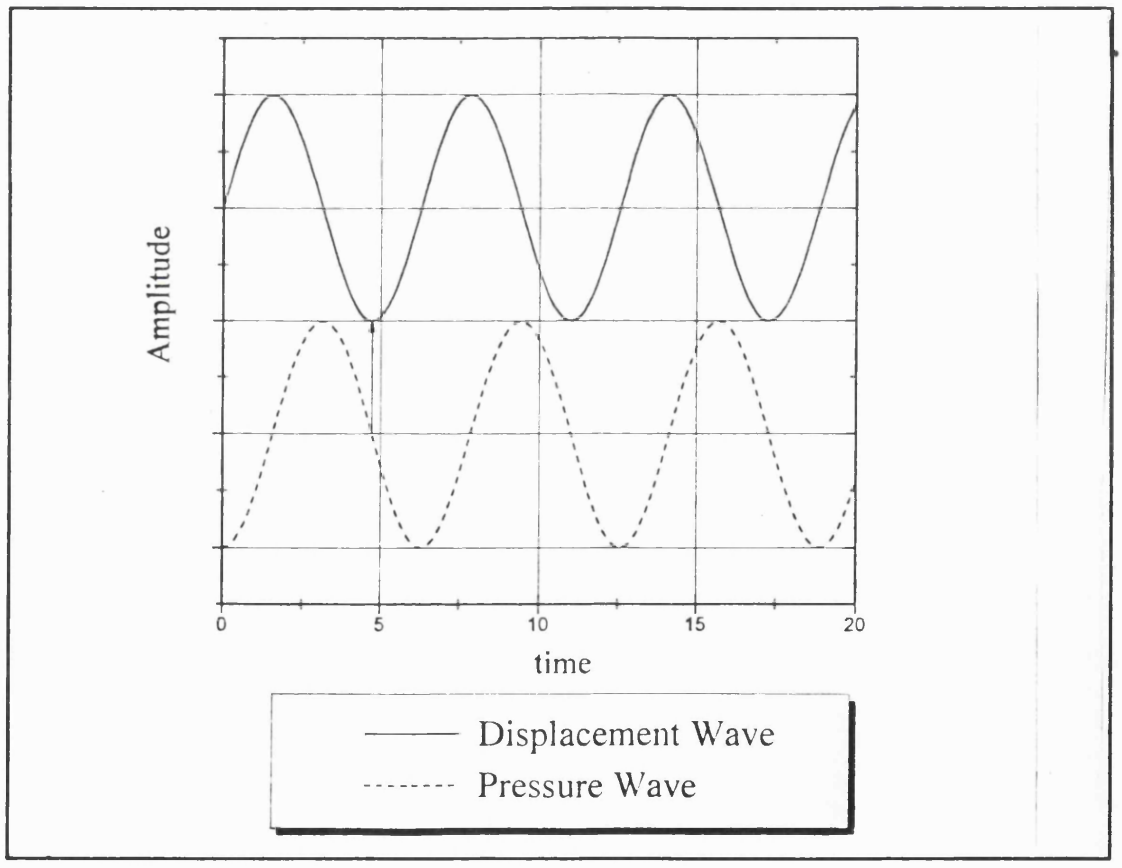

Figure 2.2 *90 Phase Delay Between Vibrational Wave and Pressure Wave.*

2.2.2.1 Intensity of Sound Wave

The intensity of a sound wave is defined as the time average rate of flow of energy per unit time per unit area of the medium through which the wave is passing. It is understood that the area through which the wave passes is perpendicular to the direction of wave propagation. The intensity, $\mathbf{I_T}$, may therefore be considered as the time averaged power transported by the wave. From the principles of mechanics intensity is equivalent to the time average of the product of the fluid element velocity **u** and the acoustic pressure $\mathbf{P_a}$.

$$I_T = \frac{P_{max}^{\ 2}}{\rho_0 c_0} \cos^2[2\pi f(t - z/c_0)] \qquad \textbf{Eq. 2.9}$$

The intensity of a travelling harmonic sound wave in the **z** direction may be calculated using **Equation 2.9**.

As **Figure 2.3** indicates, the intensity of sound waves varies over a wide intensity range. To the normal human ear sound of intensity 10^{-12} W.m^{-2} is audible. However, it is possible to produce intensities as high as 10^{12} W.m^{-2}.

Sound of intensity greater than 10,000 W.m^{-2} is sometimes referred to as macrosonic.

The sound intensities used in the experimental work presented in this thesis will be of the order of 0 to 100 kW.m^{-2}. However the maximum intensity used during experiments will be determined by the cavitation threshold intensity under the experimental conditions (see **Section 1.2.1.5**).

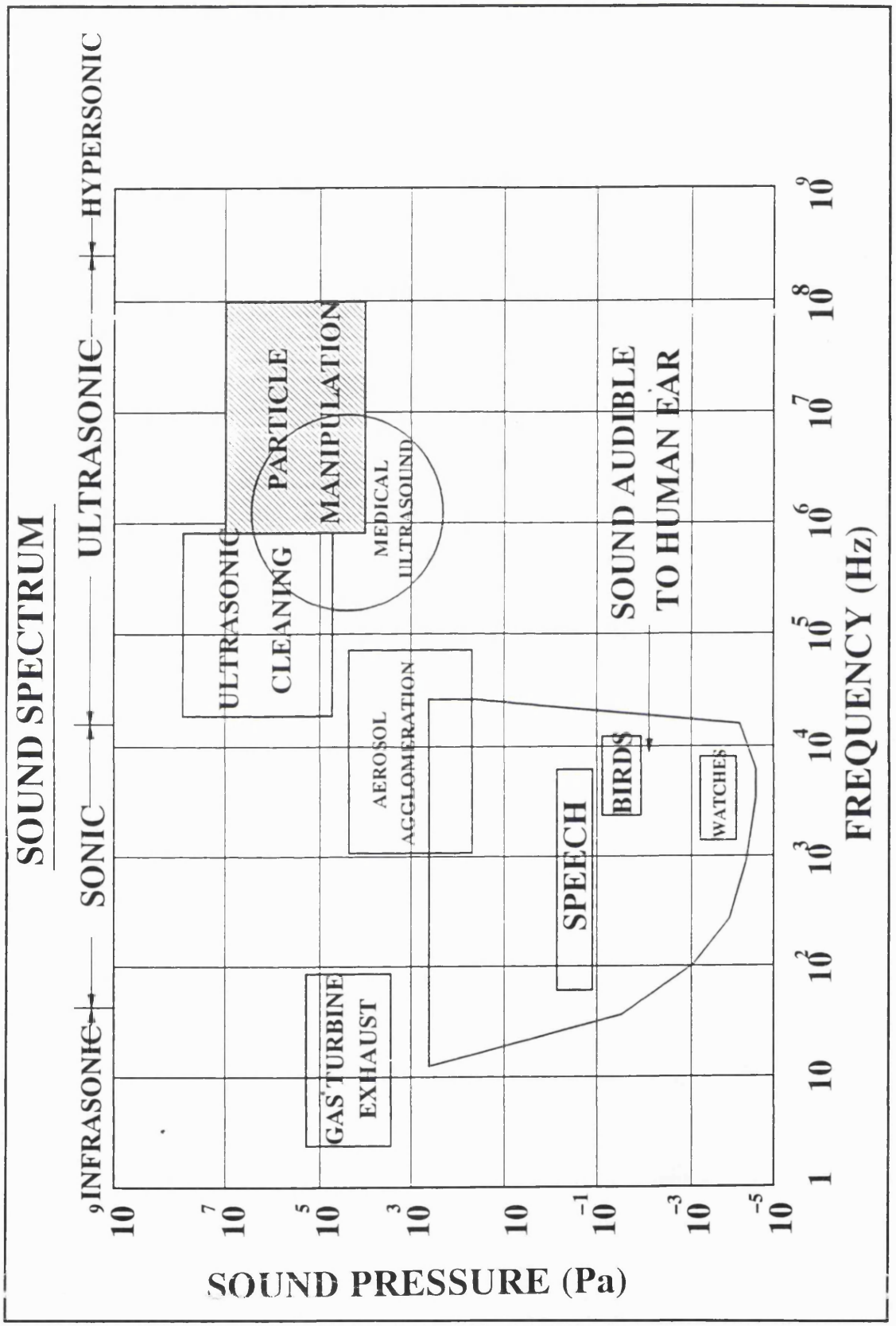

Figure 2.3 *Spectrum Diagram Indicating Region of Sound Frequency and Pressure of Interest in this Study.*

2.2.2.2 Acoustic Properties of Materials

An important property of particles which influences the way in which they respond under the application of ultrasonic energy is the acoustic impedance of the particle material. The acoustic impedance is the product of the material density and the velocity of sound through that material and hence is a measure of the ratio of sound energy that will be reflected from the material to the sound energy that will pass through the material. For particle migration in an ultrasonic standing wave field the relative acoustic impedance of the particles compared to the acoustic impedance of the suspending liquid is important. If the impedances of the liquid and the particle are identical then the sound wave would pass through the particle unhindered and there would be little or no radiation pressure exerted on the particle and hence no particle migration would result.

Table 2.1 lists some important properties of a number of different materials (Williams 1983). It is interesting to note the different properties of liquids, solids and the complex composition of biological particles (red blood cells) that have properties similar to both liquids and solids.

Material	Sound Velocity ($m.s^{-1}$)	Density ($kg.m^{-3}$)	Acoustic Impedance ($kg.m^{-2}.s^{-1}$)	Wavelength at 1 MHz (mm)
Dry Air	331.5	1.293	429	0.33
Water	1497	998	1.49×10^6	1.5
Polystyrene	2670	1050–1100	2.94×10^6	2.67
Aluminium	6420	2710	17.4×10^6	6.42
Stainless Steel (347)	5790	7900	45.7×10^6	5.79
Red Blood Cells (Wladimiroff)	1540–1560	1084–1099	1.71×10^6	1.55

2.2.3 Standing Waves

The sound waves mentioned thus far have been travelling waves, in which by definition, the peaks of excess pressure travel continuously in the direction of propagation. Another form of sound wave which are of prime importance in this work are standing or stationary waves.

Standing waves are formed when a continuous harmonic wave is reflected from a surface normal to the direction of propagation. On reflection the phase of the wave is changed by 180° (π), so that the reflected wave is always 180° out of phase with the incident wave and travelling in the opposite direction. The wave formed as the incident and reflected wave superimpose at a specific instant in time is shown in **Figure 2.5**. At one specific instant in time the waveforms are as shown in **Figure 2.4**.

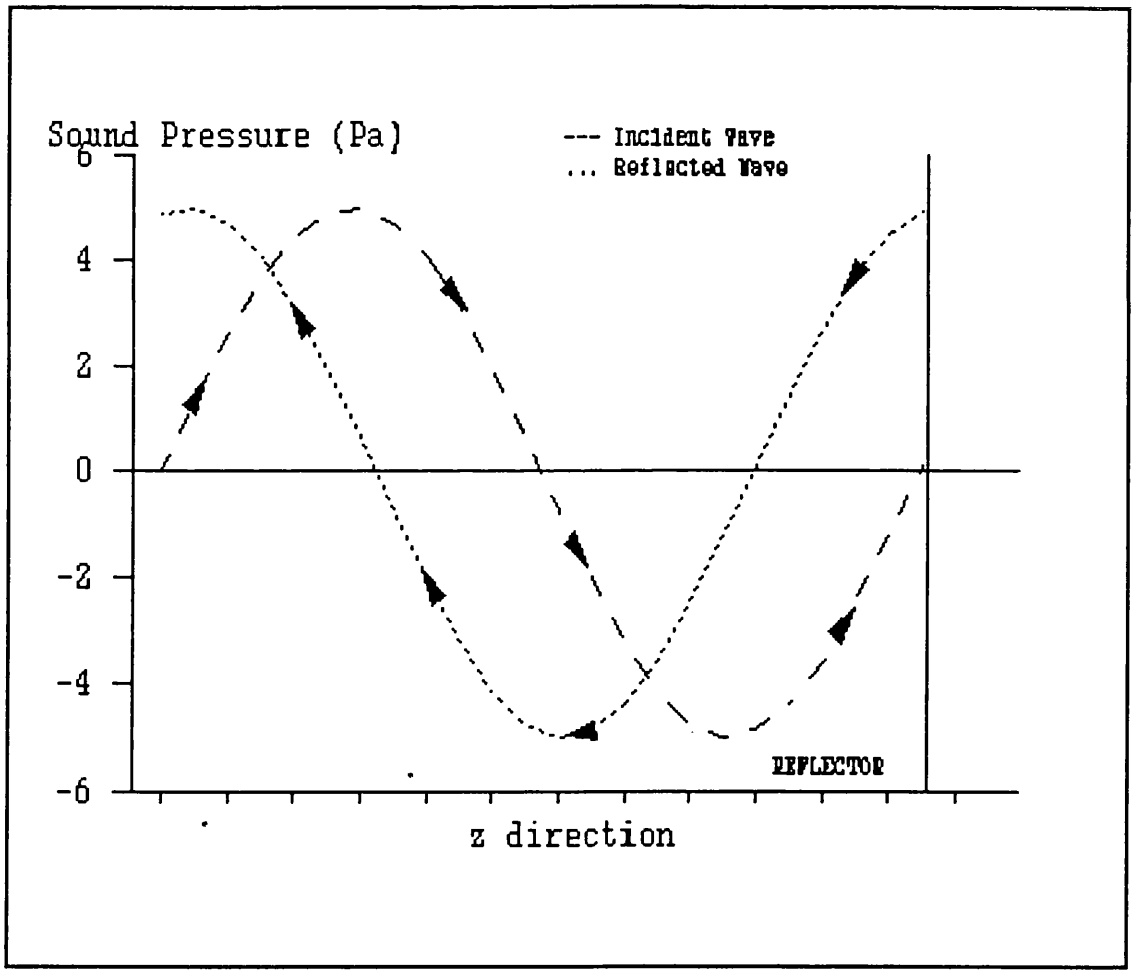

Figure 2.4 *Reflection of a Plane Harmonic Sound Wave Showing 180° Phase Shift on Reflection.*

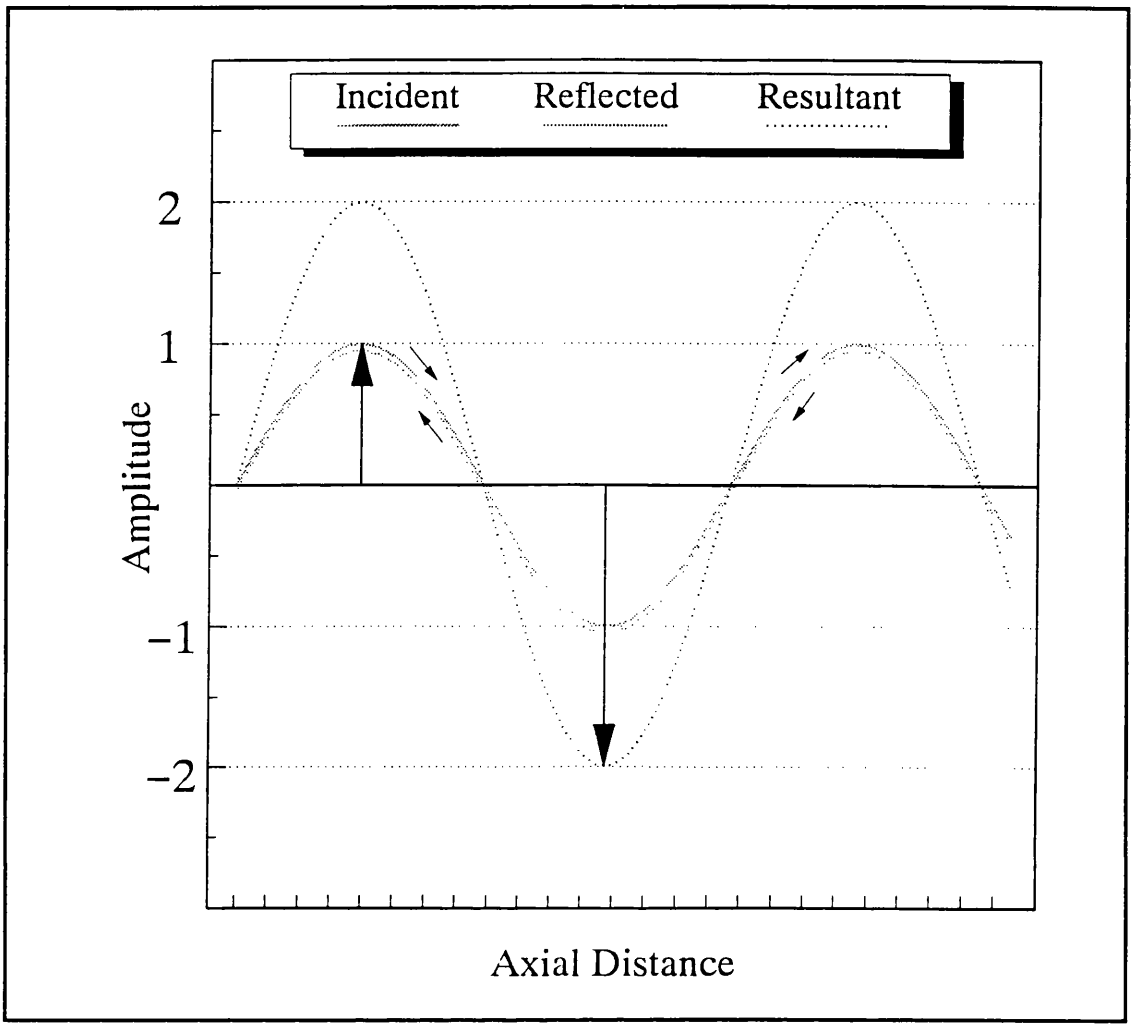

Figure 2.5 *Constructive Interference of Incident and Reflected Plane Harmonic Sound Waves.*

Both the incident and reflected wave are however travelling and hence at some subsequent instant in time a minimum will be obtained at the point X rather than the maximum shown in **Figure 2.5**.

The waveform of a standing wave can be portrayed as in **Figure 2.6**.

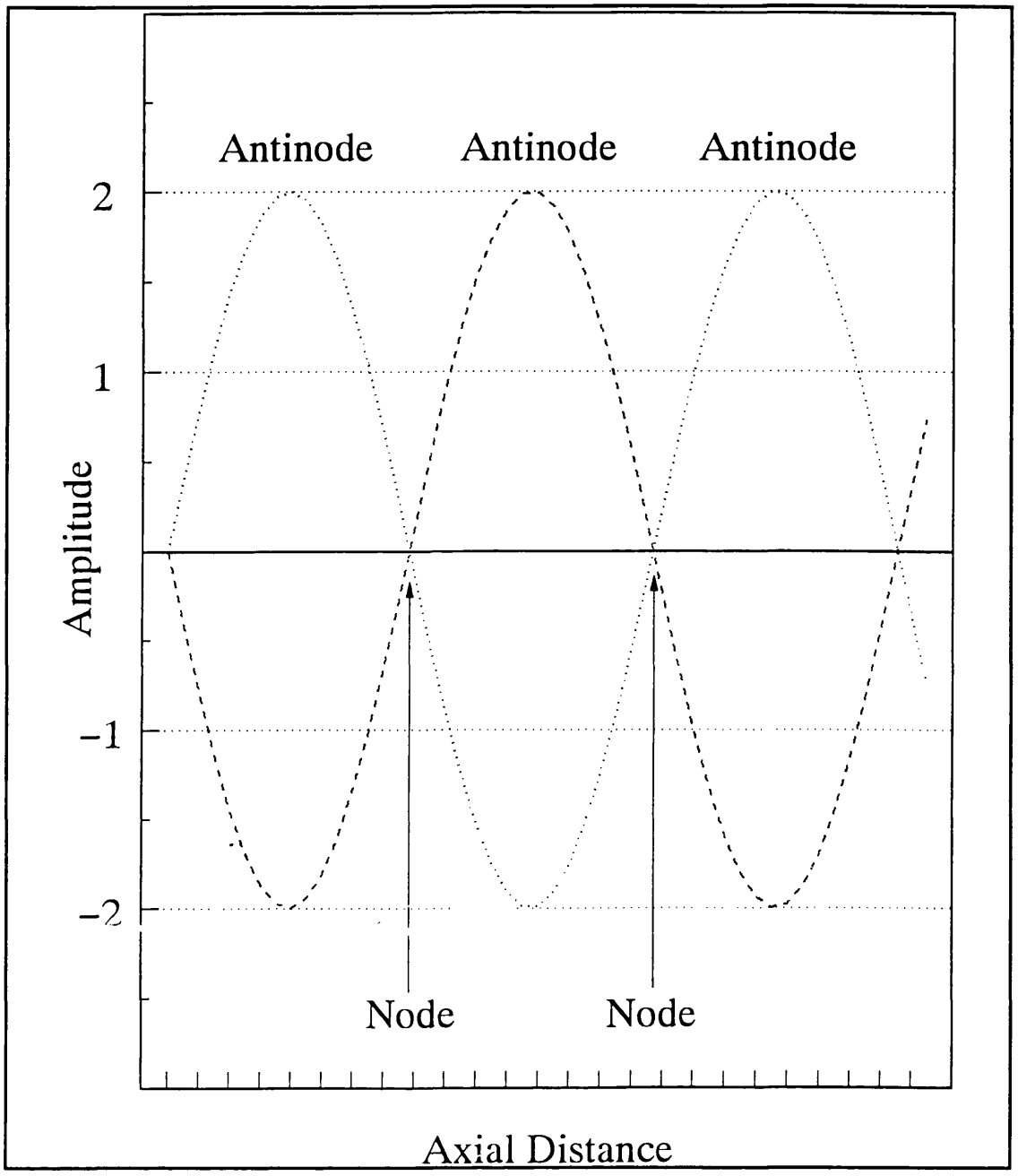

Figure 2.6 *Schematic Representation of a Plane Standing Wave Field Showing Relative Positions of the Nodes and Antinodes.*

A point in the standing wave field where the amplitude of vibration is zero is called a displacement node. Conversely points in the sound field where the amplitude of vibration is maximal are called displacement antinodes or loops. It must be noted that the sound pressure wave is 90° out of phase with the displacement wave and

hence each displacement node is a sound pressure antinode (the point of maximum sound pressure).

Nodes are spaced one half wavelength ($\lambda/2$) apart, as are the antinodes; the distance between a node and an antinode therefore being one quarter wavelength. One additional feature of a standing wave is that there is always a node at the reflector.

If the equation for the incident wave is given by:

$$P_a^i = P_{max}^i \cos[\, 2\pi f^i (t - z^i/c_0)] \qquad \textbf{Eq. 2.10}$$

then the equation of the reflected wave (r) is the same but in the opposite direction and with a phase change of π radians (180°)which gives

$$P_a^r = P_{max}^r \cos[2\pi f^r (t + z^r/c_0) + \pi] \qquad \textbf{Eq. 2.11}$$

Now superimposing the two waves and noting that

$$P_a^r = P_a^i = P_a \; ; \; P_{max}^r = P_{max}^i = P_{max} \; ; \; f^r = f^i = f$$

we obtain:

$$P_a = P_{max}[\cos(2\pi f(t - z/c_0)) + \cos(2\pi f(t + z/c_0) + \pi)] \qquad \textbf{Eq. 2.12}$$

Which rearranges to yield:

$$P_a = P_{max} \sin(2\pi f t).\sin(\frac{2\pi f}{c_0} z) \qquad \textbf{Eq. 2.13}$$

From **Equation 2.13** it is evident that the amplitude of vibration in a standing wave field is twice that of the incident wave. **Equation 2.13** is plotted in three dimensions (amplitude, z direction and time) in Figure 2.7

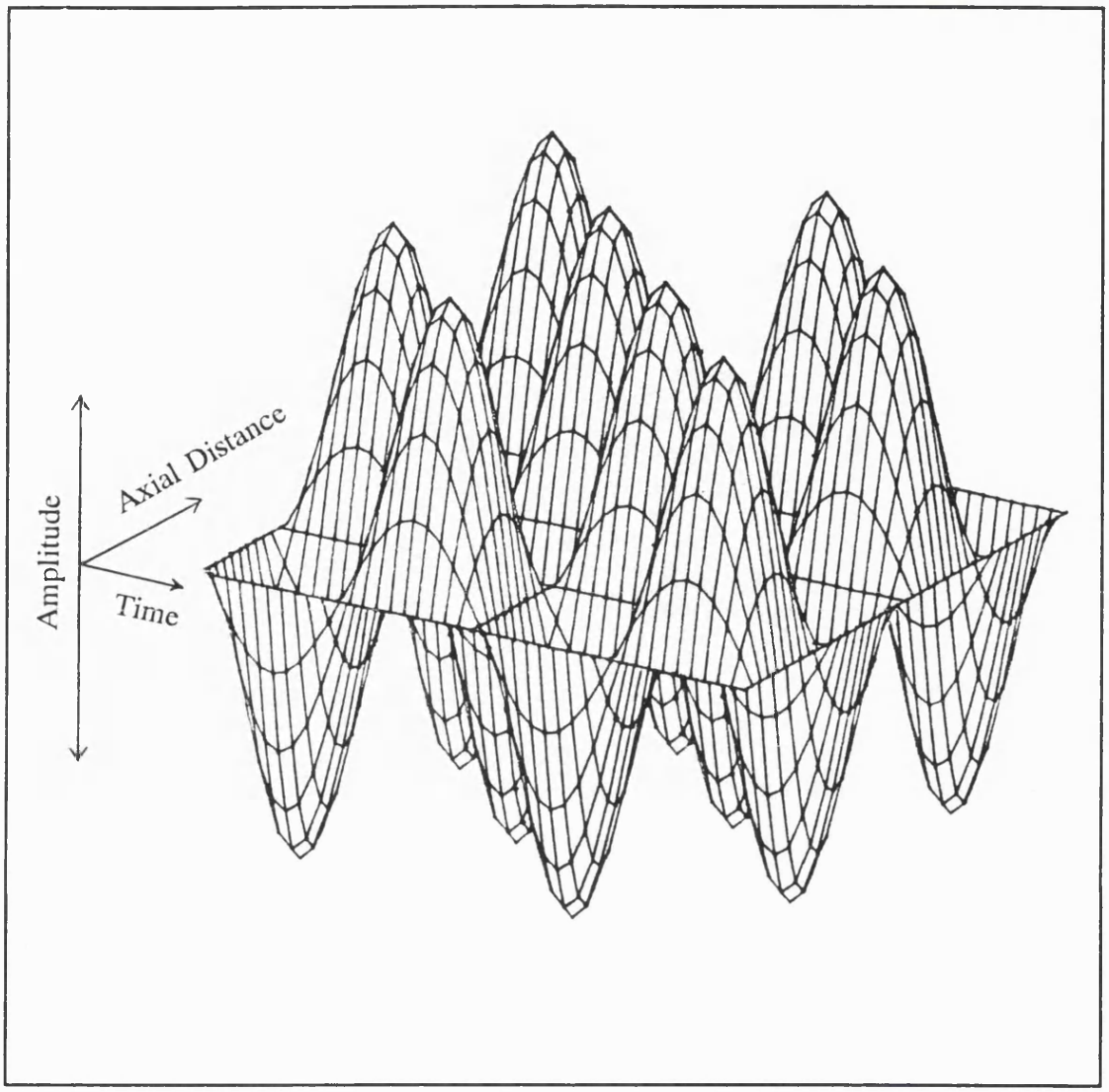

Figure 2.7 *Three Dimensional Plot of Vibration Amplitude as a Function of both Time and Axial Distance from Sound Source.*

2.2.3.1 Intensity and Energy Density of Standing Waves

The sound intensity of a standing wave field is an ambiguous concept as it can only be determined for a specific point in space and time. Furthermore the average sound intensity is equal to zero (in the case of the two sound waves being of equal amplitude and frequency). Thus the concept of sound intensity can only be used realistically in reference to a progressive wave, but for standing waves it is convenient to use the notion of a mean sound energy density which is defined as follows.

At the nodes of a standing wave the velocity is zero and the density of the kinetic energy is also zero, whilst the mean (time averaged) potential energy density is given by:

$$E_p = \frac{P_{max}^2}{\rho_0 C_0^2} \qquad \text{Eq. 2.14}$$

At the antinodes the mean potential energy density is zero whilst that of the kinetic energy equals

$$E_k = 2\,\frac{P_{max}^2}{\rho_0 c_0^2} \qquad \text{Eq. 2.15}$$

Therefore the total mean energy density at any point of the standing wave field is equal to twice the energy density in each of the component waves.

$$\bar{E} = [\frac{P_{max}^2}{\rho_0 c_0^2}\sin^2 \kappa z + \frac{P_{max}^2}{\rho_0 c_0^2}\cos^2 \kappa z] = \frac{P_{max}^2}{\rho_0 c_0^2} \qquad \text{Eq. 2.16}$$

2.2.4 Absorption of Ultrasound

During the propagation of a plane sound wave through a medium the intensity of the wave decreases as the distance from the source increases. The energy in the sound field is lost through viscous and thermal effects occurring on a molecular level. This attenuation of the sound intensity as the wave passes through an elastic medium can be represented as follows:

$$I = I_0 \exp(-2\alpha d) \qquad \text{Eq. 2.17}$$

where $\mathbf{I_0}$ is the initial sound intensity, **I** is the intensity of the wave at a distance **d** from the source and α is the absorption coefficient. The absorption coefficient depends on the nature of the fluid, the temperature of the fluid and the frequency of the sound wave. Mathematical relationships relating the absorption coefficient to frictional losses and thermal conduction losses in liquids have been developed but calculated values are in poor agreement with observed vaiues. However observations have determined that the value of α/f^2, where **f** is the sound frequency, for a given liquid is constant at a given temperature and for water is equal to 2.15×10^{-14} m^{-1}. By substituting this value into **Equation 2.17** the graphical data in **Figure 2.8** may be generated.

It is evident from **Figure 2.8** that when considering the scale–up of processes involving ultrasonic energy the frequency of the sound wave required strictly limits the distance across which the ultrasonic wave can be transmitted effectively. In addition relatively small variations in sound intensity across the sound field ie those caused by the absorption of the ultrasonic wave can cause acoustic streaming (See **Section 1.2.2.2**) that would disrupt the migration of particles to the nodes of the standing wave field.

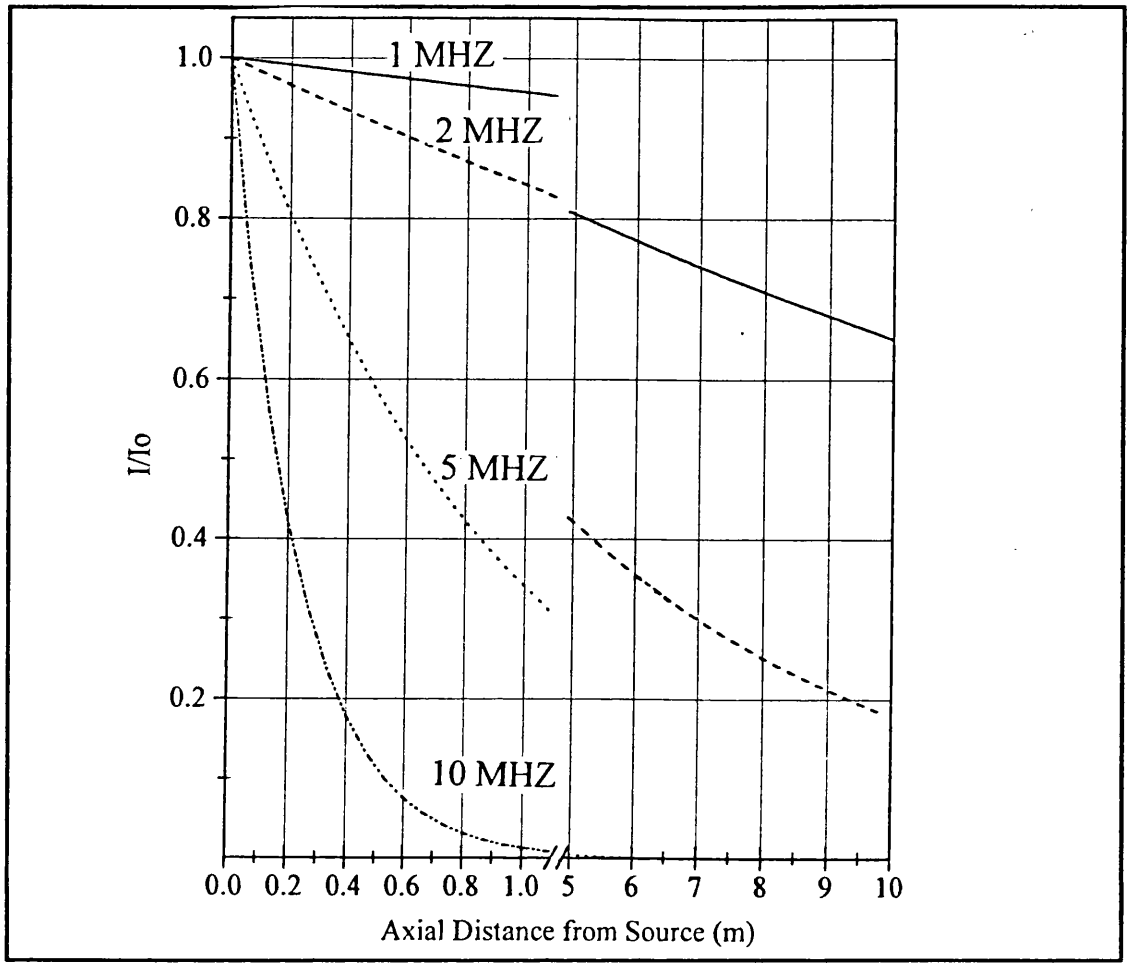

Figure 2.8 *Absorption of Ultrasound as a Function of Axial Distance from Ultrasound Source.*

2.3 Forces on Particles in Standing Wave.

This section describes the forces that exist within an ultrasonic standing wave field in a suspension of particles.

2.3.1 Introduction

There are a number of forces that act upon solid, liquid and gaseous bodies when placed in an ultrasonic standing wave field. Some of these forces act to cause the formation of Kundt's tube striations, others act to prevent their formation.
The following forces are exerted upon single particles in a sound field:

- Radiation Pressure
- Gravity
- Acoustic Streaming Forces
- Hydrodynamic Drag Force

There are also forces present that act between particles:

- Diffusion
- Bernoulli Attraction
- Bjerkne's Force

The following sections consider each of these forces in turn and develop expressions relating them to the parameters of a sound field that can be influenced to achieve the most effective use of the forces to aid in the segregation of biological particles in an ultrasonic standing wave field. The magnitude of each force as experienced by a 6 μm diameter biological particle, of density 1050 $kg.m^{-3}$, suspended in water in a 2 MHz standing wave field with a maximum sound pressure amplitude of 10,000 Pa will be given as being representative of the conditions pertaining in much of the work described in this thesis.

2.3.2 Forces on Single Particles

The following section describes the forces experienced by single particles in suspension in a standing wave field.

2.3.2.1 Radiation Pressure

Radiation pressure is defined as the steady pressure exerted on a surface in a sound field. The radiation pressure acting on a rigid sphere freely suspended in a non-viscous fluid, in travelling and standing waves was first calculated by King (1936). The force due to radiation pressure on a particle of radius a in a plane stationary wave field may be given by **Equation 2.18**

$$F_P = 2\pi a^3 \kappa \sin(\kappa z) J \bar{E} \qquad \textbf{Eq. 2.18}$$

where J is a correction factor for the difference in density of the particle and the fluid.

$$J = \frac{1 + 2/3(1 - \frac{\rho_0}{\rho_1})}{2 + (\frac{\rho_0}{\rho_1})}$$

The predictions of **Equation 2.18** are in close agreement with experiments made in liquid with spheres of very hard materials such as stainless steel. However with softer particles, such as biological materials, the effect of compressibility must be considered.

Yosioka and Kawasima (1955) extended the theory of King to include particle compressibility. The modified expression for the radiation pressure is given in **Equation 2.19** .

$$F_P = \frac{2\pi^2 f a^3 P_{max}^2 F \sin(2\kappa z)}{3\rho_0 c_0^3} \qquad \textbf{Eq. 2.19}$$

Where **F** is a correction factor which accounts for the effect of particle compressibility.

$$F = \frac{\nabla + (2/3(\nabla - 1))}{1 + 2\nabla} - \frac{1}{3\nabla\sigma^2} \qquad \textbf{Eq. 2.20}$$

and

$$\nabla = \frac{\rho_1}{\rho_0} \qquad \sigma = \frac{c_1}{c_0}$$

The subscripts 0 and 1 refer to the fluid and particle properties respectively.

As can be deduced from **Equation 2.19** the radiation pressure exerted on a spherical particle is proportional to the particle radius cubed and therefore the

migration of particles in a standing wave field is strongly dependent on the particle size and decreases rapidly with a reduction in particle diameter. In comparison the radiation pressure is only linearly proportional to the frequency of the sound field.

The magnitude of the force radiation pressure force as described by **Equation 2.19** exerted on a typical particle under the conditions specified in **Section 2.3.1** is approximately 1.05×10^{-14} N.

2.3.2.2 Hydrodynamic Drag Force

Hydrodynamic drag forces act on particles suspended in a viscous fluid and arise as a result of relative fluid–particle motion. Stokes (1851) derived an expression, to account for this drag force, F_D.

$$F_D = 6 \pi \mu a u \qquad \textbf{Eq. 2.21}$$

where **u** is the velocity of the particle of radius **a**. This equation only holds true when the modified Reynolds Number Re′ for the particle, as defined below, has a value of between 0.001 and 0.2.

$$Re' = \frac{2au\rho}{\mu} \qquad \textbf{Eq. 2.22}$$

This range of Re′ values is consistent with the range of particle diameters and fluid velocities encompassed by the experimental work of this thesis.

Plots of the hydrodynamic drag force and radiation pressure exerted on a particle as a function of both particle diameter and ultrasonic energy density in a standing wave field for the same relative particle–fluid velocity (or relative node/fluid velocity) are shown in **Figure 2.9**.

At low particle diameters and sound energy densities the hydrodynamic drag force is of greater magnitude than the radiation pressure exerted on the particle. Under these circumstances particles would be carried through a standing wave field with the flow of liquid with possibly only a slight decrease in the velocity of the particle as it is 'delayed' by the forces acting at the nodes of the sound field. The intersection of the

two curves which represents the point at which the two forces are of the same magnitude and this theoretically predicts the conditions of fluid velocity and ultrasonic energy density that are required for the particles to be held stationary at the nodes of the sound field against a flow of liquid (See experiments in **Section 6.5.5**).

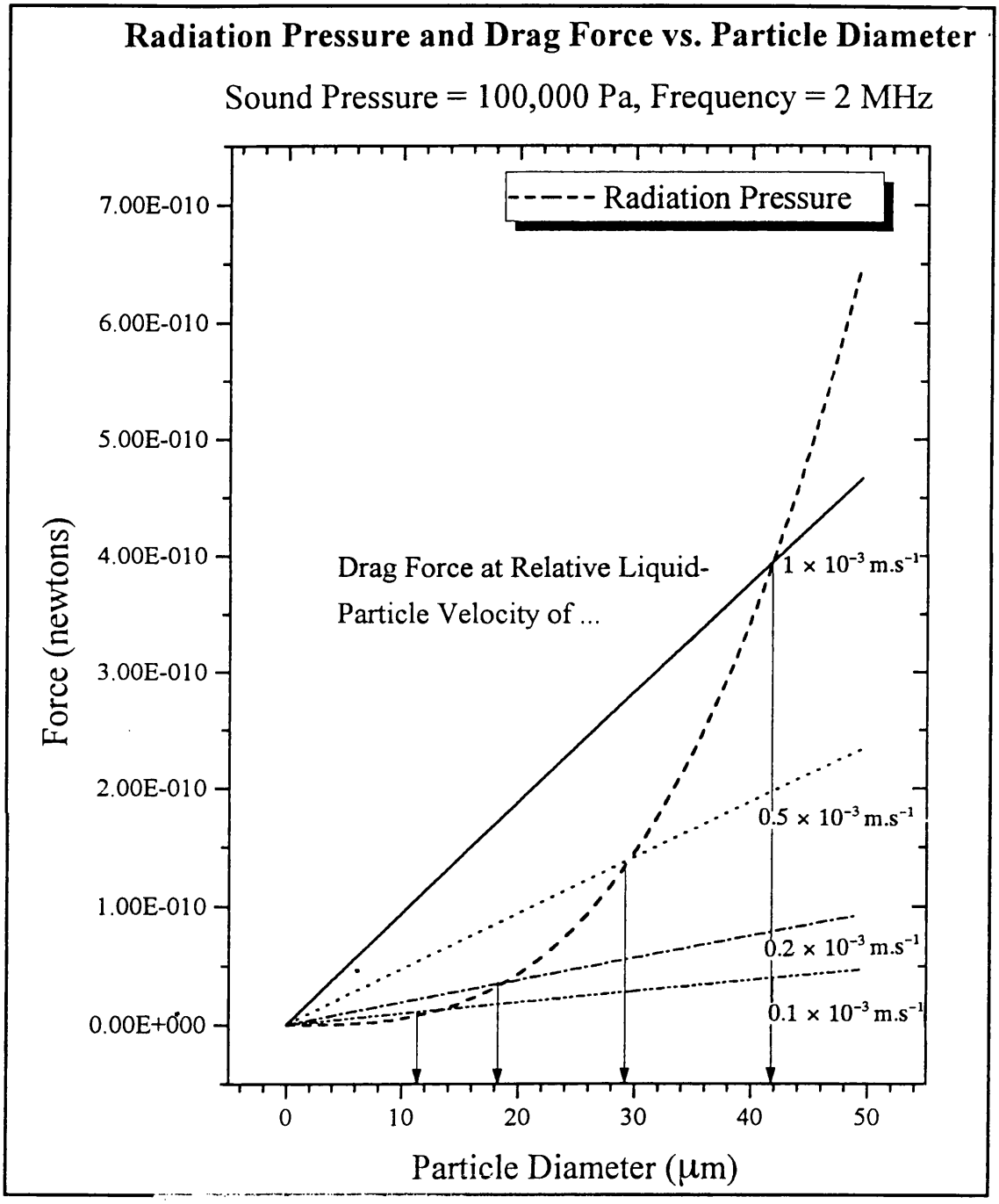

Figure 2.9 *Plot of Hydrodynamic Drag Force and Radiation Pressure on a Particle Versus Both Particle Diameter and Sound Pressure, for the Same Relative Fluid Velocity.*

2.3.2.3 Force Due to Gravity

Even though the particles under study in this thesis are of very small dimensions it can be shown that the force due to gravity exerted on the particles is of the same order of magnitude as the ultrasonic forces experienced by the particles.

The gravitational force, F_G, on a particle of volume **V** is given by the following:

$$F_G = V(\rho_1 - \rho_0)g \qquad \textbf{Eq. 2.23}$$

where **g** is the acceleration due to gravity and ρ_1 and ρ_0 the densities of the particle and fluid respectively.

For a spherical particle of volume **V** where **Equation 2.23** becomes

$$F_G = \frac{4}{3}\pi a^3(\rho_1 - \rho_0)g \qquad \textbf{Eq. 2.24}$$

The force due to gravity on a 6 μm diameter cell is approximately 5.5×10^{-14} N.

2.3.2.4 Acoustic Streaming Forces

Acoustic streaming is a time–independent flow due to the presence of non–linear effects in a sonicated fluid. The pattern of the flow induced in a channel between two walls, of intermediate to large separation compared to the wavelength of the sound, bordering a standing wave field (Rayliegh type streaming) is shown in **Figure 2.10**. The streaming that is produced is of a vortex nature and is repeated every half wavelength in the direction of propagation of the sound wave.

For liquid in a vertical cylinder of radius **R** the streaming velocity in the axial direction may be taken to be:

$$U_z = [\frac{-3P_{max}^2}{8\rho_0^2 c_0^3}].[1 - 2(r/R)^2] \sin(2\kappa z) \qquad \textbf{Eq. 2.25}$$

where **r** is the radial distance from the axis of the cylinder. Streaming in the radial direction is given by **Equation 2.26**:

$$U_r = [\frac{3P_{max}^2 \kappa r}{8\rho_0^2 c_0^3}].[1 - (r/R)^2]\cos(2\kappa z) \qquad \textbf{Eq. 2.26}$$

The axial streaming velocity is independent of frequency while the radial streaming velocity is linearly proportional to frequency through the term κ, the wave number. The axial streaming velocity has maxima determined by the term $[1-2(r/R)^2]$ at the cylinder axis (**r=0**) and at the cylinder walls (**r=R**), and is zero at **r = 0.7R**. Because the radial streaming velocity depends on the term $r[1-(r/R)^2]$ it has a value of zero at the cylinder axis and at the wall, and has a maximum value at r = **0.57R**. These relationships are shown in **Figure 2.10**.

The force exerted on a particle due to acoustic streaming is dependent on the initial position of the particle with regards to the nodal plane and also with regards to the axis of the sound field. As the streaming is a rotational flow of liquid within the sound field the force exerted on the particle is also dependent on particle properties such as shape and diameter (the force is apparent as a drag force on the particle as the fluid streams past), whether the particle is trapped at a node or free in the internodal space, and therefore the magnitude of the radiation pressure exerted on the particle. These characteristics of acoustic streaming mean that it would be very difficult to determine the exact force exerted by the acoustic streaming on a particle. However it can be said that the rotational flow of liquid may aid the formation of concentrated bands of particles (especially very small particles) by carrying the particles closer to the nodal planes, areas of higher particle concentration, where particle interactions would cause the particles to join the band of particles.

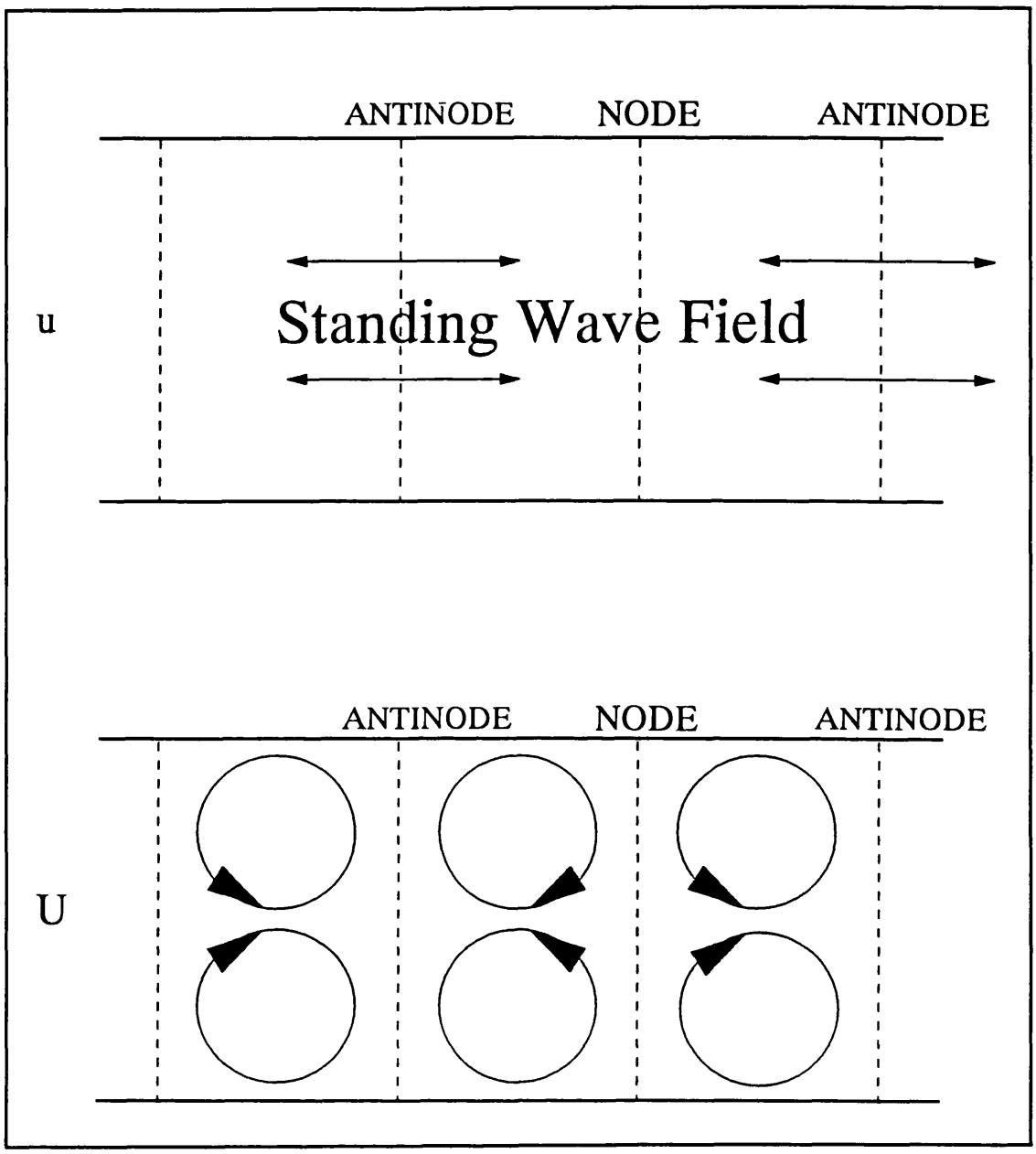

Figure 2.10 *Acoustic Streaming in an Ultrasonic Standing Wave Field.*

2.3.3 Inter-Particle Forces

Particles suspended in an ultrasonic standing wave field experience a number of forces that are a direct result of the interaction of the ultrasonic waves with other particles suspended in the sound field. These inter-particle forces are described in the following section.

2.3.3.1 Bernoulli Attraction

Bernoulli attraction is defined as the force normal to the direction of sound propagation that is generated by fluid flow between two spherical particles of radius **a** separated by a small distance **D**. If the particles are sufficiently large they will not move in phase with the fluid as it oscillates due to the passage of the sound wave. Because of the resultant velocity differential set up between the fluid and the particles there will be an alternating flow of fluid through the space between the two particles. The fluid velocity in the space will be higher than the fluid velocity would have been if the particles had not been present. This increase in fluid velocity leads to a reduction in the fluid static pressure and a corresponding attractive force between the particles according to the Bernoulli equation. It can be shown that the average attractive force F_A acting between spheres of equal diameter (**2a**) is given by :

$$F_A = - \frac{\pi a^6 P_{max}^2}{4 \rho_0 c_0^2 D^4} \qquad \textbf{Eq. 2.27}$$

Typical values of the attractional force between 6 μm diameter biological particles separated by a distance equal to a single particle diameter (ie typical distance between particles when being concentrated in a standing wave field.) are in the region of 4×10^{-14} N.

2.3.3.2 Bjerknes Force

The Bjerknes force is that force exerted on an particle suspended in an ultrasonic stationary wave field due to the compressibility of the particle alone.

The time averaged Bjerknes force, F_B, is most commonly expressed as

$$F_B = [V(t)\ grad\, P_a(r,t)] \qquad \textbf{Eq. 2.28}$$

where **V(t)** is the volume of the particle and **grad** P_a the acoustic field pressure gradient.

This general expression may also be used to calculate the force exerted on an object of radius **a** due to the ultrasonic field re-radiated by another particle in the sound field, provided that $\kappa a \ll 1$ and that the centres of the object are separated by a distance **D** such that $\kappa D \ll 1$.

For the case where the wavelength is sufficiently large that the radius of the compressible sphere **1** is not affected by the pressure field generated by sphere **2** and is the same as that which would result if sphere **2** did not exist, then the change in radius of sphere **1** caused by the original sound wave is given by:

$$a_1(t) = a_1 + \Delta a_1 \sin(2\pi ft) \qquad \textbf{Eq. 2.29}$$

where $\mathbf{a_1}$ is the constant equilibrium radius, and $\Delta\mathbf{a_1}$ is the pulsation amplitude. A similar expression can be derived for sphere **2**.

For the case when the radial position of the particle is much less than a wavelength ($\mathbf{r \ll \lambda}$), so that the re-radiated field of one particle affects another, the pressure field generated by sphere **1** at the site of sphere **2** is given by the **Equation 2.30**.

$$P(r,t) = -[\frac{\rho a_1^2}{r}].[2\pi f]^2 . \Delta a_1 \sin[2\pi ft] \qquad \textbf{Eq. 2.30}$$

For small pulsations the volume of sphere 2 can be expressed as

$$V_2(t) = \frac{4}{3}\pi a_2^3 + 4\pi a_2^2 \Delta a_2 \sin[2\pi ft + \theta] \qquad \textbf{Eq. 2.31}$$

where θ is the phase angle between $\mathbf{a_1(t)}$ and $\mathbf{a_2(t)}$ (and is equal to zero in this case).

To evaluate the pulsation amplitude $\Delta\mathbf{a_1}$ it is necessary to consider the compressibility of the host liquid, β_0, as well as that of the particle, β_1. Hence **Equation 2.31** becomes:

$$V_2(t) = V_0[1 + P_a \sin(2\pi ft).\beta_0(1 - \frac{\beta_1}{\beta_0})] \qquad \textbf{Eq. 2.32}$$

and according to **Equation 2.31**

$$\Delta a_2 = \frac{V_0 P_a \beta_0 (1 - \frac{\beta_1}{\beta_0})}{4\pi a_2^2} \qquad \textbf{Eq. 2.33}$$

Δa_1 is evaluated in the same manner. Substituting and assuming two identical spheres ($a_1 = a_2 = a$) and $\Delta a_1 = \Delta a_2 = \Delta a$, then the Bjerknes force on spheres **1** and **2** is given by **Equation 2.34**

$$F_B = - \frac{\rho_0 (2\pi f)^2 . [V_0 P_a \beta_0 (1 - \frac{\beta_1}{\beta_0})]^2}{4\pi D^2} \qquad \textbf{Eq. 2.34}$$

where V_0 is the volume of a spherical particle. Note that the force is negative and therefore an attractional force between the particles.

2.3.3.3 Diffusion

Particles which are randomly fluctuating with time are acted upon by the following smoothed-out thermodynamic force [Batchelor (1976)]

$$F_{DIFF} = -k_B T \frac{\partial}{\partial z} \ln \psi \qquad \textbf{Eq. 2.35}$$

where k_B is the Boltzmann constant, **T** is the temperature and ψ the probability density function of the particles which closely follows a Gaussian profile. The force is repulsive and therefore hinders the the banding of very small particles (0 - 200 nm diameter) where the radiation pressure exerted on the particles is very small with respect to the diffusional forces.

Both Bjerknes Force and the forces due to diffusion have significant magnitudes when the particles are in very close proximity (distances comparable to

the particle diameter). Therefore the forces are only of importance when the suspension is very concentrated or when the particles form concentrated bands at the nodal planes.

2.3.4 Summary of Forces on a Particle

The previous sections have described the forces that are exerted upon particles in a sound field (listed below). This section discusses the combined effects of these forces upon particles suspended in a standing wave field.

- Radiation Pressure
- Gravity
- Acoustic Streaming Forces
- Hydrodynamic Drag Force
- Bjerkne's Force
- Bernoulli Attraction
- Diffusion

The forces listed above act in a number of different directions with respect to the direction of propagation of the ultrasonic waves. The radiation pressure, according to theoretically ideal conditions, acts solely in the direction of propagation of the ultrasonic waves whereas the Bernoulli attraction is exerted in a plane normal to the axis of sound propagation and is dependent on the relative position of the particles to one another therefore being a function of the particle concentration in the liquid. The diffusion and Bjerknes forces are exerted in more than one direction and are also dependent on the concentration of the particles in the liquid. The forces due to acoustic streaming act in a number of directions depending on position within the standing wave field and, as the acoustic streaming is a liquid flow phenomenon, the forces are manifested as a hydrodynamic drag on the particle in the sound field. The

forces due to gravity and the drag force developed from liquid flow are dependent on the specific geometry of the vessel containing the standing wave field.

The relative magnitude of the forces can be readily determined at the instant of application of the standing wave field. However due to the increase in concentration of the particles caused by particle migration towards the antinodes of the standing wave field and the corresponding change in relative position of the particles it is very difficult to predict the forces exerted on a single particle at a time other than the initial instant of application of the sound waves or the equilibrium state achieved after an infinite period of application of the standing wave field.

2.4 Conclusions

From the preceding sections it is clear that the main force exerted on a particle suspended in an ultrasonic standing wave field is the radiation pressure caused by the impingement of the ultrasonic wave on the particle.

The radiation pressure and the hydrodynamic drag forces exerted on the particles are the only two parameters affecting the separation of particles in a standing wave field that can be varied in a controlled and reproducible manner during experimentation to optimise the efficiency of ultrasonic separation. The radiation pressure can be varied by controlling the ultrasonic energy input and the drag force on the particle can be varied by controlling the fluid velocity within the standing wave field. Gravity, diffusion, Bernoulli attraction, Bjerknes force are parameters that are not subject to direct control in this study and to a certain degree are the forces arising from acoustic streaming. And therefore in this thesis experimentation into the application of ultrasonic standing wave fields to the separation of particles will involve experiments in which the forces exerted on the particles in suspension are varied by controlling the ultrasonic energy density of the standing wave and the fluid velocity within the standing wave field.

CHAPTER 3 MATERIALS AND METHODS

3.1 Introduction

This chapter describes the methods and techniques which are common to the following experimental sections. A number of other experimental procedures are detailed within the relevant sections where they have been applied.

3.2 Measurement of Particle–Supension Properties.

During this study the measurement of particle size and concentration was performed using a number of analyzers each of which employed a different method of measuring particle size and/or concentration. Due to the inherent differences in the measurement mechanisms each of the analyzers could only be applied to the analysis of certain samples and to defined particle size ranges. The following sections briefly describe the mechanism each analyzer employs and discusses the application of the data generated within the context of this study. The density of latex particles was determined using a procedure outlined in **Section 3.2.4**.

3.2.1 Elzone Particle Analyzer

The Elzone instrument (Particle Data Ltd., Unit 2, Goose's Foot Industrial Estate, Kingstone, Hereford, U.K.) uses the electrozone measurement principle to determine particle size distributions and number concentration. During analyses particles suspended in an electrolyte are caused to flow through a small orifice through which is passing an electric current. As a particle travels through the orifice it displaces its own volume of the electrolyte passing through the orifice and therefore causes a sharp change in the level of the electric current which is registered as a single pulse by the instrument. Under suitable conditions of particle concentration the particles travel through the orifice singly, causing electrical pulses at rates between 100's and 1,000's per second depending on the flow velocity, orifice size and particle concentration. The amplitude of each pulse is directly proportional to the volume of the particle as sensed by it's "electrical envelope" displacement within the orifice.

Therefore analysis of the frequency and amplitude of the pulses can be used to determine the particle size distribution and concentration of a suspension.

The limits of detectable particle size are dependent on the diameter of the orifice being used and are between, approximately, 2 and 50 % of the orifice diameter. Orifices are available in diameters ranging from 12 to 1900 μm and therefore accommodate the analysis of a large range of particle sizes. The orifices used during this research were 24 μm and 30 μm in diameter.

One drawback of this analyzer is that the particles must be suspended in an electrically conducting solution of adequate ionic strength to support the passage of the sensing current through the orifice. Reducing the electrolyte strength requires the reduction of the sensing current and subsequent loss of resolution. High electrolytic strength can cause plasmolysis of biological cells and particles (therefore reducing the actual diameter of the particles and delivering a false size distribution) or could cause the denaturation and structural deformation of proteins in solution or suspension. The concentration of the particles in suspension should be low enough to prevent the passage of more than one particle at a time through the orifice (termed coincidence). If two or more particles enter the orifice at the same time the analyzer interprets the resulting pulse as that caused by a large particle of volume equal to the sum of the volumes of the particles in the orifice. A coincidence level of 1% is considered to be acceptable, above this level the results of the particle size distribution analysis indicate the presence of large particles not present in the suspension and therefore the distribution is distorted.

In this study samples were diluted in known volumes of electrolyte solution (isotonic phosphate buffered saline, or 5 – 10 wt% solutions of sodium acetate). Measured volumes (50 μL) of the suspension were automatically drawn through the orifice under a vacuum to enable the concentration of the particles in the suspension to be determined together with the size distribution. For all of the particle suspensions examined in the experimental work of this thesis either a 24 μm or a 30 μm orifice was used for the analyses. These gave detectable size ranges of 0.48 μm to 12 μm and 0.6 μm to 15 μm respectively. All particle size distribution determinations were made as a series of repeated measurements and the particle number concentrations quoted were all found to lie within ± 5 %.

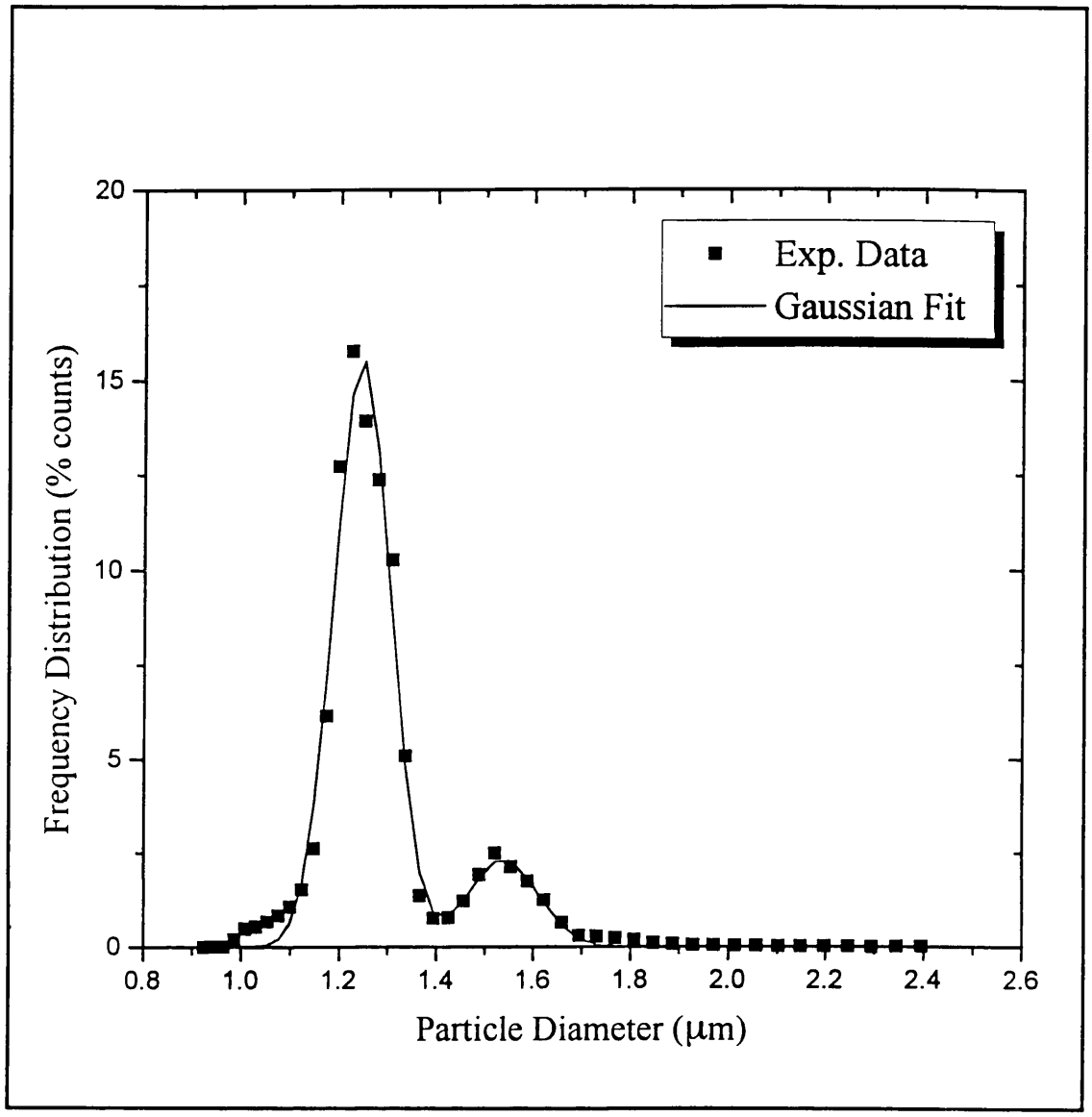

Figure 3.1 *Example of Particle Size Analysis Performed on the Elzone Instrument.*

Figure 3.1 displays the results of a typical particle size distribution analysis performed on the Elzone instrument.

3.2.2 Malvern 4700 Submicron Particle Analyzer

The Malvern Instruments 4700 Submicron Particle Analyzer (Malvern Instruments, Malvern, Worcestershire, UK.) is a dynamic light scattering device that determines the particle size distribution of a dilute particle suspension by measuring the diffusion coefficients of the suspended particles. The diffusion coefficient is

determined by monitoring the intensity fluctuation of laser light scattered by the particles as they move under the influence of Brownian motion. Computerised correlators process this information and present the particle size distribution of the particles in the range of 0.5 to 3,000 nm. The analyzer was used to measure the size distribution of suspensions of particles with diameters below 1,000 nm. Each analysis comprises of ten individual light scattering measurements made by the device, the most representative of which are then used by the correlator to determine the particle size distribution. Repeated analyses of each sample were made to ensure reproducability; the mean particle size determined from each analysis was found to be within ± 3 % at particle diameters above 1,000 nm, rising to ± 5 % for particles between 50 and 500 nm.

The analyzer cannot be used to measure the concentration of the particles in suspension and only provides information on the proportion of the scattered light intensity associated with particles within a certain channel. Therefore if a particle species within the suspension has a greater scattering efficiency than the other particles it will appear that the particle species is present in greater amounts than actually occur.

The vast majority of samples to be analyzed with this instrument need to be diluted many times to reduce the total intensity of the scattered light to the operation levels of the photomultiplier of the analyzer and also to prevent multiple scattering (light scattered by one particle impinges on another particle before entering the analyzer and therefore causes inaccuracies in the resulting distribution).

Particle size analysis can be seriously impaired by the presence of particles larger than the 3,000 nm maximum particle size limit of the analyzer. The presence of the large particles causes the mean size of calculated size distribution to be shifted towards that of the large particles.

Such problems require careful sample preparation prior to analysis and also preclude the analysis of many of the suspension under examination in this thesis. An example of the data generated by the analyzer is displayed in **Figure 3.2** which shows the results of a size distribution analysis on yeast homogenate.

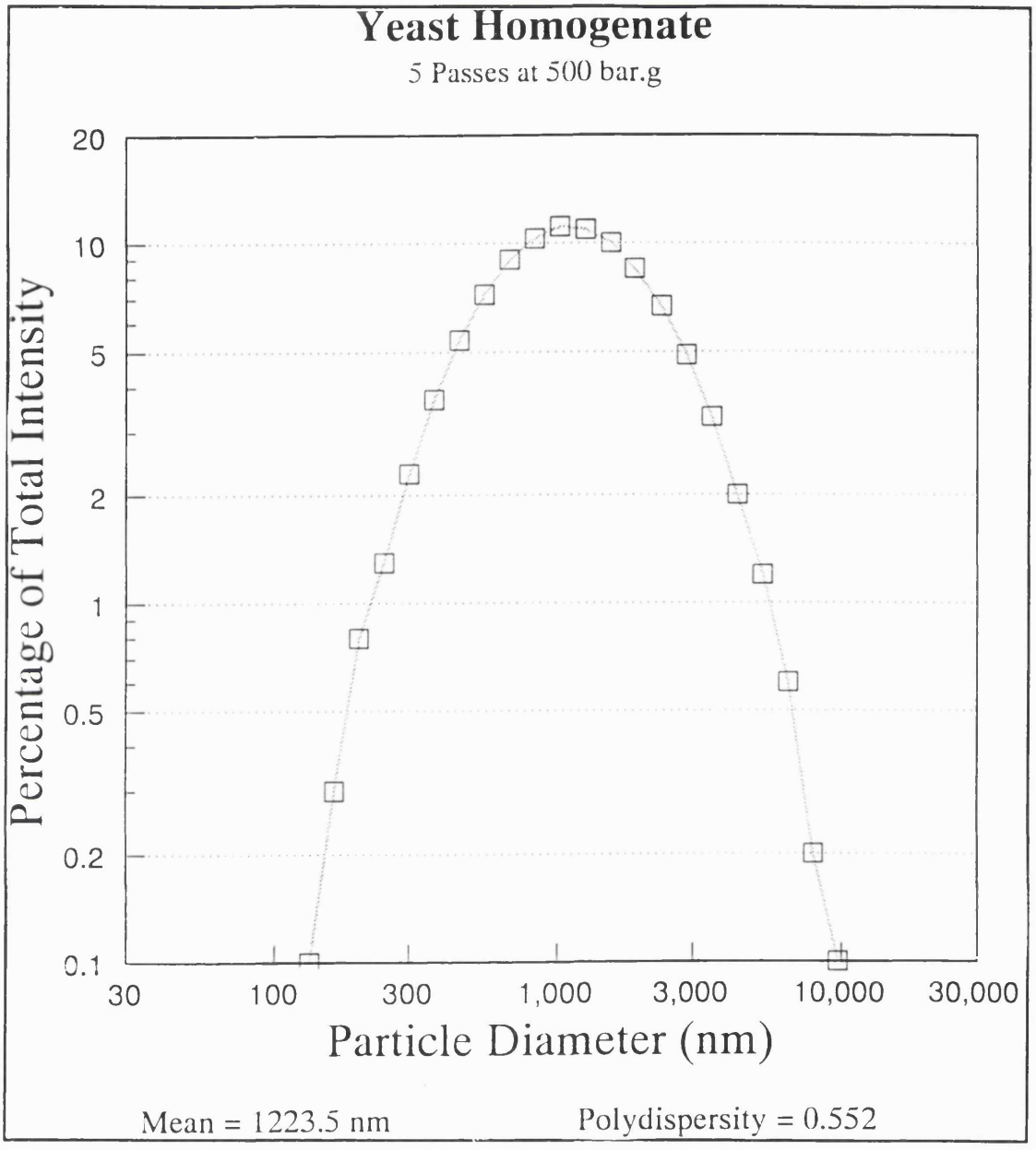

Figure 3.2 *Example of Particle Size Analysis Performed by the Malvern 4700.*

3.2.3 Brookhaven Disc Centrifuge

A disc centrifuge (Brookhaven Instruments Corporation, 750 Blue Point Road, Holtsville, New York, USA) was used to determine the size distribution of particulate samples by the rapid measurement of the rate of centrifugal sedimentation of the particles. In operation the sample to be analyzed is injected onto the surface of a liquid with a density gradient contained within a spinning disc. The density gradient

is formed by the partial mixing of water and a miscible liquid of suitable density (either greater or less than the density of water). A less dense liquid such as methanol can be used to increase the rate of sedimentation of small particles and conversely a solution of sucrose or glucose can be used to reduce the sedimentation rate of larger or more dense particles.

As the particles sediment radially outward through the liquid a distribution is formed depending on the density, shape and diameter of the particles. The particles pass a white light source and a photodetector which measures the light intensity as the particles scatter or absorb the light as a function of time. From this raw data, and *a priori* information entered by the operator, the analyzer estimates the particle size distribution. The properties the estimated particle size distribution are extremely sensitive to the density of the particles involved which must be known accurately before analysis.

The analyzer provides particle size distributions with high resolution (approximately ± 4 nm for the example shown in **Figure 3.3**). Reproducibility is dependent on maintaining a constant spin fluid temperature and in such a case the reproducibility of the mean particle size determined is within ± 2 %.

Figure 3.3 shows an example of the results of particle size analyses obtained performed on the Brookhaven DCP 100.

3.2.4 Determination of the Density of Polystyrene Latex Particles

Many of the experiments conducted during this research required knowledge of the density of the particles involved and this section describes the method employed to determine the density of the polystyrene latex particles used throughout this work.

Solutions of analytical grade Nycodenz [systematic name: 5- (N-2, 3-di-hydroxypropylacetamido)-2, 4, 6-tri-iodo-N, N'-bis(2, 3 dihydroxypropyl) isophthalamide), Nycomed AS, Pharma, Diagnostic Division, P.O. Box 4284 Torshov, N-0401 Oslo 4, Norway] were prepared by dissolving precise weights (0.064 kg and 0.090 kg) of Nycodenz powder in one litre of filtered, deionised water to give two solutions of density 1040 ± 2 $kg.m^{-3}$ and 1060 ± 2 $kg.m^{-3}$ respectively. The density of the Nycodenz solution was determined by two separate methods. A standard

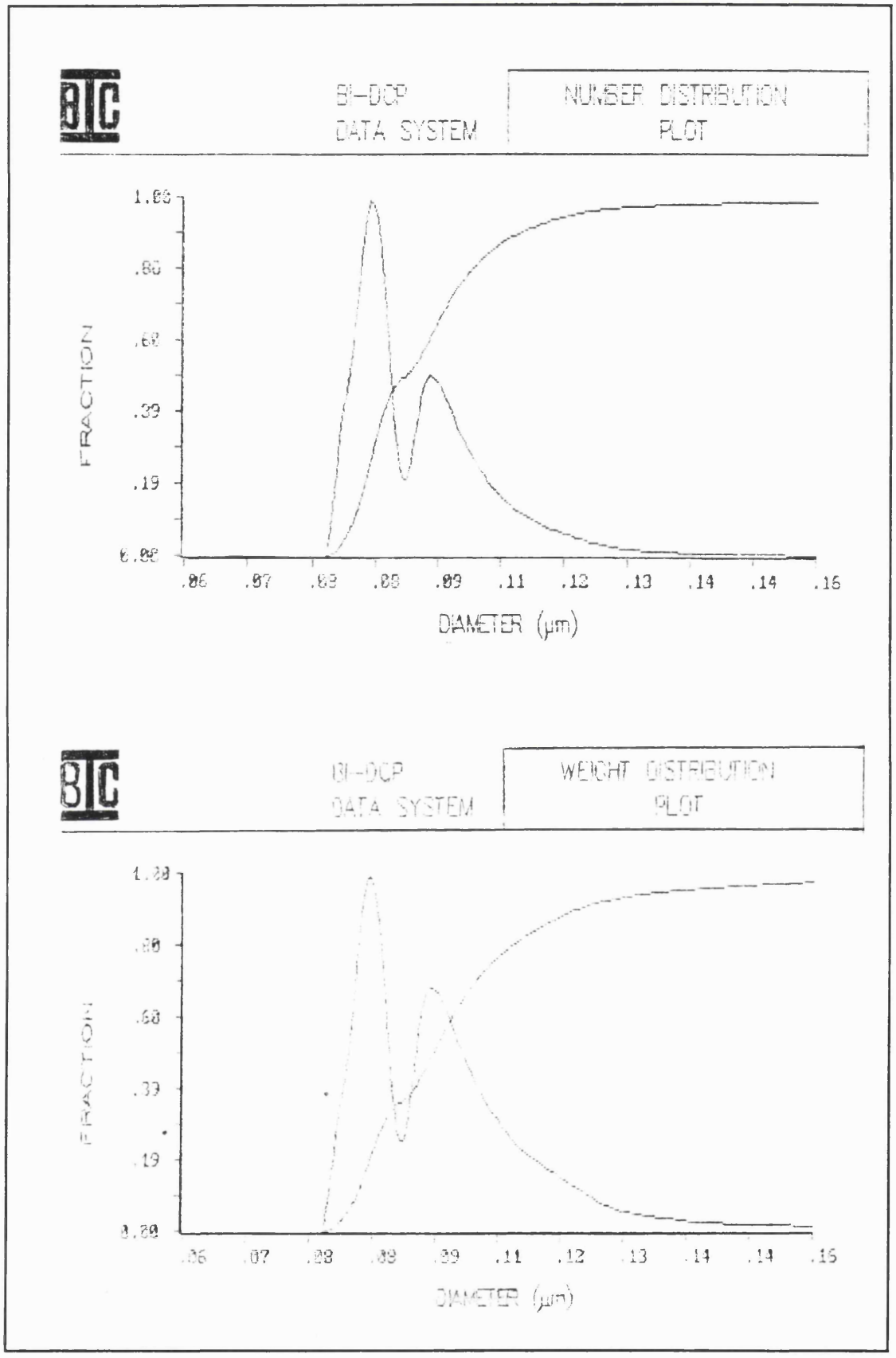

Figure 3.3 *Results of Particle Size Analysis Performed on Brookhaven DCP 100.*

laboratory hydrometer measuring specific gravity at 293 K [BDH (Merck Ltd.)] was used together with an optical density method suggested by the manufacturers.

The density of the Nycodenz solution can be related to the optical density at 350 or 360 nm by the following relations:

$$Density\ (kg.m^{-3}) = 0.0815\ O.D._{350\,nm} + 1.0 \qquad \textbf{Eq. 3.1}$$

or:

$$Density\ (kg.m^{-3}) = 0.1325\ O.D._{360\,nm} + 1.0 \qquad \textbf{Eq. 3.2}$$

The optical density was measured on a Lambda II spectrophotometer (Perkin–Elmer Ltd.)

A small volume (approx. 20 mL) of the 1060 $kg.m^{-3}$ density solution was pipetted into a standard 50 mL plastic centrifuge tube on top of which was carefully pipetted a similar volume of the 1040 $kg.m^{-3}$ Nycodenz solution so that the two solutions did not mix and formed two separate layers within the tube. Two drops of the 2.5 wt% polystyrene latex suspension of 3.09 μm particle diameter were placed on top of the Nycodenz solutions in the centrifuge tube and the tube placed in the MSE M24 centrifuge. The suspension was centrifuged at 10,000 rpm for ten minutes. After centrifugation the centrifuge tube was examined to determine the final settling position of the latex particles. It was found that the latex particles formed a narrow band between the two liquid layers in the tube and therefore the density of the particles was between 1040 and 1060 $kg.m^{-3}$. The experiment was repeated several times using Nycodenz solutions of densities ranging between 1040 and 1060 $kg.m^{-3}$ with 2 $kg.m^{-3}$ step changes in density. This allowed the density of the polystyrene latex particles to be determined to ± 2 $kg.m^{-3}$.

The polystyrene particles were found to remain in suspension when centrifuged in a Nycodenz solution of density 1054 ± 2 $kg.m^{-3}$ and therefore the density of the polystyrene latex particles was determined to be 1054 ± 2 $kg.m^{-3}$. As the Nycodenz solution is stable for up to five years when stored at room temperature a suspension of 3.09 μm latex particles in the Nycodenz solution was left tightly stoppered in a cupboard for several weeks to ensure that no settling of the latex occurred through a slight mismatch in density. After that long period of time no settling or 'creaming' of

the latex particles had occurred and therefore the density of the latex particles was confirmed to be 1054 ± 2 $kg.m^{-3}$.

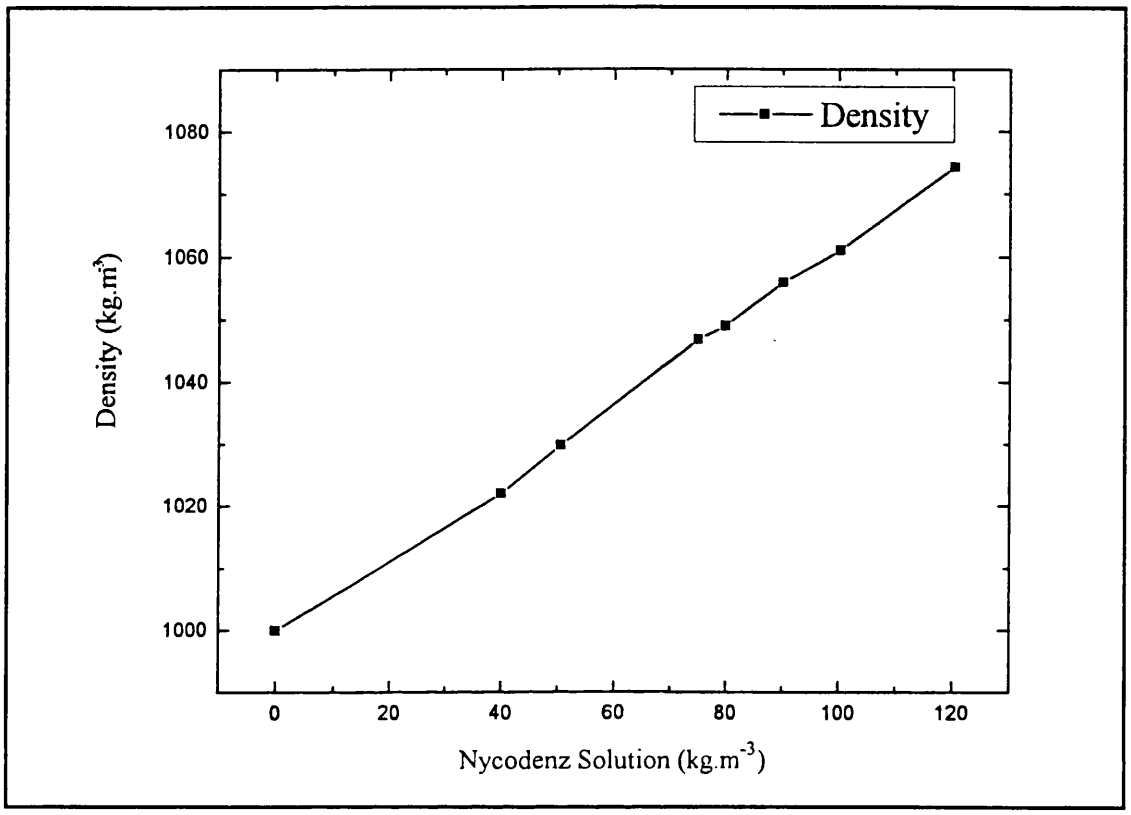

Figure 3.4 *Calibration Curve of Density vs. Nycodenz Concentration.*

3.3 Ultrasonic Equipment.

Key features of the ultrasonic equipment are described in the following sections. Specific details of apparatus used for individual experiments are dealt with separately within the relevant chapters.

3.3.1 Transducer Mounting

During the course of study a method was developed for mounting piezoelectric ceramic transducers onto aluminium support blocks.

The transducers were supplied with a fired-on silver electrode, several micrometers thick, to which the electrical contacts could either be soldered or

cemented with a conducting adhesive. Care was taken when soldering onto the transducers so as not to exceed the Curie temperature (Morgan Matroc Ltd. sales literature) of the material (approximately 250°C for lead zirconate titanate. See **Section 2.4.**) at which point the piezoelectric properties of the ceramic are destroyed. Conducting adhesives were used to overcome this problem but are of low bond strength and not easy to apply effectively. It was therefore decided to use a low melting point solder (ERSIN, 5 core, 362 flux, liquidus/solidus 179°C; Multicore Solders Limited, Kelsey House, Woodlane End, Hemel Hempstead, Hertfordshire, UK.) and a temperature controlled soldering iron to avoid depolarization whilst achieving a stronger bond.

The transducers were cemented onto the machined aluminium mounting blocks for use in the ultrasonic separation experiments as described in **Section 6.4** (See **Figure 3.5**). The ceramic transducers were supported by the circular ring of the front face of the mounting block with the majority of the transducer backed by air to provide more efficient transmission of ultrasonic energy from the transducer. Cementing the entire area of the transducer to a surface would have altered the resonant frequency of the transducer by a degree that would be extremely difficult to reproduce, making the use of a pair of matched frequency transducers rather difficult. Each transducer was cemented onto the aluminium with a two-part heat conducting adhesive (553-251, RS Components Ltd.) which also provides electrical insulation and a water proof seal between the transducer and the aluminium block. A heat conducting adhesive was chosen to provide a small degree of heat sinking to the transducer mounting blocks and the structure of the separation device. Finally several thin layers of conformal coating (567-682, RS Components Ltd) were sprayed onto the assembled transducer unit to prevent water from short circuiting the electrodes and from being absorbed by the porous ceramic of the transducer.

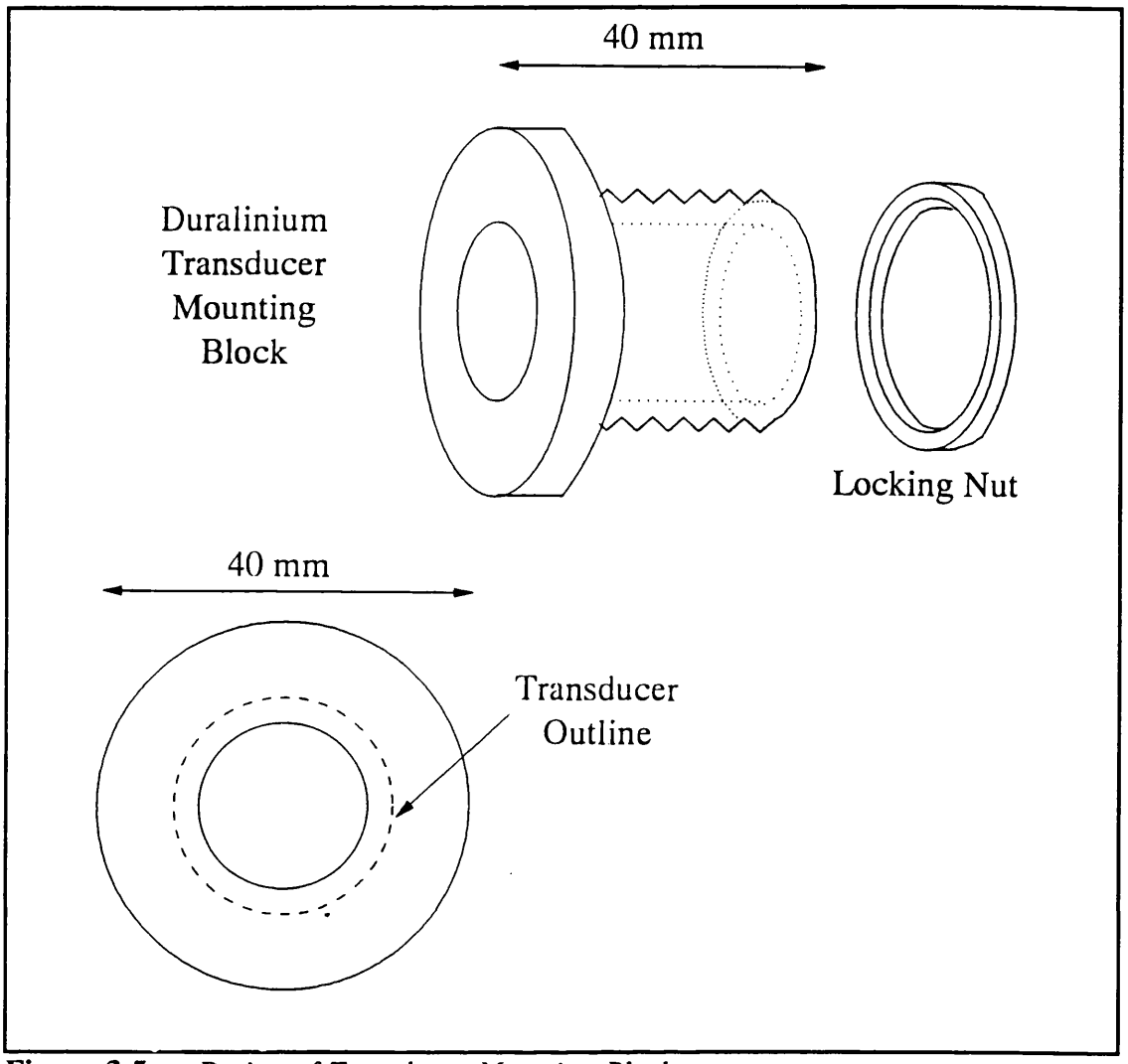

Figure 3.5 *Design of Transducer Mounting Blocks.*

3.3.2 Piezoelectric Transducer Materials

This section describes the piezoelectric ceramic and polymer transducers used in this research.

3.3.2.1 Piezoelectric Ceramic Transducers

The ceramic transducers used throughout this research were purchased from Morgan Matroc Ltd, Unilator Division, Ruabon, Wrexham, Wales. A list of the more relevant properties of the lead zirconate titanate, PC4, ceramic material is presented

in **Appendix I** together with a table showing the dimensions of the transducers used during the research.

The PC4 material is designed to operate continuously at high power levels making it suitable for the present application. For optimum efficiency the transducers are operated at their resonant frequencies, f_r, which for a disc is represented by the following equation when the transducers are polarised to resonate in thickness mode:

$$f_r = \frac{N_T}{T} \qquad \textbf{Eq. 3.1}$$

where N_T is the frequency constant (Hz.m) for the particular material and T is the thickness of the ceramic disc (m). The transducer can be tuned to its resonant frequency by operating the transducer at the frequency, f_m, where the transducer displays its minimum impedance, as shown in **Figure 3.6** .

The ceramic material is subject to several operating limitations such as maximum operating temperature, voltage, stress and acoustic pressure. As the operating temperature approaches the Curie temperature of the material (573 K for PC4) the piezoelectric performance of the transducer decreases and is lost completely at temperatures above the Curie point; elevated temperatures also increase the ageing rate of the material. Therefore a means of cooling the transducer may be required to remove the heat generated by electrical inefficiency of the transducer to prevent the transducer from reaching the Curie temperature.

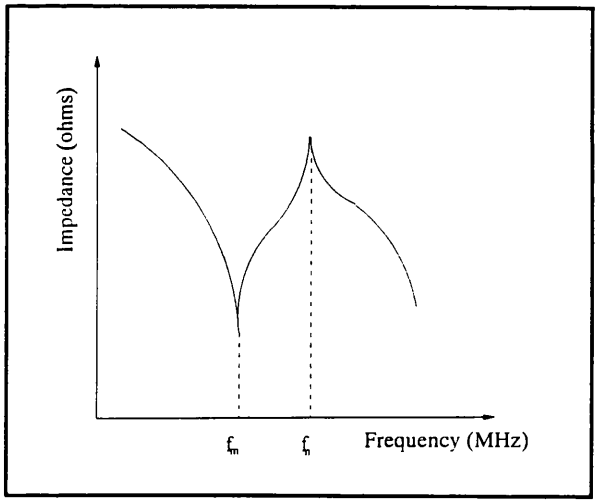

Figure 3.6 *Frequency Dependence of the Impedance of a Transducer.*

Piezoelectric ceramics can be depolarized by strong electric fields with polarities opposite the original poling voltage. The exact limit is dependent on the temperature, duration of exposure to the field and the type of material but is normally

within the range of 500 – 1000 $V.mm^{-1}$. The alternating voltage used to drive the transducer can depolarize the material when the half cycle of the signal that opposes the original poling voltage exceeds the limiting voltage.

The acoustic power handling capacity of the transducer is limited by the following factors: mechanical strength; reduction in efficiency due to dielectric losses and mechanical losses; depolarization due to elevated electric field and temperature; and instability due to positive feedback between dielectric losses and internal heating. High frequency continuous duty transducers are generally limited by temperature and the operating efficiency is dependent on the rate of removal of heat from the transducer. However the specific power limitation is dependent on the mechanical design of the transducer unit and an absolute value of the power limitation cannot be determined without thorough knowledge of the operating conditions.

3.3.2.2 Polyvinylidene Fluoride Piezoelectric Polymer

Polyvinylidene fluoride (PVDF) elements were used in the design and manufacture of the hydrophones as described in **Section 5.3**. The properties of the PVDF piezoelectric film are given in **Appendix V**. The film can be used to either transmit or receive ultrasound over a very wide frequency range thus making it ideally suited for use in a hydrophone. The sensitivity of the film when used as a hydrophone is typically 10^{-5} – 10^{8} $N.m^{-2}$ with a frequency range of less than 1 Hz to GHz frequencies.

The disadvantages of using PVDF rather than a ceramic material are the operating temperature and electric field limitations. The operating temperature range is 233 K to 373 K where the upper limit is only possible after special treatment during manufacture. This means that the film will not withstand the temperatures generated by steam sterilization or normal cleaning–in–place procedures. The maximum operating voltage is 30 $V.\mu m^{-1}$ with a breakdown voltage of 100 $V.\mu m^{-1}$ and as a combined result of the capacitance of the material (3.8×10^{-9} $F.m^{-2}$) the PVDF film can not be used to generate high intensity ultrasound.

3.3.3 Phase Shifting

The Audley Scientific Dual Ultrasonic Amplifier (Audley Scientific Ltd, Audley Way, Ascot, Berkshire, U.K.) included an electronic circuit that enabled the phase of one transducer driving signal to be shifted with respect to the other transducer driving signal. The rate of phase shift was controllable via a TTL compatible 8-bit digital signal supplied externally either by a microcomputer or similar device.

By changing the phase of one transducer signal with respect to the other the relative spatial positions of the nodes of the standing wave field in a fluid could be altered to a fine degree and made to move continuously through the fluid. Particles accumulated at the nodal planes of the standing wave field will be forced, by the radiation pressure, to move with the nodes as they move under the influence of phase shifting. A maximum effective nodal velocity occurs when the phase shift employed moves the nodes at a velocity greater than that particle velocity generated by the radiation pressure on the particles, when, in which case the particles will remain dispersed in suspension and not be caused to concentrate. The maximum effective rate of phase shift is investigated experimentally in **Chapter 6.**

The rate of phase shift was controlled by computer programs that sent an eight bit digital control word in the range of 0 to 255 to the phase shifting circuit in the ultrasonic amplifier. When the eight bit control word equals zero the two transducer signals are in phase, as the control word increases in value the two signals gradually shift out of phase until the control word equals 255 when the two signals are one cycle or wave length out of phase (and therefore essentially back in phase). The program controls the rate of the phase shift by varying the rate at which the control word increases from 0 to 255.

An oscilloscope was used to measure the actual rate of phase shift in terms of cycles per second. The concentrated bands of particles accumulated in the standing wave field moved a distance of half a wavelength for every phase shift of one full cycle.

3.3.4 Electronic Circuits

During this research project a number of electronic circuits were constructed for the control of a piece of apparatus or for the amplification of electrical signals.

3.3.4.1 Laser Driver Circuit.

A laser driver circuit was necessary to control the current supplied to the 30 milliwatt Sharp LT024MD laser diodes (Access Pacific Ltd, Kymbrook School House, Kimbolton Road, Keysoe, Bedford, U.K.) used during the relevant experiments in this project (**Chapter 5** and **Chapter 7**).

The power output of a laser diode can vary with fluctuations in the ambient temperature and therefore a control mechanism is required to maintain a constant output. The circuit incorporates an integrated circuit (IC) chip [Sharp IR3C01N] and requires a power supply to generate +5 and −12 volts DC. The laser diode package also incorporates a photodiode that monitors the output of the laser diode. The output of the monitor photodiode is sent to a power control circuit within the IC and a feedback control loop is set up between the monitor photodiode output and the laser power input. The circuit (as shown in **Appendix VII**) also features a slow start characteristic that prevents damage to the laser diode from power surges.

3.3.4.2 High-Speed Amplifier.

A high-speed amplifier was constructed to amplify the signals generated by the miniature ultrasonic hydrophones used to measure the sound pressure in a standing wave field (described in **Chapter 5**).

The amplifier consisted of a ultra high frequency operational amplifier [op-amp] (NE5539N, 300-221, RS Components Ltd) and associated printed circuit board (435-664 RS Components Ltd). A twin rail power supply was also required to provide the +12 and −12 volts DC required to drive the op-amp (Verospeed, PSU 203, 89-10667L, Farnell). The circuit constructed (See circuit diagram in **Appendix VII**) incorporated variable gain of the input signal which allowed the amplified signal to

be adjusted to utilise the full range of the Amplicon PC30–AT board used to monitor and record the hydrophone output.

3.4 Preparation of Suspensions for Ultrasonic Tests.

A number of suspensions and buffers were needed for experiments. The details of their preparation are given below.

3.4.1 Water Preparation.

Water used for sample preparation, agar gel preparation, transducer cooling and for use during experiments was taken from a deionised supply and degassed before being filtered if necessary.

Degassing was achieved by placing the water in a conical vacuum flask that had been rinsed with deionised and filtered water. The flask was placed on a hot plate and the water was heated and held at 373 K for approximately five minutes. The water was allowed to cool to approximately 320 – 330 K at which point the conical flask was sealed with a clean rubber bung and connected to a water driven vacuum pump.

Upon application of the vacuum the water was seen to bubble violently for several minutes. After ten minutes and/or the cessation of bubbling the vacuum was removed and the water placed in a clean airtight container and used within a few hours of degassing.

Filtered, degassed water was prepared using a small filtration system assembled to provide filtered water at a rate of several litres per hour. A peristaltic pump (330–812, 330–828, 330–799, RS Components Ltd) was used to pump degassed water via silicone rubber tubing through a Millipore GF/F glass fibre filter disc (Millipore [UK] Ltd, The Boulevard, Blackmore Lane, Watford, Herts, UK.) to remove any large contaminating particles. The filtered water then passed through a 0.1 μm pore size filter membrane (Millipore Ltd). The filter membrane discs were replaced after every ten litres of water filtered.

3.4.2 Sample Preparation

Sample suspensions of polystyrene latex particles and yeast (whole cells and homogenate) were prepared for experiments in the following manner.

3.4.2.1 Polystyrene Latex Particles

Polystyrene latex beads were supplied by Park Scientific Ltd (Park Scientific Ltd, 24 Low Field Road, Moulton Park, Northampton, UK.), and consist of a 2.5 wt% suspension of particles in water. For each experiment a measured quantity of well mixed latex suspension were mixed with degassed, filtered deionized water to provide a suspension of approximately the required concentration. The suspension was then sonicated in a standard laboratory ultrasonic bath for between 10 and 20 seconds to disrupt any particle aggregates that may have formed whilst in the latex bottle.

If an accurate measure of the particle number concentration was required then a sample was taken for analysis on the Elzone Particle Analyzer as described in **Section 3.2.1**. For suspensions of particles smaller than the minimum particle size range of the Elzone analyzer the concentration was estimated by measuring the absorbance of the suspension at 780 nm on a Perkin–Elmer Lambda II spectrophotometer (Perkin–Elmer Limited., Post Office Lane, Beaconsfield, Buckinghamshire, U.K.) and comparing the value with a calibration curve of absorbance against particle concentration (See **Appendix III**). The calibration curve was generated by making suspensions of polystyrene latices, measuring the dry weight of the particles from a precisely measured weight and volume of suspension and measuring the absorbance of serial dilutions of the suspension. Curves were prepared for several sizes of polystyrene latex particles.

3.4.2.2 Whole Yeast Cells

Suspensions of whole yeast cells were prepared by suspending pieces of block Baker's yeast (Distillers UK) in phosphate buffer (See Section 3.9). Suspensions were prepared to an approximate wet weight percent concentration, the actual concentration being measured on the Elzone Particle Analyzer as described above.

The yeast suspensions were washed with fresh phosphate buffer before particle analysis to remove cell debris and other contaminants of small size by spinning down the yeast cells in a centrifuge at low spin speeds for a few minutes then removing and replacing the supernatant with fresh buffer. This procedure was repeated to ensure the removal of the majority of the contaminants.

3.4.2.3 Preparation of Phosphate Buffer

Phosphate buffer, for the suspension of whole yeast cells and yeast homogenate, was prepared from solutions of di-potassium hydrogen orthophosphate and potassium dihydrogen orthophosphate, $K_2H.PO_4$ and $KH_2.PO_4$ respectively both at a strength of 0.1 M. The solutions were made with deionized water and analar grade reagents (P/5240/53 and P/4800/50, Fisons Scientific Equipment, Bishop Meadow Road, Loughborough, Leicestershire, U.K.). Equal volumes of the solutions were mixed to give a solution of pH 6.5. On occasion the pH of the solution required correction with a few drops of 2.5 M sodium hydroxide solution (NaOH) to achieve a pH of 6.5.

3.4.2.4 Preparation of Yeast Homogenate

Blocks of Baker's yeast were broken up and mixed by hand with phosphate buffer (**Section 3.9**) to give 3 – 5 litres of a 60 % wet wt. suspension of whole cells. Homogenisation was carried out on an APV Lab 50 homogeniser (APV, Crawley, West Sussex, U.K.) at 500 bar.g pressure. Five passes through the homogeniser produced sufficient disruption of the yeast cells. To remove the lipid fraction released by disruption the homogenate was centrifuged at 14,000 g for 30 minutes at approximately 277 K after which the lipid was easily manually lifted off the supernatant and the remaining homogenate mixed to resuspend the sediment formed.

3.4.3 Preparation of Sonically Transparent Agar Plugs

The glass sample vessel of the ultrasonic separation apparatus used in the experiments of **Chapter 6** (See **Figure 6.2**) required the space between the cling film at the ends of the tube and the inlet–outlet ports to be filled to prevent solids and air bubbles from collecting in the space that would be formed. The material used to fill this space had to be selected such that it would allow the virtually unhindered passage of ultrasonic waves from the water bath to the particle suspension. To achieve this objective it was decided to use an aqueous agar gel of 0.5 % wt/vol agar which was prepared in the following manner:

Degassed, filtered, deionized water (50 mL) was placed in a 100 mL glass beaker on the heated plate of a magnetic stirrer. The water was heated a little to aid the mixing of approximately 0.25 g of agar powder (BDH [Merck Ltd], Broom Road, Poole, Dorset, U.K.) with a magnetic stirring bar. The mixture was heated to boiling point whilst stirring to dissolve the agar powder fully. After a short period to allow entrapped air bubbles to disperse, the hot agar solution was injected into the glass sample tubes with a pasteur pipette so that the meniscus formed was level with the edge of the inlet–outlet port. The agar gel was allowed to solidify and the procedure repeated with the other end of the glass tube.

The agar plugs consisted of 99.5 % water and therefore have essentially the same acoustic impedance as the particle suspension under study and the water in the water baths either end of the glass tube. The agar plugs proved to be long lasting under experimental conditions and were only replaced when particles were forced into the gel by the ultrasonic forces and the effect of phase shifting and therefore constituted a potential source of contaminating particles to subsequent experiments.

CHAPTER 4 INITIAL INVESTIGATIONS

4.1 Introduction

The aim of these experiments was to investigate the use of megahertz frequency ultrasonic standing wave fields in the separation of fine biological particles.

Before purchasing expensive electronic equipment and apparatus it was necessary to become accustomed with the phenomenon of particle aggregation in ultrasonic standing wave fields and to investigate equipment designs appropriate to the separation of fine biological particles.

To achieve this several simple pieces of apparatus were designed and assembled. Initial investigations were undertaken to determine the operational limits of the ultrasonic separation technique. For example, to ascertain the transducer driving signal voltages required to generate ultrasonic standing waves of sufficient intensity to cause effective particle migration to the nodal planes of the standing wave field. Other constraints such as the size range of particles influenced by megahertz frequency standing wave fields and basic apparatus design limits were also the subjects of study in these initial experiments.

4.2 Cuvette Experiments

This section describes a series of experiments in which suspensions of particles were subjected to ultrasonic standing wave fields. For convenience these experiments were performed using plastic spectrophotometer cuvettes as the vessels.

4.2.1 Materials and Methods

Plastic spectrophotometer cuvettes, 4 mL volume, (40 x 10 x 10 mm) were chosen as sample containers because of their clear walls which aided visual observation and also because the cuvettes were of similar dimensions to the ultrasonic transducers used in the experiments described in **Section 4.2.4**. Two aluminium blocks 50 x 50 x 10 mm were machined and polished to act as waveguides for the ultrasound and to provide heat sinking for the transducers (See **Figure 4.1**). The transducers and

cuvettes were fixed to the aluminium blocks using a non-conducting heat sink compound (503-357, RS Components Ltd, Corby, Northants, UK).

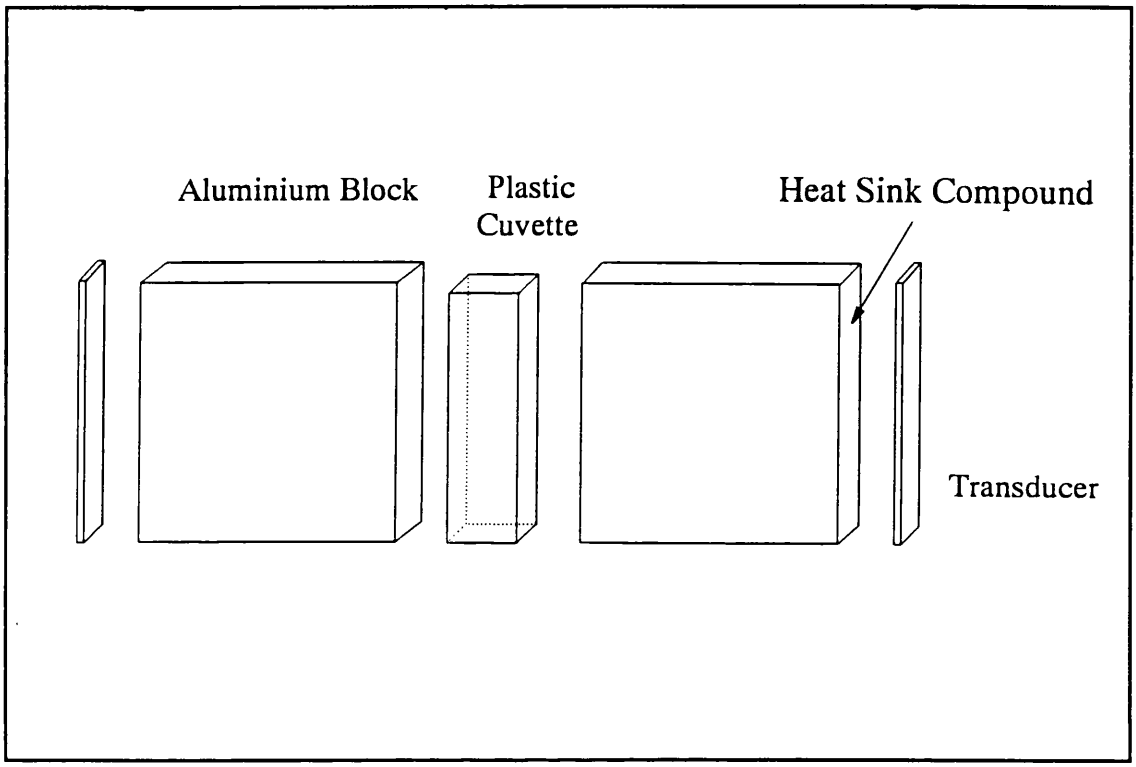

Figure 4.1 *Schematic Diagram of Cuvette Apparatus used During Initial Investigations of Ultrasonic Standing Wave Particle Segregation.*

4.2.2 Electronic Equipment

The ultrasonic transducers used were two 40 x 10 mm PC4 lead zirconate titanate piezoelectric ceramic pieces with resonant frequency of 2 MHz (Morgan Matroc, Unilator Division, Ruabon, Wrexham, Wales). To drive the transducers a standard laboratory function generator was employed (Wavetek XCG Waveform Generator, Model 183, Wavetek, San Diego, California, USA). This device had a frequency range of 0 to 5 MHz and a maximum electrical power output of 1.3 watts.

A Hitachi VC-6050 digital storage oscilloscope (Hitachi Denshi Ltd., Garrick Industrial Centre, Garrick Road, Hendon, London, U.K.) was used to monitor the waveform of the current driving the transducers and to tune the signal generator to the resonant frequency of the ultrasonic transducers.

4.2.3 Particulate Systems

Suspensions of monodispersed polystyrene latex beads of several particle sizes were obtained from Polysciences Ltd. The range of particle diameters used was 15.8 μm – 2.01 μm, with a quoted particle density being 1050 $kg.m^{-3}$. The particle sizes were confirmed using particle size analysis equipment and methods described in **Section 3.2**. These particles were therefore representative of typical biological cells, for example *E.coli* at approximately 2 μm, yeast cells at approximately 6 μm and mammalian cells at over 10 μm.

4.2.4 Experimental Procedure

Two sets of experiments were performed; the first involving the use of just one of the ultrasonic transducers, and the second involving both of the transducers operating simultaneously. The object of having two sets of experiments was to establish whether there was any benefit to be gained from operating with two transducers rather than only one. The use of a single transducer would have attractive advantages because of the saving in capital outlay and running costs on a scaled-up process.

As quantitative results were not sought at this stage the latex suspensions were diluted with deionized water to provide a suitably opaque suspension. At this stage of the research the possible dependency of the ultrasonic effects upon the concentration of the particles in suspension was not under investigation. Hence the suspensions were intentionally prepared to be dilute to avoid any possible complications arising from the effects of high particle concentrations.

The contents of the cuvette were thoroughly stirred and the electrical supply to the transducers switched on; the frequency having been previously set at the resonant frequency (approximately 2 MHz) and the power output to the maximum of 1.3 watts total output.

The appearance of the contents within the cuvette were studied and the time taken for any visible effects to occur recorded. This procedure was repeated for each suspension containing particles of discrete size. Each set of experiments was repeated and the appearence of the duplicates recorded.

For the experiments using a single transducer the sound waves produced reflected off the interface of the opposite aluminium block and the air to form the standing wave field required. The results of these experiments are listed in **Table 4.1** and may be compared with the results obtained using a pair of transducers to generate the standing wave field. The results of these experiments are listed in **Table 4.2.**

4.2.5 Results

Upon the application of a sound field to the suspensions the formation of a vertically orientated banding pattern was rapid and unmistakeable with the bands of particles being spaced approximately a third of a millimetre apart, corresponding to the half wavelength distance of 350 μm for a 2 MHz sound wave in water. Efficient removal of particles from the volume of fluid between the bands resulted in clearly defined regions of concentrated particles and clear liquid.

After approximately half a minute of irradiation flow patterns were observed in the cuvettes during both sets of experiments. The velocity of the flow observed was in the region of 0.002 $m.s^{-1}$ (determined through visual observation of the movement of the concentrated particles against the banding pattern of bands of particles spaced at half wavelength distances i.e. 0.35 mm at 2 MHz in water). **Figure 4.2** is a schematic representation of the formation and disruption of the concentrated bands within the cuvette at successive periods of time after the start of sonication.

Latex Particle Diameter (μm)	Time Taken for Particle Aggregation (seconds)
15.8	6
13.1	6
11.0	7
8.7	7
5.96	15
2.02	No visible banding

Table 4.1 *Single Transducer Experimental Results*

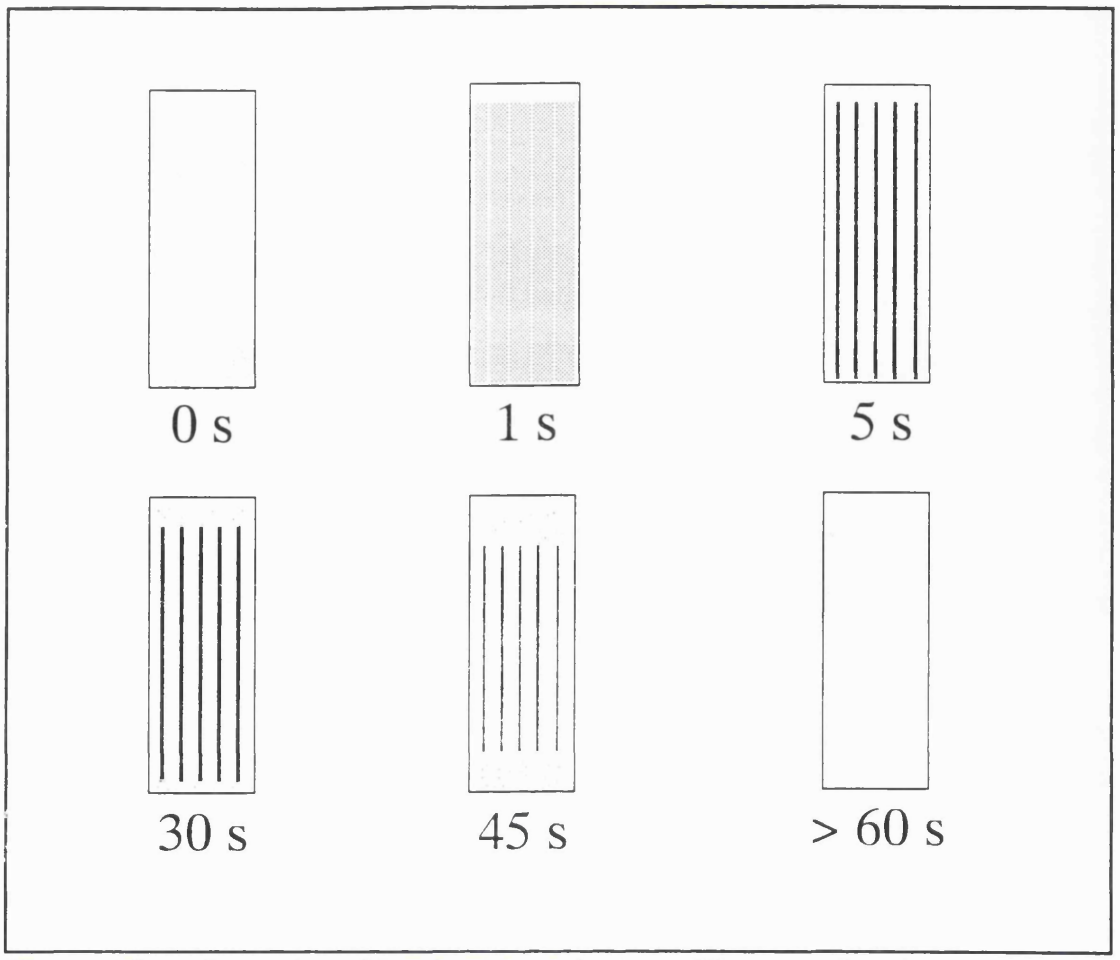

Figure 4.2 *Formation of Bands of Particles in an Ultrasonic Standing Wave Field.*

Latex Particle Diameter (μm)	Time Taken for Particle Aggregation (seconds)
15.8	4.0
13.1	3.5
11.0	4.0
8.7	4.0
5.96	4.5
2.02	No visible banding

Table 4.2 *Twin Transducer Experimental Results*

4.2.6 Discussion

The devices used in the initial experiments enabled only a very limited range of experimental conditions to be examined. Results however gave a gross indication of the power levels required to cause particle migration and also the influence of particle diameter and time.

The power output of the function generator used was very low and the sound intensity generated had a theoretical maximum of approximately 1.5 $kW.m^{-2}$ (ignoring any impedance mismatch between the transducers and the function generator, and the inefficient conversion of electrical energy to sound energy). This value of sound intensity is at the lower end of the range of intensities quoted in the literature surveyed (See **Section 1.2**) as being sufficient to cause particle migration to the nodes of a standing wave field. However very definite banding was observed and the clarity of the internodal spaces suggested a high level of separation.

The formation of the banding patterns was seen to be more rapid when the two transducers were used together. The inferior performance of the single transducer was most probably caused by less than perfect reflection and absorption of the ultrasonic energy at the cuvette–aluminium and aluminium–air interfaces. More rigorous alignment was clearly necessary to achieve a satisfactory standing wave field. Another feature of the twin transducer experiments was that the concentrated bands of particles appeared to have a greater uniformity of density and were more compact, again suggesting a more effective concentration of the particles at the nodes of the standing wave field than that achieved with only one transducer.

The flow patterns arising after prolonged irradiation (See **Figure 4.2**) may be attributed to the generation of acoustic streaming forces (See **Section 1.2** and **Section 2.2.4.2**). Flow may have been caused by the presence of a net force at the top of the cuvette due to the fact that the transducers were slightly shorter than the cuvette which resulted in a small volume of liquid not being subjected to irradiation. Convection currents, due to heating of the liquid, were ruled out as a cause of the flow patterns because the flow stopped the instant the ultrasound was switched off; clearly a time lag would have been observed if heat transfer was the driving force behind the induced flow.

4.2.7 Conclusions

The experiments performed in the previous section confirmed that it was possible to cause the aggregation of micron sized particles suspended in an aqueous suspension by the application of megahertz frequency ultrasonic standing waves.

An indication of the ultrasonic intensity required to cause the particle migration to the nodes of the sound field was established and found to be at least 1.5 $kW.m^{-2}$.

It was concluded that the aggregation effect was more pronounced when using a pair of transducers rather than a single transducer and that future experiments would be performed using a matched pair of transducers. The use of two transducers reduced the need for the very accurate alignment necessary for successful experiments with a single transducer.

4.3 Alternative Geometry Experiments

Following consideration of the previous experimental results appropriate electronic equipment was made to carefully chosen specifications that would allow far more flexibility in future experiments as regards the frequencies and powers available for use in the experiments. Specifications for electronic equipment included a twin channel amplifier, with an integral phase shifting device and an operational frequency range of between 0.2 and 10 MHz and a total electrical power output of 25 watts.

The aim of this phase of the research was to use the above electrical equipment to perform a quantifiable separation of a well characterised particulate system on a slightly larger scale than achieved during the previous section.

4.3.1 Materials and Methods

The design of the sample container used in these experiments was governed by the geometry of the transducers purchased for the majority of this work (See **Section 4.3.2**). A perspex tube of 30 mm internal diameter was chosen as the sample vessel. Two duralinium cylinders were machined to fit into the open ends of the perspex tube to act as mounting blocks for the transducers and wave guides for the

ultrasound (See **Figure 4.3**). The tubular perspex vessel had an internal wetted length of 100 mm and therefore had an effective volume of approximately 0.07 L.

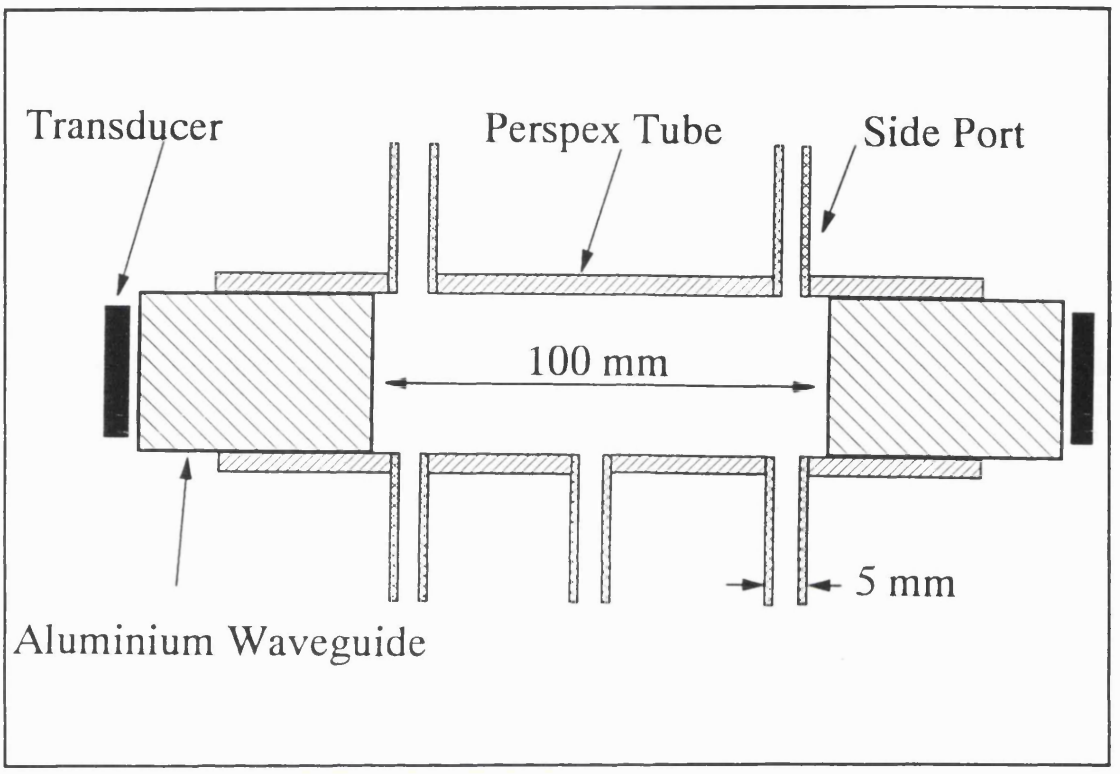

Figure 4.3 *Diagram of Sample Vessel and Transducer Mounting Blocks Designed for Use in the Experiments of* **Section 4.3**.

4.3.2 Transducers

A number of piezoelectric ceramic transducers were purchased (Morgan Matroc Ltd, Unilator Division, Vauxhall Industrial Estate, Ruabon, Wrexham, Clwyd, Wales). The pieces used in this set of experiments were 1 MHz lead zirconate titanate, PC4 piezoelectric ceramic discs, 22 mm in diameter and 2 MHz PC4 discs 25 mm in diameter. The transducers were fixed to the aluminium support blocks with the heat transfer compound used previously (See **Section 4.2.1**).

4.3.3 Electronic Equipment

A number of items of electronic equipment were required to enable quantifiable separation experiments to be performed. The high frequency signal generator, ultrasonic amplifier and phase shifting device were purchased after consultation with the manufacturer (Audley Scientific Ltd, Audley Way, Ascot, Berkshire, U.K.) who designed the equipment to meet the specifications mentioned earlier (**Section 4.3**).

4.3.3.1 Super-Stable High Frequency Generator

A super-stable high frequency generator unit with a frequency range of 0 to 40 MHz and stable to 1 part per million per degree centigrade per hour was specified for subsequent work. The frequency stability of the signal generator is crucial since it prevents the frequency of the signal from drifting away from the resonant frequency of the transducer at which the transducer has the greatest output. During all experiments using this unit a square wave of the desired frequency and a voltage of 15 volts peak to peak was used to supply a dual ultrasonic amplifier.

4.3.3.2 Dual Ultrasonic Amplifier

An amplifier capable of driving two channels at operational frequencies of 200 kHz to 10 MHz with a total electrical power output of 25 watts was used in these experiments. The unit had in addition an integral digital phase shifting device. This device allowed externally controlled shifting of the phase of one output channel with respect to the other. External control of the rate and duration of phase shift was achieved using a personal microcomputer (Apple II Microcomputer, Apple Computer Inc, 10260 Bandley Drive, Cupertino, California, USA.) to supply the amplifier with an eight bit control word. **Appendix II** contains a sample listing of a program used to control the phase shift on the Apple II computer.

4.3.3.3 Digital Storage Oscilloscope

A high frequency (60 MHz) digital storage oscilloscope was used to monitor the amplitude and waveform of the signal driving the transducers (Hitachi VC-6050, Hitachi Denshi Ltd., Garrick Industrial Centre, Garrick Road, Hendon, London, U.K.).

4.3.4 Particulate Systems

Experiments were conducted using suspensions of latex particles in deionised water and also suspensions of whole Baker's yeast cells in an appropriate phosphate buffer as defined in **Section 3.4.2.2.**

4.3.5 Experimental Procedure

Suspensions were made up as 1:100 dilutions of the latex samples with deionised water giving a final concentration of 0.025 % w/v. The suspensions were then pumped into the apparatus, expelling all air bubbles which could induce mixing during the application of a standing wave field. Sonication with a pair of transducers had been shown to be preferable to a single transducer (See **Section 4.2**) and hence these experiments were conducted with a pair of matched transducers.

The experiments were designed to quantify the concentration of particles achieved during separation and to assess the use of the phase shifting device as a tool to aid separation. To achieve these aims the particle suspensions were sonicated at various power levels and phase shifting was employed to manipulate the concentrated bands of particles that formed in order to provide a mechanism of continuously removing the concentrated bands of particles from the sound field.

4.3.6 Results and Observations

Particle migration to the nodes of the sound field was observed at various points in the perspex tube and on several experimental runs banding was observed throughout the vessel. However a number of problems were encountered whilst using

this apparatus the most severe being heating of the liquid in the vessel and acoustic streaming of the liquid which tended to disrupt any bands of particles that had formed.

At high transducer voltages (over 50 volts peak to peak) temperatures of 340 to 350 K were reached after only a few minutes of irradiation. A rapid streaming pattern was generated after several minutes operation which led to disruption of the accumulated particles at the nodal planes. These problems were not easily overcome and quantifiable results on the efficiency of the separation effect were not obtained.

4.3.7 Discussion

Although banding was achieved in the perspex tubular design the onset of bulk mixing effectively negated the ultrasonic effect. The mixing and the associated heating problem were most probably caused by heat generated by electric loss in the transducers being conducted through the duralinium support blocks into the particle suspension. It was decided that future designs would have to provide for the removal of this excess heat. Streaming was further exacerbated by the large diameter of the tube compared to the transducer diameter (1.2 times). This led to a variation in sound intensity across the diameter of the tube causing Eckart streaming (See **Section 1.2.2.2**). To overcome this problem subsequent sample vessel designs were such that the vessel diameter was a smaller diameter than that of the transducer.

4.4 Overall Conclusions.

Preliminary experiments showed that megahertz frequency ultrasonic standing wave fields would cause the migration of micron size particles towards the nodes of the standing wave field. Initial experiments indicated that performing particle aggregation in a megahertz frequency ultrasonic standing wave field is more effective when the standing wave field is generated with the use of two opposing transducers compared to that formed using a single transducer and a reflector.

In order to avoid streaming effects the vessel diameter should not exceed that of the transducer. This has obvious implications when the aspect of process scale–up

is considered and could be the limiting factor in deciding the potential throughput of an ultrasonic separation device.

On the basis of the above experiments it was evident that future experimental apparatus would need to be designed with careful attention being paid to avoiding the problems of acoustic streaming and would necessitate the very fine adjustment of transducer alignment.

(**Chapter 6** covers the design of an ultrasonic separation device based on these findings and the experiments performed with the apparatus.)

The next phase of research concentrated on determining the levels of acoustic intensity required to cause particle migration.

CHAPTER 5 DETERMINATION OF ULTRASONIC INTENSITY

5.1 Introduction

This chapter describes methods developed in this study to determine the intensity of the ultrasound generated by the piezoelectric transducers during experiments. This information is important for the comparison of experimental findings with theoretical relations and to enable design of scaled–up equipment.

It is difficult to quantify the ultrasonic energy emitted by an ultrasonic transducer in a standing wave field. One way to assess the ultrasonic power output is to measure the electrical power used by the transducer with a power meter, however at best this would only indicate the maximum possible output as it does not account for inefficiencies in the transducer. Another method would be to measure the sound pressure amplitude by means of a hydrophone. This method has problems due to the need for the hydrophone to be calibrated before it can be used and due to the anisotropic nature of the standing wave field. Also since the nodes and antinodes of the sound field (the planes of minimum and maximum sound pressure) are separated by only a quarter of a wavelength (175 μm at 2 MHz in water) then using a hydrophone itself physically larger than the wavelength of the sound wave will result in the sound pressure indicated being close to zero (The reading will equal the summation across several nodes and antinodes). Hydrophones smaller than one quarter of a wavelength are extremely difficult to make and will only give the sound pressure amplitude at a very specific point in the sound field as the sound pressure varies sinusoidally between each half wavelength. Miniature thermistor probes coated with an ultrasound absorbing material (rubber or epoxy resin) have also been suggested as a means of measuring the ultrasonic intensity of a sound field [Martin and Law, (1980)] but once again calibration is required and problems may be encountered due to fluctuations in the liquid temperature.

In this study a method for the absolute determination of the sound pressure at any point in an ultrasonic sound field through the application of a light diffraction technique has been investigated as a means of determining the actual energy densities generated in the standing wave fields used during the experimental work of this thesis. Comparative investigations on the use of electrical power measurements and

hydrophonic measurements are also presented. The following sections consider each available method in turn and report on the research conducted and the conclusions drawn.

5.2 Electrical Power Measurement

Direct measurement of the electrical power used by the transducers could provide a simple method of estimating the ultrasonic power generated by the transducers (accounting for the transducer efficiency). However problems in measurement occur due to the nature of the signal required to drive the transducers. Firstly the frequency of the signals is much higher than the range of most simple multimeters and therefore it is very difficult to measure the current supplied to the transducers with such a device. Secondly the very low impedance of the ceramic transducers (a few ohms) causes difficulties because most measurement equipment operates at either 50 or 75 Ω and therefore the power used by the transducers cannot be measured by radio-frequency power meters operating at these impedances.

Although it was not possible to overcome these difficulties with the resources available to this project an electrical device was built to measure the ratio of the power travelling to the transducer, to the power being reflected from the transducer under standing wave conditions. As a direct result of mismatched impedances at 5 MHz and above, greater than 50% of the power supplied by the amplifier was found to be reflected from the transducers. Consequently very little power was actually available to the transducers at these frequencies. At 1 and 2 MHz as much as 20% of the power was reflected from the transducers.

5.2.1 Conclusions

It was concluded that measurement of the electrical power supplied to the ultrasonic transducers was an ineffective means of establishing the actual level of ultrasonic power generated by the piezoelectric ceramic transducers during experiments. The inefficiencies of the ultrasonic amplifier when attempting the difficult task of driving the ceramic transducers became apparent as a consequence of

the investigations described above and highlighted the need to measure the ultrasonic energy directly as a means of assessing the ultrasonic power used during experiments.

5.3 Hydrophonic Measurements

An extensive literature survey revealed the possibilities of using miniature ultrasonic hydrophones to investigate the properties of ultrasonic fields. This section describes the fabrication of miniature hydrophones and the experiments performed with the devices to determine the sound pressure amplitudes generated by the ceramic transducers used during separation experiments.

5.3.1 Introduction

Hydrophones can be described as underwater microphones. They operate by being sensitive to the variations of pressure in the fluid caused by the passage of a sound wave. At ultrasonic frequencies a piezoelectric material is required as the sensing element. Hydrophones have been made from piezoelectric ceramic materials in a wide range of sizes [Filmore and Chivers (1986), Moffett, Powers and Clay (1988) and Shorter and Bridge (1986)], however the need for very small dimensions when using hydrophones in megahertz standing wave fields means that the ceramic hydrophones are very difficult to manufacture. Piezoelectric polymeric materials such as polyvinylidene fluoride (PVDF) are easier to manipulate and allow the manufacture of very small sensing elements [Bacon (1981), DeReggi, Roth, Kenney, Edelman and Harris (1981), Habeger, Wink and Van Zummeren (1988), Lewin (1981), Lewin and Jensen (1979), Platte (1985), Sasady, Hartig and Bjorno (1979) and Shotton, Bacon and Quilliam (1980)]. The PVDF hydrophones can be made in two basic forms: membrane hydrophones and miniature probes. Membrane hydrophones consist of a piece of the PVDF polymer stretched over a former such as a plastic ring and are usually large with respect to the ultrasonic wavelength. Hydrophones in the form of miniature probes can consist of very small areas (1 mm^2) of PVDF material as the sensitive element positioned at the end of a fine tube or rod which allows their use in standing wave fields.

5.3.2 Experimental Procedure

During this study a number of small area hydrophone probes were assembled to the following design (See **Figure 5.1**) from PVDF polymer elements (KH–028K, Atochem Sensors Ltd., 22 Ridge Way, Hillend Industrial Park, Fife, Scotland). Some relevant properties of the PVDF film material are listed in **Appendix V**. The electrodes on the PVDF film were connected to fine platinum wires by silver loaded epoxy adhesive (RS Components Ltd) and the platinum wires joined to low loss coaxial cable. The PVDF film was then attached to the end of a steel tube which could be bent to any desired angle. The whole assembly was finally sprayed with a conformal coating lacquer which formed a thin water proofing layer over the hydrophone.

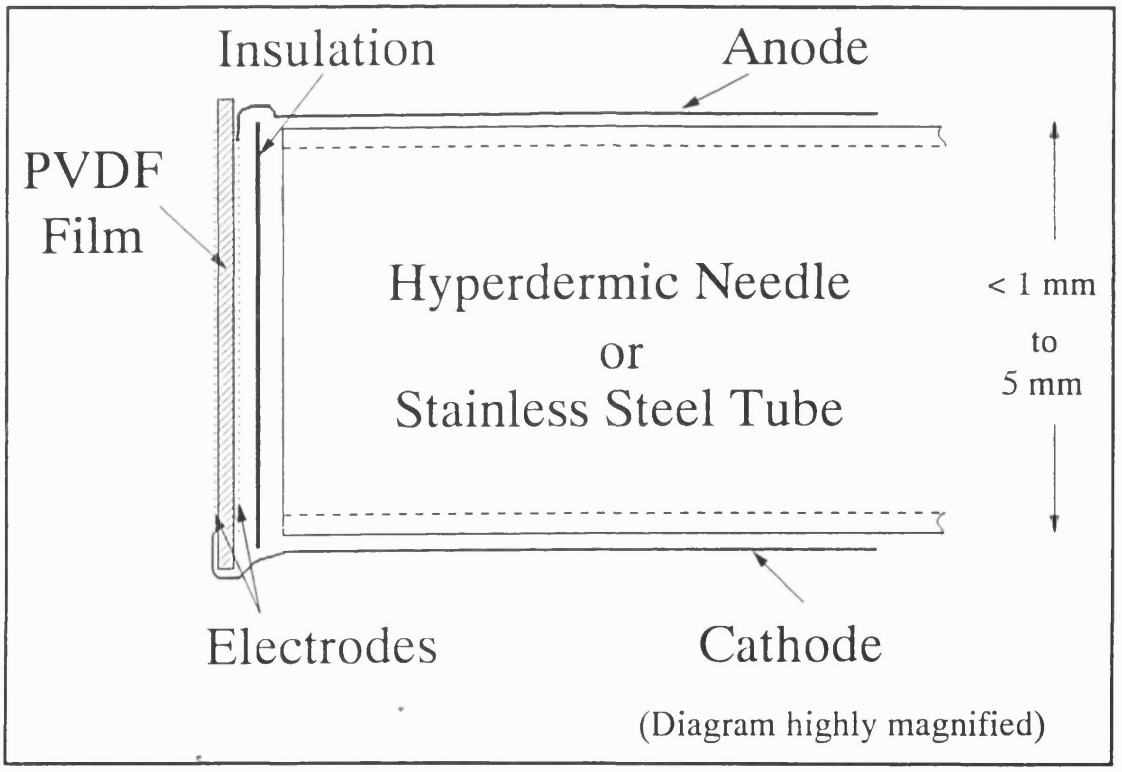

Figure 5.1 *Schematic Design of PVDF Hydrophone.*

A small high–frequency amplifier was also designed and assembled to allow the signal generated by the hydrophone to be sampled by the PC–30AT data acquisition board (Amplicon Liveline Ltd) installed in a personal computer. The

amplifier consisted of a ultra high-frequency op-amp (300-221, NE5539N, RS Components Ltd) combined with a printed circuit board (435-664, RS Components Ltd) and associated electronic circuitry allowing variable gain of the signal from the hydrophones (See **Section 3.3.4.2** and circuit diagram in **Appendix VII**).

The aim of the experiments using hydrophones was to determine the ultrasonic pressure amplitudes generated by the ultrasonic transducers when operating at known peak to peak driving signal voltages.

The ultrasonic transducers were placed in a water bath approximately 0.15 m in depth so that standing wave fields (or travelling wave fields) of the required length (0.20 m) could be formed. The hydrophone was placed in the water at set distances between the two transducers and the signal produced was either recorded on the personal computer or monitored with a Hitachi VC-6050 digital storage oscilloscope (Hitachi Denshi Ltd., Garrick Industrial Centre, Garrick Road, Hendon, London, U.K.).

5.3.3 Observations

Several problems were encountered when the hydrophones were used.

- The hydrophones suffered from electrical pick-up from the transducer driving signals that proved to be many times greater than the voltage generated by the hydrophonic detection of the ultrasonic field. Using screened cables to remove this problem was only of limited benefit. Separating the transducer and hydrophone by a non-conducting membrane dividing the water bath had no effect in reducing the electrical pick-up.

- The hydrophones were found to be highly directional and required very precise alignment, perpendicular to the propagation of the ultrasound, within the standing wave field to produce reproducible readings.

- It was not possible set up a truly travelling wave field within the water bath made for the hydrophone experiments. Reflections of the incident waves from rubber and foam materials used to absorb the ultrasound in an attempt to prevent standing

waves meant that partial standing waves were formed which caused a spatial variation in the sound field that once again necessitated very precise hydrophone alignment.

5.3.4 Conclusions

The use of hydrophones for the determination of ultrasonic energy generated by the transducers was found to be unsuitable in the present application due to the problems discussed in **Section 5.3.3**.

The considerable amount of work that would be required to overcome the problems described above was determined to be beyond the scope of the objectives of this study. However as outlined in the aims of this thesis the determination of the level of ultrasonic energy used to effect separation is of prime importance when considering the scale-up of equipment. Ultrasonic hydrophones do show promise in the measurement of sound pressure and future work involving such equipment is discussed in **Chapter 11** of this thesis.

5.4 Laser Light Diffraction

A third method for determining the ultrasonic intensity was experimentally investigated. The following section describes an investigation of the use of an optical method for the determination of the intensity of an ultrasonic beam travelling through water. The method allows the absolute determination of the ultrasonic intensity in a travelling or standing wave.

5.4.1 Introduction

The passage of a parallel beam of collimated light through an ultrasonic wave field can be used to measure the sound pressure amplitude at any point in the sound field. The theoretical background of the method will be described first.

5.4.2 Theoretical Background

This section is a brief account of the theory of ultrasonic diffraction of light as a means of determining ultrasonic intensity. An in-depth discussion of the theory of the ultrasonic diffraction of light is given by Raman & Nath (1935) and a comprehensive discussion of the practicalities of measuring the ultrasonic diffraction of light is given by Haran & Cook (1975).

A beam of ultrasound produces a periodic density variation in the medium of propagation. If a beam of collimated, monochromatic light is normally incident to the beam of ultrasound then the phase of the light will be retarded proportionally to the local sound pressure. The result is a Fraunhofer diffraction pattern in which the $\mathbf{n^{th}}$ order normalised light intensities $\mathbf{I_n}$ vary as shown in **Equation 5.1**.

$$I_n = J_n^2(\nu) \qquad \textbf{Eq. 5.1}$$

where $\mathbf{J_n}$ is the $\mathbf{n^{th}}$ order Bessel function and ν is a measure of the maximum optical phase retardation (known as the Raman-Nath parameter). The phase retardation, ν, is directly proportional to the local peak acoustic pressure.

The determination of ν from the light intensities of each of the diffraction orders can be accomplished by using two or more diffraction orders (See **Equation 5.1**) and values for the Bessel functions. This technique assumes that the acoustic waveform is a pure sinusoid. Bessel functions of argument ν are also defined by the recursion relation described in **Equation 5.2**.

$$\nu\,(J_{n-j} + J_{n+j}) = 2n \cdot J_n \qquad \textbf{Eq. 5.2}$$

When the two equations above are combined, the parameter ν may be calculated from the normalised light intensities.

Relating the experimentally determined values of the phase retardation ν to the acoustic power requires some knowledge of the influence the acoustic field radiated by a plane piston source has on the integrated optical effect. It has been shown [Ingenito & Cook, (1969)] that for a circular piston of radius **a** and centred on the **z** axis, the optical phase retardation is given by:

$$\nu(z) = \nu_0 \left(\frac{ka}{2}\right) \cdot \left(\frac{\pi}{2k\eta}\right)^{1/2} \cdot J_0^2 (k\xi)^{1/2} \qquad \textbf{Eq. 5.3}$$

where

$$\nu_0 = \frac{4\pi u_0 \rho_0 c a \kappa}{\lambda_1} \qquad \textbf{Eq. 5.4}$$

$$\xi = \frac{(z^2 + a^2)^{1/2} - z}{2} \qquad \textbf{Eq. 5.5}$$

$$\eta = \frac{(z^2 + a^2)^{1/2} + z}{2} \qquad \textbf{Eq. 5.6}$$

and $\mathbf{J_0}$ and $\mathbf{J_1}$ are zero and first-order Bessel Functions, κ is the wave number of the sound. **Equations 5.3** and **5.4** apply to a transducer of velocity amplitude $\mathbf{u_0}$ radiating into a semi-infinite nondissipative medium of density ρ_0 and sound velocity $\mathbf{c_0}$, λ_1 is the wavelength of the light and **k** is the adiabatic piezo-optic coefficient. The term ν_0 is a measure of the phase retardation at the source (ie **z=0**).

With **Equation 5.3** one may experimentally determine ν at some finite distance from the face of a source and simply convert back to the value ν_0 at the face of the crystal. The assumption that $\kappa\mathbf{a}$ is large and that $\mathbf{p = u_0 c \rho_0}$ permits ν_0 to be written as

$$\nu_0 = \frac{2\pi L p \kappa}{\lambda_1} \qquad \textbf{Eq. 5.7}$$

where **L** is the source diameter (**2a**) and **p** is the peak acoustic pressure.

Equation 5.8 gives the total acoustic power output **P** in terms of the measured parameter ν.

$$P = \left(\frac{1}{2\pi\rho_0 c}\right) \cdot \left(\frac{a\lambda_1}{2L\kappa}\right)^2 \nu_0^2 \qquad \textbf{Eq. 5.8}$$

(ν is determined from **Equation 5.1** or **Equation 5.2** and substituted into **Equation 5.3** thereby determining ν_0 which is then substituted into **Equation 5.7** or **Equation 5.8** to give the total acoustic power output , **P**.)

It must be noted that this experiment must be performed in the far–field zone as **Equation 5.3** is only valid in the optical phase grating region or far–field region of the sound wave.

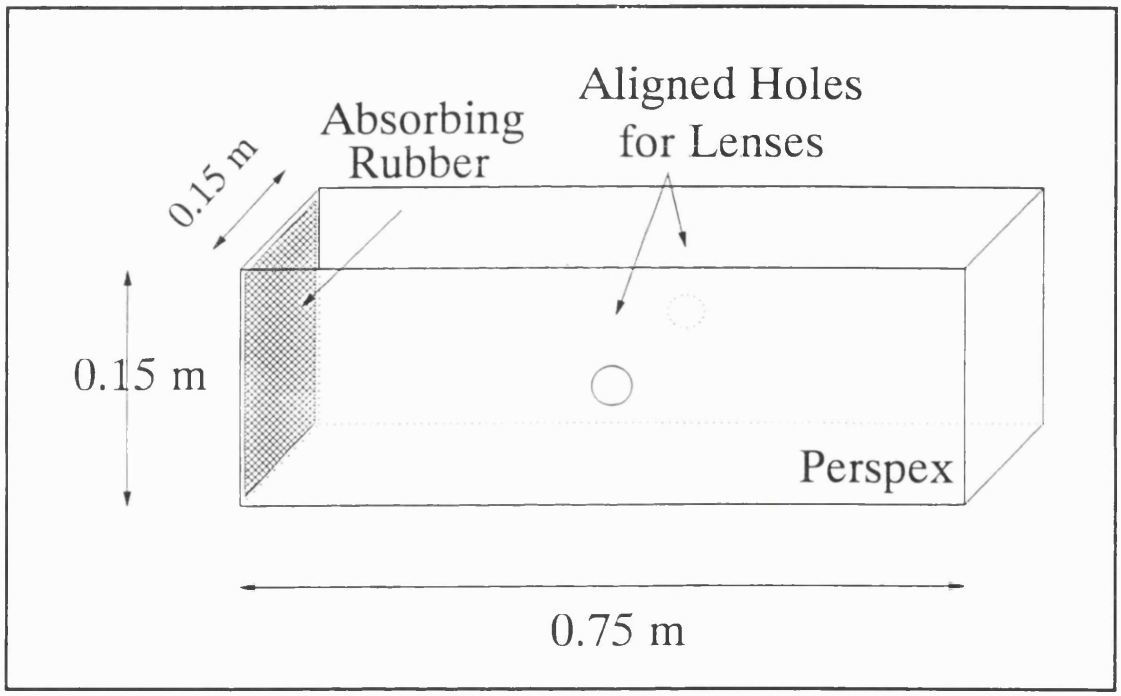

Figure 5.2 *Perspex Tank Used in Diffraction of Laser Light Experiments to Determine Ultrasonic Power.*

5.4.3 Apparatus Design

The design of the experimental apparatus was based around an optical system composed of a laser diode and several lenses used to expand and to collimate the laser light emitted by the diode which then passed as a parallel beam through the sound field before being refocussed ready for detection with a photodetector. The optical system is schematically described in **Figure 5.3**.

A rectangular, perspex water–tank (as shown in **Figure 5.2**) was constructed to contain an ultrasonic beam of sufficient length to allow the light diffraction

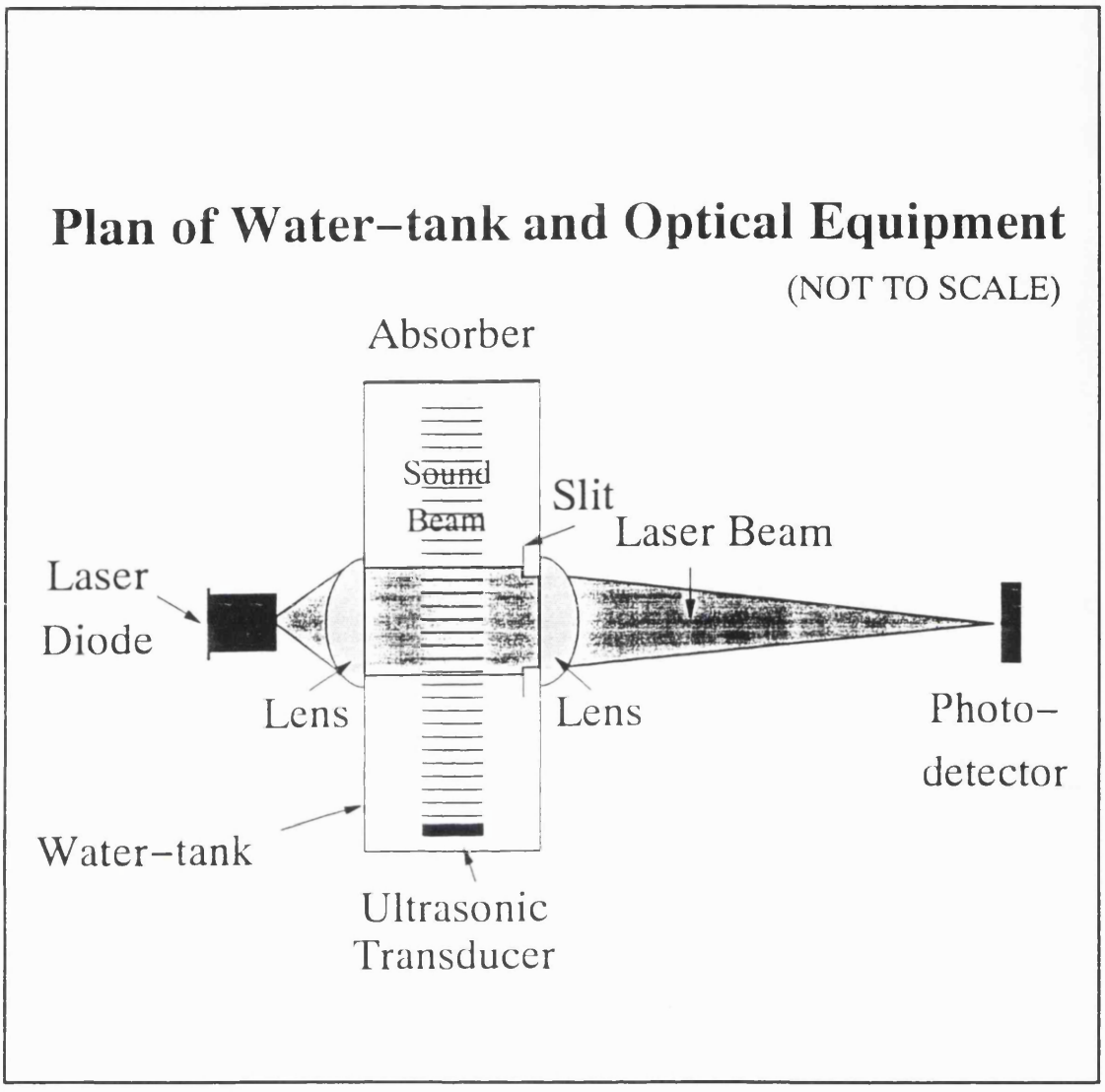

Figure 5.3 *Schematic Diagram of Optical System for Laser Diffraction Studies.*

experiments to be performed at several distances from the transducer face.

Two concentrically aligned 20 mm diameter holes were drilled through the longest sides of the water–tank to permit two lenses to be mounted in the walls of the tank. The lenses were 20 mm diameter plano–convex glass lenses (Melles Griot Ltd.); the lens on the front wall had a focal length of 25 mm and the lens on the far wall had a focal length of 100 mm. The diameter (20 mm) and focal length of the first lens (25 mm) were chosen to collect the diverging laser light emitted by a laser diode placed 25 mm in front of the lens which then produced a parallel beam of laser light approximately 12 mm in diameter. The parallel beam then travelled through the tank and ultrasonic field, through a 12 × 1 mm slit to remove stray reflected light, and

through the opposite lens which reconverged the light to a focal point 100 mm away where it fell upon a photodetector.

A 30 milliwatt laser diode (Access Pacific Ltd, Kymbrook School House, Kimbolton Road, Keysoe, Bedford, U.K.), operating at 780 nm, was driven by a circuit which allowed the control of the output power of the diode (See **Section 7.4**) and was mounted in a die-cast aluminium box (RS Components Ltd.)

5.4.4 Experimental Procedure

A 25 mm diameter, 2 MHz transducer was chosen to produce the ultrasonic field for the evaluation of the experimental apparatus due to the relatively short length of the near field generated by the transducer which would enable both the near and far field to be investigated with the laser beam. The transducer was water-proofed and mounted on a duralinium mounting block (See **Section 3.3**) which was then screwed into a right angled piece of aluminium which stood on the floor of the water-tank.

The laser beam was passed through the water-tank prior to sonication so as to measure the total intensity of the light at the focal point and thereby relate the intensity of each point (or order) of the diffraction pattern, produced by the interaction of the laser beam and ultrasonic beam, to this total intensity measurement. The transducer was then driven by a 20 volt peak to peak signal (the lowest possible with the 2 MHz transducer) from the Audley Scientific Dual Ultrasonic Amplifier producing a travelling ultrasonic wave field through the water in the tank. The laser beam was passed through the central axis of the ultrasonic beam and focused onto a white card so as to determine the position of the exact focal point and to examine the diffraction pattern produced by the passage of the laser beam through the sound field. This procedure was repeated several times, each time passing the laser beam through the ultrasonic beam at a different distance from the ultrasonic transducer.

5.4.5 Observations and Discussion

A diffraction pattern was only visible at the very highest transducer voltage of 48 volts peak to peak and was only discernable as a widening of the original focused

spot. The diffraction pattern produced did not vary with the distance of the laser beam from the face of the transducer. It was not possible to identify the different orders of the diffraction pattern and further more the widening of the laser spot was not symmetrical on either side of the zero order position suggesting that at the high transducer voltages there was significant distortion of the ultrasonic wave. This distortion would have made it extremely difficult to determine the intensity of the ultrasonic wave as the theoretical relations used for this purpose depend upon the assumption that the wave is purely sinusoidal.

The resulting diffraction pattern was improved somewhat by increasing the focal length of the second lens in the system to 200 mm. However it remained impossible to distinguish the individual orders of the pattern and hence to measure the light intensity at each order.

5.4.6 Conclusions

It was concluded that the apparatus constructed to perform the experiments would require a great deal of development to allow the intensity of the ultrasonic wave to be determined. The distortion of the waveform encountered at the highest transducer voltage would have prevented the determination of the ultrasonic intensity by this method and therefore limited its application to relatively low levels of transducer driving voltage.

5.5 Overall Conclusions.

The preceding sections have described the problems faced when attempting to measure the ultrasonic power generated by a pair of piezoelectric ceramic transducers using a variety of methods. None of the methods investigated (electrical power measurement, hydrophonic measurements and optical diffraction measurements) gave satisfactory results. It was concluded that exact measurement requires highly sophisticated electronics and was beyond the scope of this project.

For the purposes of recording the levels of ultrasonic energy used during experiments it was decided to measure the voltage supplied to the transducers by

means of a Hitachi VC-6050 digital storage oscilloscope (Hitachi Denshi Ltd., Garrick Industrial Centre, Garrick Road, Hendon, London, U.K.) and to use this as a direct measure of power input. This may tend to over-estimate the ultrasonic power input to the system, especially at the higher frequencies, due to the inefficiencies of the amplifier and the mismatching of the transducers to the amplifier.

The next section of work discusses the use of ultrasonic standing waves for the separation of biological suspensions and uses results from previous chapters (**Chapters 4 & 5**) to formulate an engineering design framework for the design and operation of ultrasonic separators.

CHAPTER 6 ULTRASONIC SEPARATION

6.1 Introduction

This chapter describes work using a novel ultrasonic separation device which incorporates design features developed to overcome the problems associated with the earlier experimental apparatus described in **Chapter 4**.

The following section details the design features of the device and **Sections 6.5.1** to **6.5.7** describe the experiments performed to investigate the operational limits of a small scale ultrasonic separation device.

6.2 Equipment Design

The ultrasonic separator design included a number of features, listed below, that reduce the probability of acoustic streaming and heating of the sample process liquid each of which is detrimental to the efficient application of ultrasonic standing waves to effect the separation of biological particles.
The main features of this design were as follows:

- The small internal diameter of the tube (5 mm). The small diameter of the tube compared with the diameter of the ultrasonic transducers (20–25 mm) reduces the problems associated with acoustic streaming of the fluid by ensuring that the amplitude of the sound waves did not vary greatly across the cross section of the tube hence creating a uniform field within the test apparatus.

- The glass tube was positioned over the axes of the transducers – the area of maximum amplitude generation. Alignment with the central axis may be expected to generate an even sound pressure profile by excluding the troughs of vibration amplitude found at certain radii of the transducers (See **Figure 6.1**)

- The test liquid was separated from the transducers by water baths containing degassed water (See **Section 3.6**). The water absorbed any heat produced by the transducers through electrical inefficiency whilst providing excellent transmission of

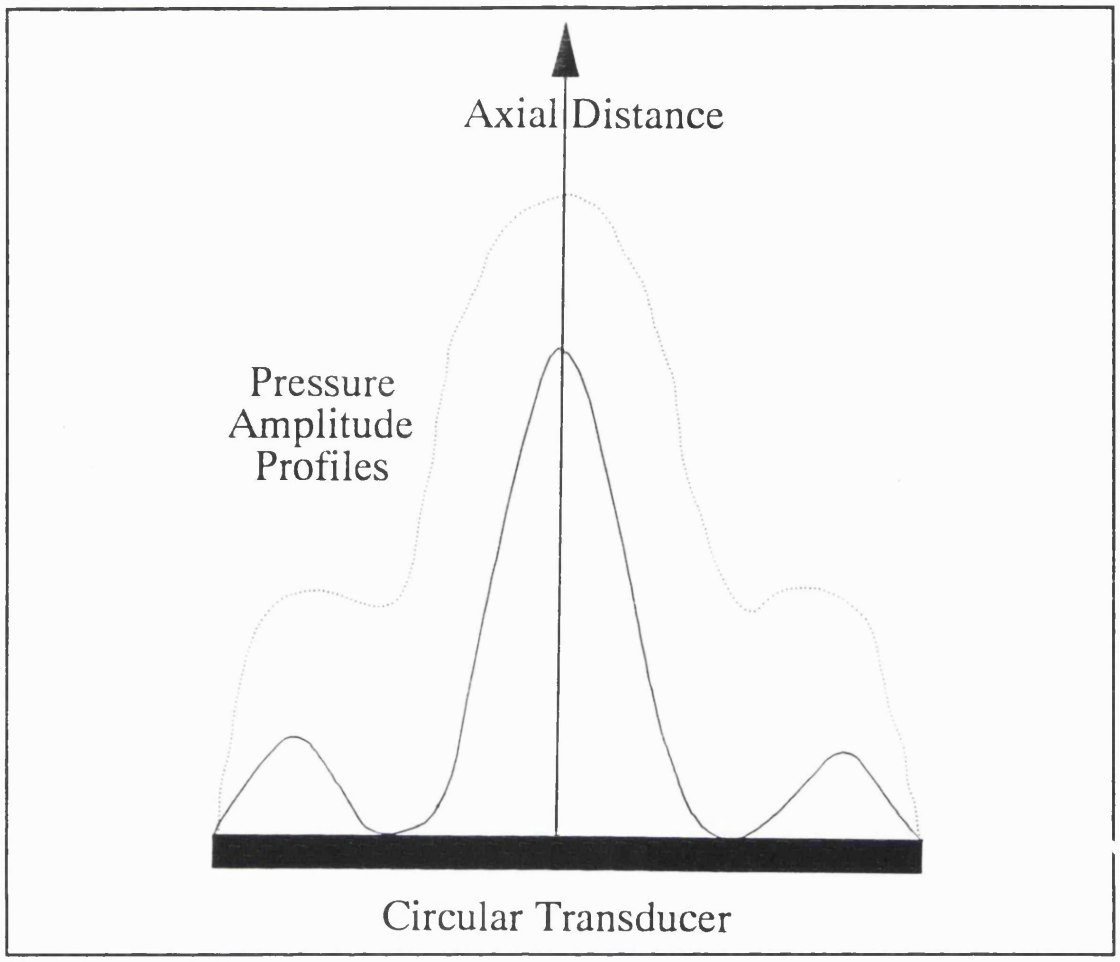

Figure 6.1 *Sound Pressure Amplitude Across the Face of a Circular Transducer.*

the ultrasonic waves. Degassing the water was necessary to prevent cavitation and the formation of bubbles on the glass tube as the dissolved gas in the water is removed from solution by the ultrasound. The bubbles would have caused random reflections of the ultrasonic waves, disrupted the standing wave pattern, and led to acoustic streaming effects.

● The upper transducer was mounted on a micropositioner (411–05s, Newport Ltd, Pembroke House, Thompsons Close, Harpenden, Hertfordshire, UK) which allowed the distance between the two transducers to be adjusted with an accuracy of ± 1 μm. Although it was not necessary to operate this ultrasonic separation device with the two transducers spaced at an exact multiple of the half wavelength, exploratory experiments had shown that doing so adds stability to the standing wave

field when moving concentrated bands of particles by phase shifting (See **Section 3.3.3**).

- The glass tubing was not permanently attached to the stand and could be exchanged for another manufactured of a different material (e.g. acrylic) or with alternative port arrangements thus allowing many different experiments to be performed on the same apparatus (See **Section 6.4.3**).

- Since the transducers could be removed it was possible for the separator to be used to experiment with various transducers of different resonant frequencies and different dimensions (See **Section 6.4.2**).

6.3 Experimental Aims

There were several objectives to this section of experimentation :

- To compare the theoretically determined minimum particle size and minimum ultrasonic power limit of ultrasonic particle aggregation with experimental observations.
- To study particle migration with relation to ultrasonic standing wave fields of different frequencies (1, 2, 5, and 10 MHz) and intensities.
- To confirm that particle migration in a standing wave field is possible with particles and suspending liquid of identical densities.
- To measure the fluid velocity perpendicular to the standing wave field required to remove particles from the banding position by causing viscous drag forces to exceed the radiation pressure exerted on the particle and similarly to determine the maximum and optimum particle velocities achievable through the application of phase shifting.
- To assess the efficiency of removal of particles from a liquid using ultrasonic standing wave and phase shifting technology.

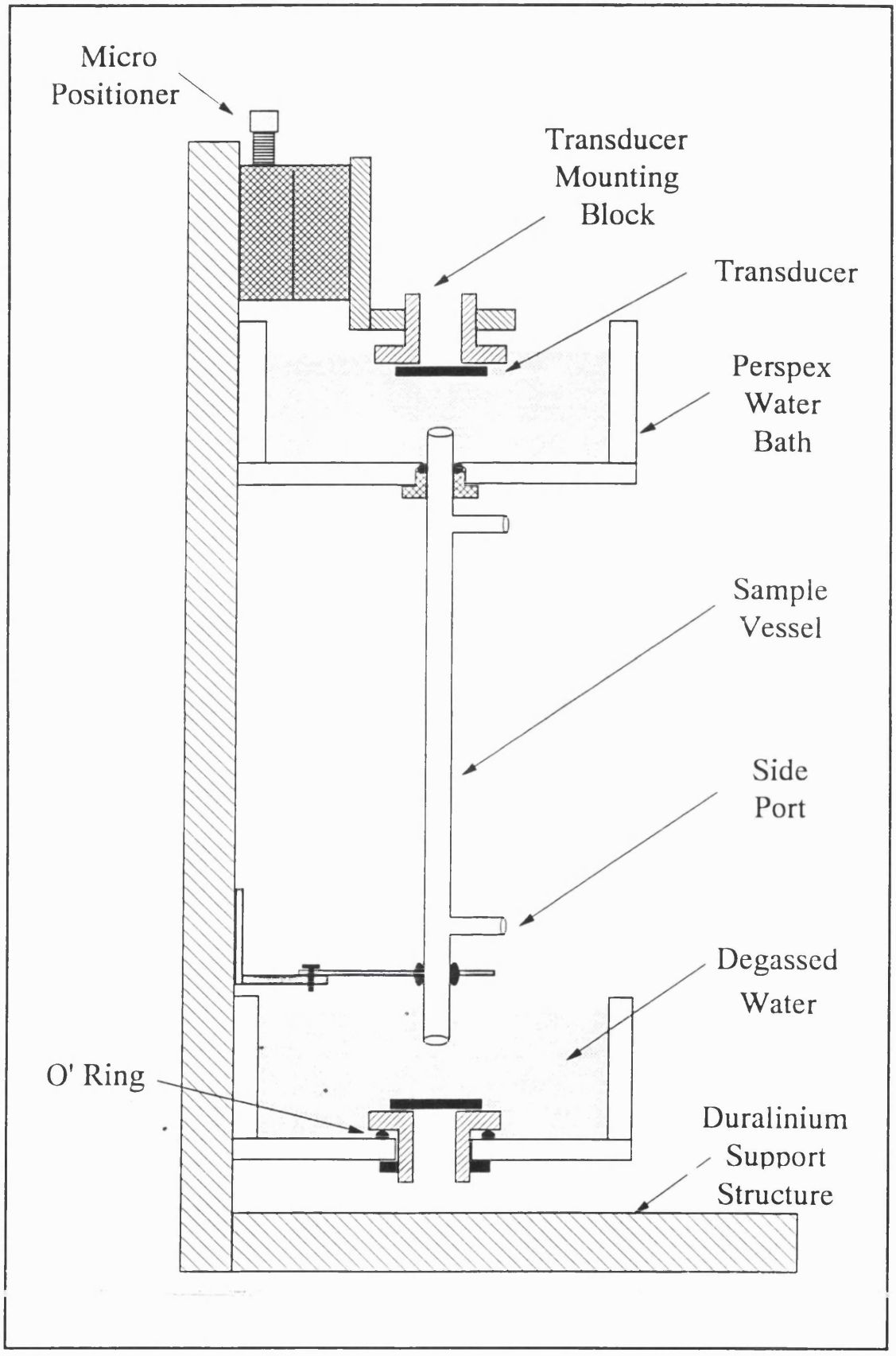

Figure 6.2 *Schematic Diagram of Ultrasonic Separation Apparatus.*

6.4 Materials and Method

This section describes the equipment and procedures used to perform the experiments outlined in **Section 6.3**.

6.4.1 Transducer Mounting

The piezoelectric ceramic transducers were cemented on to specifically designed aluminium mounting blocks that could be screwed into the separation apparatus.

The aluminium mounting blocks (See **Section 3.3.1, Figure 3.4**) were designed so that several different sizes and types of ultrasonic transducer could be used in the same piece of apparatus. The design allows for the ceramic transducers to be supported by the front face of the mounting block but that the majority of the transducer is backed by air to provide more efficient transmission of ultrasonic energy from the opposite face (See **Section 3.3**). Each transducer was cemented onto the aluminium with a two-part heat conducting adhesive (553-251, RS Components Ltd, Corby, Northants, UK.) that also provides electrical insulation and a water proof seal between the transducer and the aluminium block. A heat conducting adhesive was chosen to provide a small degree of heat sinking to the transducer mounting blocks and to the structure of the separation device.

6.4.2 Ultrasonic Transducers

The source of ultrasound used in this set of experiments (See **Section 6.5**) were PC4 material (lead titanate zirconate) piezoelectric ceramic transducer discs (Morgan Matroc Ltd.,Unilator Division, Ruabon, Wrexham, Clwyd, Wales.).

Transducers of four different resonant frequencies were used in the following experiments, 1, 2, 5 and 10 MHz approximately (See **Appendix I**). The transducers were mounted as described in **Section 6.3.1** and then sprayed with a conformal coating preparation commonly used in the manufacture of electronic circuit boards. The conformal coating provided a long lasting, resilient water proof layer that also

insulated the transducer preventing shorting of the electrical supply (567-682, RS Components Ltd., Corby, Northants, UK).

6.4.3 Design of Glass Sample Tube

Glass tubes of various geometries (See **Figure 6.3**) were fabricated by the glass blower in the Department of Chemistry, UCL. Each glass tube was designed to allow a specific mode of operation to be investigated. For example tube **(a)** in **Figure 6.3** was designed as a simple flow cell in which the suspension of particles was made to flow along the tube in the direction of propagation of the sound field. Tube **(b)** was constructed with an extra side arm thereby facilitating the continuous removal of two separate fractions of the flow of liquid. This arrangement could be used to separate a suspension into a concentrated suspension of particles and a clarified stream of liquid. Diagram **(c)** describes a more complex arrangement where the suspension entry port is adjacent to one of the exit ports and separated by a thin wall. The purpose of this design was to enable the maximum length of the glass tube and therefore the maximum number of nodal planes to be used to maximise the ultrasonic separation effect when performing the separation of different particle sizes.

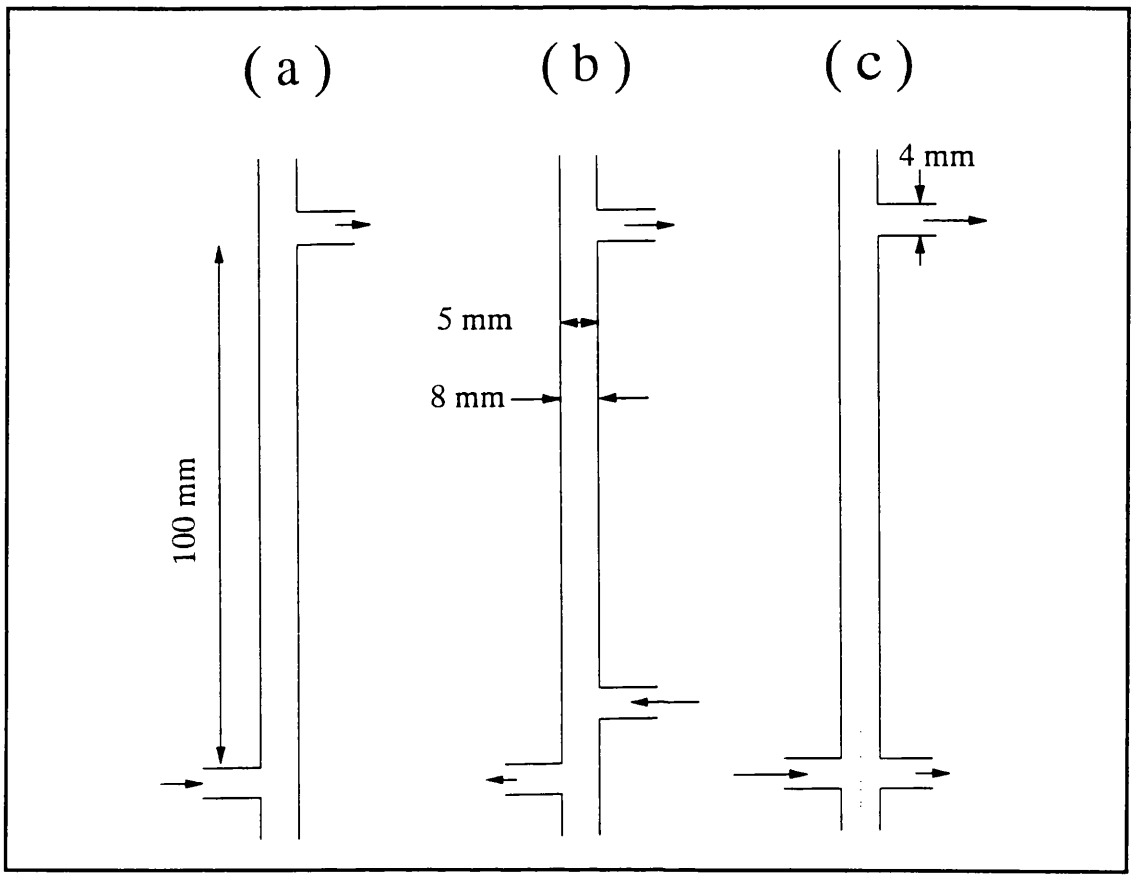

Figure 6.3 *Design of Glass Tubes Used as Ultrasonic Separation Vessels.*

6.4.4 Sample Preparation

Before experimenting with complex biological particles it was necessary to characterise the possible separation achievable with this apparatus by experimenting with particles of known properties. Particle diameter and density are the two most important parameters affecting the radiation pressure force acting on a particle in an ultrasonic standing wave field. It was decided to use polystyrene latex particles (Park Scientific Ltd [Polysciences], 24 Low Farm Place, Moulton Park, Northampton, UK.) because of their narrow size distribution, monodispersity and near constant density of 1050 $kg.m^{-3}$.

The polystyrene particles were supplied as suspensions 2.5 w/v % in water. Details of the particles used are given in **Appendix III**. The concentrated suspensions of latex beads were accurately diluted with 0.1 μm filtered, deionised water and the actual number concentration of particles was measured on an Elzone Particle Analyzer (See **Section 3.2.1**). For particles below the minimum size range of the Elzone (a

particle diameter of approximately 0.5 μm), the particle concentration was calculated by taking turbidity measurements of the suspensions on a spectrophotometer (Perki-Elmer Lambda II, Perkin-Elmer Ltd., Post Office Lane, Beaconsfield, Buckinghamshire, U.K.) at a wavelength of 700 nm and comparing the readings with a calibration curve constructed by accurate dilutions of suspensions of known weight concentration. The particle size distribution was also studied on two other devices the Brookhaven DCP 100 disc centrifuge particle analyzer (Brookhaven Instruments Corporation, 750 Blue Point Road, Holtsville, New York, USA) and the Malvern 4700 Sub-micron Particle Analyzer (**Section 3.2**). It was necessary to resort to three different particle analyzers and methods because of the different limitations of each of the methods (See **Section 3.2**). For example the minimum particle size measured accurately with the Elzone Particle Analyzer is approximately 0.5 μm, whereas the Brookhaven and Malvern instruments can measure particle sizes below 0.1 μm but do not measure the concentration of the particle suspension as is possible on the Elzone instrument.

Suspensions of whole yeast cells were made by mixing samples taken from blocks of Baker's yeast with volumes of potassium phosphate buffer to the concentration required in the experiments (See **Sections 3.4.2.2 & 3.4.2.3**). The suspensions of yeast were spun down in a centrifuge and washed with fresh buffer to remove cell debris and other matter included in the original blocks of yeast.

Yeast homogenate was prepared using an APV Lab 60 homogeniser from an initial 60 wt % (wet basis) suspension of whole Baker's yeast cells and diluted with phosphate buffer to the desired concentration to be used in the separation experiments. The typical procedure used to produce the homogenate is described in **Section 3.4.2.4**.

6.4.5 Phase Shifting

The standard method employed during the following experiments (See **Section 6.5**) was to introduce a standing wave field into the suspension held in the glass sample tube to cause the particles to accumulate at the nodal areas of the standing wave field. Once particle accumulation has been achieved there are a number of different ways of removing the liquid phase from the particles.

- Flow the suspension through the sound field thus retaining the particles at the nodes and producing a stream of clarified liquid.

- Physically move the vessel containing the suspension through the sound field thereby forcing the particles to one particular position in the vessel to facilitate removal of the particles.

- Allow the increased concentration of the particles at the nodes of the sound field to accelerate the rate of sedimentation of the particles by intermittently removing the ultrasonic standing wave field from the suspension and allowing sedimentation to occur.

However in this study a more sophisticated, practical and controllable method of moving the particles with respect to the fluid was used. Since the electrical signals delivered to the transducers are generated and amplified electronically it is therefore possible to create a device to alter the phase of one of the signals being amplified. Changing the phase of one signal with respect to the other causes the nodes of the standing wave field to move between the two transmitting transducers at a speed determined by the rate of phase shift. The sound field is not then a true stationary wave but a pseudo-standing wave. If the nodes are moved slowly then the particles accumulated at the nodes may be expected to also move through the liquid. The theoretical maximum rate of movement will be equal to the velocity at which the Stokes' drag force (See **Section 2.3.2.2**) on the particle equals the radiation force holding the particle at the node (assuming that the radiation pressure is the only ultrasonic force acting on the particle). **Equation 6.1** describes the Stokes Drag Force on a spherical particle; **Equation 6.2** represents the radiation pressure on the spherical particle.

$$F_D = 6 \pi \mu a u \qquad \textbf{Eq. 6.1}$$

$$F_P = 4\pi\kappa a^3 \overline{E} F \sin(2\kappa z) \qquad \textbf{Eq. 6.2}$$

If the Stokes Drag Force and the Radiation Pressure equations are equated then the result is **Equation 6.3** which describes the theoretical maximum particle velocity U_{MAX} achievable through phase shifting (Assuming the particle is at the antinode; which is acceptable as the particles will have migrated to the antinodes under the influence of the radiation pressure).

$$U_{MAX} = \frac{2\kappa a^2 \overline{E} F}{6\mu} \qquad \textbf{Eq. 6.3}$$

Figure 6.4 is a plot of U_{MAX} versus particle radius.

Phase shifting was accomplished through the use of an Audley Scientific phase shifting device which was controlled by a personal computer via a data acquisition–control board. Short computer programs are required to use the phase shifting device (See **Appendix V** for listing of program). In this study only a relatively simple shifting algorithm was investigated. However there is substantial scope for writing complex control programs to enhance the separation being performed (See **Section 11.6**).

6.4.6 Fluid Flow

The suspensions of particles being studied were pumped through the glass tube of the ultrasonic separator by a micro peristaltic pump (Eyela MP–3, Microtube Pump, Tokyo Rikakikai Co. Ltd., Tokyo, Japan). The flow rate delivered by the pump was adjustable to a fine degree the range of 0.03 to 3 $L.h^{-1}$ through the use of 1 mm and 5 mm bore silicon rubber tubing. The range of fluid velocities used during the experiments was between 0 and 0.015 $m.s^{-1}$. The typical Reynolds Number for the flow of liquid through the tube was of the order of $10^1 - 10^2$.

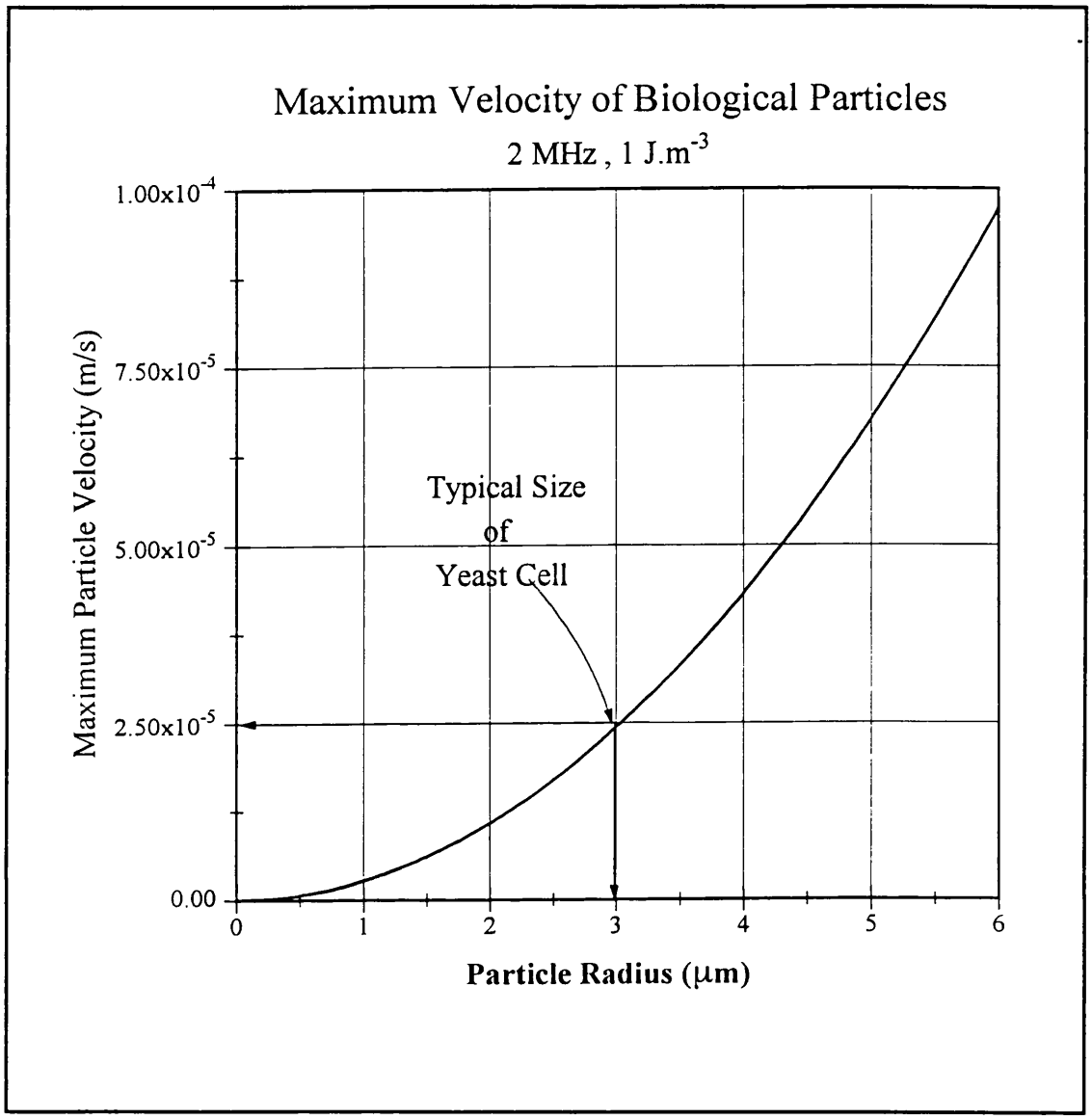

Figure 6.4 *Plot of U_{MAX} versus Particle Radius.*

6.5 Experimental Procedures

This section describes the various experimental procedures used to accomplish the objectives (**Section 6.3**) set out prior to the sections on design and construction of the ultrasonic separator. All experiments were conducted on the ultrasonic separation apparatus described in **Figure 6.2**.

6.5.1 Minimum Particle Size Limit for Aggregation

The following experiments were performed to determine the size of the smallest particles that could be forced to migrate to the nodes of an ultrasonic standing wave field.

6.5.1.1 Method

The experimental apparatus was assembled as is described in **Section 6.1**. The following experiments were performed using ultrasonic transducers of four different resonant frequencies; 1.0 MHz, 2.0 MHz, 5.0 MHz and 10.0 MHz (See **Appendix I**).

Suspensions of polystyrene latex particles of similar weight percent concentration were prepared by dilution with deionised water (See **Section 6.4.4**). The suspension under investigation was then pumped into the glass tube of the ultrasonic separator with care being taken to exclude any air bubbles as noted earlier in **Section 6.2**.

The glass tube and particle suspension were insonated for 30 seconds only during which time the suspension was observed for visible signs of particle aggregation at half wavelength spacing of approximately 0.74 mm, 0.37 mm, 0.15 mm and 0.075 mm, at frequencies of 1.0, 2.0, 5.0,and 10.0 MHz respectively.

The voltage of the transducer driver currents were monitored during the experiments using a Hitachi VC-6050 digital storage oscilloscope (Hitachi Denshi Ltd., Garrick Industrial Centre, Garrick Road, Hendon, London, U.K.). During the experiments using the 1 and 2 MHz transducers the voltage was maintained at 40 volts peak to peak. The dual ultrasonic amplifier was not able to provide enough power to drive the 5.0 and 10.0 MHz transducers above 10 volts peak to peak and therefore during these experiments the transducers were driven at the maximum amplifier output at 5 and 10 MHz, which were 17 and 5 volts respectively.

The sizes of particles used in this experiment were 0.06 μm, 0.16 μm, 0.73 μm, 0.99 μm, 3.09 μm, 5.83 μm and 9.21 μm. The properties of the particles are listed in **Appendix III**.

6.5.1.2 Results

During the experiments the appearance of the suspension was recorded along with the elapsed time to the onset of visible banding. If no particle aggregation was observed after an insonation period of 30 seconds then it was determined that negligible particle aggregation had been obtained at the relevant particle diameter and sound intensity. Each set of experiments was repeated and the average recorded. Values of Banding threshold times were found to be within ± 5%.

The results of several repeat experiments are displayed **Table 6.1**.

Samples	Banding Threshold Time (seconds)			
Particle Diameter	1 MHz 40 volts	2 MHz 40 volts	5 MHz 17 volts	10 MHz 5 volts
0.06 μm	No Banding	No Banding	No Banding	No Banding
0.16 μm	> 45	20	No Banding	No Banding
0.73 μm	17	5.2	No Banding	No Banding
0.99 μm	4.6	3.0	15	No Banding
3.03 μm	2.25	0.9	7.2	No Banding
5.55 μm	0.9	0.5	5.1	No Banding
9.21 μm	0.5	0.1	2.0	>40

Table 6.1 *Banding Threshold Times for Polystyrene Latex Particles in Deionized Water and Different Frequency Standing Wave Fields.*

The results displayed in **Table 6.1** show that particle aggregation was observed at all particle diameters, other than at 0.06 μm, when the ultrasonic standing wave field was applied at the frequencies of 1.0 and 2.0 MHz. This suggests that the minimum diameter of a polystyrene particle that can be manipulated with an ultrasonic standing wave field is somewhere between 60 and 160 nm. This range is in agreement

with the 100 nm diameter limit quoted by Higashitani *et al* (1981) and the theory put forward that particles below this diameter experience diffusional forces that are similar or greater in magnitude than the ultrasonic forces impinging on the particle (See **Section 2.3.3.3**).

The time required to create concentrated bands of particles decreases rapidly with increasing particle diameter and also decreases with the increase in frequency from 1 to 2 MHz. For the frequencies above 2 MHz the unavoidably reduced transducer voltage used during the experiments means that a direct comparison with the results obtained at 1 and 2 MHz would not be strictly valid.

At 10 MHz frequency the half wavelength distance is only 75 μm and together with the fact that the concentrated bands of particles that would be formed at this frequency would only contain the particles migrated from a very much smaller volume of suspension than at other frequencies means therefore that any banding pattern formed would have been very difficult to see with the naked eye and possibly only visable when particle migration had reached its full extent. A magnifying lens was used to examine the suspensions in the standing wave field, but banding was only evident with the 9.21 μm particles.

6.5.1.3 Conclusions

The experiments described above have shown that the migration of fine particles to the nodes of a standing wave field is achievable for polystyrene particles with diameter greater than 160 nm when transducer voltages of the order of 40 volts peak to peak are employed.

The frequency of the standing wave field employed is of obvious importance and is the subject of experimentation in the following section.

6.5.2 Frequency Dependency of Particle Migration

The aim of the following experiments was to study the effect of the frequency of the ultrasonic standing wave field on the aggregation of polystyrene latex spheres within the constraints imposed by the experimental apparatus.

According to theoretical relations (See **Section 2.3.2.1**) the radiation pressure exerted on a spherical particle in an ultrasonic standing wave field is linearly proportional to the frequency of the sound waves forming the standing wave field. To examine this relationship the following experiment was performed.

6.5.2.1 Method

Suspensions of 0.16 to 9.21 μm diameter polystyrene latex particles were prepared as described in **Section 6.4.4** the concentration of each suspension was measured on an Elzone Particle Sizer (See **Section 3.2**).

The following procedure was repeated using each of the 1, 2 and 5 MHz transducers. The experimental apparatus was set up as described in **Section 6.1**. The suspension of polystyrene latex particles was pumped into the glass tube of the separator expelling all air bubbles. The amplifier was set to deliver 20 volts peak to peak to each of the transducers used in the experiments.

The following parameters were examined :

- Time taken for visible banding to occur.
- Maximum effective fluid velocity possible during separation before particle segregation is disrupted.
- The efficiency of the separation[1] achieved.

The fluid velocity used in all separation efficiency experiments was 1.7×10^{-3} $m.s^{-1}$. The procedure was then repeated for each set of different diameter particles.

---

[1] The eficiency is determined by measuring the concentration of the particles in the fluid leaving the standing wave field and comparing the particles removed, as a percentage, with the concentation of the feed stream entering the standing wave field.

6.5.2.2 Results

The results of repeated maximum fluid velocity and separation efficiency experiments are shown in **Table 6.2** and **Table 6.3** and the banding time experimental results are displayed in **Figure 6.5**.

Particle Diameter (μm)	Maximum Fluid Velocity ($\times 10^{-3}$ m.s^{-1} $\pm$ 0.1 $\times$ 10^{-3} m.s^{-1}) at 20 volts peak to peak.		
	1 MHz	2 MHz	5 MHz
0.16	0	0	0
0.73	0	0	0
0.99	0.7	0.8	0
3.03	1.5	1.7	0.8
5.55	1.7	2.5	3.2
9.21	2.5	3.2	4.1

Table 6.2 *Results of Experiments on the Frequency Dependency on the Maximum Permissable Fluid Velocity through the Standing Wave Field.*

Particle Diameter (μm)	Separation Efficiency (%) ± 2%, at 20 volts peak to peak.		
	1 MHz	2 MHz	5 MHz
0.16	0	0	0
0.73	0	2	0
0.99	2	4	2
3.03	20	92	4
5.55	80	96	96
9.21	98	99	99

Table 6.3 *Results of Experiment to Determine the Separation Efficiency of Various Particle Sizes as a Function of Ultrasonic Frequency.*

The results of the experiments studying the effect of ultrasonic frequency on the maximum fluid velocity permissable through the standing wave field and on the separation efficiency, listed in **Table 6.2** and **Table 6.3** respectively, show that frequency has a strong influence on the segregation of particles in a standing wave field. The results of experiments performed at 1 MHz are significantly poorer than those performed at 2 MHz with a reduction in both the separation efficiency and the maximum effective fluid velocity through the sound field.

The results of the experiments performed at 5 MHz, and the maximum voltage that was possible (17 volts peak to peak), show that at larger particle diameters the segregation effect is more pronounced than at both 1 and 2 MHz frequency. However this superior effect is not evident at the lower particle diameters (less than 3 μm) and this result is possibly due to an effect of the very much closer banding positions at this frequency. The heterogeneities in the standing wave fields formed in the apparatus mean that particles are less strongly influenced by the ultrasound in some areas than

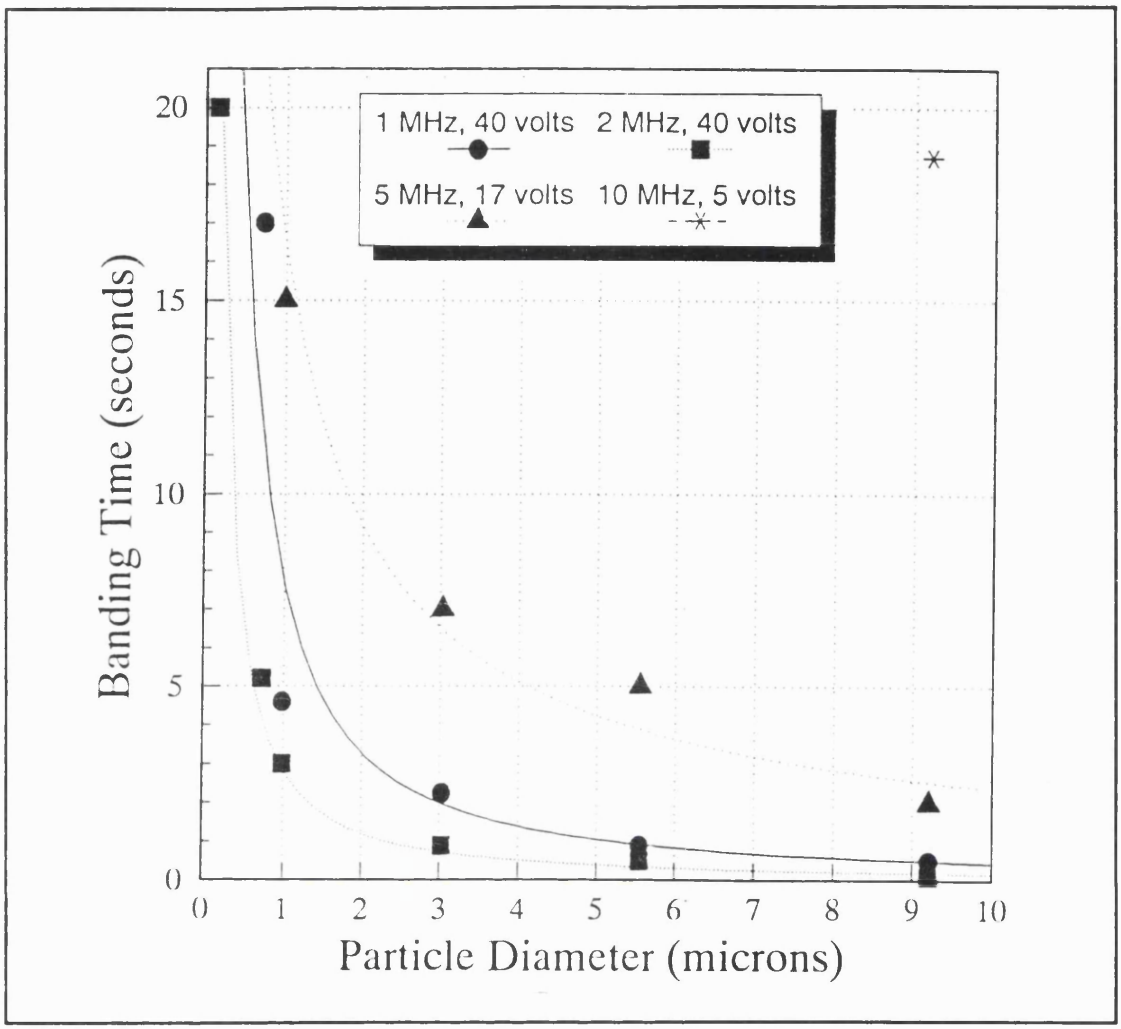

Figure 6.5 *Plot of Banding Time versus Particle Diameter for Latex Particles.*

in others and this fact coupled with the closer banding positions would make it very much easier for particles to escape from one "weak" band to another and eventually exit from the standing wave field. Another factor of importance at higher frequencies is the absorption of the ultrasonic energy; as much as 15 % of the initial ultrasonic energy would be absorbed along the length of the glass vessel used during the experiments (See **Figure 2.8**). Due to the higher particle number concentration of the suspensions of small diameter particles and the shorter ultrasonic wavelength at these frequencies there would be an increase in the scattering of the ultrasound and therefore a greater degree of absorption may occur as the ultrasound propagates through the suspension. This fact may account for the reduced effects seen at the lower particle diameters.

From the results displayed in **Figure 6.5** it is clear that the migration of latex particles to the nodes of a standing wave field is more rapid at 2 MHz than at the other frequencies studied in the experiment.

The curves fitted to the data points follow the power law function described below where *y* has the units of seconds and *x* the units of μm.

$$y = ax^b \qquad \textbf{Eq. 6.4}$$

The 1 MHz data can be approximated by the curve described in **Equation 6.5**:

$$y = 7.8x^{-1.23} \qquad \textbf{Eq. 6.5}$$

and the 2 MHz data by the curve described in **Equation 6.6**:

$$y = 2.4x^{-1.23} \qquad \textbf{Eq. 6.6}$$

The value of **a** in **Equation 6.6** is in between one quarter and one third of the value of **a** in **Equation 6.5** whilst the value of **b** remains constant. This finding would agree with the theoretical relations that suggest a reduction of banding threshold diameter with increasing sound frequency (**Section 2.3.2.1**) as the radiation pressure on the particles increases monotonically with the frequency of the standing wave field. This would cause the banding time to be halved, however at 2 MHz **a** is almost four times smaller than at 1 MHz. This is explained by the halving of the ultrasonic wavelength from 1 to 2 MHz which leads to the particles having to migrate only half the distance in a 2 MHz standing wave field than in a 1 MHz standing wave field. Hence the banding time is inversely proportional to the radiation pressure exerted on the particle, to the ultrasonic wavelength, and therefore, for a constant energy density, the banding time is inversely proportional to four times the frequency of the ultrasonic standing wave field. The slight disagreement in the experimental data is due to problems encountered when measuring very short banding times by hand where slightly longer banding times than actually occuring are recorded.

The higher threshold diameters suggested by the experiments performed at 5 MHz are questionable due to the reduced sound intensity applied during these sets of experiments (**Section 6.4.2**) and to the inefficiency of the ultrasonic amplifier at these higher frequencies leading to the unavoidable, over–estimation of the magnitude of the ultrasonic intensity used during the experiments.

The transducer voltages used during the 5 MHz experiments (17 volts p–p) was slightly below that of the 1 and 2 MHz experiments and could account for the reduction in efficiency of migration at 5 MHz and above; a more powerful amplifier would be required to generate the transducer voltages required for effective banding of particles at 5 MHz and above (See **Section 5.2**) and therefore the technique may be more energy intensive. The increased absorption of the ultrasonic energy at greater than 5 MHz would also have an adverse influence upon the rate of particle migration during the experiments.

6.5.2.3 Conclusions

The frequency of the ultrasonic standing wave has a strong influence on the rate of particle migration within the standing wave field.

A frequency of 2 MHz was found to be the most effective frequency for ultrasonic separation in this experimental apparatus. In general, for identical values of transducer voltage, an increase in frequency causes a reduction of banding time and an increase in the efficiency of separation. However at frequencies greater than 5 MHz the particle segregation effect is limited by factors such as absorption and difficulties in generating sufficient ultrasonic intensity.

The difference in rate of migration determined experimentally between 1 and 2 MHz is as predicted by the theoretical relations described in **Chapter 2**. The 1 MHz data was represented by the curve described in **Equation 6.5**:

$$y = 7.8x^{-1.23} \qquad \textbf{Eq. 6.5}$$

and the 2 MHz data by the curve described in **Equation 6.6**:

$$y = 2.4x^{-1.23} \qquad \textbf{Eq. 6.6}$$

The value of **a** in **Equation 6.6** is approximately one quarter of the value of **a** in **Equation 6.5** whilst the value of **b** remains constant which confirms the theoretical relation which predicts that the rate of migration of a particle is a factor of the increasing radiation pressure associated with increasing ultrasonic frequency and a factor of the reduction of the ultrasonic wavelength with increasing frequency.

Further work is required to investigate the frequencies between 2 and 5 MHz which may prove to be the optimum frequency range for ultrasonic particle separation.

The next section of research examines the effect of particle–liquid density on particle migration.

6.5.3 Density Dependency of Particle Migration

The principal objective of this section of experimentation was to determine whether the non–invasive technique of particle separation in an ultrasonic standing wave field could effect the separation of a neutrally buoyant particle – a separation that is impossible to achieve by centrifugation.

The radiation pressure exerted on a compressible sphere suspended in a standing wave field can be described by **Equation 6.7**

$$P_r = 4\pi a^3 \kappa E F \sin(2\kappa x) \qquad \textbf{Eq. 6.7}$$

where the Compressibility Factor **F**

$$F = \frac{\Lambda + 2(\Lambda - 1)/3}{1 + 2\Lambda} - \frac{1}{3\Lambda\sigma^2}$$

and where

$$\Lambda = \frac{\rho_1}{\rho_0} \quad , \quad \sigma = \frac{c_1}{c_0}$$

ρ is density and σ is the velocity of sound through the material. The subscripts **0** and **1** refer to the fluid and particle respectively.

From the plot of Compressibility Factor **F** against the density difference between particle and suspending fluid (**Figure 6.6**) it is clear that the Compressibility Factor **F** can become zero or very nearly zero. Should this occur then the radiation pressure experienced by the particle suspended in the sound field would also approach zero and hence no particle migration could occur. For the case of polystyrene particles

F would approach zero when the fluid surrounding the particle has a density of approximately 1,400 $kg.m^{-3}$.

The compressibility factor will heavily influence the efficiency of separation of biological particles when both the density and sound velocity through the particle material are similar to those of the suspending fluid due to the high degree of hydration typical of such particles.

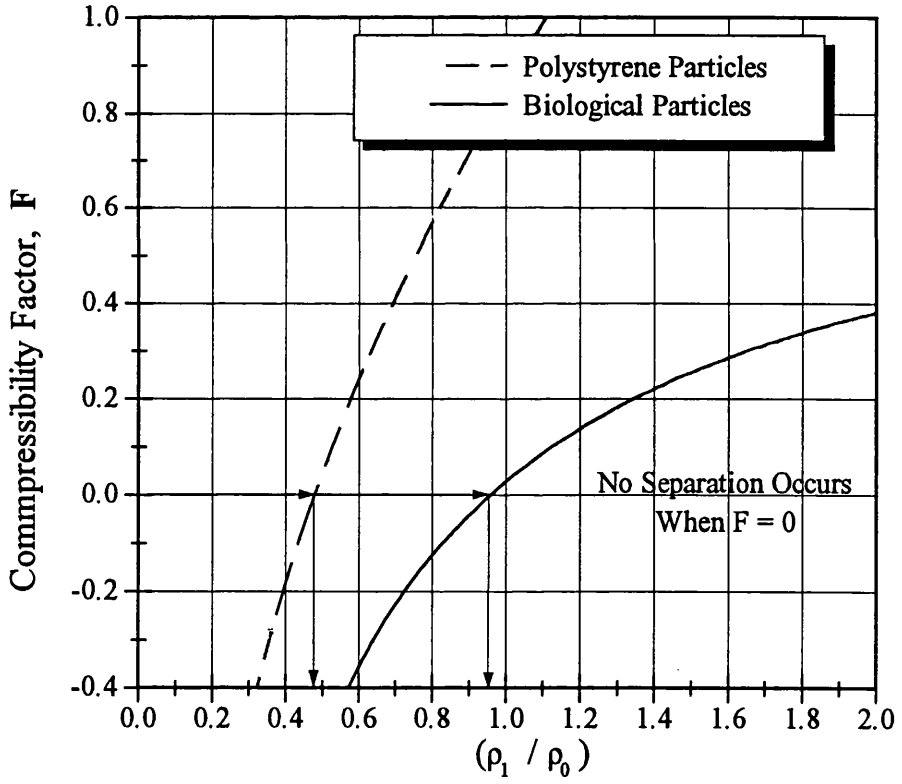

The properties of the biological particles featured in the above figure are the mean values of a variety of different cell types.

Figure 6.6 *Plot of Acoustic Compressibility Factor, F, versus Ratio of Particle–Liquid Densities.*

6.5.3.1 Experimental Procedure

The experimental apparatus was assembled as previously described in **Section 6.1**. As it is rather difficult to independently and simultaneously control the density of a fluid and the sound velocity through the fluid only the density of the suspending fluid was adjusted during the following experiments.

The density of polystyrene latex particles was quoted to be in the region of 1050 $kg.m^{-3}$ by the manufacturers Polysciences Inc. This value was checked by the experiment detailed in **Section 3.2.4** and the actual density found to be 1054 ± 2 $kg.m^{-3}$. This value for the density of polystyrene particles is used during the following experiments described below.

The density of yeast cells was taken to be 1050 $kg.m^{-3}$ and is a figure quoted frequently in the literature (P. Ward, Ph.D. Thesis, University of London).

To alter the density of the suspending fluid used in the experiments a proprietary material, Nycodenz (Nycomed AS, Pharma, Diagnostic Division, P.O. Box 4284 Torshov, N–0401 Oslo 4, Norway), used in the laboratory scale centrifugal separation of cell organelles was used. Nycodenz is a non–ionic, non–toxic material that is not metabolized by living cells. The Nycodenz powder was diluted with filtered deionized water until the density of the solution was within 2 $kg.m^{-3}$ of the desired density. The density of the solution was measured by the use of a hydrometer and by measuring the absorbance of the solution at 350 and 360 nm wavelengths as described in **Section 3.2.4**. To reduce the density of the suspending liquid to below that of water solutions of water and 96 vol% ethanol were prepared. The densities of the ethanol solutions were measured with an alcohol hydrometer.

A dilute suspension of 3.09 μm polystyrene latex particles in the Nycodenz or ethanol solution was prepared and pumped into the ultrasonic separator. The transducers were powered at 30 volts peak to peak at a resonant frequency of 2.0 MHz.

The procedure was repeated for several liquid densities below, above and exactly the same as the density of the latex spheres.

6.5.3.2 Results

The time taken for concentrated bands of particles to form was measured along with the maximum effective fluid velocity through the separation vessel and the maximum effective rate of phase shift. Duplicate experiments were performed and the reproducibility of the measurements of maximum fluid velocity and maximum rate of phase shifting were found to be within ± 10 %.

The results of repeated experiments are listed in **Table 6.4** and a graph of the raw results is presented in **Figure 6.7**.

Fluid Density ($kg.m^{-3}$)	Banding Time (s)	Maximum Fluid Velocity ($m.s^{-1}$)	Maximum Rate of Phase Shift
798	0.5 ± 0.2	7.5×10^{-3}	4.0 $\lambda.s^{-1}$
954	2.1 ± 0.2	$< 10^{-4}$	1.1 $\lambda.s^{-1}$
975	4.5 ± 0.2	$< 10^{-4}$	0.4 $\lambda.s^{-1}$
1000	0.9 ± 0.2	3.0×10^{-3}	1.6 $\lambda.s^{-1}$
1054	0.9 ± 0.3	2.1×10^{-3}	1.4 $\lambda.s^{-1}$
1100	1.7 ± 0.2	$< 10^{-4}$	1.0 $\lambda.s^{-1}$
where λ is the wavelength and period of the sound wave			

Table 6.4 *Results of Density Difference Experiments with 3.09 μm Polystyrene Latex Particles.*

6.5.3.3 Discussion

The reduction in particle migration efficiency apparent at the densities of 954 and 975 $kg.m^{-3}$ are most probably due to the viscosity of the ethanol solution used to reduce the density to below that of water. Ethanol–water solutions have higher viscosities than either pure water (0.001 Pa.s) or pure ethanol (0.0014 Pa.s), for a 40 vol% solution of ethanol in water the viscosity is 0.003 Pa.s. The velocity at which the particles move through the liquid under the influence of the radiation pressure is

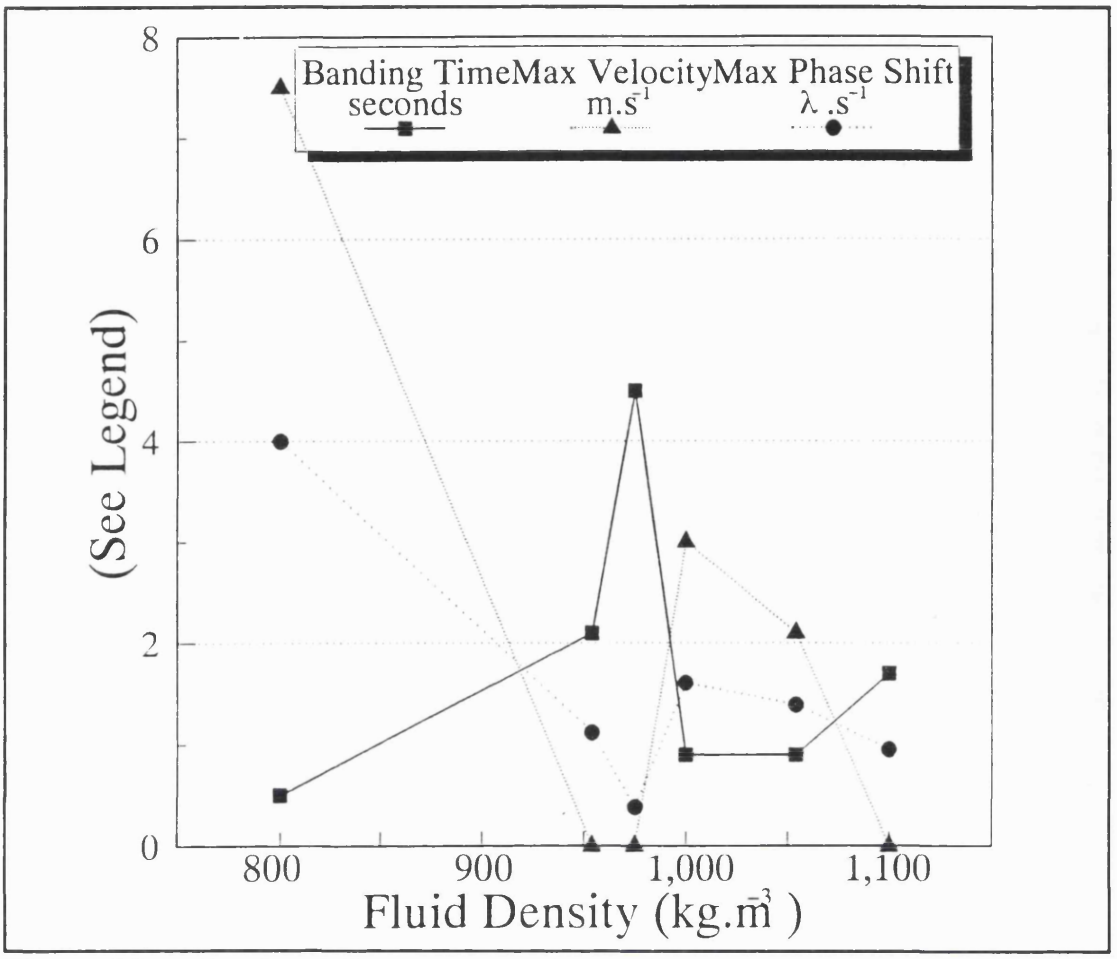

Figure 6.7 *Results of Experiments to Determine the Effect of Change in Liquid Density on the Migration of Particles.*

linearly dependent on the viscosity of the liquid, as the drag force exerted on the particle increases with the liquid viscosity. For this reason the experimental data listed in **Table 6.4** has been corrected to remove the effect of the changing viscosity of the solutions and is presented in **Figure 6.8** and **Figure 6.8a**.

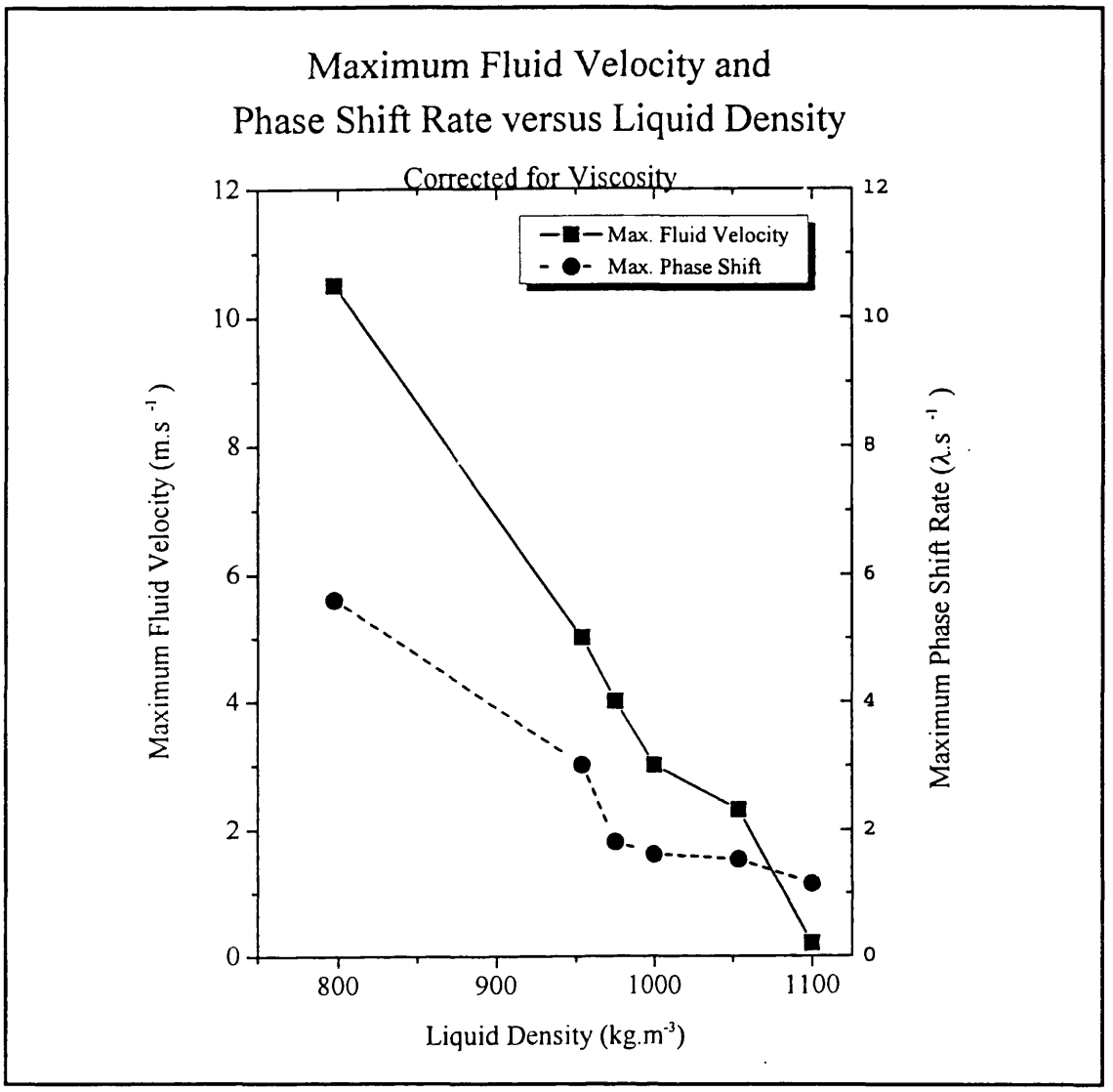

Figure 6.8 *Corrected Results of Experiment to Determine the Effect of Change in Liquid Density on the Migration of Particles.*

6.5.3.4 Conclusions

The results listed in **Table 6.4** and displayed in **Figure 6.7** show that particle migration occurs even when the particles are suspended in a fluid of the same density. This means that the ultrasonic separation technique is able to separate neutrally buoyant particles from a fluid, a process which would be impossible to achieve with conventional centrifugal separation techniques that rely on the density difference between particle and fluid to effect separation. This result agrees with the theory described in **Section 2.3.2.1** and **Section 6.3**.

Having established the ability to separate neutrally buoyant particles and also the maximum rate of phase shifting subsequent work looked at the effect of flow velocity on the degree of separation achieved.

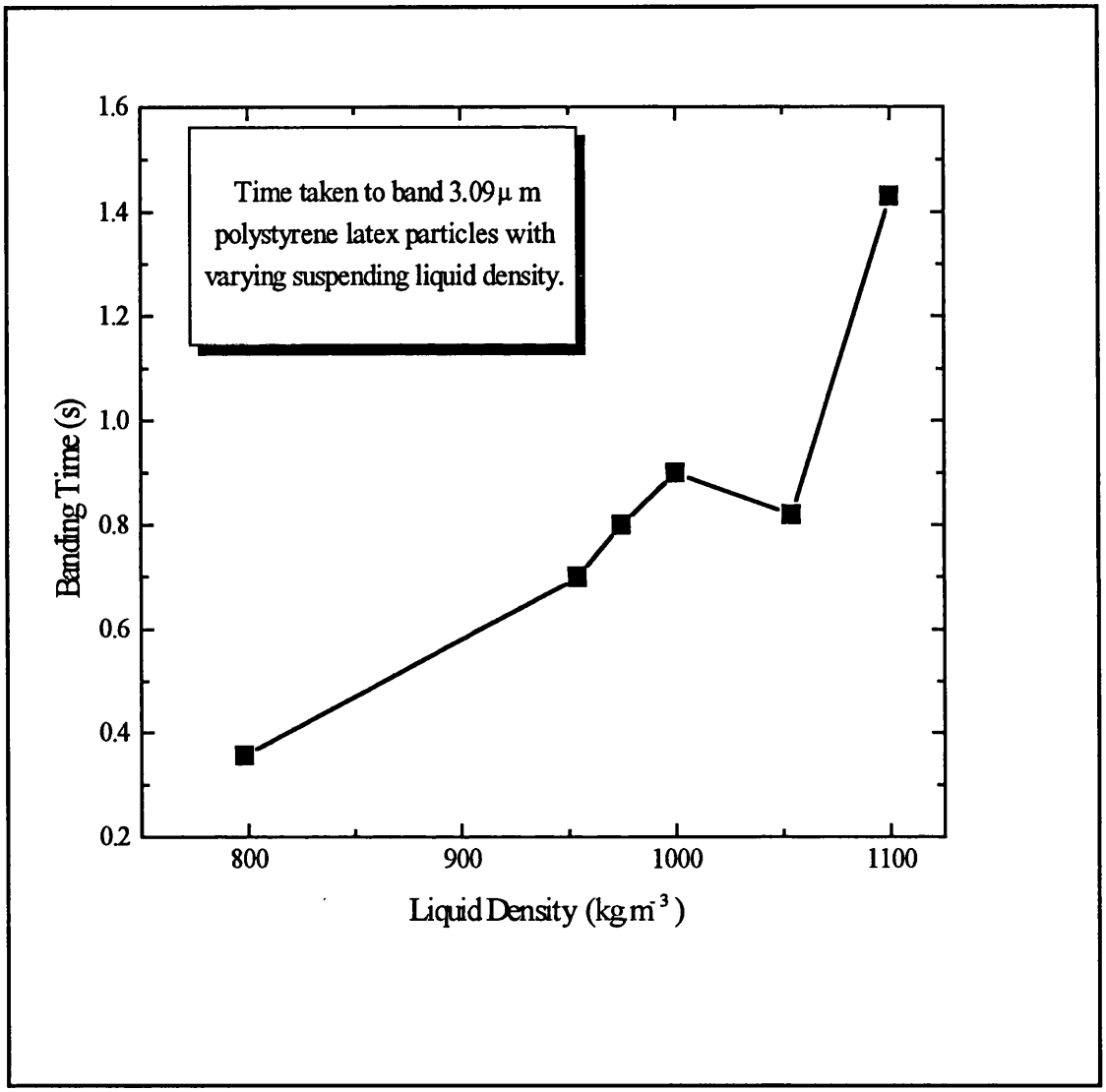

Figure 6.8a *Corrected Results of the Influence of Density on Particle Migration.*

6.5.5 Maximum Fluid Velocity

Experiments were performed to study the effect of fluid flow perpendicular to the nodal planes of the ultrasonic standing wave field. The aim was to determine the liquid velocity relative to the nodes of the standing wave field that caused the particles aggregated at the nodes to be forced away from the nodes by viscous drag, the point

at which separation is no longer possible. This information is key to the scale-up of ultrasonic separation.

See **Section 2.3.2.2** for a theoretical discussion of the drag force exerted on a particle in a fluid, and **Figure 6.4** for a plot of maximum particle velocity versus particle diameter.

6.5.5.1 Experimental Procedure

The apparatus was set up as previously described in **Section 6.1**. Suspensions of 1.5, 5.71, and 9.21 μm polystyrene latex particles **(Appendix III)** were prepared by diluting the 2.5 weight % suspensions with deionized water. The particle concentrations of the prepared suspensions were then measured on the Elzone Particle Analyzer (See **Section 3.2**).

The suspensions were pumped at a measured flowrate through a standing wave field generated by a measured and controlled voltage from the ultrasonic amplifier. Samples of the fluid passing through the standing wave field were collected. After 10 mL of sample was collected the flowrate of suspension into the standing wave field was increased, the suspension was allowed to flow through for two minutes to ensure the concentration of particles in the fluid leaving the standing wave field was constant and samples were then collected as before.

The above procedure was repeated for three different transducer voltages and for each of the three polystyrene latex suspensions.[2]

2

Note: The experimental procedure was carefully designed to make it easier to detect the maximum effective fluid velocity achievable under the varying conditions of ultrasonic standing wave field. Throughout each experiment, as the flowrate is gradually increased, the particles are being removed from the suspension and concentrated at the nodes of the sound field. When the critical flowrate is exceeded the particles previously removed from the flowing suspension are released from the nodes of the standing wave field and are carried out of the separation vessel with the flow of suspension thus causing the concentration of the particles in the sample suspension to greatly exceed the feed suspension concentration. The concentration of particles in the suspension leaving the separation vessel then drops to that of the feed suspension as all of the previously separated particles are washed from the nodes of the standing wave field and further

(continued...)

6.5.5.2 Results

The results of the above experiments are displayed graphically in **Figures 6.8** to **6.10**. The fluid velocities refer to the maximum fluid velocity through the glass sample tube assuming a laminar flow profile where the maximum fluid velocity is at the axis of the tube and is twice the value of the average fluid velocity through the tube.

There appears to be a critical fluid velocity through the sound field that causes all of the particles accumulated at the nodal planes to be released from the banding positions and carried with the flow of the fluid. As the fluid velocity increases towards the critical point there is a steady increase in the concentration of particles in the fluid leaving the standing wave field. This value of the critical flowrate increases with the diameter of the particles in the suspension under observation and also increases with the voltage of the transducer driving current (energy density of the standing wave field). The regions of the plots below the feed concentration show where the magnitude of the radiation force is greater than the drag force on the particle and indicate the operational windows for an effective continuous ultrasonic separation technique where particles could be continuously removed from a flowing stream of suspension (**Figure 2.9**).

---

[2](...continued)
separation does not occur due to the high drag force exerted on the particles. In this manner the critical velocity is then determined as the point at which the concentration of the suspension leaving the separation vessel exceeds the feed suspension concentration.

If, alternatively, a single sample was taken, the separation vessel emptied, cleaned and refilled for each different flowrate studied then the data collected would generate a curve where the sample concentration gradually approached the feed concentration, making it rather difficult to determine the exact point at which the fluid velocity reached the critical value.

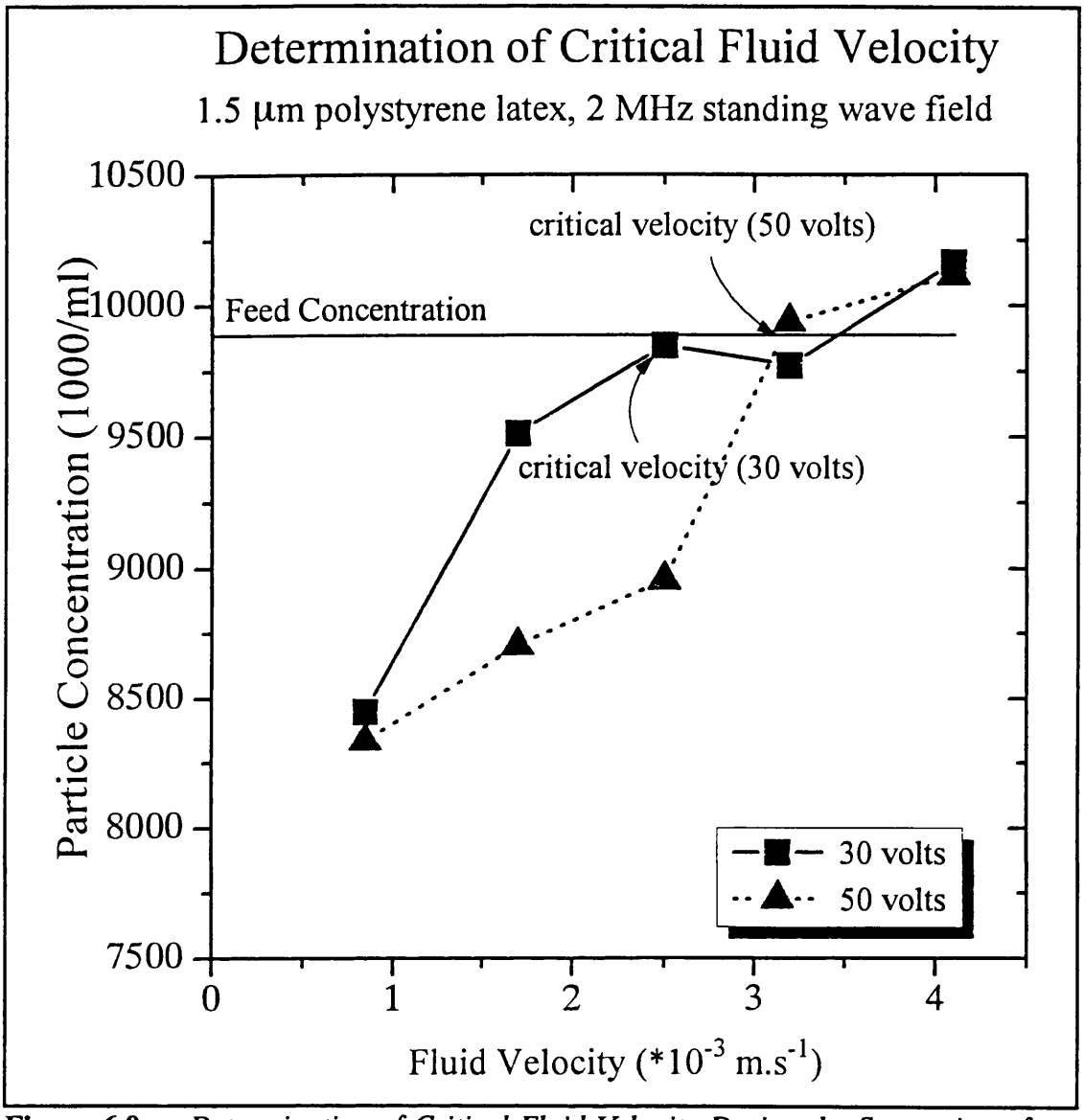

Figure 6.9 *Determination of Critical Fluid Velocity During the Separation of 1.5 μm Latex Particles.*

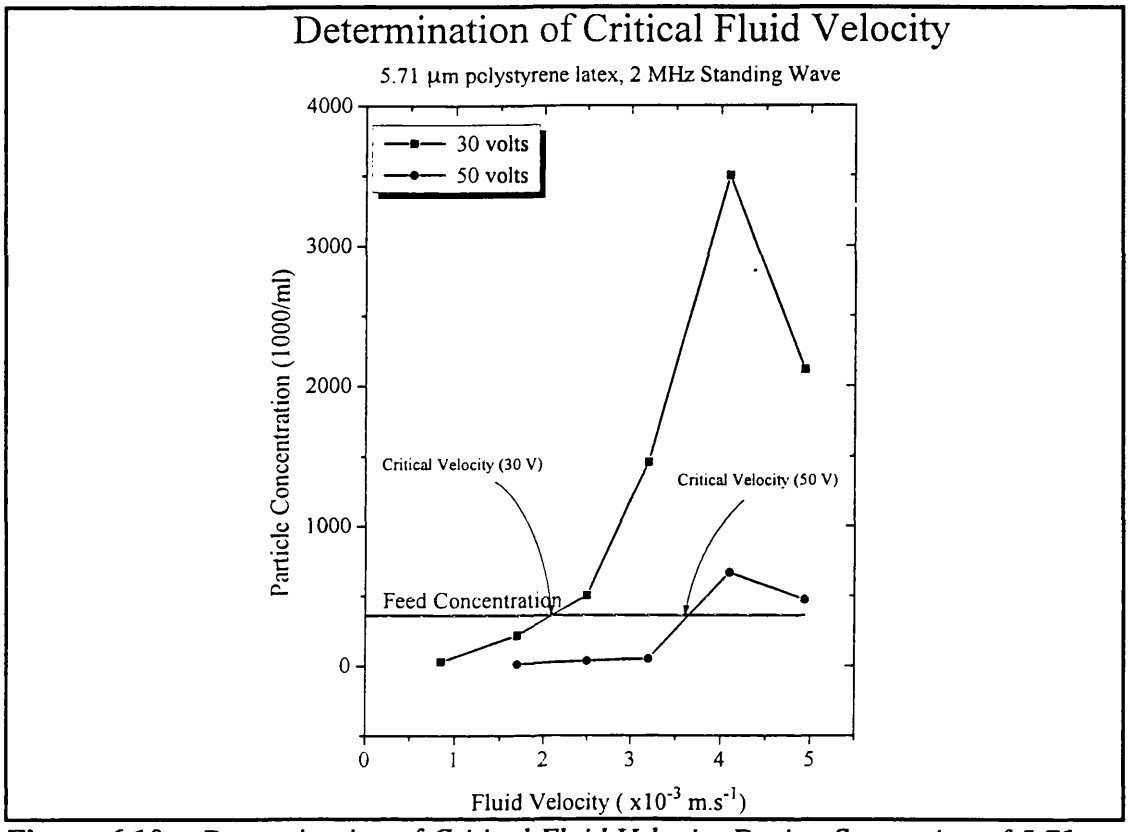

Figure 6.10 *Determination of Critical Fluid Velocity During Separation of 5.71 μm Polystyrene Latex Particles.*

Figure 6.12 is a plot of the critical fluid velocities versus the transducer voltages used in the above experiments and shows the general increase in critical velocity with increasing transducer voltage. There appears to be a greater rate of increase with transducer voltage for the larger diameter particles than smaller diameter particles.

Figure 6.13 is a plot of critical fluid velocity versus particle diameter and shows a general increase in the critical velocity with increasing particle diameter which agrees with the trend suggested by theory.

6.5.5.4 Discussion.

The steady increase in particle concentration in the exit stream is due to a percentage of the particles in the suspension escaping the full force of the standing wave by travelling through the inhomogeneities in the standing wave field established within the apparatus. This phenomenon can be compared to a "pinhole" in a filter membrane – the increase in particle concentration is linearly proportional to the increase in the fluid flowrate as there is a corresponding increased flowrate through the "pinhole". If the filter membrane analogy is maintained then the critical point in the fluid flowrate during ultrasonic separation can be compared to the "bursting pressure" or point of total mechanical failure of the filter membrane where all of the previously filtered particles are released.

Comparison of the experimentally determined maximum fluid velocities with theoretical maximum fluid velocities as predicted by equating the radiation pressure exerted on a particle with the Stokes' Drag Force on the particle reveals that the

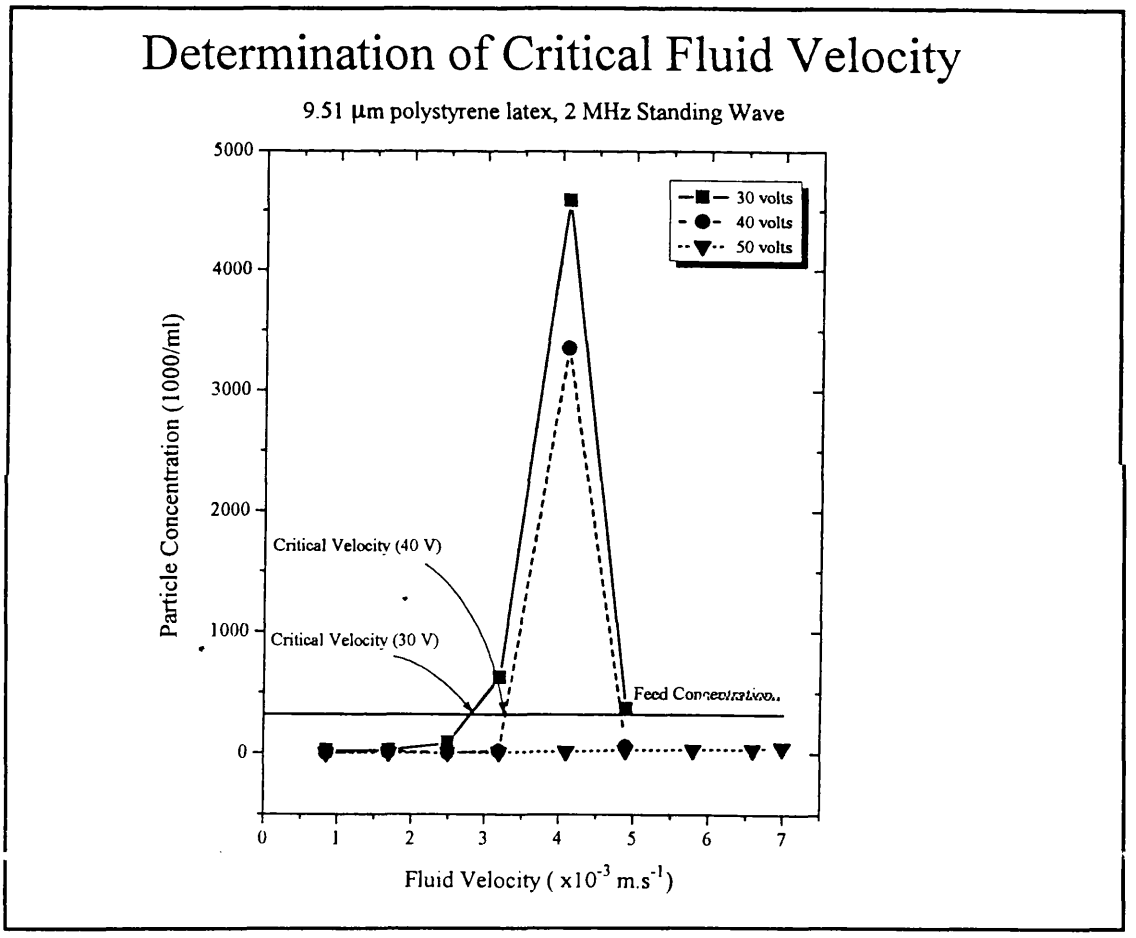

Figure 6.11 *Determination of Critical Fluid Velocity During The Separation of 9.21 µm Polystyrene Latex Particles.*

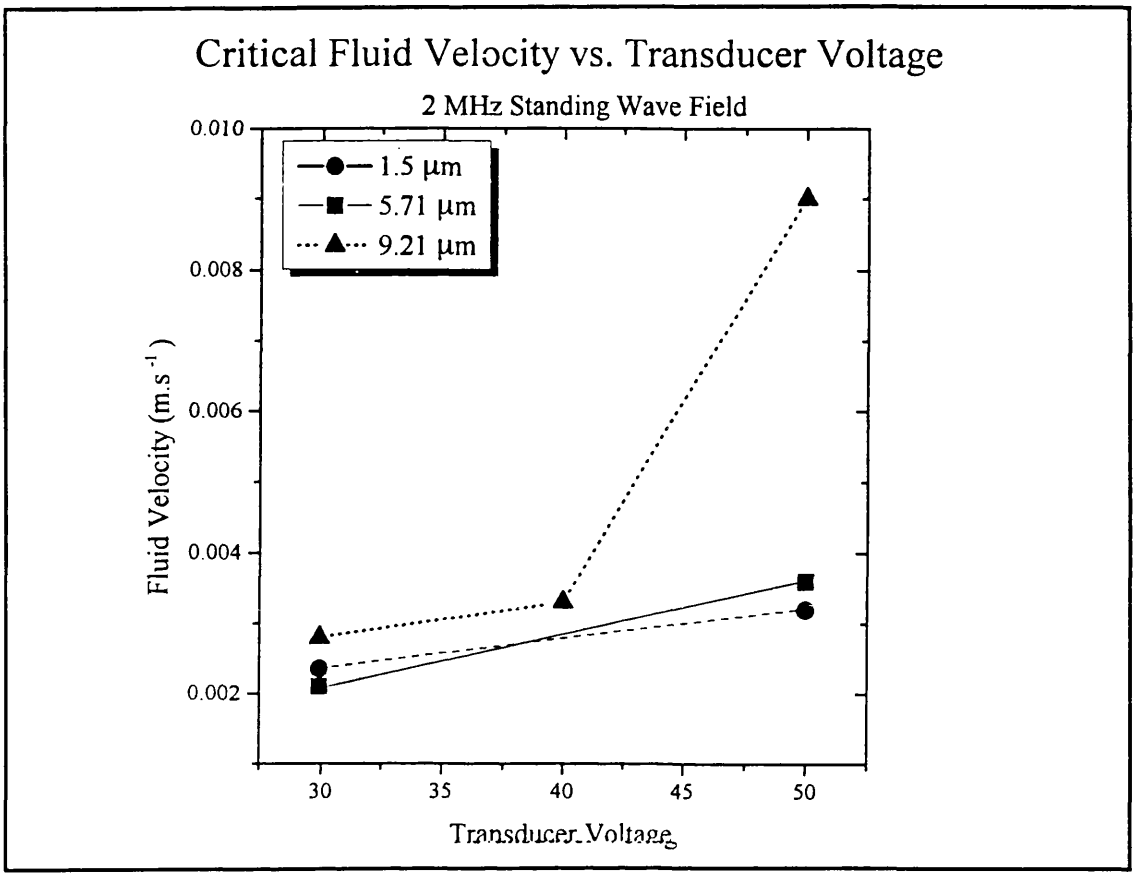

Figure 6.12 *Critical Fluid Velocity versus Transducer Driving Voltage.*

observed values are greater than the theoretical predictions (See **Figure 6.14**). The reason for this difference may be attributed to the way in which the particles accumulate in the standing wave field. Visual observations of the concentrated bands of particles at the nodes of the standing wave field reveal that the particles do not migrate to form a band of uniform concentration across the cross section of the sample tube. The particles accumulated at the bands migrate within the bands in directions at right angles to the direction of propagation of the sound waves to form "clumps" of particles (A phenomenon also reported by Coakley [1992]). These clumps of particles may contain a great number of particles in very close proximity and as such behave as a single particle of very much larger diameter. The radiation pressure exerted on such clumps of particles would be considerably greater than the radiation pressure exerted on a single particle (radiation pressure is proportional to the particle radius cubed) and would account for the increased values of maximum fluid velocity through the sound field that can be tolerated before the particles are fully entrained in the flow

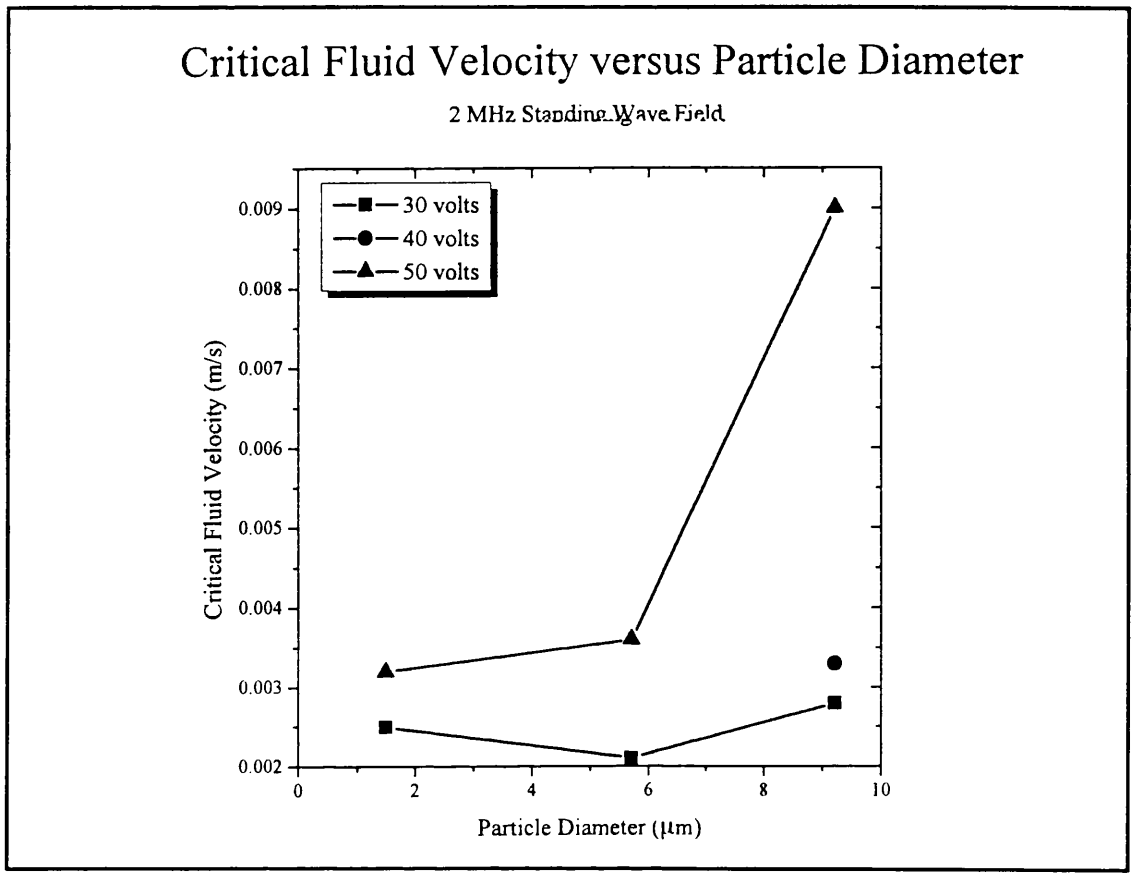

Figure 6.13 *Critical Fluid Velocity versus Particle Diameter.*

and the separation effect is negated. The corresponding increase in drag force is only linearly dependent on the particle diameter and therefore would be orders of magnitude less than the increase in radiation pressure.

6.5.5.5 Conclusions.

The critical fluid velocities determined for the 1.5, 5.71 and 9.21 μm diameter particles were found to increase with applied transducer voltage and were found to be 3.2, 3.6 and 9 × 10^{-3} $m.s^{-1}$ respectively at the highest transducer voltage of 50 volts peak–peak (2 MHz).

The experimentally determined critical velocities were found not to agree with the theoretically determined critical velocities and a hypothesis for this aberration has been presented.

The next section of research investigates the use of phase shifting in ultrasonic separation and discusses the experimental results in light of the theoretical relations

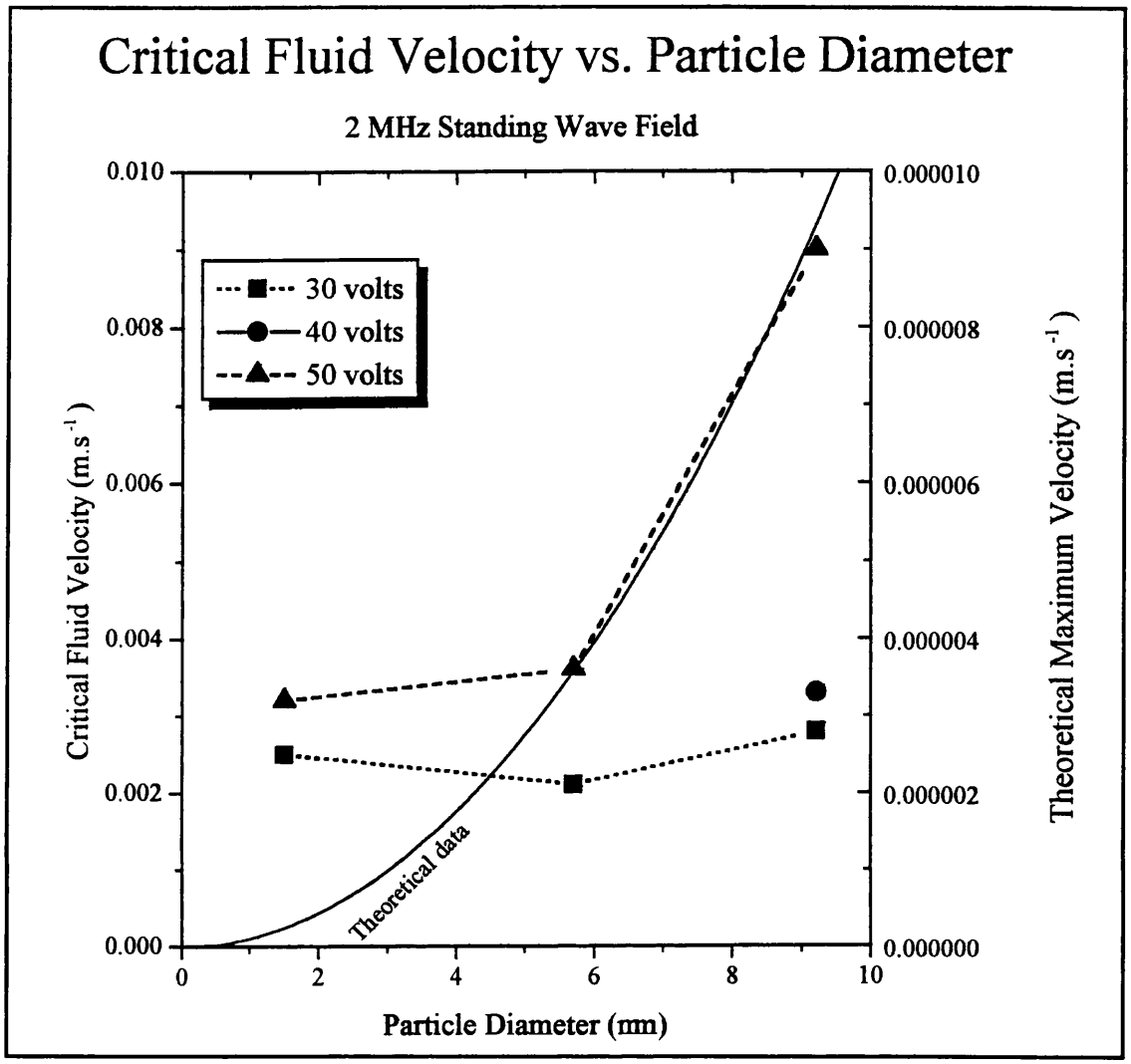

Figure 6.14 *Plot of Experimentally and Theoretically Determined Critical Fluid Velocities.*

detailed in **Chapter 2.**

6.5.6 Maximum Effective Rate of Phase Shifting.

This section describes work to determine the operational limitations of the phase shifting technique used in continuous ultrasonic separation.

6.5.6.1 Introduction

The use of phase shift has been described in **Sections 3.3** and **Section 6.4.5**. The technique facilitates the continuous separation of particles from a suspension by moving the concentrated bands of particles accumulated at the nodal planes towards one port of the glass tube used as the separation vessel (see **Figure 6.3**). The concentrated suspension, formed at the exit port, is removed from the glass tube. By controlling the ratio of the flow of liquid from the two outlet ports the concentration of the particle slurry can be varied.

6.5.6.2 Experimental Procedure

The rate of phase shift was controlled by the computer program listed in **Appendix II**. The method of determination involved creating a standing wave field in a suspension of 5.71 μm polystyrene latex particles and a suspension of whole yeast cells (prepared as described in **Chapter 3**) contained in the glass sample tube as detailed in **Figure 6.2**. Ultrasonic frequencies of 1, 2, and 5 MHz were used to create standing wave fields with transducer voltages of 30, 30 and 17 volts peak – peak respectively. The experiments were performed after two different lengths of time after the formation of the standing wave field. Firstly the phase shifting was begun at the same time as the formation of the standing wave field, and secondly the phase shifting was begun 30 s after the formation of the standing wave field.

The rate of phase shift was initially set at a quarter of a wavelength per second ($0.25\ \lambda.s^{-1}$) and gradually increased until particles accumulated at the nodes of the standing wave fields were observed to remain stationary in the liquid as the nodal planes moved through the liquid. The rate of phase shift at this point was determined to be the absolute maximum practical rate of phase shifting at the specified conditions of standing wave field and particle suspension.

6.5.6.3 Results

The experiments performed at a frequency of 5 MHz proved inconclusive whilst studying both yeast and polystyrene latex particles. In the case of simultaneous phase shifting and formation of the standing wave field no band formation was

observed over a period of 30 s. During the second set of experiments despite the satisfactory formation of concentrated bands of particles after 30 s the initiation of phase shifting caused only erratic movement of the concentrated bands of particles and soon disrupted the bands forming a homogeneous suspension once more. This result was repeated at phase shifting rates as low as 0.05 $\lambda.s^{-1}$.

The results of several repeated experiments at 1 and 2 MHz are listed in **Table 6.5** where the average value of maximum phase shift determined from experiments was found to be reproducible within an error of ± 10 %.

Maximum Phase Shift ($\lambda.s^{-1}$ ± 10 %)				
Sample	Polystyrene Latex		Yeast Cells	
Frequency	1 MHz	2 MHz	1 MHz	2 MHz
After 0 s	0.5	1.3	0.3	1.3
After 30 s	0.7	1.7	0.8	2.2

Table 6.5 *Results of Phase Shifting Rate Experiments on Yeast and 5.71 μm Polystyrene Latex.*

6.5.6.4 Discussion

The maximum possible rate of phase shift determined by the experiments described above was found to be greater when the standing wave field had been established for a period of 30 s than when the phase shifting was initiated with the formation of the standing wave field. This is explained by the growth of large aggregates of particles at the nodal planes caused by the secondary ultrasonic forces (Bernoulli and Bjerknes forces **Section 2.3**) that are present in significant magnitudes when the particles are concentrated at the nodes of the standing wave field under the action of the radiation pressure. The resulting large diameter aggregates experience a very much greater radiation pressure than the single particles and therefore can be phase shifted against a correspondingly larger drag force than the single particles. When the phase shift is initiated simultaneously with the standing wave field the

particles do not have time to form large aggregates and therefore the maximum phase shift possible is determined by the magnitudes of the drag force and radiation pressure on the single particles.

The experiments with whole yeast cells reveal a greater possible rate of phase shift even though the mean cell diameter was of the order of 5.5 μm and therefore identical to the polystyrene particle diameter. This result can be explained by the fact that the aggregates or flocs of yeast cells formed in the standing wave field are very stable and to not fragment or disperse as single particles unlike the aggregates of polystyrene particles. This enables the flocs of yeast to withstand a greater drag force before being dispersed as single particles, and therefore a greater phase shifting rate.

The difference in phase shifting rate between 1 and 2 MHz is explained by the fact that the wavelength, λ, is 1490 μm at 1 MHz and 750 μm at 2 MHz therefore a phase shifting rate of 1 $\lambda.s^{-1}$ at 1 MHz is equal to 2 $\lambda.s^{-1}$ at 2 MHz. However the absolute values are less at 1 MHz than at 2 MHz and this may be explained by the reduction in radiation pressure associated with a reduction in ultrasonic frequency (see **Chapter** 2 and **Section 6.5.5**).

Phase shifting at the higher frequencies of 5 and 10 MHz was very ineffective and was determined to be caused by deficiencies in the phase shifting circuits of the ultrasonic amplifier. (It was very difficult to obtain a uniform change of phase at these frequencies resulting in relatively sudden "jumps" in the position of the nodal planes.) Development of the phase shifting electronics would be required to successfully use phase shifting at these frequencies.

6.5.6.5 Conclusions

Phase shifting was found to be most effective at a frequency of 2 MHz. The maximum rate of phase shifting possible was found to be 1.7 $\lambda.s^{-1}$ for 5.71 μm diameter polystyrene particles and 2.2 $\lambda.s^{-1}$ for yeast cells at a frequency of 2 MHz and transducer voltage of 30 volts.

The maximum rate of phase shifting was found to be greater if the particles in supension in the standing wave field were allowed to form large aggregates.

The results of the preceeding experimental sections were considered when studying the separation of particles from liquid using an ultrasonic standing wave field which is described in the following section.

6.5.7 Efficiency of Ultrasonic Separation

This section describes experiments performed to study the use of megahertz frequency ultrasonic standing wave fields as a mechanism for the removal of particles from a suspension, under varying conditions of standing wave field and fluid flow.

6.5.7.1 Introduction

The objective of this section of experimental work was to collate the findings of the previous experiments, **Sections 6.5.1** to **6.5.6**, and study the efficiency of removal of particles from a suspension using an ultrasonic standing wave field to aggregate and segregate the particles. A 2 MHz frequency standing wave was employed to effect the separation as previous experiments **(Section 6.5.3)** proved that this frequency was most effective at causing rapid particle migration towards the nodes of the sound field.

6.5.7.2 Experimental Procedure

The apparatus was assembled as described in **Section 6.1**. The glass sample tube chosen for the experiments was as shown in **Figure 6.15**.

The experiment was divided into two sections where the standing wave field was used to separate the particles under different conditions:

1. As a static batch mode filter where the suspension was pumped through the sound field whilst **Valve A** was open and **Valve B** was closed. The particles accumulated at the nodal planes, gradually increasing in number and no phase shifting was employed.
2. As a continuous filter where phase shifting was employed and the flow through both **Valves A** and **B** controlled to provide continuous flows of clarified liquid from **Port A** and concentrated suspension from **Port B**.

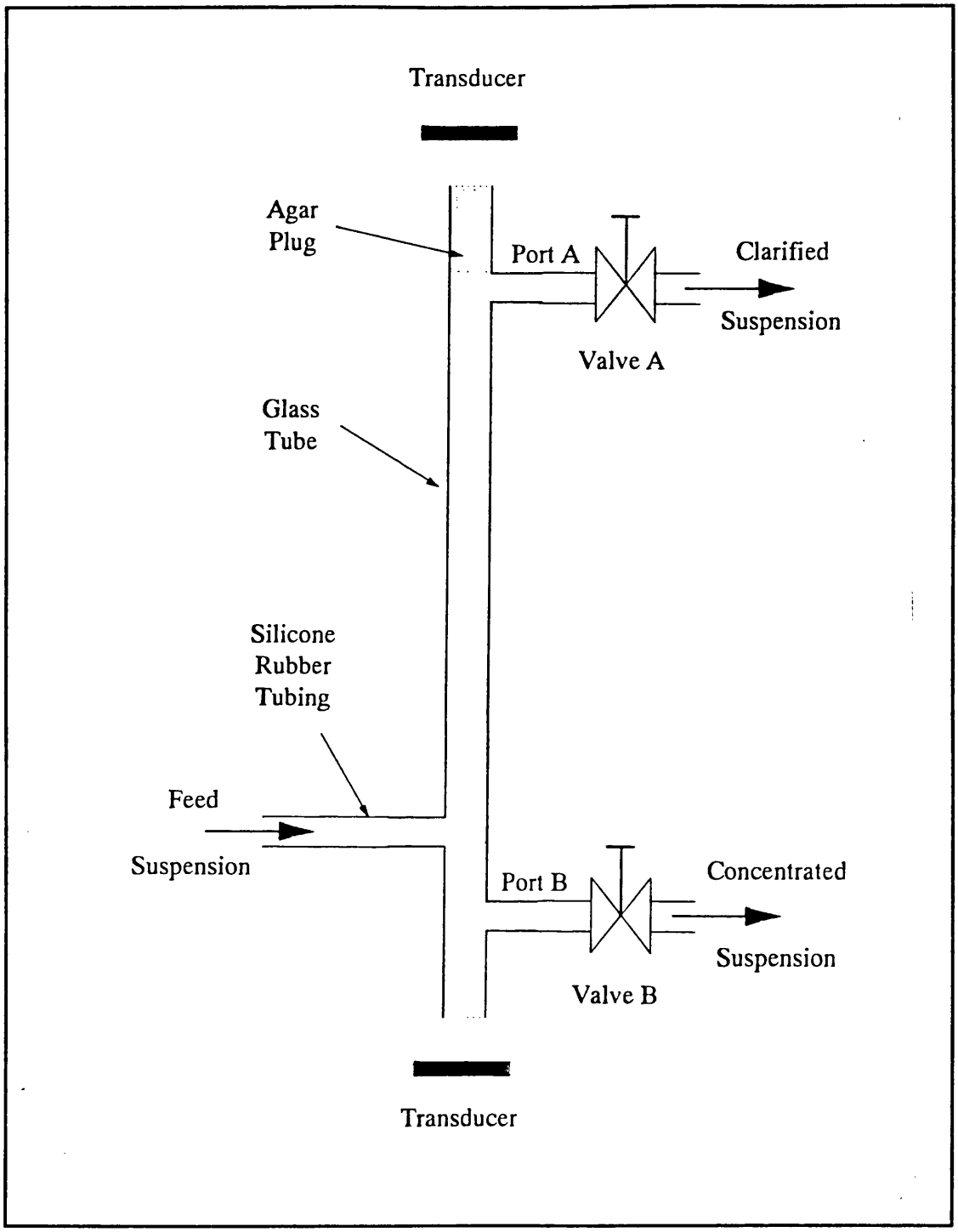

Figure 6.15 *Diagram of Ultrasonic Separation Apparatus Used to Determine the Removal Efficiency of Particles from Suspension.*

The following procedure was common to each of the experiments described above. The suspension was pumped into the glass tube and left to flow through for

several seconds. Samples of the suspension leaving both port **A** and **B** were collected as controls. An ultrasonic standing wave field of the desired intensity (transducer voltage) was formed in the glass sample tube. After setting **Valves A** and **B** to the desired positions the feed suspension was pumped into the feed port at a measured flowrate. After a period of several seconds which was required to flush unsonicated suspension from the outlet ports, samples of the liquid leaving the glass tube were collected.

The above procedure was repeated for the various suspensions described below and for different values of transducer voltage and suspension flowrate.

The suspensions used in the experiments were a wide range of polystyrene latex particles of different diameters (See **Appendix III**) prepared as dilute suspensions in distilled water as described in **Section 3.4.2.1**, a suspension of mammalian cells in a culture medium, samples of whole yeast cells in suspension in both distilled water and fermentation medium, and a suspension of yeast homogenate prepared as in **Section 3.4.2.2** and diluted 1:4 with phosphate buffer.

The concentrations of the suspensions were measured using the Elzone Particle Analyzer (See **Section 3.2**). Due to the monodispersity of the polystyrene latex suspensions the concentration of a suspension was determined by counting the particles within a narrow size range around the mean particle diameter of the latex sample and hence the removal efficiency was calculated by subtracting the number of particles counted in the sample from the number of particles counted in the feed suspension. For the more complex mixtures of yeast cell and yeast homogenate suspensions the removal efficiency was calculated across the whole size range of the sample.

The experiments performed on yeast homogenate were conducted as in the second set of experimental conditions as described above where continuous flows of concentrated suspension and clarified suspension were sampled. Two experiments were performed where the fluid velocity of the suspension flowing through the sound field was 1.7×10^{-3} m.s^{-1} and 3.2×10^{-3} m.s^{-1} respectively. The rate of phase shift used was 0.5 λ.s^{-1} in both cases.

6.5.7.3 Results

Results of duplicated experiments performed using polystyrene latex particles are displayed in **Figure 6.16**. The experimental errors were found to be ± 3 % of the separation efficiency.

This graph clearly reflects the very strong dependence on particle size of the ultrasonic separation effect. Virtually complete removal of particles is achieved for polystyrene latex particles of diameter greater than 2 μm when using the higher transducer voltages. It is also evident that the separation effected at each value of particle diameter is very dependent on the transducer voltage applied.

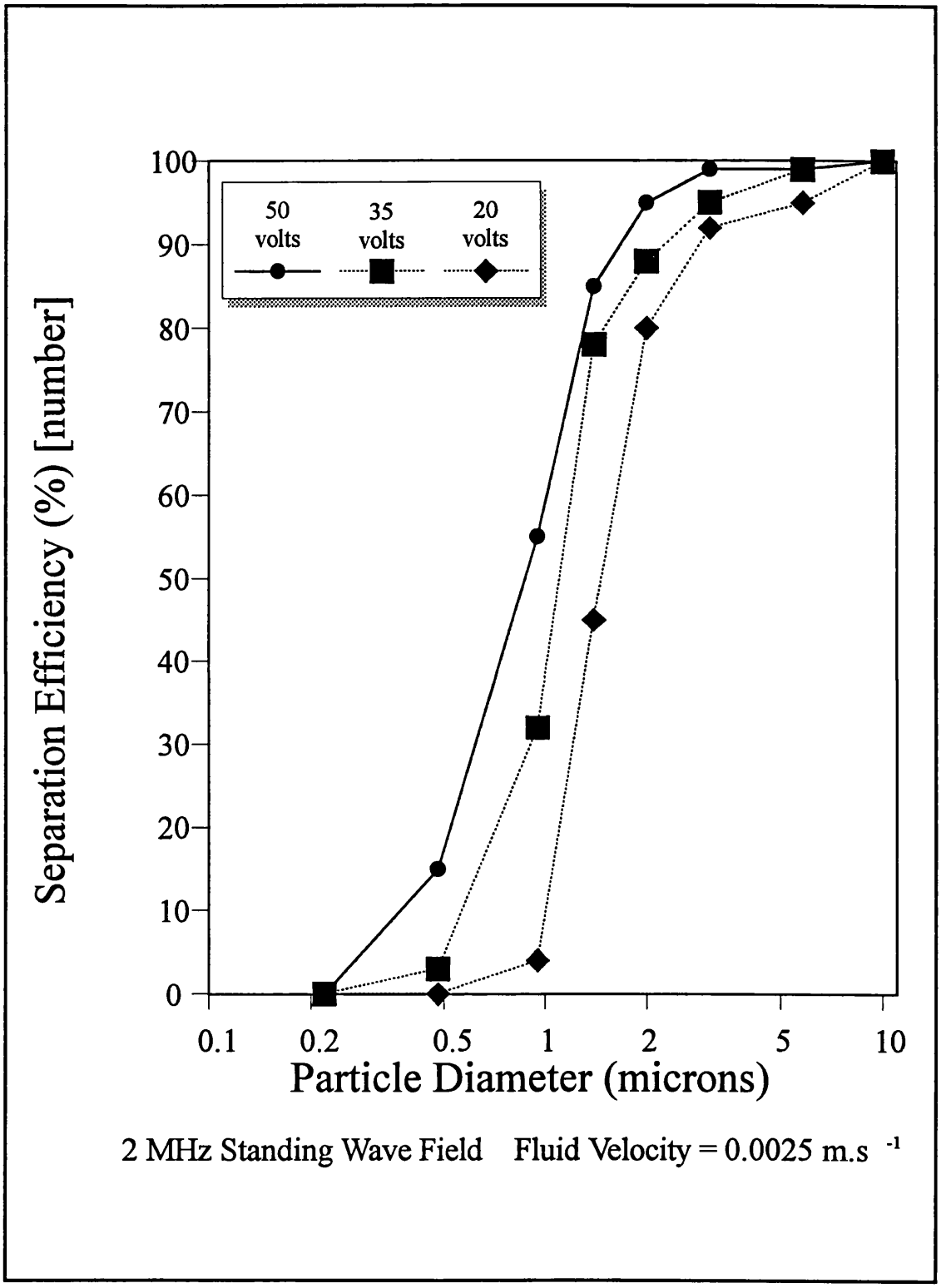

Figure 6.16 *Results of Separation Efficiency (Based on Number Concentration) Experiments on Monomodal Dispersions of Polystyrene Latex Particles.*

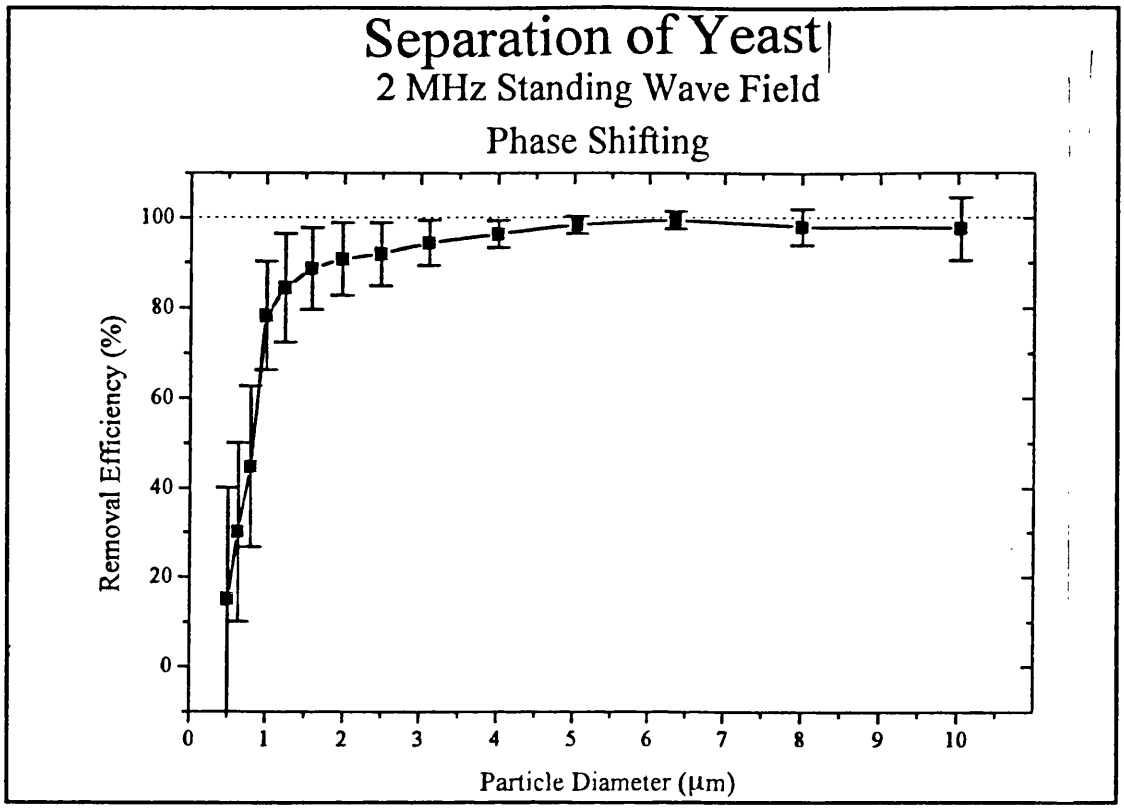

Figure 6.17 *Results of Separation Efficiency Experiments with Whole Yeast Cells.*

Results of numerous experiments using yeast cells in phosphate buffer (See **Section 3.9**) are displayed in **Figure 6.17**. The removal of the whole yeast cells, in the region of 4 – 7 μm diameter, is close to 100% and is not so effective at lower values of particle diameter; however it must be noted that the concentration of particles in the region of 0.5 – 4 μm was orders of magnitude less than the concentration of the yeast cells in the sample and therefore the experimental errors (represented by the error bars on the graph) involved in the determination of the concentration and efficiency of removal are considerable in this region; the true results may indeed agree with the results of the latex particle experiments in this size range.

Results from repeated experiments performed on yeast homogenate proved more difficult to obtain (**Figure 6.18**). The main reason for this difficulty was due to the minimum size limit of the Elzone Particle Analyzer (See **Section 3.2**) which was greater than the size of a substantial proportion of the particles present in the yeast homogenate samples. For this reason the analysis of the experimental samples was

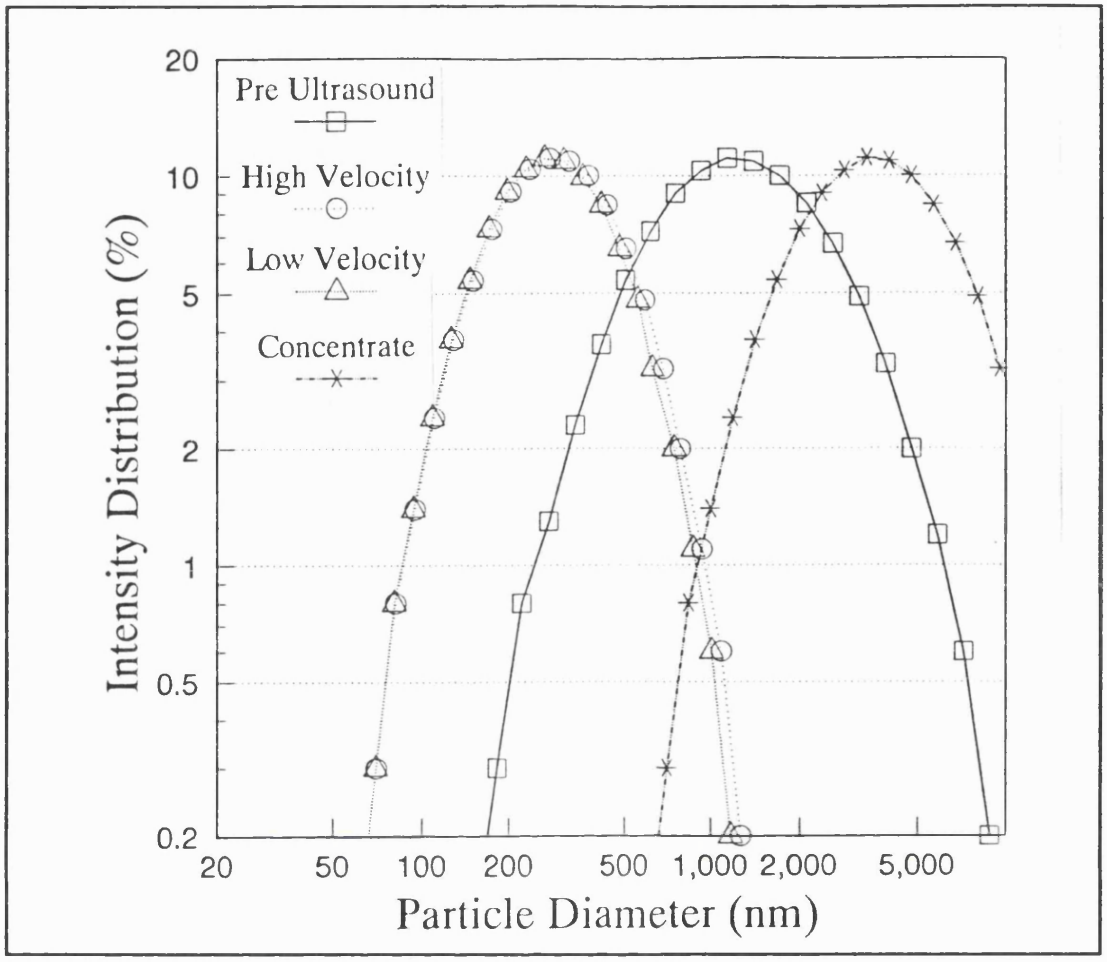

Figure 6.18 *Results of Separation Efficiency Studies on Yeast Homogenate.*

performed on the Malvern 4700 instrument permitting only the analysis of the size distribution of the samples (the samples were diluted 1:100 with filtered phosphate buffer to bring the sample concentration within the range of the instrument).

A significant reduction in the mean size of the yeast homogenate distribution after ultrasonic treatment is shown in **Figure 6.18** and as described in **Section 6.5.7.2**. The solid line represents the particle size distribution of the yeast homogenate feed to the ultrasonic separator and displays a mean diameter of 1,590 nm (standard deviation = 1,260 nm). The low velocity clarified stream is represented by the dashed line and displays a mean diameter of 317.6 nm (standard deviation = 176.0 nm) therefore showing the substantial removal of large particles from the yeast homogenate suspension. Examination of the distributions of the feed and clarified samples shows that the majority of particles of diameter greater than 900 nm were removed during the separation. The dotted line represents the higher velocity clarified stream and has

a mean diameter of 332.8 nm (standard deviation = 189.6 nm) which again indicates the significant removal of large particles from the yeast homogenate suspension but suggests the slightly less efficient removal of large particles at higher flowrates. The concentrated product stream of the separation experiments is represented by the chained–line plot and has a mean diameter of 4,290 nm (standard deviation = 2,820 nm) which clearly demonstrates the size dependency of the efficiency of ultrasonic particle removal.

6.5.7.4 Conclusions

The separation of micron and submicron sized polystyrene latex particles has been succesfully demonstrated in both batch mode separation and continuous separation processes. Approximately 20 % of particles of 0.4 μm diameter are removed and 80 % of particles of 1 μm diameter are removed.

The application of megahertz frequency ultrasonic standing waves to the segregation and recovery of whole yeast cells and yeast cell debris from suspension has been investigated and found to be an effective means of small scale separation for such biological particles, removing close to 100 % of particle over 4 μm in diameter from suspension.

The results of this section of work reflect the strong influence of particle diameter and ultrasonic energy level on the efficiency of separation of particles using a standing wave field.

6.6 Overall Conclusions

The results of the experimental work described in this chapter have demonstrated that effective separation of biological particles from liquid can be achieved with the application of a megahertz frequency ultrasonic standing wave field.

It has been demonstrated that:

- Particle segregation is possible for polystyrene particles with diameter greater than 160 nm when transducer voltages of the order of 40 volts peak to peak are employed.

- The frequency of the ultrasonic standing wave has a strong influence on the rate of particle migration within the standing wave field. A frequency of 2 MHz was found to be the most effective frequency for ultrasonic separation in this experimental apparatus.

- The time required to form concentrated bands of particles in a standing wave field decreases with decreasing ultrasonic wavelength and with increasing radiation pressure.

The difference in rate of migration determined experimentally between 1 and 2 MHz is as predicted by the theoretical relations described in **Chapter 2**. The 1 MHz data was represented by the curve described in **Equation 6.5** where y has the units of seconds and x the units of μm.

$$y = 7.8x^{-1.23} \qquad \textbf{Eq. 6.5}$$

and the 2 MHz data by the curve described in **Equation 6.6**:

$$y = 2.4x^{-1.23} \qquad \textbf{Eq. 6.6}$$

- Particle migration occurs even when the particles are suspended in a fluid of the same density. This means that the ultrasonic separation technique is able to separate neutrally buoyant particles from a fluid, a process which would be impossible to achieve with conventional centrifugal separation techniques that rely on the density difference between particle and fluid to effect separation. This result agrees with the theory described in **Section 2.3.2.1** and **Section 6.3**.

- The maximum operational fluid velocities determined for the 1.5, 5.71 and 9.21 μm diameter particles were found to increase with applied transducer voltage and were found to be 3.2, 3.6 and 9×10^{-3} $m.s^{-1}$ respectively at the highest transducer voltage of 50 volts peak–peak (2 MHz). The experimentally determined critical velocities were

found not to agree with the theoretically determined critical velocities and a hypothesis for this aberration has been presented.

- Phase shifting was found to be most effective at a frequency of 2 MHz. The maximum rate of phase shifting possible was found to be 1.7 $\lambda.s^{-1}$ for 5.71 μm diameter polystyrene particles and 2.2 $\lambda.s^{-1}$ for yeast cells at a frequency of 2 MHz and transducer voltage of 30 volts. The maximum rate of phase shifting was found to be greater if the particles in supension in the standing wave field were allowed to form large aggregates.

- The separation of micron and submicron sized polystyrene latex particles has been succesfully demonstrated in both batch mode separation and continuous separation processes. Approximately 20 % of particles of 0.4 μm diameter are removed and 80 % of particles of 1 μm diameter are removed.

- The application of megahertz frequency ultrasonic standing waves to the segregation and recovery of whole yeast cells and yeast cell debris from suspension has been investigated and found to be an effective means of small scale separation for such biological particles, removing close to 100 % of particle over 4 μm in diameter from suspension.

The conclusions of this section of work indicate the strong influence of particle diameter and ultrasonic energy level on the rate of particle migration and hence on the efficiency of separation of particles using an ultrasonic standing wave field. The next chapter describes research into a novel method of rapidly determining the rate of particle migration in a standing wave field.

CHAPTER 7 LASER SCANNING OF STANDING WAVE FIELDS

This chapter describes the development of a novel measurement technique designed for the study of the migration of particles to form concentrated bands of particles in an ultrasonic standing wave field.

7.1 Experimental Aims

The main objective of this section of work was to develop a method of collecting information on the migration of particles towards the nodal planes during the initial moments following the formation of an ultrasonic standing wave field in a suspension. A subsidiary objective of this work was to interpret the information gathered with the aim of providing process specifications for the design of separation equipment for manipulating suspensions of biological particles.

7.2 Introduction

To design equipment to separate particles from a suspension by a specific method it is necessary to know the mechanism of separation being employed and also how individual particles behave within the separation device. For example the trajectory of a particle inside the bowl of a disc–stack centrifuge is an important factor in the design of efficient centrifuges, similarly the rate of movement of a particle towards the nodes of the standing wave field is an important factor in the design of an efficient ultrasonic separation technique.

The migration of particles to the nodes of an ultrasonic standing wave field can be easily demonstrated and described in the broad terms of the agglomeration of the particles into concentrated bands and the clarification of the suspension. However for the design of a separation device it is important to know the forces acting on the particle that cause the migration towards the node and the time taken for a particle at any point in the sound field to reach the node of the standing wave field. The former question is the subject of previous chapters, whilst the latter question though difficult to answer, and the subject of this chapter.

In previous chapters the time taken for visible concentrated bands of particles to appear during an experiment has been used as a measure of the effectiveness of the ultrasonic separation effect. This measurement is simple to make but only gives limited information about the separation taking place. During the course of this work a need arose for more precise data on the rate at which particles migrate towards the nodes of the sound field so that residence times for a suspension flowing through an ultrasonic standing wave field separation device could be derived allowing the design of larger scale separation devices.

Measurements of the rate of particle migration in a standing wave field must be made on the scale of a single wavelength as the particles only migrate a maximum distance of one half of the wavelength of the sound field (which at a frequency of 2 MHz is only a distance of approximately 350 μm). Optical equipment such as travelling microscopes can be used to observe the migration of particles but seriously limit the design of the experimental equipment. Since the limit of resolution of an optical microscope is approximately 1 μm such apparatus is not suited to the measurement of sub–micron particles which are of key importance in many biological fluids [Bell, (1983)]. More seriously such measurements are limited by factors such as individual researchers eyes and reflexes. Given these limitations and in order to collect accurate data on the migration of sub–micron particles an alternative method was developed.

7.3 Theoretical Considerations

The objective of the equipment design (described below) was to repeatedly measure the distribution in concentration of particles across a single node of a standing wave field (a distance of less than 750 μm at 1 MHz in water) during the initial formation of a standing wave field (0 – 5 seconds). Two conflicting issues had to be resolved in the design, namely the requirement for high precision measurement at a high speed.

A system based on the measurement of the intensity of light transmitted through the suspension in the standing wave field was chosen to measure accurately the distribution in particle concentration across a single node (a distance of less than

750 μm) with sufficient resolution to give useful results. A laser diode was chosen as the light source because of the capability to finely focus the laser beam to produce a "waist" diameter below 10 μm which would give high resolution of the particle concentration distribution. Even with such small laser beam dimensions it was only possible to conduct experiments at a frequency of 1 MHz where the wavelength was relatively large (See **Section 7.8**). The monochromatic nature of the emitted laser light was seen as a further advantage. With laser light the wavelength can be selected to enable natural light to be filtered out, either before or at the photodetector, thus reducing the level of signal noise during the experiments.

Experiments conducted in **Chapter 6** revealed that particle migration towards the nodes of the standing wave field occurred during the first seconds of the formation of the sound field. Therefore it was required to measure the intensity of light transmitted through several successive points across the developing band of particles many times a second. To achieve this a scanning focused laser beam was designed to move across a number of nodes twice a second thus enabling very rapid detection of changes in particle concentration across a node. Providing the standing wave field formed is homogeneous and that the initial suspension of particles is well mixed, it is reasonable to assume that a small number of adjacent nodes can be considered identical. The data collected from many such nodes can then be regarded as being representative of that collected from a single node. In this manner the equipment was used to monitor changes in particle concentration occurring over time periods less than 5 ms long (the approximate time taken for the laser beam to cross a node). Such small time periods require high rates of data collection that are not feasible with equipment such as simple chart recorders, for example and therefore a high speed computerised data acquisition system was used to sample the signal produced by the transmitted laser light falling on a high speed photodetector at rates sufficient to provide several tens of data points across a single node of the standing wave field.

7.4 Equipment Design

The diagram below **Figure 7.1** is a schematic representation of the equipment designed, built and developed during this research with the sole function of studying the formation of the concentrated bands of particles in a standing wave field.

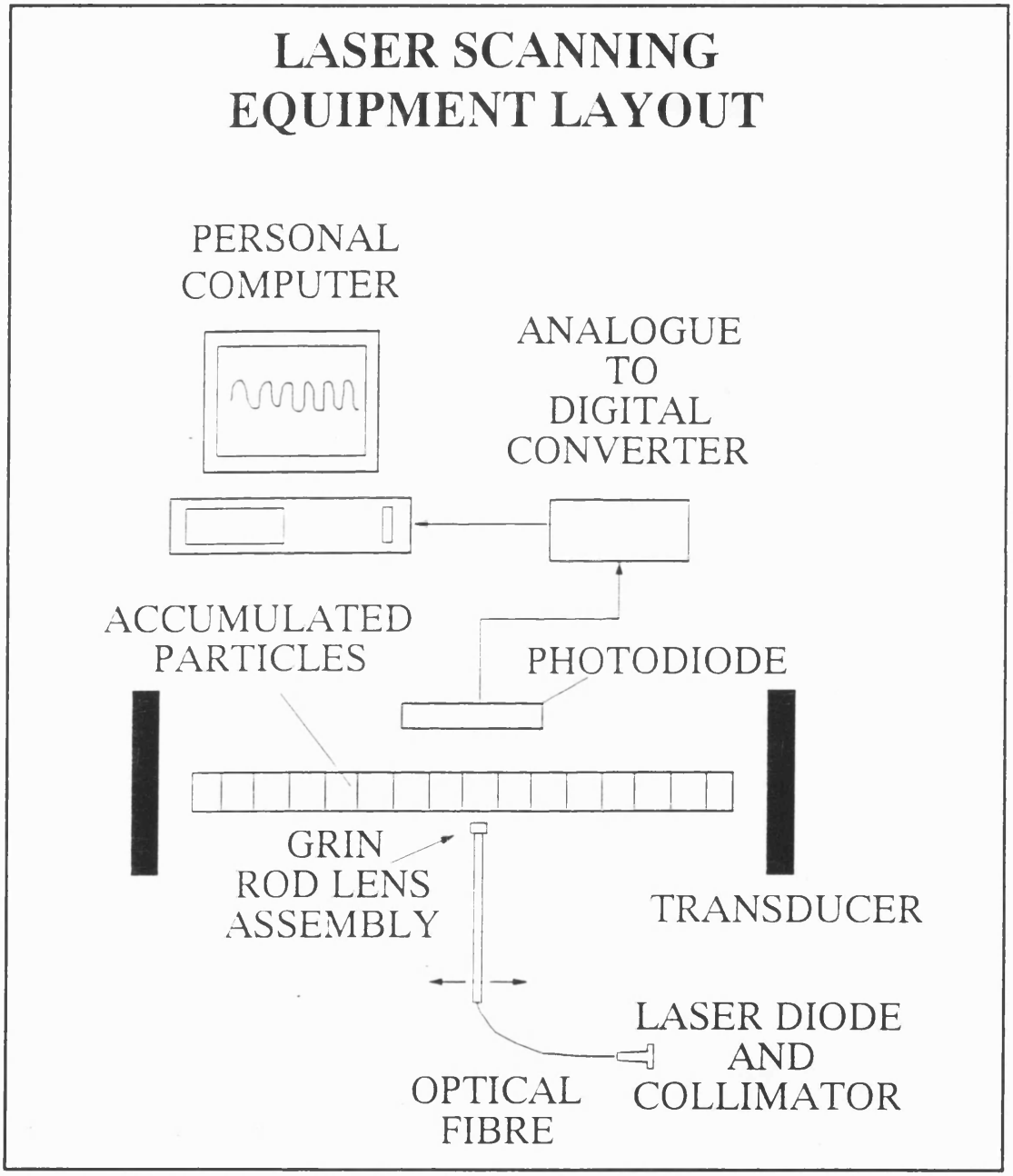

Figure 7.1 *Schematic Representation of the Ultrasonic Standing Wave Laser Scanning System.*

The device employs a finely focused laser beam produced by a 30 milliwatt Sharp LT024MD laser diode (Access Pacific Ltd, Kymbrook School House, Kimbolton Road, Keysoe, Bedford, U.K.) operating at 780 nm, coupled to an optical fibre (Kaytech Ltd, Bletchley, Milton Keynes, Buckinghamshire, UK.) which in turn was coupled to a Graded Index rod lens (GRIN rod lens, Melles Griot, 1 Frederick Street, Aldershot, Hampshire, UK.) focusing the laser beam to a waist of approximately 10 μm in diameter. The miniature assembly coupling the GRIN rod lens to the optical fibre was designed and built in-house (See **Figure 7.2**).

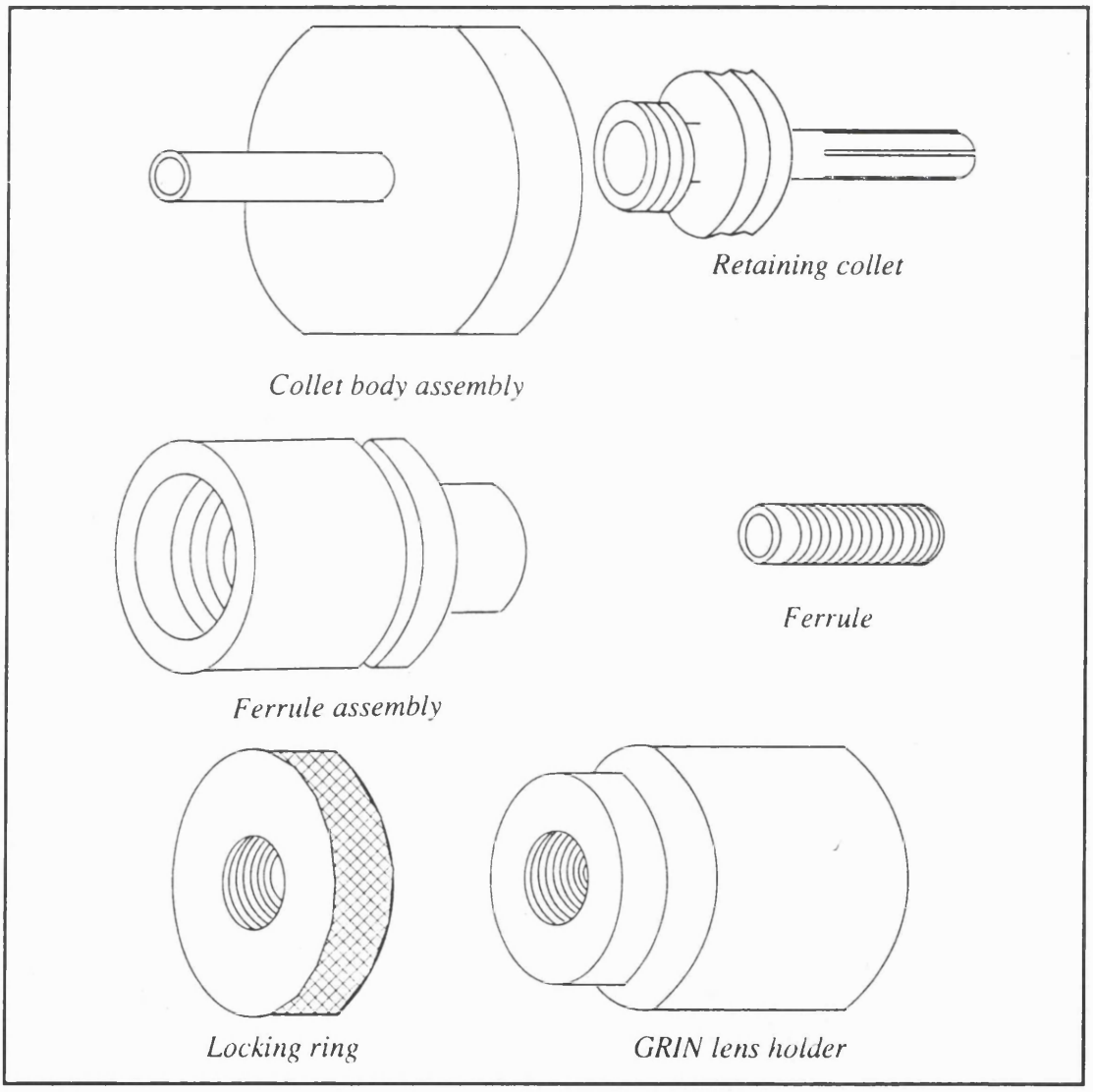

Figure 7.2 *Design of Miniature Assembly for the Coupling of a Graded Index Lens to an Optical Fibre.*

Measurements were made by scanning the laser beam across the suspension within which a standing wave field was forming. The scanning of the laser beam was effected by means of a PTFE cam (manufactured in-house) eccentrically mounted on a rotating shaft powered by a small 12 volt DC motor (336-315, RS Components Ltd.). The stainless steel tube through which the optical fibre ran and to which the GRIN rod lens assembly was attached was held against the cam by a spring, as the cam rotated the eccentric mount caused the steel tube to move from side to side thus scanning the laser beam back and forth (See **Figure 7.3**). The electric motor driving the cam operated at one revolution per second therefore the laser beam scanned the standing wave field twice a second (once in each direction of travel). The light emerging from the suspension was detected by a medium area (0.5 cm^2) high speed photodiode (651-995, RS Components Ltd) attached to the window of the sample cell. The signal from the photodiode was analyzed by a PC30AT data acquisition computer card (Amplicon Liveline Ltd, Centenary Industrial Estate, Brighton, East Sussex, UK) which sampled the analogue signal at rates up to 100 kHz converting the voltages to digital data and storing the data on the DELL System 210 computer (DELL Computer Corporation Ltd., Milbanke House, Western Road, Bracknell, Berkshire, U.K.).

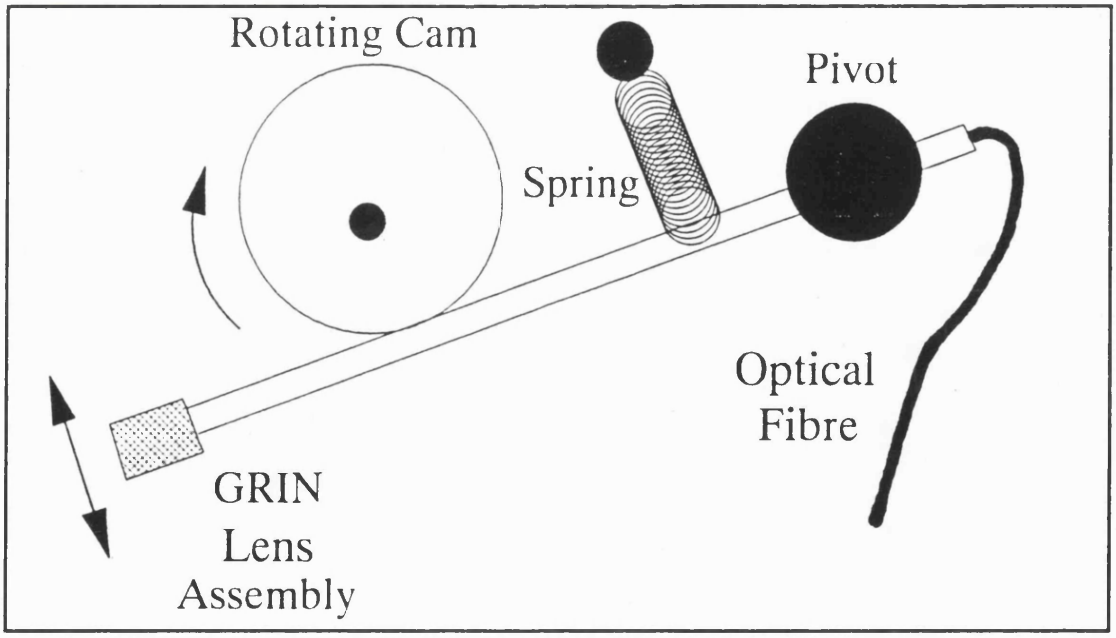

Figure 7.3 *Detail of Laser Scanning Mechanism.*

The data collected with this equipment is a measure of the laser light travelling through the suspension in the sound field. Initially the suspension has a uniform particle concentration throughout and therefore the light transmitted through the suspension has a uniform intensity across the sound field. As the particles migrate towards the nodal planes of the sound field the laser beam scans across areas of higher and lower particle concentration and therefore the intensity of the emerging light will vary across the sound field. In this fashion a series of intensity measurements are collected that monitor the change with time of the concentration of particles across a number of wavelengths as the standing wave field is forming. **Section 7.6.1** describes the methods used to analyze the raw data collected on computer disk.

The change in concentration profile across a wavelength with time can be studied under many conditions of fluid flow, phase shift, sound field and fluid–particle properties.

7.5 Calibration Procedure

A method of calibration was required for the apparatus before experiments could proceed. Standard suspensions of polystyrene latex particles of various particle diameters and of known concentration were prepared. The absorbances at 780 nm wavelength were measured in a ultraviolet–visible spectrophotometer (Perkin–Elmer Lambda II spectrophotometer, Perkin–Elmer Ltd., Post Office Lane, Beaconsfield, Buckinghamshire, U.K.) for series dilutions of the standard suspensions to create a calibration curve of absorbance versus particle concentration for each particle diameter. The 780 nm wavelength on the spectrophotometer was chosen to approximate to the light emitted by the laser diode which operated in the near infra–red region.

Each of the series dilutions was then placed in the sample cell of the laser scanning apparatus. Laser light intensity measurements were made for each of the diluted suspensions and a second calibration curve was created for each particle diameter.

The two sets of calibration curves were then used to convert the light intensity information collected by the data acquisition package into particle concentration hence

providing particle concentration profiles across several wavelengths of the standing wave fields.

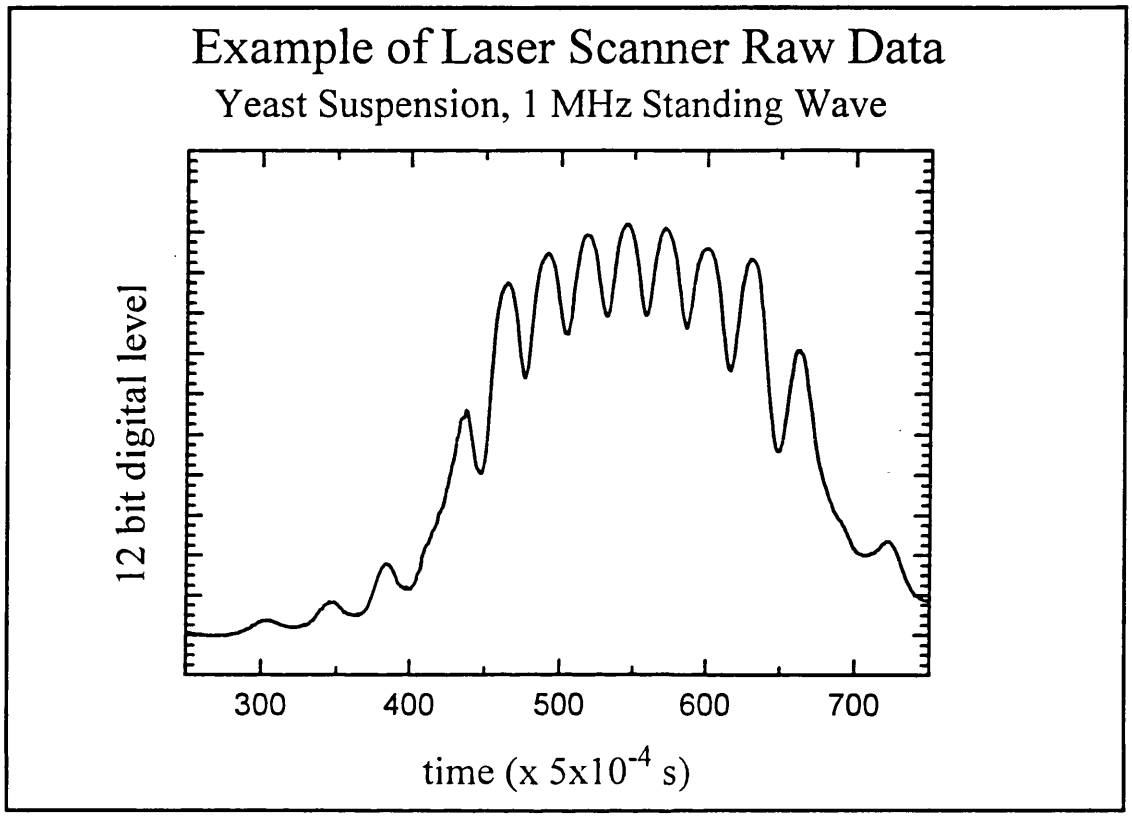

Figure 7.4 *Raw Data of Calibration Scans for Yeast Suspension.*

7.6 Experimental Procedure

The experiments performed on the laser scanning apparatus were aimed at accurately measuring the time taken for concentrated bands of particles to form at the nodal plane of a 1 MHz standing wave field and to assess the effectiveness of the apparatus to determine the concentration profile of the suspension across a nodal plane of a standing wave field.

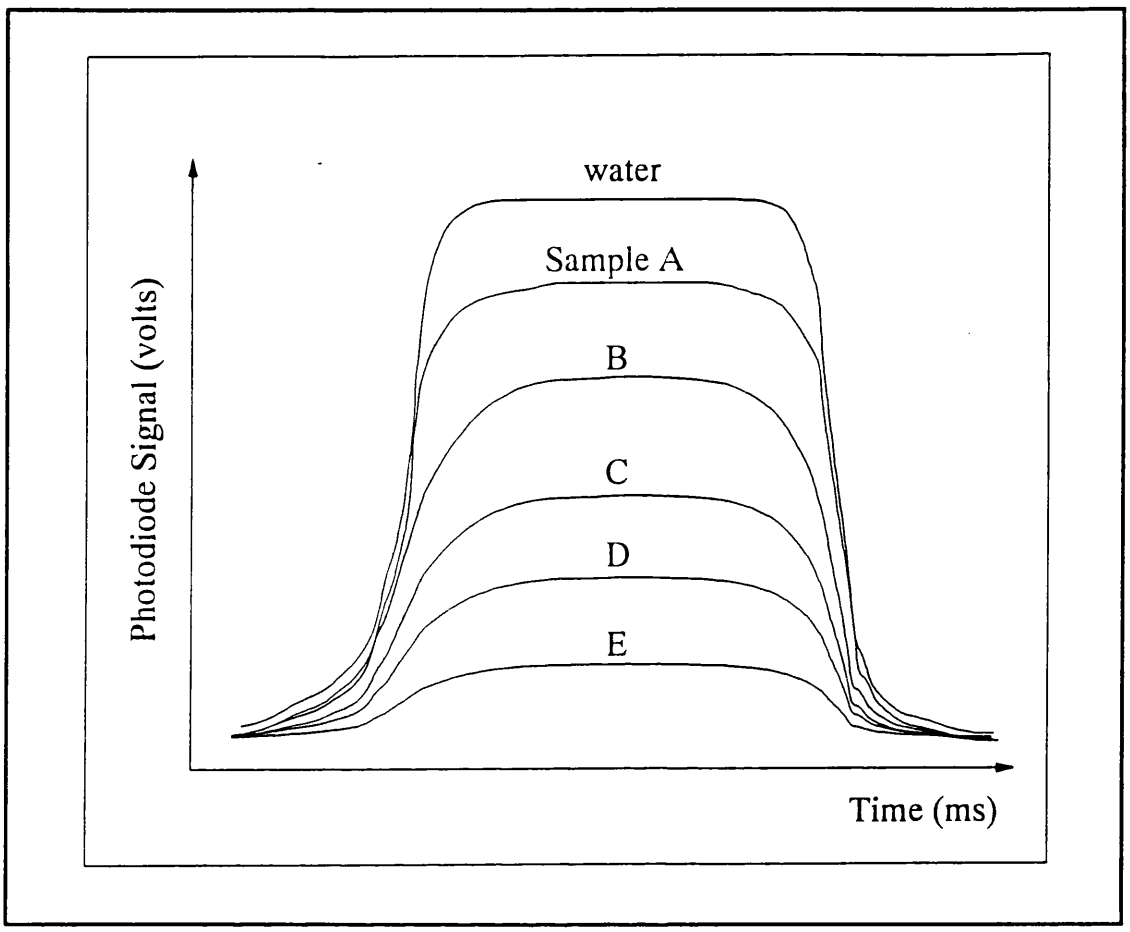

Figure 7.5 *Schematic Representation of Calibration Curves for Data Analysis.*

7.6.1 Method

Suspensions of known concentrations of particles of various diameters were prepared and a sample of the suspension was placed in the sample holder of the apparatus. Laser scanning of the sound field was initiated and the collection of data started at exactly the same instant as the ultrasonic radiation producing the standing wave field. After a thirty second period of ultrasonic radiation data collection was halted.

Analysis of the data was based on the time taken for the full extent of particle concentration to have occurred in the sound field, this was presumed to have been complete when two successive passes of the laser beam produced scans of data that were indistinguishable from each other.

7.7 Results

Examples of raw data collected during these experiments can be found in **Appendix VI** along with a graphical representation of the numerical data.

Figure 7.6 lists the results of several repeated experiments described in **Section 7.6** the values of banding time recorded were found to be very reproducible with an overall error of only 2 %. The graph follows the same curve as the results of the visual observations of banding time determined in the experiments of **Chapter 6**. The time required to form concentrated bands of particles in a standing wave field decreases with increasing particle diameter. However the time required to form concentrated bands of particles determined by the laser scanner method seems to be slightly longer. This is most probably due to the visual appearance of banding occuring some time before the bands reach their final concentration (which is the criteria for banding time in the laser scanner experiments).

7.7.1 Data Analysis

The analyses performed on the experimental results obtained from the above procedures consisted of taking measurements of the photodiode signal levels corresponding to samples of deionised water and suspensions of varying concentration of particles as described above to produce a set of calibration traces against which experimental results could be compared. The maxima and minima of the experimental results were compared with the calibration curves thus giving a measure of the concentration of the suspension at the nodes and at the internodal spaces.

7.8 Discussion

The results of the investigation confirm that this technique is capable of rapidly determining the rate of particle segregation in a standing wave field. The experimental results were found to be more reproducible than the visual observation made in Chapter 6 due to the simple definition of the point of formation of a concentrated band of particles used in the experiments described above. Rapid segregation was observed for particle diameters in excess of 2 μm. At particle diameters below 2 μm

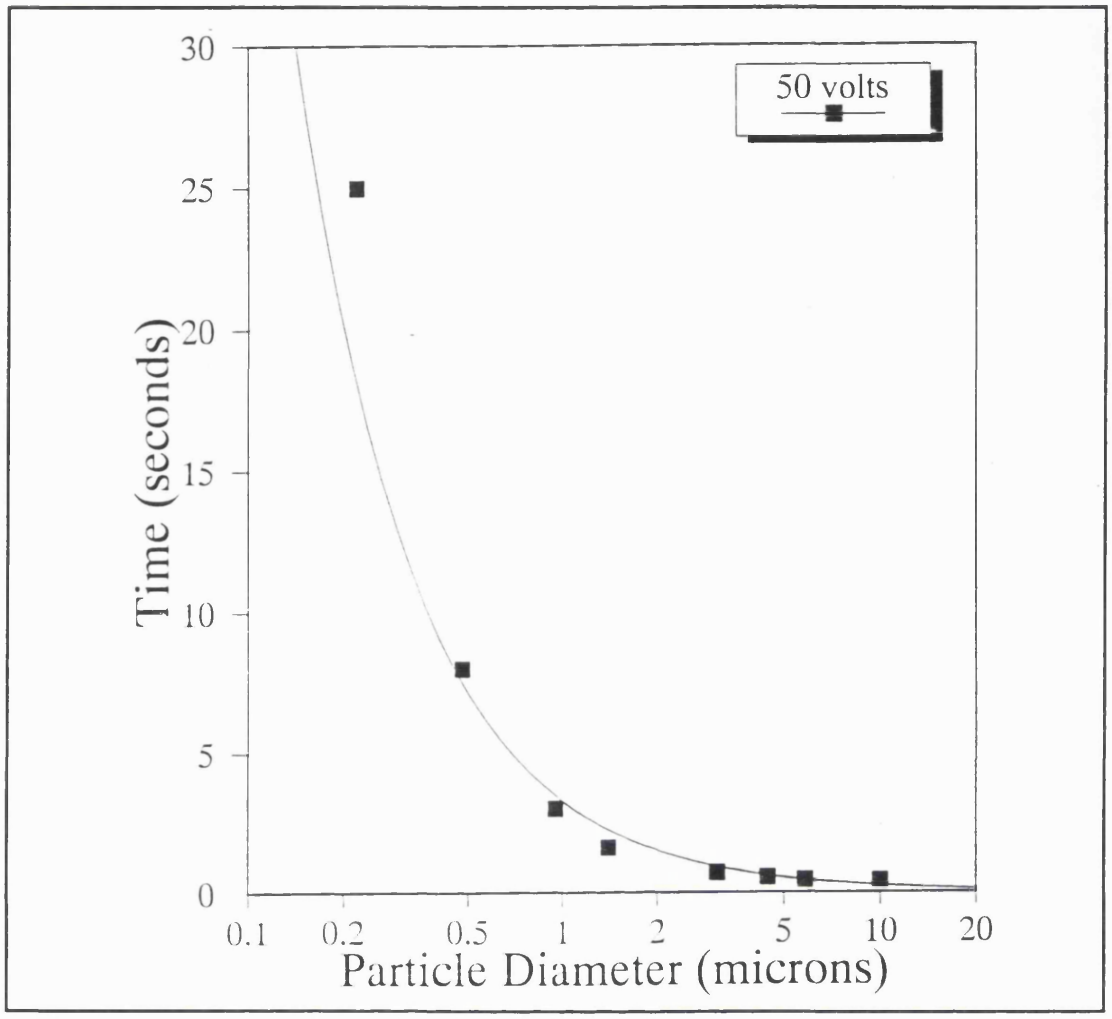

Figure 7.6 *Time Taken to Form Concentrated Bands of Particles in Standing Wave Field : Laser Scanner Experimental Results.*

the rate of particle migration reduces sharply and the banding time for such particles increases rapidly.

It became apparent that the experimental data held a great deal of information that would require sophisticated data analysis and deconvolution routines to extract. For example, although the laser was focused to a very small waist, the gaussian profile of the laser beam light intensity would cause the desired experimental data to be super-imposed with a complex waveform produced as the guassian light intensity profile crosses the areas of high and low particle concentration. This system error could be removed from the data if the laser beam light intensity profile was accurately known and easily described mathematically.

The guassian profile of the laser beam becomes apparent in the data at the point when the suspension in the standing wave field has been sonicated for several seconds and the vast majority of the particles have accumulated at the nodes. During the initial moments of sonication the data took the form of a sinusoidal curve (See **Figure 7.7**) which was as expected due to the sinusoidal distribution of the radiation pressure forces in the standing wave field.

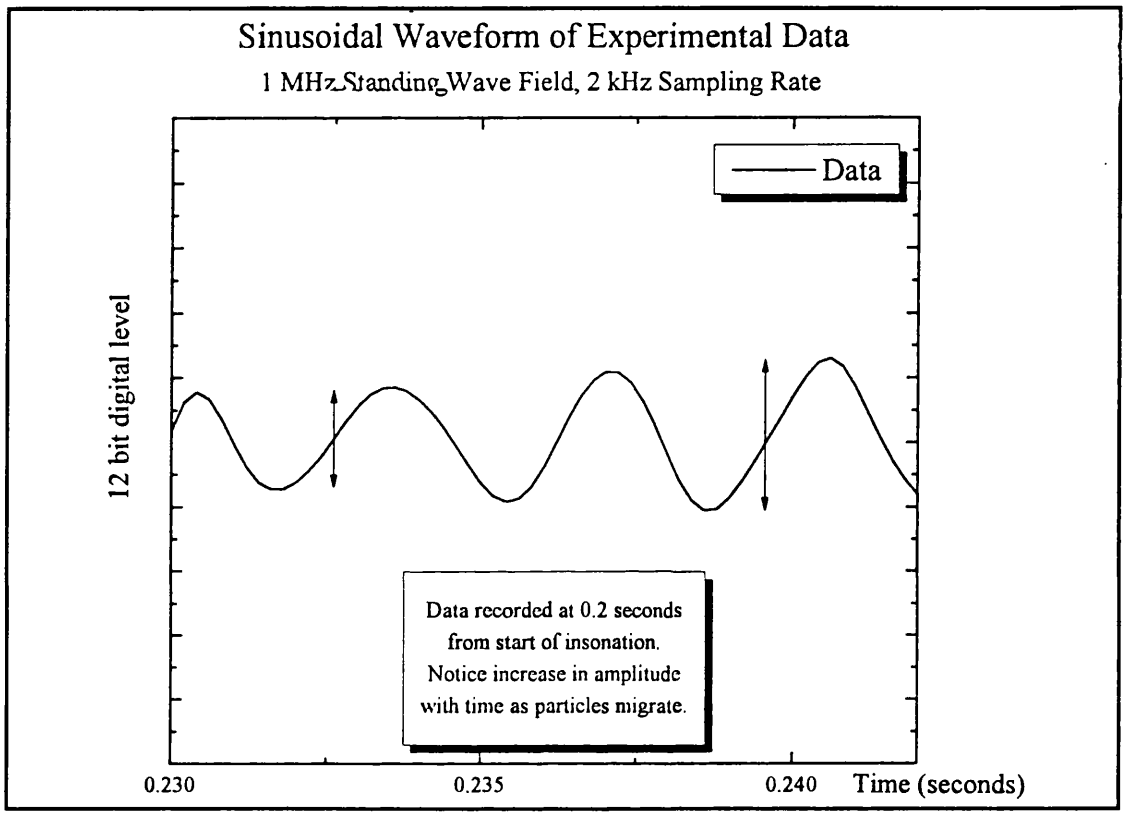

Figure 7.7 *Example of Sinusoidal Waveform of Experimental Data During Early Stages of Standing Wave Formation.*

After several seconds of sonication the data would be expected to take the form of a square wave as the laser beam passed across successive bands of very high particle concentration and particle free liquid. However the experimental data took the form of a curve as shown in **Figure 7.8** where the square wave was replaced by near gaussian curves.

The experimental data from a scan showing four bands of the standing wave field plotted together with a gaussian fit of the data performed using the fitting function shown below are given in **Figure 7.8.**

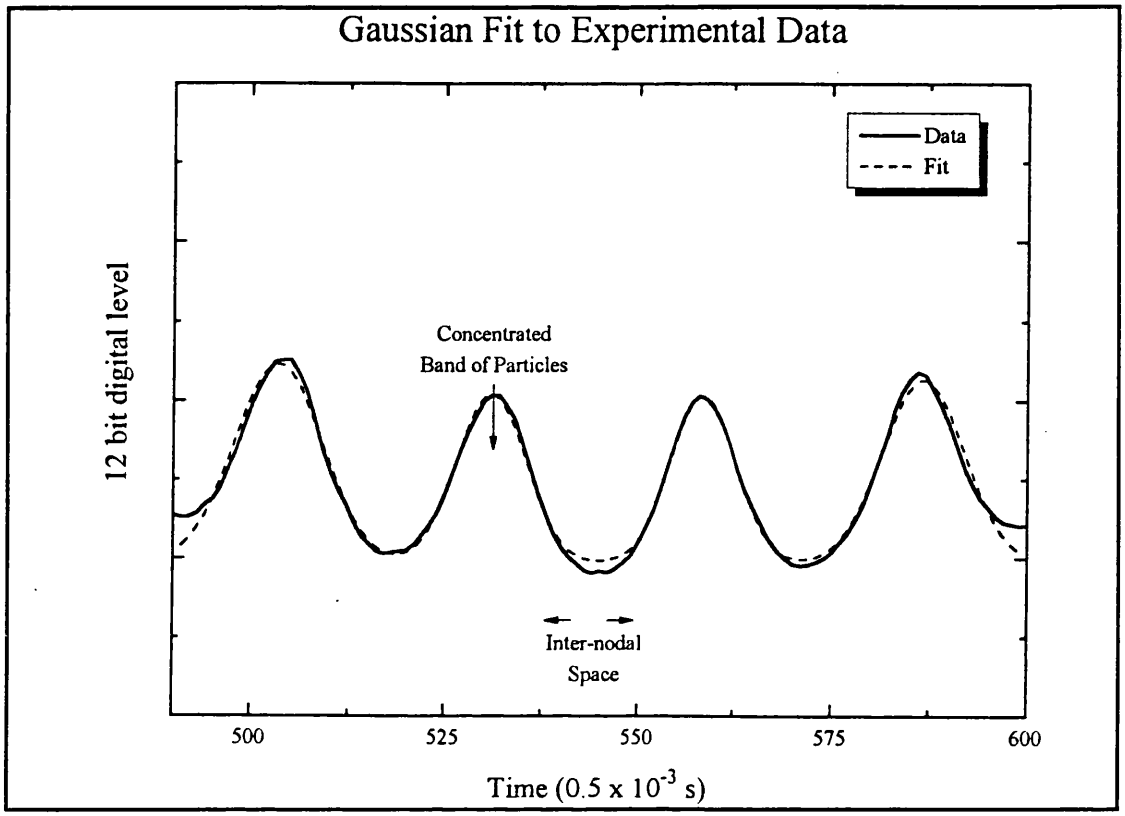

Figure 7.8 *Multiple Gaussian Fit to Experimental Data.*

$$F(x) = Y_0 + \frac{A}{w\sqrt{\frac{\pi}{2}}} \cdot e^{-\frac{2(X - X_0)^2}{w^2}} \qquad \textbf{Eq. 7.1}$$

where $\mathbf{Y_0}$ is the offset of the fitted curve, **A** is the total area under the curve, $\mathbf{X_0}$ is the coordinate of the center of the peak, and **w** is the width of the peak at half height. As can be seen from the two curves the gaussian function is an acceptable approximation of the experimental data. This confirms the earlier statement that experimental data recorded after several seconds of particle migration will not accurately reflect the concentration profile of the particles across the nodes of the standing wave fields. It is certain that the gaussian-like curves resulting from the scanning of the bands of particles will under-estimate the concentration of the particles accumulated at the nodes and at the same time seriously over-estimate the concentration of particles in the inter-nodal spaces.

7.9 Conclusions

The novel experimental technique described in this chapter has been shown to provide a rapid method of investigating the rate of migration of fine particles in an ultrasonic standing wave field.

The times required to segregate polystyrene latex particles in the range of 0.16 to 10 μm diameter have been determined. Latex particles of 5 μm diameter, approximately the diameter of a yeast cell, have been shown to form concentrated bands in a standing wave field in a time of approximately one second.

The development of this experimental apparatus could provide a rapid measurement technique for the assessment of the rate of migration of particles in a standing wave field. Exhaustive analysis of the experimental data produced, including deconvolution of the particle concentration data (**Section 7.8**), will enable the prediction of the efficiency of ultrasonic separation of a particulate sample under the chosen, precisely controlled, conditions of fluid flow and ultrasonic standing wave field.

Further work is required to investigate methods of extracting the information on the concentration profile of the particles across the nodes of the standing wave field from the experimental data and is discussed further in **Chapter 11**.

The final experimental chapter, **Chapter 8**, describes research to investigate the application of ultrasonic standing waves for in-line sample preparation.

CHAPTER 8 ULTRASONICS IN LASER PARTICLE SIZING

This chapter covers an area of work that developed as an application of the megahertz frequency standing wave separation technology being studied as the main subject of this thesis. The work is a joint project between two separate PhD programmes: this thesis on the optical monitoring and signal evaluation relating to particulate properties during purification of biological suspensions (Holwill, PhD Thesis, University of London).

The ability of ultrasonic standing waves to manipulate fine particles in suspension can find applications in many areas of technology. The application described in this chapter is an example of the exploitation of the non-invasive nature of the technique and describes the development of an *in situ*, sample preparation stage for particle size measurement in a photon correlation spectroscopy (**PCS**) submicron particle size analyser.

The results of experiments described in **Section 6.5.7** demonstrated the effect that the ultrasonic standing wave technology could have on the particle size distribution of a suspension of yeast homogenate and initiated research into the present application. The attractive feature of the ultrasonic technology in this application is the ability to selectively manipulate particles of large size difference with the aim of effectively *cleaning* the sample by using standing waves to "band" dust and particles away from the sampling volume of the laser particle sizer.

The following sections describe the theoretical aspects of **PCS** and the application of ultrasonic standing waves and present results demonstrating the effectiveness of this non-invasive technique.

8.1 Introduction

Photon correlation spectroscopy is a technique for measuring particle diffusion coefficients in suspension. It has been applied to many biological systems in the past as it is a fast, accurate and non-invasive measure which can be used for inferring particle size distribution. In the present application the technique is being applied to the analysis of complex process streams on-line in a biochemical pilot plant [Holwill (1992)], as part of a monitoring and control system which uses information including

particle size distribution and concentration to optimise yield in a multistage purification process, where a wide distribution of particle size is present. One of the problems encountered in such an application is the ability to achieve the fast and non–invasive sample preparation needed to remove unwanted particulates from the suspension prior to measurement. This chapter presents research showing how separation of such particles utilising ultrasonic standing waves may be a promising solution to this problem. Results of experiments with polystyrene latex and yeast homogenate are presented in following sections.

8.2 Photon Correlation Spectroscopy

A full discussion of photon correlation spectroscopy (**PCS**) and its application to bioprocesses is presented elsewhere [Holwill, PhD Thesis, University of London, (1992)]. Dynamic light scattering analyzers measure scattered light intensity fluctuations from a suspension of particles undergoing Brownian motion and from the temporal charcteristics of such fluctuations a diffusion coefficient is calculated which can be related to particle size. The relation for the relaxation rate of the fluctuations and diffusion coefficient for a polydisperse suspension are shown below in **Equations 8.1** and **8.2**.

$$g^{(1)}(\tau) = \int_{\gamma_{min}}^{\gamma_{max}} \exp(-\gamma\tau)\, G(\gamma)\, d\gamma \qquad \textbf{Eq. 8.1}$$

where

$$\gamma = D_C k^2$$

Here γ is the decay constant corresponding to a particular diffusion coefficient and τ is the experimental sampling interval, $G(\gamma)$ is the required distribution, and D_C, the Diffusion Coefficient, which for spherical particles is given by:

R_H is the hydrodynamic radius, k_B is Boltzmans constant, T is the temperature and η is the viscosity of the liquid.

$$D_C = \frac{k_B T}{G \pi \eta R_H} \qquad \text{Eq. 8.2}$$

The scattering vector **k** is given by the following equation

$$k = \frac{4 \pi n_0}{\lambda_L} \sin(\frac{\Theta}{2}) \qquad \text{Eq. 8.3}$$

where λ_L is the wavelength of the light, n_0 is the refractive index of the liquid and Θ is the scattering angle.

There is substantial literature concerned with the inversion of such data into size distributions and a multitude of computer programs that can be applied. *A priori* information about the size distribution may also be included to aid the deconvolution programs. However, improvement of the data quality must be the first step to a reliable measurement system.

8.2.1 Signal and Noise Considerations

In particular the baseline of the correlogram must be accurate to within about 0.1% to ensure a reliable inversion of the complete size distribution. This is a practical limit taking into account the fundamental noise inherent in the technique. The expression for experimental signal to noise ratio for a monodisperse suspension is shown below in **Equation 8.4**. This only accounts for photon counting noise and not noise due to dust or any systematic errors.

$$\frac{Signal}{Noise} = \sqrt{\gamma T} \qquad \text{Eq. 8.4}$$

Here **T** is the experimental duration. This shows that a determining factor for noise on the correlogram is the largest particle size present (assuming a constant sample time). Thus, apart from increasing the experimental time the only other way to improve the ratio is to increase γ. This can be done by using larger scattering

angles. If alternatively the maximum particle size is reduced however this will increase γ as there is an inverse relation between the two (See **Equation 8.2**). In practice multiple sample time correlators are used so that a wide range of particle size distribution can be covered. Better resolution is possible however with a narrower size range and a correspondingly narrower spacing of sample times. Keeping **T** as low as possible is important in on-line applications to ensure the rapid response of control systems. Better accuracy should therefore be accomplished in this situation by reducing the range of particle size to be measured and keeping the maximum size of particles in the sample as low as possible.

The smaller particles in suspension are often those of most interest in biochemical engineering applications i.e. they may be the product and the larger particles unwanted contaminants. Examples are the virus-like particles or hepatitis B virus surface antigen vaccine particles both of which can be expressed in yeast, where downstream of fermentation the yeast cells and their components become contaminants. Yeast homogenate covers a wide range of particle size from whole cell ghosts of about 5 μm down to the 200 nm region. For photon correlation measurements the upper detectable size limit is about 3 μm and the presence of particles larger than this compromises the results substantially [Chu (1991)]. Usually filtration or centrifugation is required to remove the larger contaminants although their size and quantity are still an important measure in the present situation. More recently a two aqueous phase operation has been used to separate the smaller contaminants. Previous work [Hoare (1990)] has used a miniaturised centrifuge in part to remove unwanted components rapidly and for small sample volumes (0.25 mL). Work by Chu *et al* used an in-line filter to remove dust particles from samples.

In this application the presence of these large particles which due to the much greater scattering efficiency associated with large particles tend to distort the resulting size distribution or indeed hide the smaller particles altogether so that sample preparation is essential prior to measurement [Holwill (1992)]. The errors in the baseline can do more than simply shift the distribution. The larger particles can contribute an almost constant offset to the baseline when their size is such that it is out of range of the correlator.

Megahertz frequency ultrasonic standing waves can be used to cause the larger particles or dust particles to migrate away from the laser beam (See **Figure 8.1**) thus aiding better data collection. Additionally it is possible to do this rapidly and *in situ* so that a crude sample may be put into the apparatus avoiding filtration or centrifugation steps and their associated problems. The use of this technique may in some cases make possible for the first time the non-invasive measurement of soluble or insoluble products in untreated process fluids.

This analysis technique has been termed Internodal Light Scattering (**ILS**).

8.3 Ultrasonic Technique

This section briefly describes the attributes of the megahertz frequency ultrasonic standing wave separation technique that are of interest in this particular application of **PCS** particle size analysis.

8.3.1 Theory

The main driving force of particle migration in an ultrasonic standing wave field is the radiation pressure exerted on each particle in suspension. **Equation 8.5** describes the radiation pressure exerted on a spherical particle in a plane stationary wave (See **Chapter 2** for details).

$$P_r = 4\pi a^3 \kappa E F \sin(2\kappa x) \qquad \text{Eq. 8.5}$$

From **Equation 8.5** it is clear that there is a very strong dependence of the radiation pressure on the particle radius **a**. The radiation pressure, $\mathbf{P_r}$, is proportional to the particle radius, **a**, cubed which in practice means that the separation driving force falls off rapidly with decreasing particle diameter. This factor can be used to separate particles of different diameters. The radiation pressure displays only a relatively weak dependence on the particle density ρ_1 and sound velocity through the particle medium c_1 and therefore particle size is the determining factor in the migration of the particles in the sound field.

By controlling the energy density of the standing wave field **E** produced any particles over a chosen size can be immobilised or "banded" at the nodal plane of the stationary wave leaving the smaller particles free (unbanded) in the inter–nodal spaces.

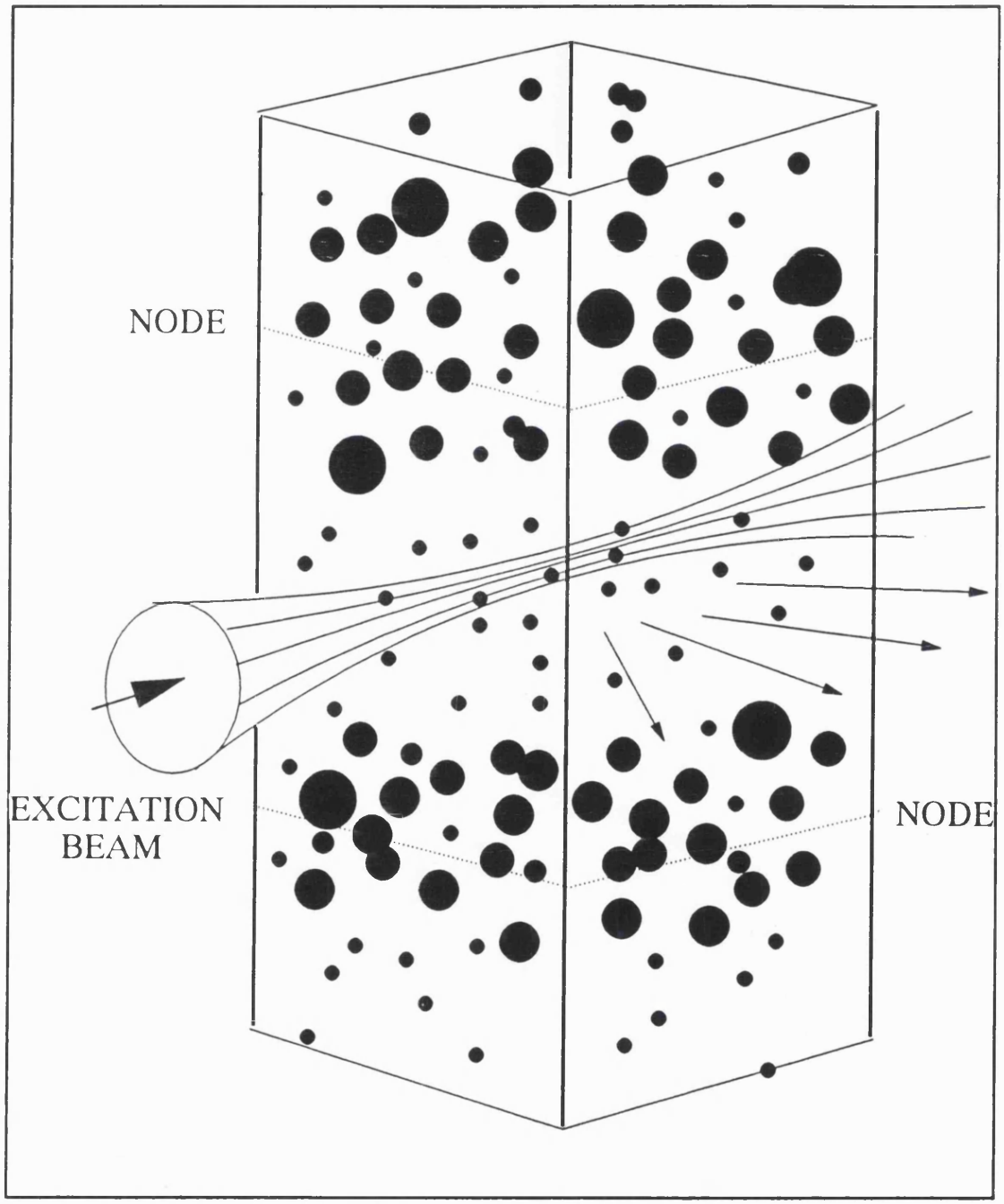

Figure 8.1 *Schematic Representation of Laser Beam Passing Between the Concentrated Bands of Large Particles Accumulated at the Nodes.*

To achieve successful **ILS** the laser beam of the dynamic light scattering analyser must pass between the concentrated bands of large particles formed at the nodes of the standing wave field and impinge on the smaller particles remaining in the inter-nodal spaces. The distance between the centres of the bands of particles is 750 μm at 1 MHz and 370 μm at 2 MHz, however the bands of particles have a finite thickness (dependent on the initial concentration of the suspension and the ultrasonic energy density in the standing wave field) and therefore the internodal space is in the order of 500 and 250 μm wide respectively. The dimensions of the laser beam waists used in dynamic light scattering analyses are in the order of 10's to 100's of μm. therefore careful consideration of the frequency of the standing wave field and the dimensions of the laser beam must be made to ensure the laser beam can be positioned within the inter-nodal space.

8.4 Experimental Work

Ultrasonic frequencies in the region of 1 MHz were chosen for this research due to the relatively large distance between nodal planes of the generated sound field (The half wavelength distance at 1 MHz in water is approximately 750 μm.) for ease of laser beam alignment, and because of the efficient separation that is performed with sound waves of this frequency (See **Section 6.4**).

An Audley Scientific Super Stable Frequency Signal Generator and Dual Ultrasonic Amplifier were used to drive the 25mm diameter PC4 ceramic transducer (Morgan Matroc Ltd) generating the sound field. A sample cell designed and manufactured in-house was used to conduct the experiments (See **Figure 8.2**). The ultrasonic standing wave field was formed by the reflections of the incident travelling sound wave from the transducer being reflected off the bottom surface of the quartz cuvette used to contain the sample. Although not ideal conditions (See **Chapter 4**) effective particle migration and banding was observed during the experiments.

The initial work was carried out with a Malvern 4700 photon correlation instrument (Malvern Instruments, Malvern, Worcestershire, UK) with a 30 mW, 633 nm HeNe laser and an IBM PS2 for data processing. This technique is capable of sizing particles in the range of 3 μm down to 0.5 nm. The ultrasonic sample cell was

positioned in the index matching bath (which reduces unwanted light reflections at the sample cell walls) of the Malvern 4700. Fine vertical positioning of the transducers was made possible by means of an optical component, fine positioner (Melles Griot, 1 Frederick Street, Aldershot, Hampshire, UK). Thus the laser beam could be accurately passed through any part of the sample cell required.

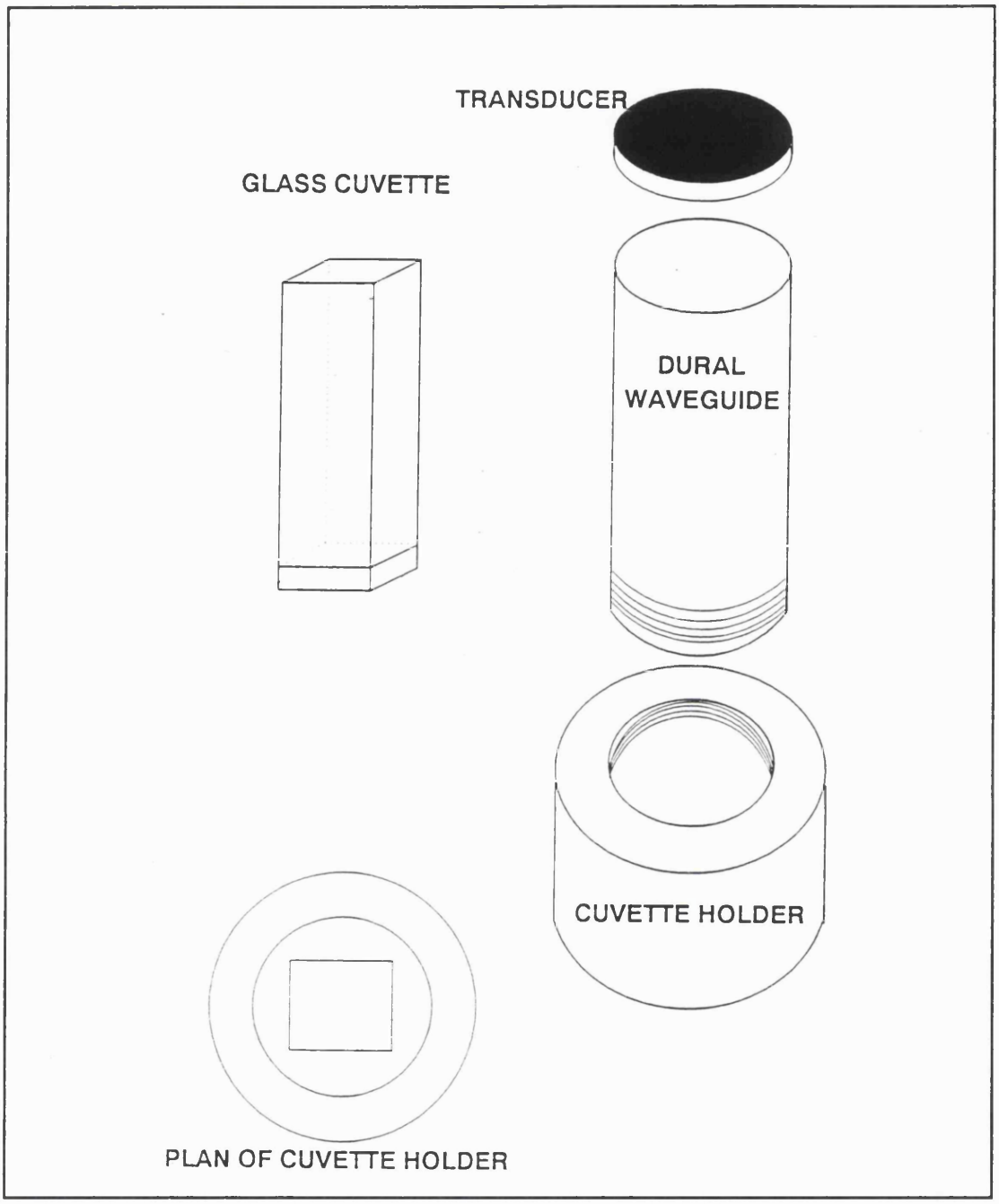

Figure 8.2 *Components of Ultrasonic Sample Cell for* ILS *Analyses.*

Polystyrene latex particles were chosen for use in this investigation (see **Appendix III**). As the aim of the work was to remove large particles from mixtures containing submicron particles, initial experiments were conducted using mixed suspensions of very small latex particles (39 nm) and larger (4,000 to 15,000 nm) particles, each separate latex suspension having a monomodal distribution. The

difference in average size between the two component particle distributions in suspension was then reduced to assess the lower size limit or the effective removal of the larger particles from the inter-nodal spaces. This included the use of 85 nm particles, 2,000 nm and 15,000 nm particles. Finally yeast homogenate diluted 1:10 with filtered phosphate buffer (See Section 3.8) was investigated with **ILS** analysis.

The transducer voltage used was in the region of 25 volts peak to peak for the experiments using polystyrene latex particles and considerably higher (50 volts p-p) for the yeast homogenate experiments. The higher power levels were required due to the low values of **F** (See **Equation 2.20**) associated with such biological particles.

8.5 Results

The following sections discuss the results of analyses conducted to assess the performance of the internodal light scattering technique. The experiments described above were repeated several times and the reproducibility of the measurements is as detailed in **Section 3.2**.

8.5.1 Polystyrene Latex Particles.

The results obtained for a mixture of polystyrene latex spheres are shown in **Figure 8.3**. Data for the results of a unimodal analysis on a mixture of 39 nm and 4,450 nm particles without the application of an ultrasonic standing wave clearly indicate that the presence of the 4,450 nm particles has seriously distorted the properties of the measured particle size distribution.

The result of the **ILS** analysis of the mixture of 39 nm and 4,450 nm particles is shown in the same figure. The mean of the distribution is given as 53.5 nm and the overall distribution is slightly broader than the 39 nm suspension distribution. However the result shows that the ultrasonic standing wave has effectively removed the 4,450 nm particles from the analysis. The slightly broader distribution of the **ILS** analysis results may be due to stray light scattered from the concentrated bands of particles at the nodes either side of the inter-nodal space entering the detector. However the distortion is very slight. This result indicates the utility of using **ILS** to

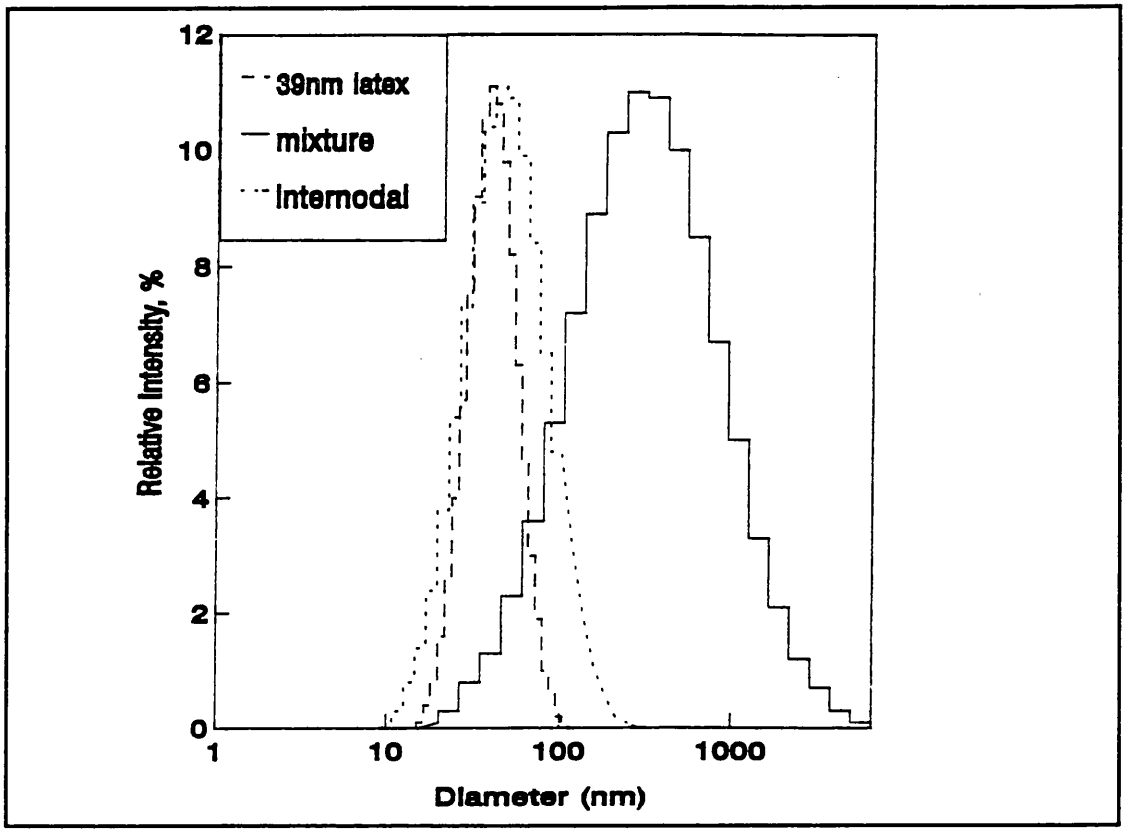

Figure 8.3 *Size Distribution of 39 nm and 4459 nm Polystyrene Latex Particles.*

pre-condition a sample for analysis of the smaller particles in suspension.

The results of ILS analysis on a mixture of 39 nm and 2,000 nm particles are shown in **Figure 8.4**. Data from the analysis performed in the internodal space shows a clear peak close to 39 nm indicating complete removal of the 2,000 nm particles from the analysis volume.

Results from an analysis performed on the concentrated bands of particles accumulated at the nodes of the standing wave field show a mean of 18,500 nm, about nine times the actual size of the 2,000 nm particles. This result may be attributed to a number of phenomonen, such as may be caused by the high concentration of the particles in this region resulting in particle interaction effects such as particles aggregating to form flocs of particles; or an effect of the ultrasonic field hindering the normal diffusion of the particles. In cases of high particle concentration multiple scattering of the light from the sample may occur which invalidates the analysis technique used by the instrument as it is based on singly scattered light. However

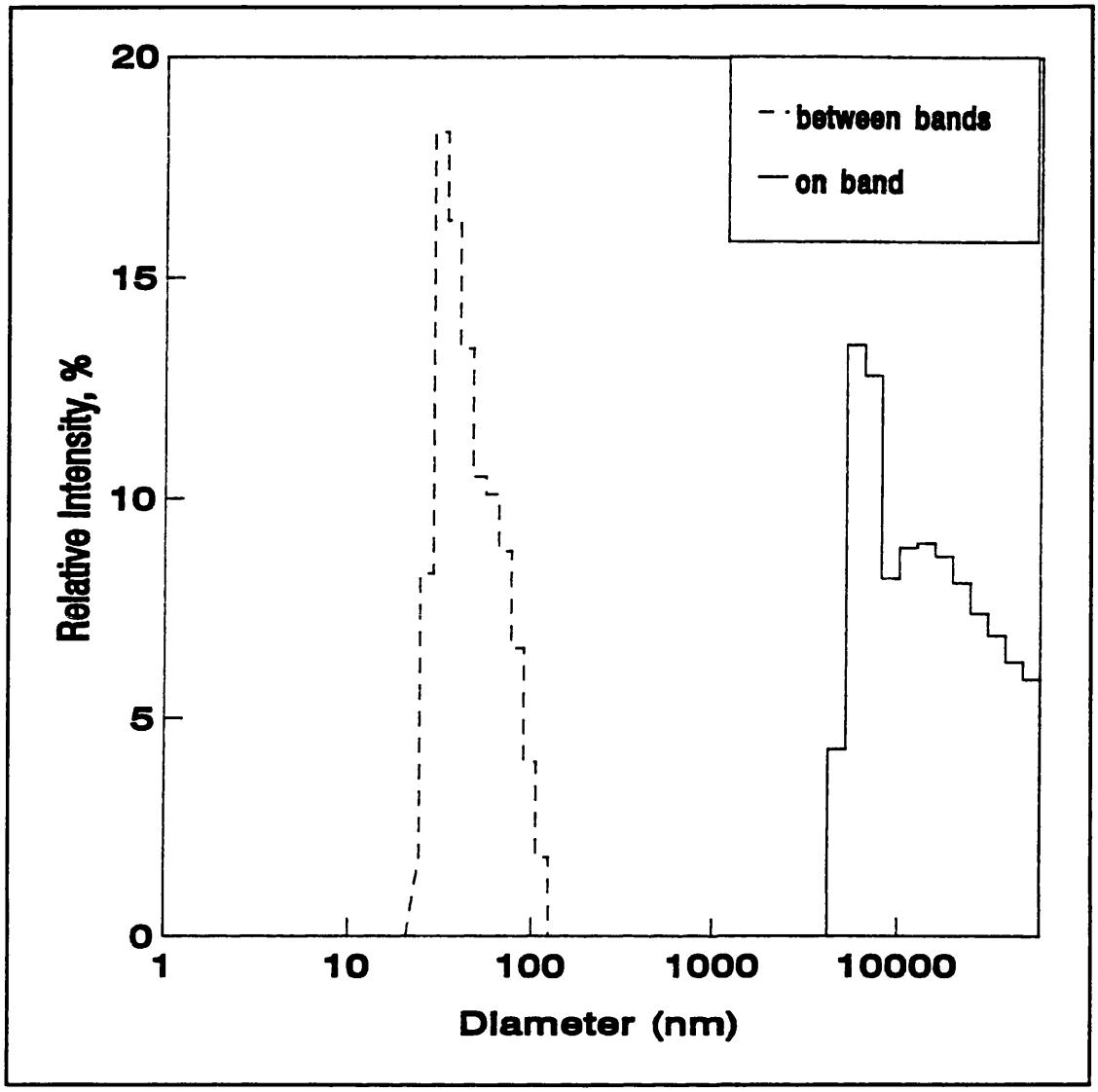

Figure 8.4 *Size Distribution of 39 nm and 2,000 nm Polystyrene Latex Particles.*

multiple scattered light, when interprated in a dynamic light scattering experiment, will give rise to a lower than expected particle size rather than a very much greater one, hence one of the aforementioned causes is likely to be the reason for the large particle size returned by the analyzer.

The results of the normal and ILS analyses of a mixture of 85 nm and 15,000 nm particles are displayed in **Figure 8.5**. The dotted line represents a normal analysis (without ultrasound) of the mixture and shows a bimodal distribution indicating the presence of 85 nm particles. The very broad peak from 5,000 nm upwards reveals the presence of contaminants and as well as the 15,000 nm particles in the mixture.

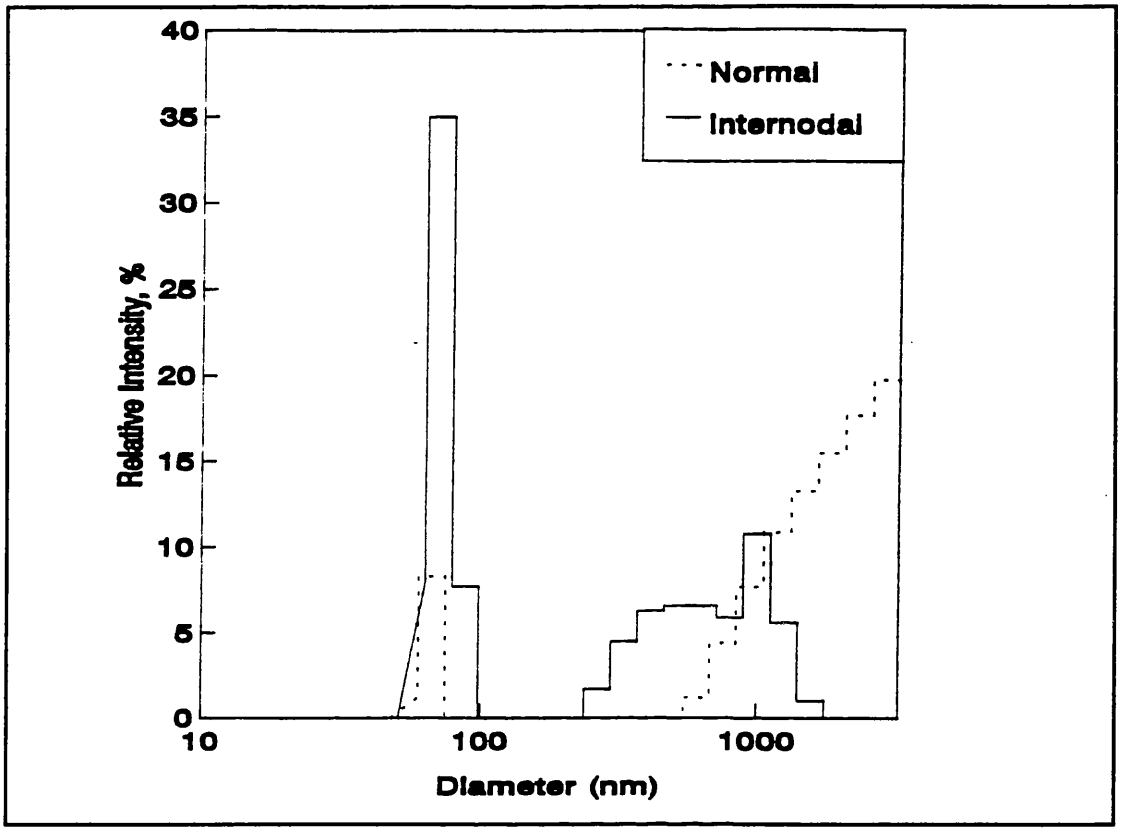

Figure 8.5 *Size Distribution of 85 nm and 15,000 nm Polystyrene Latex Particles.*

The **ILS** analysis (solid line) shows a dramatic increase in the 85 nm peak indicating the removal of the 15,000 nm particles from the inter–nodal space. The remaining signal at 200–1,200 nm represents the contaminating particles in the suspension whose distribution has now been resolved by the removal of the 15,000 nm particles by the standing wave field.

The results of an **ILS** analysis on a mixture of 85 nm and 1,400 nm particles are given in **Figure 8.6**. The original distribution (not shown for reasons of clarity) was very similar to the **ILS** result. This observation would suggest that there exists a minimum size limit for the removal of particles from the inter–nodal space for this particular experimental set up. This result does not define the absolute limit for the technique, only of this particular piece of apparatus. Redesign of the **ILS** cell, incorporating the use of two transducers and more effective ultrasonic frequencies, would be expected to reduce the minimum size limit to the order of 100's of nm by inputing a greater ultrasonic energy density and hence exposing the particles in suspension to very much greater radiation pressure forces (See **Chapter 6**).

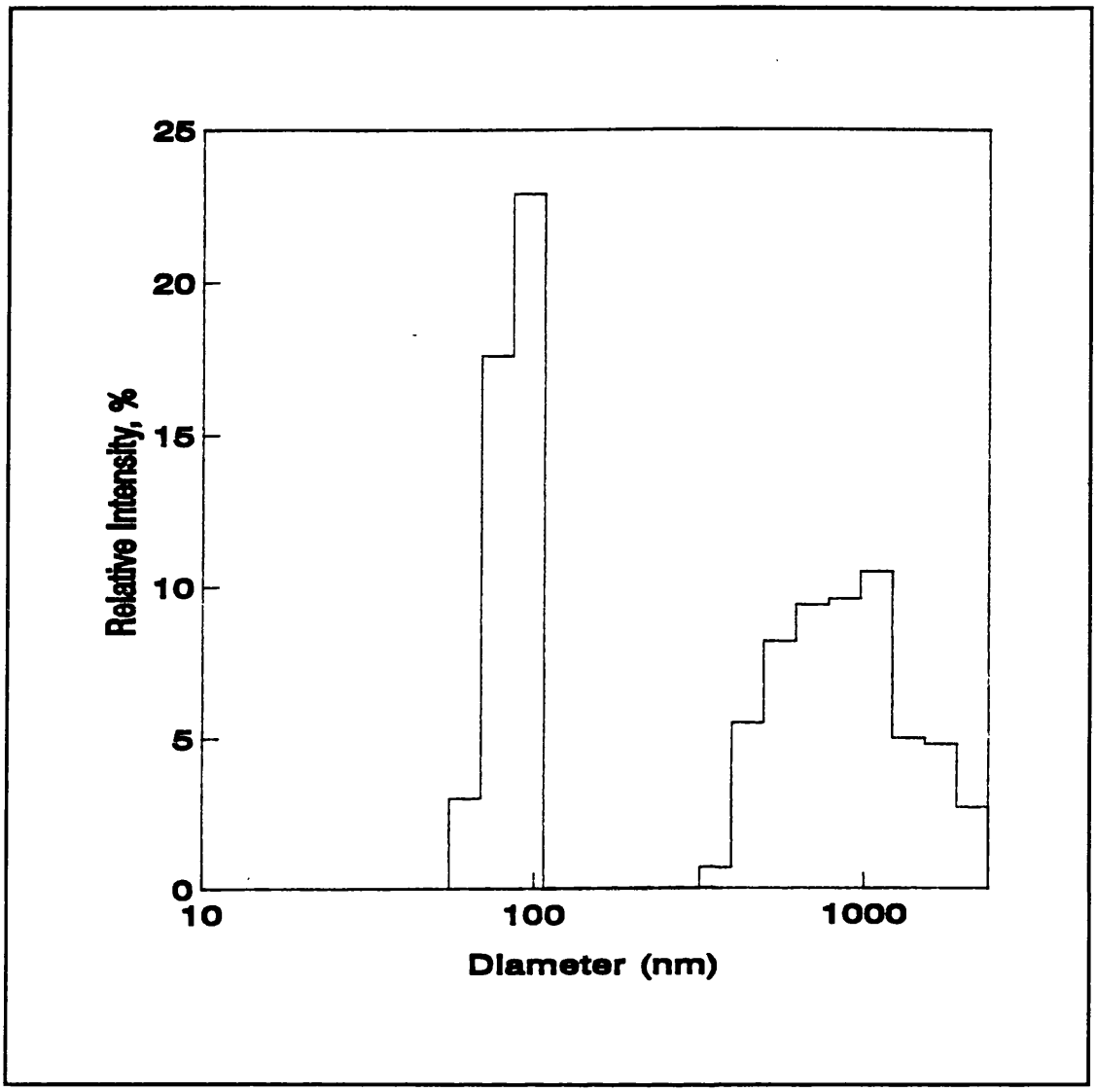

Figure 8.6 *Size Distribution of 85 nm and 1,400 nm Polystyrene Latex Particles.*

8.5.2 ILS Analysis of Yeast Homogenate

Experiments on the ILS analysis of unclarified yeast homogenate were performed to assess the possible improvements to be gained from the use of ILS in yeast based product particle size distribution analysis. Results of numerous experiments showed that at the high ultrasonic energies required to effect banding of the homogenate particles it was difficult to maintain the stability of the ultrasonic standing wave for sufficient time to record consistent and repeatable results. This observation may be attributed to the relatively high ultrasonic intensities causing the formation of gas bubbles in the homogenate suspension which in turn move spasmodically and chaotically within the standing wave field disrupting the regular banding patterns of the particles.

Results of the successful **ILS** experiments returned a mean particle size of 636 ± 215 nm with a polydispersity of 0.438 ± 0.051 for the yeast homogenate. Normal analysis (without ultrasound) of the homogenate gave a mean size of 1003 ± 328.2 nm and a polydispersity of 0.535 ± 0.186 (The polydispersity is a measure of the deviation of the particle distribution from a perfect monodisperse distribution). The 90○ scattered light from the normal and inter-nodal samples was 129.9×10^3 ± 14.4×10^3 and 79.8×10^3 ± 14.5×10^3 (counts per second) respectively indicating that particles contributing to nearly half of the scattered intensity had been shifted to the nodes of the standing wave field.

8.6 Conclusions

A novel technique for the in-situ sample preparation and subsequent particle size analysis by light scattering has been investigated. Results of experiments performed on polystyrene latex particles have sucessfully demonstrated that the technique is capable of removing particles of 1.4 μm and above from the sampling volume of the laser beam within five seconds permitting **PCS** analysis of the inter-nodal fluid unobstructed by contaminant particles. Results of separate experiments in this thesis predict a limiting minimum particle size for removal from a sample using this technique of approximately 0.5 μm.

CHAPTER 9 DISCUSSION AND APPLICATIONS

9.1 Introduction

The literature survey conducted at the start of this project (**Chapter 1**) concluded that very little research has been directed toward the specific application of megahertz frequency ultrasonic standing waves as a mechanism for affecting the separation of particles from liquid. Of the relevant research identified within the literature survey some consider the theoretical aspects of the particle migration witnessed in high frequency stationary waves whilst a similar proportion of the published work examine the very specific application of ultrasonic energy to a particular problem.

Within this chapter results of series of investigations carried out within the thesis into the use of megahertz frequency ultrasonic standing waves as a method for the separation of biological particles from liquids and attempts to provide a basic engineering understanding of the process technique will be discussed. The discussion will consider two main areas: the use of ultrasound for biological particle separation, and the use of ultrasound in combination with a laser light scattering technique to provide a rapid means of particle size distribution measurement.

9.2 Ultrasonic Separation of Biological Particles.

A review of the theories of particle migration in megahertz frequency ultrasonic standing wave fields reveals that the phenomenon is effective above certain particle size limits. The size limits are near to the size range of the biological particles of interest in biochemical engineering (approximately 0.1 to 100 μm diameter) since these are often difficult to remove from suspension.. Therefore initial experiments were performed to confirm that particle migration was indeed possible with particles in the size range of 1 – 20 μm diameter (See **Chapter 4**). The results of these experiments confirmed that particles a few micrometers in diameter could be concentrated into bands at the nodes of the standing wave field with very low levels of ultrasonic energy.

The results of investigations performed in **Chapter 6** to determine the parameters of importance during the separation of biological particles can be used in the design and specification of larger scale ultrasonic separation equipment. The features which must be considered in the design of such equipment will now be discussed.

The application of megahertz frequency ultrasonic standing waves to the segregation and recovery of whole yeast cells and cell debris from suspension has been investigated and found to be an effective means of small scale separation for such biological particles, removing close to 100 % of particles over 4 μm in diameter from suspension. The results of this section of work reflect the strong influence of particle diameter and ultrasonic energy level on the efficiency of separation of particles using a standing wave field (See **Figure 9.1**).

The flowrate through a large scale device will ultimately control the operation productivity. The maximum fluid velocities achievable during separation were found to be dependent on the ultrasonic intensity and the diameter of the particles being separated, as suggested by theory. For example, the continuous separation of yeast cells from suspension can be achieved if the mean fluid velocity is maintained below the critical velocity of 3.5×10^{-3} m.s^{-1} at 50 volts transducer voltage; for particles of diameter of 10 μm this critical velocity increases to greater than 7.0×10^{-3} m.s^{-1}. It is reasonable to assume that these fluid velocities should not be exceeded when designing a large scale separation device and therefore a device employing twinned transducers of area 1 m^2 would be capable of processing 12.6 m^3 of a typical biological suspension (such as a yeast fermentation broth) per hour at a fluid velocity of 3.5×10^{-3} m.s^{-1}. This volumetric throughput compares extremely well with conventional centrifugally based techniques. However, this simple calculation ignores the problems of acoustic streaming discussed in **Chapter 4** which would need to be overcome to achieve such large scale separation processes; this aspect requires further work (**Chapter 11**).

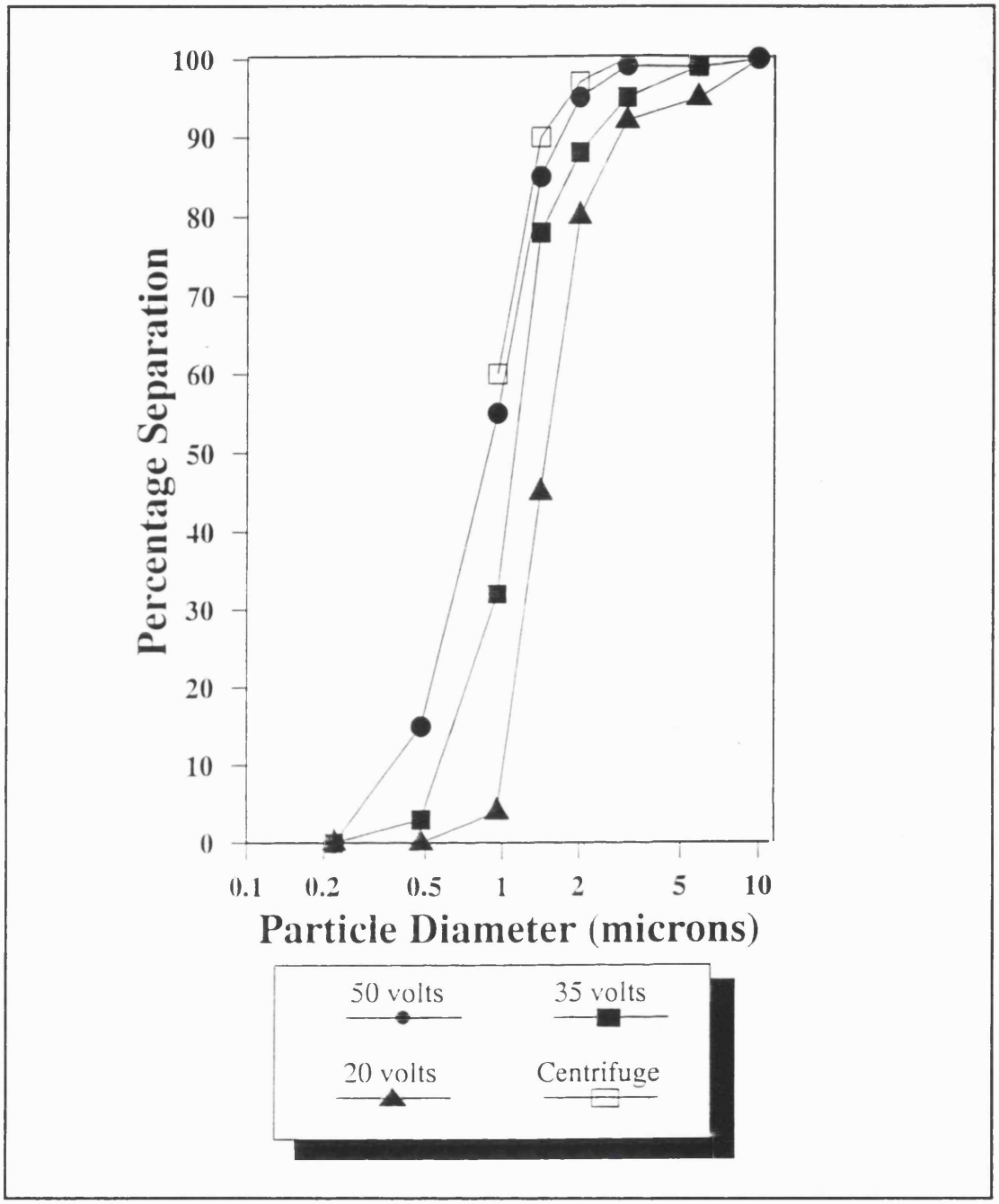

Figure 9.1 *Separation Efficiency of Ultrasonic Technique Compared With a Disc–Stack Centrifuge .*

In determining the scale–up of a separation device it will be necessary to know the levels of power input and to manipulate this to achieve the desired level of separation.

Control of the ultrasonic intensity in a system is the most direct way of controlling the radiation pressure exerted on a particle and therefore controlling the

rate of migration of particles in suspension. For this reason accurate knowledge of the levels of ultrasonic energy used to perform a specific rate of particle migration or separation efficiency will be of primary importance during the development of large scale ultrasonic devices. **Chapter 5** describes the problems faced when attempting to measure the ultrasonic power generated by a pair of piezoelectric ceramic transducers by a variety of methods. It was found that exact measurement required highly sophisticated electronics and was felt to be beyond the scope of this project.

The practice of measuring the voltage across the ultrasonic transducer, adopted as the method of determining the level of ultrasonic energy input to a system, cannot be used as an absolute measure of the ultrasonic energy input. There are a great many inaccuracies involved with this method due to problems including:

- the type of device used to measure the voltage. The frequency response or the sampling rate of the particular measurement device used will have a direct influence on the peak-peak voltage reading provided by the device.

- the waveform of the signal supplied to the transducer. The design of the signal generator and amplifier used to drive the transducers and the quality of their internal components will alter the waveform of the ultrasonic signal by introducing higher frequency harmonic noise elements to the wave. This noise may be present with similar voltage amplitudes as the fundamental frequency and therefore simple voltage measurements cannot take into account the loss of transducer efficiency caused by the harmonic noise in the signal.

- energy lost as heat. A significant proportion of the electrical energy supplied to the transducers is lost as unwanted heat energy. Transducer temperatures of 330 K are easily achieved at modest voltages.

- absorption and reflection of the ultrasound prior to entering the sample. A measurable percentage of the ultrasonic energy generated by the transducer will not reach the process stream due to absorption and reflection of the waves by the materials separating the ultrasonic transducers from the process fluid.

It is therefore critical that more detailed work be carried out to determine accurately the levels of power input during ultrasonic separation.

The rate of particle migration during ultrasonic separation is a critical design parameter. The experiments within **Chapter 7** describe the use of a scanning laser beam to study the migration of particles towards the nodal planes of a standing wave field in a 'real time' process. The results relate the time required to cause the particles in suspension to form concentrated bands within the standing wave field to the conditions of the wave field. This data could also be used in the design of flow-through ultrasonic devices using tubular ceramic transducers. In such a geometry particles are concentrated at the concentric circular nodal planes of the cylindrical standing wave field as the suspension is flowed through the transducer. Applications for such a flow-through device include, the enhancement of flocculation of cells in suspension (especially when allied with the use of a flocculating agent such as a polyelectrolyte material) where the increase in concentration of the particles at the nodal planes would increase the rate of particle collisions and hence the rate at which flocs are formed.

The information on the rate of migration of particles towards the nodal plane of a standing wave field obtained with the laser scanning technique developed in this work can be used to determine a suitable residence time for a particle within the standing wave field to allow the particles to be aggregated at the nodal planes. Hence the flow rate of suspension through the tubular transducer can be specified for a specific particle size distribution and ultrasonic field. As noted in **Chapter 11** additional research is still required however to enable the concentration of the aggregated particles within the nodes to be estimated.

9.3 Inter-nodal Light Scattering.

A novel technique for in-situ sample preparation and subsequent particle size analysis by light scattering has been investigated (**Chapter 8**). Results of experiments performed on polystyrene latex particles have successfully demonstrated that the technique is capable of removing particles of 1.4 μm and above from the

sampling volume of the laser beam within five seconds permitting photon correlation spectroscopy analysis of the inter-nodal fluid unobstructed by contaminant particles. Results of separate experiments in this thesis predict a limiting minimum particle size for removal from a sample using this technique of approximately 0.5 μm.

The applications of such an analytical tool are varied and widespread, for example:

- enhancing particle size analysis measurements (as detailed in **Chapter 8**).
- allowing accurate and rapid spectroscopy of "dirty" (particle laden) samples.
- a rapid optical method of determining the optimum dosing rate of a precipitant or flocculating agent by analysis of the internodal liquid.
- rapid analysis of excreted products (macromolecules, virus-like particles) in fermentation broths.
- increasing the accuracy of rapid optical biomass determinations by allowing the direct investigation of small particle species in the inter-nodal spaces (a cause of considerable inaccuracy at present).

To advance the application of this technique it may be necessary to subject the sample to a series of ultrasonic fields, selected so as to manipulate the suspension to form discrete portions for analysis. This may be achieved using varying levels of ultrasonic intensity for example to separate the heterogenous sample into a larger number of sub-populations which may each be sized more accurately by **ILS** (or analyzed in any optical means). Further development will also require the engineering of an improved **ILS** device with careful consideration of the coupling of the ultrasonic transducers to the cell containing the fluid to be tested.

The conclusions of the experimental investigations performed in this project are presented in **Chapter 10** of this thesis.

CHAPTER 10 CONCLUSIONS

This chapter summarises the key conclusions contained within this research thesis.

- The migration of micron and sub-micron sized particles to the nodes of an ultrasonic standing wave field has been demonstrated.

- Segregation of biological particles in the size range of 0.16 - 20 μm diameter from aqueous-liquids has been achieved by a novel non-invasive ultrasonic technique.

- An optimum frequency range for effective the separation of biological particles from aqueous liquids has been identified as lying between the frequencies of 2 and 5 MHz.

- The capacity to segregate neutrally-buoyant particles has been demonstrated.

- A laser-based technique to measure the rates of particle migration in a standing wave field has been developed. Further analysis of the data produced by this device may enable the concentration of the collected particles to be determined.

- The minimum particle diameter for the formation of concentrated bands of particles at the nodes of a standing wave field has been shown to be of the order of 0.16 μm. However rapid concentration is only achieved, at the ultrasonic power levels used in this project, with particles over 0.5 μm in diameter. A minimum particle size of approximately 1 - 2 μm is required to perform the effective continuous separation of the particle from suspension.

  The experimental data was found to be approximated by the curves described in **Equations 10.1 & 10.2** for 1 and 2 MHz standing wave fields respectively:

$$y = 7.8x^{-1.23} \qquad \textbf{Eq. 10.1}$$

$$y = 2.4x^{-1.23} \qquad \textbf{Eq. 10.2}$$

where y is the time required to band particles of diameter x (in μm).

- Maximum flow velocities of fluid in relation to the particles aggregated at the nodal planes of a standing wave field have been related to the ultrasonic energy input to the system and to the diameter of the particles in suspension and found to be in the order of $10^{-3} - 10^{-2}$ m.s^{-1}. The larger the particle or the higher the energy input the greater the permissable flow velocity.

- The use of phase shifting has been demonstrated as an effective means of facilitating a continuous separation process capable of simultaneously producing a flow of clarified suspension and a flow of concentrated particle suspension from a feed stream.

- Possible paths to scale–up of this separation process have been discussed. The experimental apparatus used in this research has been shown capable of processing suspension at a rate of approximately 2.5×10^{-3} m^3.s^{-1} per square meter of paired transducer area. Based on typical biological process stream properties this would enable 9 m^3.h^{-1} of suspension to be separated.

- Scale–up is currently limited by the problems of acoustic streaming encountered when the transducer area, and the associated liquid volume between the transducers, are increased.

- A novel and promising technique for the *in situ* preparation of samples prior to laser particle sizing has been researched. This method permits the rapid and accurate determination of particle size distribution of sub–micron sized particles in a "dirty" (particle laden) liquid. (This technique has been termed internodal light scattering **ILS**).

- The application of **ILS** to heterogeneous suspensions of latices and also to spiked cell homogenate has been used to demonstrate the feasibility of the technique.

A number of the elements of this research have yielded results which may warrant additional research. This is the subject of the final chapter of this thesis.

CHAPTER 11 FUTURE RESEARCH

11.1 Introduction.

This thesis has described a series of experimental investigations into the application of megahertz frequency ultrasonic standing waves to the segregation and separation of fine biological particles from liquids. Specific areas of the investigations have yielded results which might warrant further research which is beyond the scope of this project. These topics are described in the following sections.

11.2 Optimum Ultrasonic Frequency.

The results of investigations into the influence of the ultrasonic frequency of the standing wave on the efficiency of the separation technique (**Chapter 6**) suggested that the optimum frequency for separation of particles in the size range 0.5 μm diameter upwards may lie between the 2 and 5 MHz frequencies chosen for work within in this thesis. The piezoelectric ceramic transducers used in this study operate at maximum amplitude when they are driven at their mechanical resonant frequency. The resonant frequency is itself a function of the thickness of the transducer and is therefore of a fixed value (See **Section 3.5.1**). Further research into determining the optimum frequency for particle separation would therefore require the purchase of several sets of transducers of various resonant frequencies between 1 and 5 MHz.

High frequency standing wave fields exert a greater radiation pressure on a particle compared to a low frequency standing wave of the same intensity. However with increasing frequency there is an increase in absorption of the ultrasound and an increasing difficulty in driving the transducers to high voltages (compounded by an increase in complexity of the electronics required). Research into optimisation of the ultrasonic frequency must find a balance between these opposing relations.

11.3 Scale-Up.

As discussed in **Chapter 7** and **Chapter 9** of this thesis the results of the investigations into determining the efficacy of the separation achieved under various

conditions of ultrasonic standing wave field clearly point to the importance of the ultrasonic energy density applied during separation and to the maximum fluid velocity within the standing wave field when considering the design of large scale equipment. Further work is therefore needed in the following areas.

11.3.1 Transducers.

The next stage of research may involve experimentation with an ultrasonic separation device employing large areas of transducers. The problems encountered with acoustic streaming from large transducers need to be addressed together with the problems of preventing turbulent flow in the suspension which would cause disruption of the banding process. It may be possible to design equipment comprising of several separation "cells", divided by ultrasonically transparent material, positioned between a single pair of transducers thereby increasing the scale of the process without increasing the transducer area and the capital cost.

The problem of acoustic streaming may be overcome by dividing the liquid volume between the transducers into channels of small cross sectional area thereby inhibiting acoustic streaming in each channel but not reducing the area of the standing wave field.

11.3.2 Energy Requirements.

The energy requirements of large scale separation devices is an important aspect which requires further work. Techniques must be developed to enable the prediction and control of ultrasonic power levels employed within the ultrasonic devices. Also any novel separation process must have comparable running costs to existing equipment if it is to meet with acceptance in industrial processes. Experimentation is also needed to determine factors such as the optimum distance between a pair of transducers that can be used for the separation of particles from suspension.

The amount of energy transferred to the process stream as heat is an area of research that has not been covered in this thesis or in published literature but will be

an important consideration in the large scale use of ultrasonic equipment in biochemical engineering due to the requirement to maintain low process temperatures.

11.3.3 Transducer Materials.

The ceramic transducers currently available are capable of generating the ultrasonic intensities required for the separation of fine particles in a standing wave field but are limited in size by difficulties encountered during the manufacture of large ceramic elements. In comparison polyvinylidene fluoride polymeric material (PVDF) can be manufactured as a continuous sheet and therefore the possibility of producing large scale separation devices employing PVDF transducers can be envisaged. However the ultrasonic intensities generated by such polymer materials are very much lower than those obtained from ceramic transducers. Therefore it appears that material sciences research is required to fulfil the requirements of a transducer material suitable for large scale ultrasonic separation processes. At the time of writing of this thesis transducer manufacturers are developing hybrid materials consisting of piezoelectric ceramic particles or elements embedded in a matrix of PVDF thereby combining the advantageous properties of both materials. Future research in ultrasonic separation using these hybrid materials may solve some of the problems encountered with this technique at the present time.

11.4 Laser Scanning of Standing Wave Fields.

Chapter 7 describes the use of a laser scanning technique to measure the rate of migration of particles within a standing wave field. The experimental data generated by the laser scanning technique also contains information about the concentration profile of the particles in suspension about the nodes of the standing wave field. It was not possible within the timescale and resources of the project to utilise fully this information. Further work in this field could lead to the development of a rapid technique for the assessment of the suitability of ultrasonic standing wave fields as a means of separating a particulate system. The rate of particle migration to the nodes of the standing wave fields and the concentration of the particles at and between the concentrated bands of particles could be determined within a few seconds, thus

allowing the specification of the size and duty of the separation equipment required for a given application.

11.5 Computer Control.

In previous sections a computer program has been used to control the rate of phase shift applied during experiments. As the ultrasound used to effect separation is electrically generated the opportunity exists to develop computer control of the whole separation process, not just the rate of phase shift. For example, computer control of the energy density of the ultrasonic standing wave field may be linked to the in-line measurement of particle size distribution downstream of the ultrasonic separator. In this fashion the separation process could be controlled to produce a clarified stream of the desired quality whilst the energy requirements of the process are optimised economically. In a similar manner the control of the phase shift used could be extended to include a control loop optimising the rate of phase shift through the measurement of particle size distribution or optical density downstream.

11.6 Inter-Nodal Light Scattering.

The success of the **ILS** application described in **Chapter 8** may depend upon the ability to accurately control the removal of sub-micron particles from the laser beam sampling volume by the ultrasonic standing wave field. Prediction of the size of the smallest particles removed from the sampling volume requires exact values of the ultrasonic intensity applied in the standing wave field. Currently the selectivity of the technique is not high and future work would have to address this issue.

Further research may lead toward the use of different frequency standing wave fields for different applications depending on the design and properties of the optical system used to analyze the inter-nodal liquid and/or the concentrated particles. The use of phase shift may be advantageous in the automatic alignment of the light beam within the inter-nodal space.

Appendix I: Ultrasonic Transducers.

This table describes the piezoelectric ceramic transducers used to perform the ultrasonic separation experiments.

Resonant Frequency	Piezoelectric Material	Diameter (mm)	Thickness (mm)
1 MHz	PC4	22	2.0
2 MHz	PC4	25	1.0
5 MHz	PC4	20	0.4
10 MHz	PC4	20	0.2

Table A.I *Resonant Frequencies and Dimensions of Transducers Used During Experimentation.*

Appendix II: Computer Program Listings.

This appendix contains the listings of three programs written and used during this research.

- The first program was written in Applesoft Basic to control the phase shifting device incorporated in the Audley Scientific Dual Ultrasonic Amplifier used in preliminary ultrasonic experiments in **Chapter 4** of this work.

```
10    REM  PHASE
20    REM  THIS PROGRAM RAPIDLY
30    REM  SHIFTS THE PHASE OF
40    REM  AMPLIFIER OUTPUT B.
50    REM
60    A = 0
70    PRINT "ENTER RATE OF PHASE SHIFTING"
80    PRINT "0 TO 500 : 500 = ONE SECOND DELAY"
90    INPUT S
100   SLOT = 4
110   DIOBASE = - 16384 + SLOT * 256
120   DDRA = DIOBASE + 3
130   POKE DDRA,255
140   OUTA = DIOBASE + 1
150   PRINT "ENTER PHASE SHIFTING RANGE"
160   INPUT B
170   PRINT "TO ALTER RANGE TYPE"
180   PRINT "     'Q'    =    +1"
190   PRINT "     'W'    =    +5"
200   PRINT "     'E'    =    +20"
210   PRINT
220   PRINT "     'Z'    =    -1"
230   PRINT "     'X'    =    -5"
240   PRINT "     'C'    =    -20"
250   FOR D = A TO B
260   FOR PAUSE = A TO S : NEXT PAUSE
270   POKE OUTA,D
280   X = PEEK ( -16384)
290   POKE - 16368,0
300   IF X = 209 THEN B = B + 1
310   IF X = 215 THEN B = B + 5
320   IF X = 197 THEN B = B + 20
330   IF X = 218 THEN B = B - 1
340   IF X = 216 THEN B = B - 5
350   IF X = 195 THEN B = B - 20
```

```
360   IF B > 255 THEN B = 255
370    NEXT D
380   GOTO 250
400   END
```

● This program was written in the Microsoft QuickBasic language to control the phase shifting device in the Audley Scientific Dual Ultrasonic Amplifier via the PC30AT data acquisition-control board in **Chapters 5, 6, 7, 8** and **9** of this thesis.

```
'This programme rapidly shifts the phase of
'amplifier output B
 '$INCLUDE: 'call2630.bi'
DEFDBL S
CALL initfile
CALL setiospeed(1.25E+07)
CALL datadirection(0, 0, 0, 1)      ' A out, B out, C out
ON KEY(1) GOSUB 30
KEY(1) ON
ON KEY(2) GOSUB 40
KEY(2) ON
ON KEY(30) GOSUB 10
KEY(30) ON
ON KEY(31) GOSUB 20
KEY(31) ON
KEY 15, CHR$(0) + CHR$(82)
ON KEY(15) GOSUB 50
KEY(15) ON
KEY 16, CHR$(0) + CHR$(71)
ON KEY(16) GOSUB 60
KEY(16) ON

PRINT
COLOR 3, 1
CLS
PRINT
PRINT
PRINT "          DUAL ULTRASONIC AMPLIFIER PHASE CONTROLLER
"
PRINT "          ----------------------------------------"
PRINT "          CONTROL KEYS :"
PRINT "                    F1 = -1        F11 = +1 "
PRINT "                    F2 = -0.1      F12 = +0.1"
PRINT
PRINT "                    7/HOME RESTORES ORIGINAL STEP SIZE"
PRINT "                    0/Ins SETS STEP SIZE TO ZERO"
```

```
  PRINT "                          SPACEBAR ENDS PROGRAM"
  PRINT
  PRINT " Phase Shifting Range   *0 to 255*"  'input B
  b = 255
  PRINT "Enter Step Size        *Larger step sizes mean greater phase shifting
rates*"
  INPUT s: x = s
  PRINT s
8  DO

          OUT &H709, d
        d = d + s
      LOOP UNTIL d >= b
         d = 0
    IF INKEY$ = " " THEN GOTO 100
   GOTO 8
10  s = s + 1: PRINT s: RETURN
20  s = s + .1: s = INT(s * 10 + .5) / 10: PRINT s: RETURN
30  s = s - 1: PRINT s: RETURN
40  s = s - .1: s = INT(s * 10 + .5) / 10: PRINT s: RETURN
50  s = 0:
    IF INKEY$ = "" THEN GOTO 50:
    PRINT s:
    RETURN
60  s = x: PRINT , b: RETURN
100 SHELL "exit "
    END
```

● This program was written in Microsoft QuickBasic to control the sampling of the photodetector signal during the experiments described in **Chapter 7**.

```
' THIS PROGRAM COLLECTS DATA FROM A SINGLE CHANNEL OF
YOUR CHOICE
' THE RATE OF DATA COLLECTION AND NUMBER OF POINTS ARE
VARIABLE
' THE RESULTS ARE STORED IN THE SC4 FILE RESULTS.CAL

  '$INCLUDE: 'pc30at.bi'
  CLS
  CALL initfile
     IF (pc30err <> 0) THEN
        PRINT "initfile failed"
     ELSE
```

```
      PRINT "initialised PC-30A package"
    END IF

  CALL setiospeed(1.25E+07)
10 PRINT
  DIM adata(1 TO 2000) AS INTEGER
  DIM radata(1 TO 2000) AS DOUBLE
  DIM f AS STRING
  DIM i AS INTEGER
  DIM x AS STRING
  DIM n AS INTEGER
  DIM adchans(0 TO 15) AS INTEGER
  c = 0
  PRINT
  PRINT "Input full path, directory, filename and extension of file to accept "
  INPUT "collected data                              "; f
  IF f = "" THEN f = "d:\sc4\data\run.cal"
  PRINT
  INPUT "Select channel for data collection (0 to 15)  "; c
  adchans(1) = c
  INPUT "Input rate of data collection in Hz          "; h
  PRINT "Input number of data points to be collected"
  INPUT "up to a maximum of one thousand (1000)       "; n
  setsoftrate (h)'collect at h Hz
  CALL SetAdChans(adchans(), 1)
  CLS
  CALL SoftScanAd(adata(), n)
    FOR i = 1 TO n
       radata(i) = rawtovolts#(adata(i))
    PRINT USING "##.###    ####.####"; (i / h); radata(i)
    rad = rad + radata(i)
    NEXT i
  OPEN f FOR OUTPUT AS #1
    FOR i = 1 TO n
        WRITE #1, (i / h), radata(i)
    NEXT i
  CLOSE #1
  PRINT
  PRINT "Take another reading ? y/n"
  DO
  x = INKEY$
  LOOP UNTIL (x = "y" OR x = "n")
  SELECT CASE x
     CASE "y"
          GOTO 10
     CASE "n"
          SHELL "exit"
  END SELECT
```

Appendix III: Properties of Polystyrene Latices.

This appendix contains a table listing the various sizes and properties of polystyrene particles used during this work and a graph describing the change in absorbance of latex suspensions with particle concentration.

Properties of Polystyrene Latex Dispersions		
Diameter (μm)	Standard Deviation (μm)	Colour
0.06	0.007	WHITE
0.16	0.01	BLUE
0.22	0.0018	WHITE
0.45	0.0041	RED
0.48	0.0021	WHITE
0.73	0.045	WHITE
0.95	0.064	WHITE
1.0	0.09	YELLOW
1.5	0.07	WHITE
2.01	0.09	WHITE
3.09	0.17	RED
4.45	0.15	WHITE
5.71	0.1	WHITE
5.83	0.189	BLUE
9.21	0.3	WHITE
9.33	0.64	VIOLET

Table A.III *List of Polystyrene Latex Particles Used During Experimentation.*

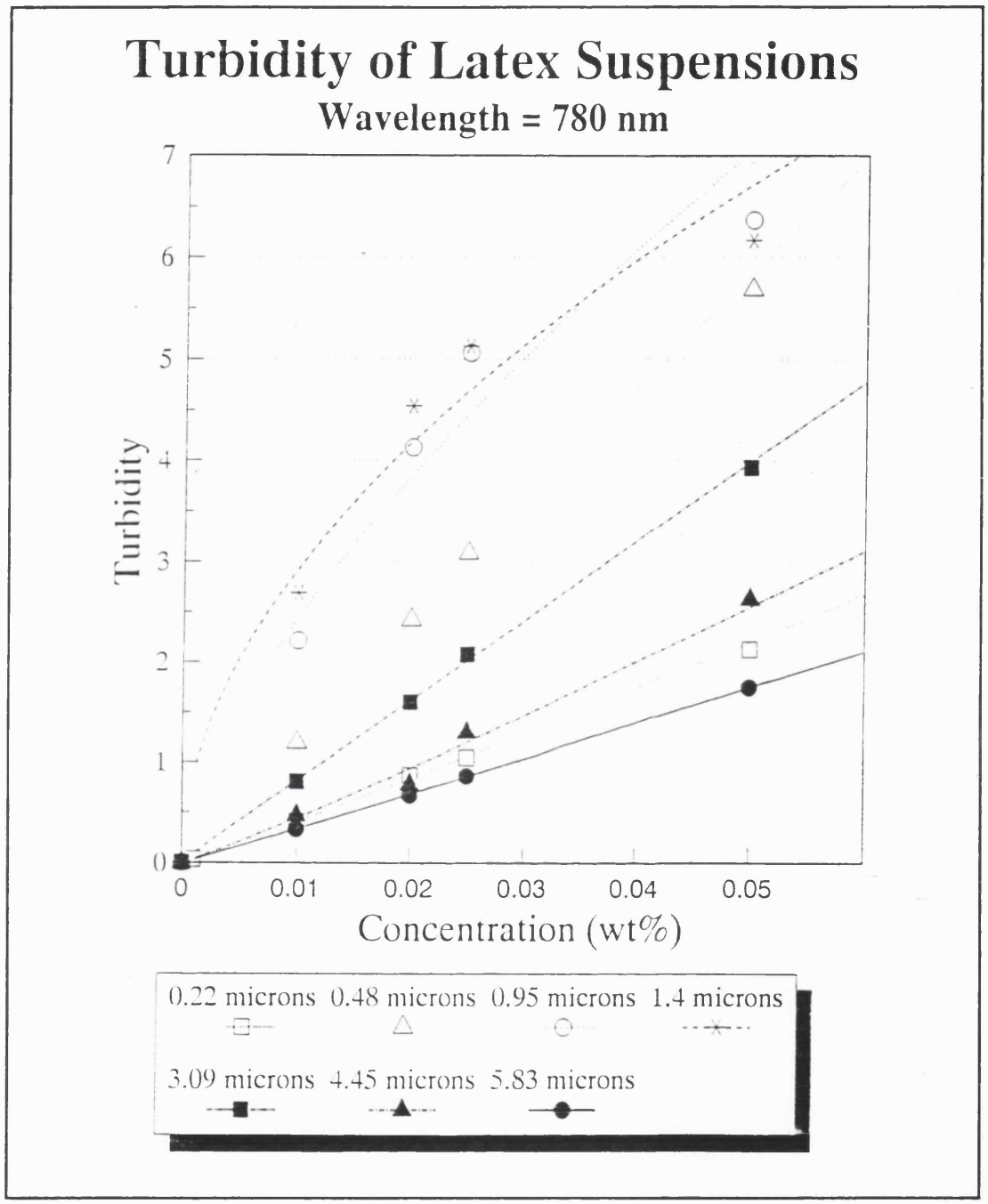

Figure A.III *Absorbance (780 nm) Against Particle Concentration (wt%) of Polystyrene Latex Suspensions.*

Appendix IV: Piezoelectric Ceramic Transducers.

This section lists the properties of the Morgan Matroc Ltd PC4 lead zirconate titanate piezoelectric ceramic transducer material. (Taken from Morgan Matroc Ltd. literature.)

Parameter	Unit	Value
Electric Low Field		
Relative Permittivity	_	1075
Dielectric Loss (tan δ)	_	0.002
Resistivity	Ω.m	10^{13}
Electric High Field at 2KV/mm		
Increase in Relative Permativity	%	1.9
Dielectric Loss	_	0.004
Coupling Factors		
k_t	_	0.45
k_p	_	0.53
k_{31}	_	0.31
k_{33}	_	0.71
Charge Constants	$\times 10^{-12}$ C.N^{-1}	
d_{31}	"	-104
d_{33}	"	287
d_t	"	79
Voltage Constants	$\times 10^{-3}$ Vm.N^{-1}	

Parameter	Unit	Value
g_{31}	"	-10.9
g_{33}	$\times 10^{-3}$ Vm.N^{-1}	30.2
g_h	"	8.3
Frequency Constants	Hz.m	
N_p	"	2292
N_{11}	"	675
N_{31}	"	570
N_s	"	1800
N_c	"	1020
N_t	"	2082
Quality Factor Qm	_	1200
Density	kg.m^{-3}	7600
Curie Temperature	K	573
Compliances	$\times 10^{-12}$ m^2.N^{-1}	
S^E_{33}	"	14.7
S^E_{11}	"	11.7
S^E_{12}	"	-3.6
S^D_{33}	"	7.4
S^D_{11}	"	10.8
S^D_{12}	"	-4.8
S_{66}	"	30.7

Table A.IV *Properties of PC4 Piezoelectric Ceramic*

Appendix V: Polyvinylidene Fluoride Polymer.

This section lists the properties of the polyvinylidene fluoride piezoelectric polymer film (Atochem Sensors Ltd, 22 Ridge Way, Hillend Industrial Park, Fife, Scotland.) used in the manufacture of experimental hydrophones (**Chapter 5**).

Property	Unit	Value
Thickness	μm	9,28,52,110,500
Strain Constant	$m.V^{-1}$ or $C.N^{-1}$	
d31		23×10^{-12}
d33		-33×10^{-12}
Stress Constant	$V.m.N^{-1}$ or $m^2.C^{-1}$	
g31		216×10^{-3}
g33		-339×10^{-3}
Electromechanical Coupling Factor		% (at 1kHz)
k31		12
k33		19
Capacitance(28 μm film)	$pF.cm^{-2}$	380
Young's Modulus	$N.m^{-2}$	2×10^{9}
Sound Velocity		$m.s^{-1}$
transverse		1,500
thickness		2,200
Density	$kg.m^{-3}$	1780
Permittivity	$F.m^{-1}$	106×10^{-12}
Relative Permittivity		12

Property	Unit	Value
Resistivity	Ω.m	10^{13}
Dielectric Loss (tanδ)		
at 10 Hz		0.015
at 100 kHz		0.02
Compressive Strength	$N.m^{-2}$	60×10^{6}
Operating Temperature Range	K	233–373
Max. Operating Voltage	$V.\mu m^{-1}$	30
Breakdown Voltage	$V.\mu m^{-1}$	100

Table A.V *Properties of PVDF Piezoelectric Polymer Film*

Appendix VI: Laser Scanner Data.

This appendix contains a sample of the raw data from the laser scanning experiments performed in **Section 7.6** as collected by the PC30A data acquisition board. A example plot of the raw data is shown in **Section 7.5 (Figure 7.4)**. The first value listed is the sample number and the second value is the 12 bit digital level of the signal (4098 = 20 volts). The frequency of sampling in this example was 2 kHz.

1	594	37	581	2005	655
2	593	38	581	2006	657
3	593	39	581	2007	657
4	592	40	580	2008	659
5	592	41	580	2009	661
6	592	42	580	2010	662
7	592	43	579	2011	664
8	591	44	579	2012	666
9	591	45	579	2013	667
10	590	46	579	2014	669
11	590	47	579	2015	670
12	589	48	579	2016	672
13	589	49	578	2017	675
14	588	50	577	2018	678
15	588	51	578	2019	681
16	587	52	577	2020	682
17	587	53	577	2021	684
18	587	54	578	2022	686
19	586	55	577	2023	687
20	586	56	577	2024	691
21	585	57	577	2025	692
22	585	58	577	2026	694
23	585	59	576	2027	697
24	585			2028	698
25	585	1993	639	2029	700
26	585	1994	639	2030	703
27	584	1995	640	2031	704
28	584	1996	642	2032	707
29	584	1997	644	2033	709
30	584	1998	645	2034	712
31	583	1999	648	2035	713
32	583	2000	649	2036	717
33	583	2001	649	2037	719
34	582	2002	650	2038	723
35	582	2003	652	2039	727
36	582	2004	653	2040	730

Appendix VII: Circuit Diagrams

This section includes circuit diagrams of the electronic circuits described in **Section 3.3.5**.

- The figure below shows the schematic layout of the laser driver circuit described in **Section 3.3.5.1**.

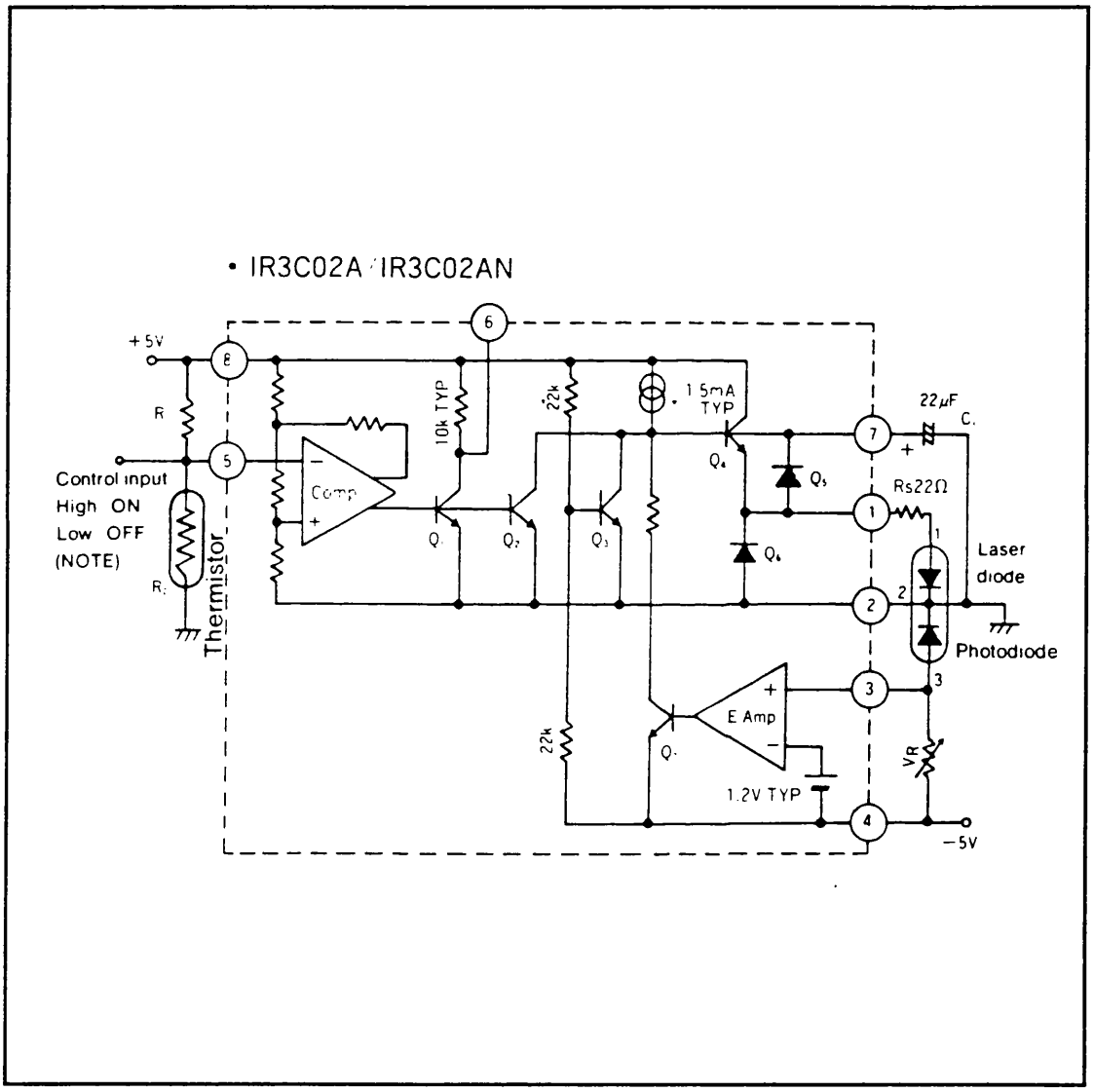

Figure A.VII.1 *Laser Driver Circuit Diagram.*

● The figure below is a circuit diagram of the ultra-high speed amplifier constructed (See **Section 3.3.5.2**) to amplify the signal generated by the hydrophones used in **Chapter 5**.

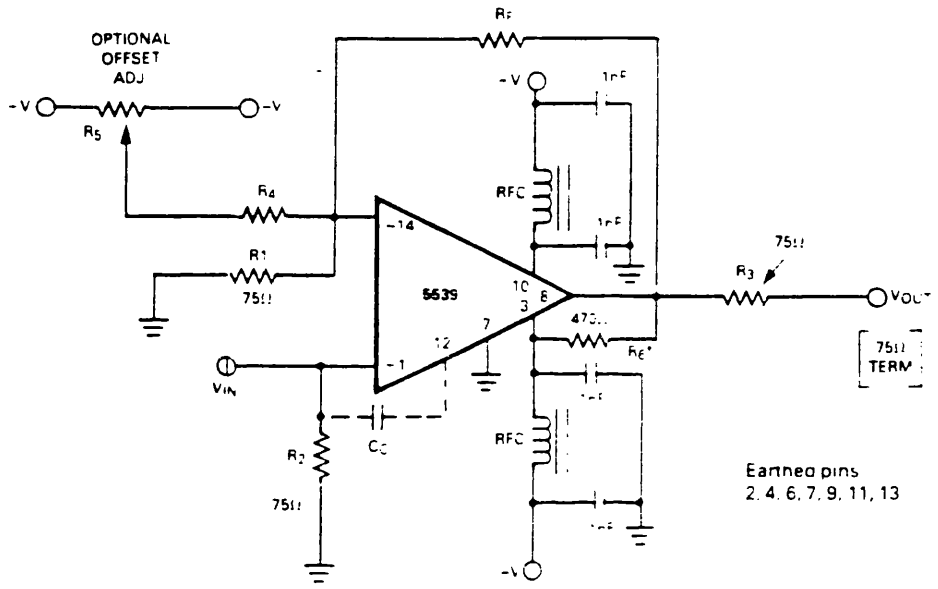

Component List

R1	=	75Ω
R2	=	75Ω
R3	=	75Ω
R4	=	33kΩ
R5	=	20k Cermet Pot
RF	=	1k5
R6*	=	470Ω
4 x Caps	=	1n
2 x RFC	=	1u, 2.7A
2 x SKT	=	BNC

Figure A.VII.2 *High Speed Amplifier Circuit Diagram.*

BIBLIOGRAPHY

Abdulla, U., Talbert, D., Lucas, M. and Mullarkey, Effects of ultrasound on chromosomes of lymphocyte cultures., 1972, BRITISH MEDICAL JOURNAL, Sept., 797–799.

Ahuja, A.S. Wave equation and propagation parameters for propagation in suspensions., 1973, J. APPL. PHYS., **44**, (11), 4863–4868.

Anada, H.R., Shah, Y.T. and Klinzing, G.E., Methods of improving settling of industrial pigment slurries, 1974, CANADIAN J. CHEM. ENG., **52**, Dec., 715–721.

Ando, T. and Kimura, T., Reactivity and selectivity in organic sonochemical reactions involving inorganic solvents., 1990, ULTRASONICS, **28**, 326–332.

Anson, L.W. & Chivers, R.C., Thermal Effects in the Attenuation of Ultrasound in Dilute Suspensions for Low Values of Acoustic Radius, 1990, ULTRASONICS, **28**, 16–26.

Anson, L.W. & Chivers, R.C., Influence of Cell Parameters on Ultrasonic Attenuation in Cell Suspensions., 1989, ACUSTICA, **69**, 276–281.

Armour, E.P. and Corry, P.M., Cytotoxic effects of ultrasound *in vitro* dependence on gas content, frequency, radical scavengers, and attachment., 1982, RADIATION RESEARCH, **89**, 369–380.

Ashkin, A., Dziedzic, J.M. and Yamane, T., Optical trapping and manipulation of single cells using infrared laser beams., 1987, NATURE, **330**, Dec., 769–771.

Bacon, D.R., Characteristics of a PVDF membrane hydrophone for use in the range 1–100 MHz., 1981, IEEE TRANS. SON. ULTRASON., **SU–29**, 1, 18–25.

Baker, N.V., Segregation and sedimentation of red blood cells in ultrasonic standing waves., 1972, NATURE, **239**, Oct., 338–339.

Bar, R., Ultrasound enhanced bioprocesses: Cholesterol oxidation by Rhodococcus erythropolis., 1988, BIOTECH. BIOENG., **32**, 655–663.

Barnes, C. and Lewis, T.J., Stimulated ultrasound absorption in aqueous solutions of biomolecules., 1991, J.ACOUST.SOC.AM., **89**,(4), 1792–1800.

Bell, D.J., Hoare, M. and Dunnill, P., The formation of protein precipitates and their centrifugal recovery., 1983, ADV. BIOCHEM. ENG. BIOTECH., **26**, 1–72.

Berlan, J. and Mason, T.J., Sonochemistry: from research laboratories to industrial plants., 1992, ULTRASONICS, **30**, (4), 203–212.

Bien, J., Ultrasonic preparation of sludges to improve dewatering., 1988, FILTRATION AND SEPARATION, **Dec.**, 425–426.

Bien, J., Kowalska, E. and Zielewicz, E., The effects of the thickening of various sewage deposits subjected to the influence of ultrasonic field., 1979, 2nd Int. Conference on Physiochem. Methods,Poland

Bjorno, L., Characterization of biological media by means of their non–linearity., 1986, ULTRASONICS, **24**, 254–259.

Bjorno, L., Finite amplitude wave propagation in fluid filled tubes., 1973, Finite–amplitude wave effects in liquids.

Bristow, F.G., Chivers, R.C. and Sluman, E.E., A simple ultrasonic transducer manipulator., 1980, ULTRASONICS, **18**, 134.

Burger, F.J. and Sollner, K., The action of ultrasonic waves in suspensions., 1936, TRANS. FARAD. SOC., **32**, 1598–1603.

Carstensen, E.L. and Schwan,H.P., Absorption of sound arising from the presence of intact cells in blood., 1959, J.ACOUST.SOC.AM., **31**, (2), 185–189.

Chapman, I.V. and Al–Hashimi, A.H.M., The influence of increased viscosity and ambient pressure on ultrasound–induced ion flux changes in mammalian cells., 1979, ULTRASONICS INTERNATIONAL, 577.

Chetverikova, E.P., Williams, A.R. et al, Interaction of therapeutic ultrasound with purified enzymes *in vitro*., 1985, ULTRASONICS, **23**, 183–188.

Chivers, R.C., The Definition and Use of Effective Geometrical Parameters for Radiating Transducers in Experimental Ultrasonics., 1990, ACUSTICA, **70**, 215–222.

Chivers, R.C. and Aindow, J.D., Wave propagation in biological tissue., 1983, ULTRASONICS INTERNATIONAL 1983.

Chu, B., Laser Light Scattering: Basic principles and practice., 1991, 2nd Edition, Academic Press USA.

Clarke, P.R. and Hill, C.R., Physical and chemical aspects of ultrasonic disruption of cells., 1970, J.ACOUST.SOC.AM., **47**, 2(2), 650–658.

Coakley, W.T., Acoustical detection of single cavitation events in a focused field in water at 1MHz., 1971, J.ACOUST.SOC.AM., **49**, 3(2), 792–801.

Coakley, W.T. et al, Cell manipulation in ultrasonic standing wave fields., 1989, J. CHEM. TECH. BIOTECHNOL., 44, 43–62.

Connolly, W. and Fox, F.E., Ultrasonic cavitation thresholds in water., 1954, J.ACOUST.SOC.AM., **26**, (5), 843–848.

Crum, L.A. and Eller, A.I., Motion of bubbles in a stationary sound field., 1970, J.ACOUST.SOC.AM., **48**, 1(2), 181–189.

Crum, L.A. and Nordling, D.A., Velocity of transient cavities in an acoustic stationary wave., 1972, J.ACOUST.SOC.AM., **52**, 1(2), 294–301.

Culshaw, B., Fiddy, M.A., Hall, T.J. and Kingsley, S.A., Fibre optic acoustic sensors., 1979, ULTRASONICS INTERNATIONAL, 267–272.

Cum, G., Galli, G., Gallo, R. and Spadaro, A., Role of frequency in the ultrasonic activation of chemical reactions., 1992, ULTRASONICS, **30**, (4), 267–270.

Danckwerts, P.V., Industrial Gas Cleaning., INTERNATIONAL SERIES OF MONOGRAPHS IN CHEMICAL ENGINEERING, **8**, 1974.

Defebvre, A., Pouliquen, J. and Deparis, J.P., Cardioid directivity conditions for a hydrophone., 1983, ULTRASONICS INTERNATIONAL, 408–413.

DeReggi, A.S., Roth, S.C., Kenney, J.M. and Edelman, S., Harris, G.R., Piezoelectric polymer probe for ultrasonic applications., 1981, J.ACOUST.SOC.AM., **69**, 3, 853–859.

Devereux, N., Hoare, M., Dunnill, P., Bell, D.J., The Development of improved methods for the industrial recovery of protein precipitates., 1984, SOLID–LIQUID SEPARATION, Ed. J. Gregory., Chichester: Ellis Horwood Ltd, 143–160.

Dion, J.–L., Valade, J.L. and Law, K.N., Evolution d'une suspension de fibres dans un champ ultrasonore stationnaire., 1988, ACUSTICA, **65**, 284–289.

Doktycz, S.J. and Suslick, K.S., Interparticle collisions driven by ultrasound., 1990, SCIENCE, **247**, 2 March, 1067–1069.

Dunnill, P., Trends in Downstream Processing of Proteins and Enzymes., 1983, PROCESS BIOCHEMISTRY, October, 9–13.

Dupont, L.A., Kruus, P. and Patraboy, J., Polymerisation initiated by ultrasonic cavitation., 1983, ULTRASONICS INTERNATIONAL 1983.

Dutta, S.K. and Sinha, A.P., Process applications of ultrasonics., 1974, CHEMICAL PROCESSING, Aug.

Dyson, M., Woodward, B. and Pond, J.B., Flow of red blood cells stopped by ultrasound., 1971, NATURE, **232**, Aug., 572–573.

Elder, S.A., Cavitation Microstreaming., 1959, J.ACOUST.SOC.AM., **31**, (1), 54–64.

Eller, A.I. and Crum, L.A., Instability of the motion of a pulsating bubble in a sound field., 1970, J.ACOUST.SOC.AM., **47**, 3(2), 762–767.

Ellwart, J.W., Brettel, H. and Kober, L.O., Cell membrane damage by ultrasound at different cell concentrations., 1988, ULTRASOUND MED. BIOL., **14**, (1), 43–50.

Filmore, P.R. and Chivers, R.C., Measurements on batch produced miniature ceramic ultrasonic hydrophones., 1986, ULTRASONICS, **24**, 216–229.

Freedman, A., Sound Field of a Rectangular Piston., 1960, J.ACOUST.SOC.AM., **32**, (2), 197–209.

Gaertner, W., Frequency dependence of ultrasonic cavitation., 1954, J.ACOUST.SOC.AM., **26**, (6), 977–980.

Galloway, W.J., An experimental study of acoustically induced cavitation in liquids., 1954, J.ACOUST.SOC.AM., **26**, (5), 849–857.

Gong, X–f., Zhu, Z–m., Shi, T. and Huang, J–h., Determination of the acoustic nonlinearity parameter in biological media using FAIS and ITD methods., 1989, J.ACOUST.SOC.AM., **86**, (1), 1–5.

Goss, S.A., Frizzell, L.A., Dunn, F. and Dines, K.A., Dependence of the ultrasonic properties of biological tissue on constituent proteins., 1980, J.ACOUST.SOC.AM., **67**, (3), 1041–1044.

Gould, R.K., Coakley, W.T. and Grundy, M.A., Upper sound pressure limits on particle concentration in fields of ultrasonic standing–wave at megahertz frequencies., 1992, ULTRASONICS, **30**, (4), 239–244.

Graham, E., Hedges, M., Leeman, S. and Vaughan, P., Cavitational bio–effects at 1.5 MHz., 1980, ULTRASONICS, **18**, (Sept.), 224–228.

Habeger, C.C., Wink, W.A. and Van Zummeren, M.L., Using neoprene–faced, pvdf transducers to couple ultrasound into solids., 1988, J.ACOUST.SOC.AM., **84**, (4), 1388–1396.

Haran, M.E. and Cook, B.D., Comparison of an acousto–optic and a radiation force method of measuring ultrasonic power., 1975, J.ACOUST.SOC.AM., **57**, (6)

Hasegawa, T., Kido, T., Takeda, S., Inoue, N., Matsuzawa, K., Acoustic radiation force on a rigid sphere in the near field of a circular piston vibrator., 1990, J.ACOUST.SOC.AM., **88**, (3), 1578–1583.

Hayward, G., A systems feedback representation of piezoelectric transducer operational impedance., 1984, ULTRASONICS, **22**, 153–162.

Higashitani, K., Fukushima, M. and Matsuno, Y., Migration of suspended particles in plane stationary ultrasonic field., 1981, CHEM. ENG. SCI., **36**, (12), 1877–1882.

Hoare, M. and Dunnill, P., Biochemical Engineering Challenges of Purifying Useful Proteins., 1989, PHIL. TRANS.R. SOC. LOND.B, **324**, 497–507.

Hobaek, H., On some observations on standing acoustical waves in a medium with a density gradient., 1973, FINITE-AMPLITUDE WAVE EFFECTS IN LIQUIDS.

Hunicke, R.L., Industrial applications of high power ultrasound for chemical reactions., 1990, ULTRASONICS, **28**, 291–294.

Hunt, J.W., Arditi, M. and Foster, F.S., Ultrasound Transducers for Pulse-Echo Medical Imaging., 1983, IEEE TRANS. BIOMED. ENG., **BME 30**, (8).

Inoue, M., Church, C.C., Brayman, A., Miller, M.W. and Malcuit, M.S., Confirmation of the protective effect of cysteamine in *in vitro* ultrasound exposures., 1989, ULTRASONICS, **27**, 362–369.

Inoue, M., Miller, M.W. and Church, C.C., Alternative explanation for a postulated non-thermal, non-cavitational ultrasound mechanism on *in vitro* cells at hyperthermal temperatures., 1990, ULTRASONICS, **28**, 185–189.

Kilburn, D.G., Clarke, D.J., Coakley, W.T. and Bardsley, D.W., Enhanced sedimentation of mammalian cells following acoustic aggregation., 1989, BIOTECH. AND BIOENG., **34**, 559–562.

King, R.O. and Forster, C.F., Effects of sonication on activated sludge., 1990, ENZYME MICROB. TECHNOL., **12**, 109–115.

Kober, L.O., Ellwart, J.W. and Brettel, H., Effect of the pulse length of ultrasound on cell membrane damage *in vitro*., 1989, J.ACOUST.SOC.AM., **86**, (1), 6–7.

Kolb, J. and Nyborg, W.L., Small scale acoustic streaming in liquids., 1956, J.ACOUST.SOC.AM., **28**, (6), 1237–1242.

Kowalska, E., Kowalski, W. and Bien, J., Changes of some physical properties of sonated suspensions., 1979, ACUSTICA, **43**, 260–265.

Kundt, A. and Lehmann, O., Ueber longitudinale Schwingungen und Klangfiguren in cylidrischen Flüssigkeitssäulen., 1874, ANNALEN DER PHYSIK UND CHEMIE, **153**, (9), 1–12.

Kweik, P. and Reibold, R., Experimental investigation of the ultrasonic phase–amplitude diffraction grating in the optical nearfield., 1990, ACUSTICA, **71**, 69–71.

Lakestani, F., Baboux, J.C., Jayet, Y. and Perdrix, M., Theoretical and experimental study of the efficiency of an ultrasonic transducer., 1983, ULTRASONICS INTERNATIONAL, 402–407.

Lenart, I. and Auslander, D., The effect of ultrasound on diffusion through membranes., 1980, ULTRASONICS, **18**, 216–218.

Lewin, P.A., Miniature piezoelectric polymer ultrasonic hydrophone probes., 1981, ULTRASONICS, **19**, 213–216.

Lewin, P.A. and Bjorno, L., Acoustic pressure amplitude thresholds for rectified diffusion in gaseous microbubbles in biological tissue., 1981, J.ACOUST.SOC.AM., **69**, (3), 846–852.

Lewin, P.A. and Jensen, F., The use of miniature ultrasonic transducers for measurement in penetrable media., 1979, ULTRASONICS INTERNATIONAL, 279–286.

Luche, J.L., Developments of the new 'experimental theory' of sonochemistry initiated in Grenoble., 1992, ULTRASONICS, **30**, (3), 156–162.

Macedo, I.C., and Yang, W.–J., Acoustic effects on gas bubbles in the flows of viscous fluids and whole blood., 1973, J.ACOUST.SOC.AM., **53**, (5), 1327–1335.

Martin, C.J. and Law, A.N.R., The use of thermistor probes to measure energy distribution in ultrasound fields., 1980, ULTRASONICS, **18**, 127–133.

Martin, P.D. and Ward, L.D., Reactor Design for Sonochemical Engineering., 1992, TRANS. I.CHEM.E., **70**, (A), 296–303.

Martner, J.G., Design and applications of radial tubular resonators., 1979, ULTRASONICS INTERNATIONAL, 233–238.

Mason, T.J., Lorimer, J.P. and Walton, D.J., Sonoelectrochemistry., 1990, ULTRASONICS, **28**, 333–337.

Matskevich, L.I. and Skalozubov, M.F., Effect of acoustic vibrations on the coagulation of a carbonate slurry., 1969, TR. NOVOCHERKASSK. POLITEKH. INST., **197**, 14–19.

Mc Clements, D.J., Povey, M.J.W., Jury, M. and Betsanis, E., Ultrasonic characterization of a food emulsion., 1990, ULTRASONICS, **28**, 266–272.

Meister, R. and St.Laurent, R., Ultrasonic absorption and velocity in water containing algae in suspension., 1960, J.ACOUST.SOC.AM., **32**, (5), 556–559.

Middelberg, A.P.J., Bogle, I.D.L. and Snoswell, M.A., Sizing biological samples by photosedimentation techniques., 1990, BIOTECHNOL. PROG., **6**, 255–261.

Miller, D.L., Particle gathering and microstreaming near ultrasonically activated gas-filled micropores., 1988, J.ACOUST.SOC.AM., **84**, (4), 1378-1387.

Miller, D.L., Gas body activation., 1984, ULTRASONICS, **22**, (Nov.), 261-269.

Miller, D.L., Williams, A.R. and Gross, D.R., Characterization of cavitation in a flow-through exposure chamber by means of a resonant bubble detector., 1984, ULTRASONICS, **22**, (Sept.), 224-230.

Miyazaki, K., Takahashi, Y. and Shiomi, K., Classifying particles in a slurry by ultrasonic filter., 1990, FILTRATION & SEPARATION, Jan., 28-31.

Moffett, M.B., Powers, J.M. and Clay, W.L.,Jr., Ultrasonic microprobe hydrophones., 1988, J.ACOUST.SOC.AM., **84**, (4), 1186-1194.

Muralidhara, H.S. and Ensminger, D., Acoustic dewatering and drying - a state of the art review., 1984, PROC. 4TH INT. DRYING SYMP., Kyoto, Japan, July 1984, Session DG, 304-315.

Narasimham. A.V., A theory of ultrasonic absorption on liquids., 1990, ACUSTICA, **71**, 233-236.

Nelson, C.D. and Glatz, C.E., Primary particle formation in protein precipitation., 1985, BIOTECH. AND BIOENG., **28**, 1434, 1444.

Neppiras, E.A., Acoustic cavitation : an introduction., 1984, ULTRASONICS, **21**, 25-28.

Neppiras, E.A. and Coakley, W.T., Acoustic cavitation in a focused field in water at 1 MHz., 1975,

Neppiras, E.A. and Noltingk, B.E., Cavitation produced by ultrasonics : Theoretical conditions for the onset of cavitation., 1952,

Nyborg, W.L., Cavitation in biological systems., 1973, FINITE-AMPLITUDE WAVE EFFECTS IN LIQUIDS.

Nyborg, W.L., Mechanisms for nonthermal effects of sound., 1968, J.ACOUST.SOC.AM., **44**, (5), 1302-1309.

Nyborg, W.L., Gould, R.K., Jackson, F.J. and Adams, C.E., Sonically induced microstreaming applied to a surface reaction., 1959, J.ACOUST.SOC.AM., **31**, (6), 706.

Obiakor, E.K., Increasing the settling rate of flocculated suspensions., 1965, NATURE, Jan., 381.

Okada, K., Fuseya, S., Nishimura, Y. and Matsubara, M., Effect of ultrasound on micromixing., 1972, CHEM. ENG. SCI., **27**, 529-535.

Petenate, A.M. and Glatz, C.E., Isoelectric Precipitation of Soy Protein: Parts I and II., 1983, BIOTECH. AND BIOENG., **25**, 3049-3078.

Peterson, S., Perkins, G. and Baker, C., Development of an ultrasonic blood cell separator., 1987, IEEE/EIGHTH ANNUAL CONFERENCE OF ENGINEERING IN MEDICINE.

Platte, M., A polyvinylidene fluoride needle hydrophone for ultrasonic applications., 1985, ULTRASONICS, **23**, 113-118.

Purchas, D., Pre-treatment of solid/liquid mixtures., 1967, INDUSTRIAL FILTRATION OF LIQUIDS.

Reibold, R. and Kwiek, P., Optical near-field investigations into the Raman-Nath and KML regimes of diffraction by ultrasonic waves., 1990, ACUSTICA, **70**, 223-229.

Raman, C.F. and Nath, N.S.N., 1935, PROC. IND. ACAD. SCI., **2**, 406-412.

Richardson, P.D., Effects of sound and vibrations on heat transfer., 1967, APPLIED MECHANICS REVIEWS, **20**, (3), 201.

Riebel, U. and Loffler, F., On line measurement of particle size distribution and particle concentration in suspensions by ultrasonic spectrometry., 1990, CHEM.ING.TECH., **62**, (5), 426-427.

Rosenfeld, E., Romanowski, U. and Williams, A.R., Positive and negative effects of diagnostic intensities of ultrasound on erythrocyte blood group markers., 1990, ULTRASONICS, **28**, 155-158.

Rozenberg, 1971, HIGH INTENSITY ULTRASONIC FIELDS.

Sanghvi, P. and Banakar, U.V., Ultrasonics: Principles and biomedical applications., 1991, BIO.PHARM., Sept., 32-40.

Sasady, N.C., Hartig, A. and Bjorno, L., Development of some transducers based on polyvinylidene fluoride., 1979, ultrasonics international, 468-475.

Schmidt, P., Rosenfeld, E., Millner, R. and Schellenberger, A., Effects of ultrasound on the catalytic activity of matrix-bound glucoamylase., 1987, ULTRASONICS, **25**, 295-299.

Schmidt, P., Rosenfeld, E., Millner, R., Czerner, R. and Schellenberge., Theoretical and experimental studies on the influence of ultrasound on immobilized enzymes., 1987, BIOTECH. AND BIOENG., **30**, 982-935.

Schuster, Von K. and Matz, W., Über stationare Strömungen im Kundt'schen Rohr., 1940.

Sears, J.T. and Clauson, M., Sonic dewatering of large particle dispersions., 1978, SEP. SCI. TECH., **13**, (8), 633–635.

Shorter, S.C. and Bridge, B., Design, manufacture and performance of narrowband ultrasonic immersion probes for multiple frequency operation in the range 3 to 170 MHz., 1986, ULTRASONICS, **24**, 117–132.

Shotton, K.C., Bacon, D.R. and Quilliam, R.M., A pvdf membrane hydrophone for operation in the range 0.5 MHz to 15 MHz., 1980, ULTRASONICS, **18**, 123–126.

Sinisterra, J.V., Application of ultrasound to biotechnology: an overview., 1992, ULTRASONICS, **30**, (3), 180–185.

Skinner, L.A., Pressure threshold for acoustic cavitation., 1970, J.ACOUST.SOC.AM., **47**, 1(2), 327–331.

Slagle, D.J., Shah, Y.T., Klinzing, G.E. and Walters, J.G., Settling of coal in coal–oil slurries., 1978, IND. ENG. CHEM. PROCESS DES. DEV., **17**, (4), 500–504.

Sliwinski, A., Acousto–optics and its perspectives in research and applications., 1990, ULTRASONICS, **28**, 195–213.

Sollner, K. and Bondy, C., The mechanism of coagulation by ultrasonic waves., 1936, TRANS. FARAD. SOC., **32**, 616–623.

Stanton, T.K., Sound scattering by spherical and elongated shelled bodies., 1990, J.ACOUST.SOC.AM., **88**, (3), 1619–1633.

Stinson, M.R., The propagation of plane sound waves in narrow and wide circular tubes, and generalization to uniform tubes of arbitrary cross-sectional shape., 1991, J.ACOUST.SOC.AM., **89**, (2), 550-558.

Suslick, K. and Doktycz, S., Sounding out new chemistry., 1990, NEW SCIENTIST, 3 Feb, 50-53.

Suslick, K.S., Editorial from Ultrasonics, Special Edition on Sonochemistry., 1990, ULTRASONICS, **28**, 279.

Suslick, K.S., The chemical effects of ultrasound., 1989, SCIENTIFIC AMERICAN, Feb, 1989.

Suslick, K.S., Doktycz, S.J. and Flint, E.B., On the origin of sonoluminescence and sonochemistry., 1990, ULTRASONICS, **28**, 280-290.

Swartz, R.G. and Plummer, J.D., On the generation of high frequency acoustic energy with polyvinylidene fluoride., 1980, IEEE TRANS. SON. ULTRASON., **SU-27**, (6), 295-303.

Tarleton, E.S., How electric and ultrasonic fields assist membrane filtration., 1988, PROCS. FILTRATION SOC., Nov/Dec, 402-406.

Tarleton, E.S. and Wakeman, R.J., Microfiltration enhancement by electrical and ultrasonic fields., 1990, FILTRATION & SEPARATION., May/June, 192-194.

Tarleton, E.S., The role of field-assisted techniques in solid-liquid separation., 1992, FILTRATION & SEPARATION., May/June, 246-252.

Taylor, R.J., Richardson, L.B. and Burton, D.T., Ultrasonics for inhibiting biofouling., 1983, ULTRASONICS INTERNATIONAL 1983.

Theumann, J.-F., Arditi, M., Meister, J.-J. and Jaques, E., Acoustic fields of concave cylindrical transducers., 1990, J.ACOUST.SOC.AM., **88**, (2), 1160-1169.

Thielsch, H., The effect of sonic vibrations on the settling rates of ground rock particles in water., 1946, TRANS. AM. INST. MIN. (METAL)ENGRS., **169**, 203-208.

Thompson ,D. and Vilbrandt, F.C., Effect of ultrasonic energy on settling of solids in phosphate tailing., 1954, IND. ENGRG. CHEM., **46**, 1172-1180.

Tilley, D., Coakley, W.T., Gould, R.K., Payne, S.E, Real time observations of polylysine, dextran and polyethylene glycol induced mutual adhesion of erythrocytes held in suspension in an ultrasonic standing wave field., 1987, EUR. BIOPHYS. J., **14**, 499-507.

Tjotta, J.N. and Tjotta, S., Mass transport sustained by oscillations of finite amplitude in a stratified fluid., 1973, ULTRASONICS INTERNATIONAL, 37-43.

Tsujino,T., Cavitation damage and noise spectra in a polymer solution., 1987, ULTRASONICS, **25**, 67-72.

Tsujino,T., Shima, A. and Oikawa, Y., Effect of polymer additives on the generation of subharmonic and harmonic bubble oscillations in an ultrasonically irradiated liquid., 1988, J.SOUND. VIB., **123**, (1), 171-184.

Urick, R.J., The Absorption of Sound in Suspensions of Irregular Particles., 1948, J.ACOUST.SOC.AM., **20**, (3), 283-289.

Veress, E. Vincze, J., The haemolysing action of ultrasound on erythrocytes., 1976/77 ACUSTICA, **36**, 100-103.

Vienken, J., Coakley, W.T., Gould, R.K. *et al*, Electro–acoustic fusion of erythrocytes and of myeloma cells., 1985, BIOCHEMICA ET BIOPHYSICA ACTA, **820**, 259–264.

Vigoureux, P., 1951, ULTRASONICS.

Wang, C.–Y., Acoustic streaming due to an oscillatory source near a plate., 1984, J.ACOUST.SOC.AM., **75**, (1), 108–111.

Watmough, D.J., Quan, K.M. and Shiran, M.B., Possible explanation for the unexpected absence of gross biological damage to membranes of cells insonated in suspension and in surface culture in chambers exposed to standing and progressive wave fields., 1990, ULTRASONICS, **28**, 142–148.

Webster, D.F., Harvey, W., Dyson, M. and Pond, J.B., The role of ultrasound –induced cavitation in the *in vitro* stimulation of collagen synthesis in human fibroblasts., 1980, ULTRASONICS, Jan, 33–37.

Whitworth, G. and Coakley, W.T., Particle column formation in a stationary ultrasonic field., 1992, J.ACOUST.SOC.AM., **91**, (1), 79–85.

Wiltshire, M.F., Symposium on the applications of high intensity ultrasound., 1990, ULTRASONICS, **28**, 338.

Wladimiroff, J.W. and Talbert, D.G., The changing fine structure of erythrocyte formations when trapped in ultrasonic standing waves, 1973, PHYS.MED.BIOL, **18**, 888–891.

Zemanek, J., Beam Behaviour within the Nearfield of a Vibrating Piston., 1971, J.ACOUST.SOC.AM., **49**, 1(2), 181–191.